

Numerical Simulation of Groundwater
in the Umm er Radhuma Aquifer at
Shadco Project – Eastern Province

by

Rajai Samih Al Assar

A Thesis Presented to the

FACULTY OF THE COLLEGE OF GRADUATE STUDIES

KING FAHD UNIVERSITY OF PETROLEUM & MINERALS

DHAHRAN, SAUDI ARABIA

In Partial Fulfillment of the
Requirements for the Degree of

MASTER OF SCIENCE

In

CIVIL ENGINEERING

January, 1992

INFORMATION TO USERS

This manuscript has been reproduced from the microfilm master. UMI films the text directly from the original or copy submitted. Thus, some thesis and dissertation copies are in typewriter face, while others may be from any type of computer printer.

The quality of this reproduction is dependent upon the quality of the copy submitted. Broken or indistinct print, colored or poor quality illustrations and photographs, print bleedthrough, substandard margins, and improper alignment can adversely affect reproduction.

In the unlikely event that the author did not send UMI a complete manuscript and there are missing pages, these will be noted. Also, if unauthorized copyright material had to be removed, a note will indicate the deletion.

Oversize materials (e.g., maps, drawings, charts) are reproduced by sectioning the original, beginning at the upper left-hand corner and continuing from left to right in equal sections with small overlaps. Each original is also photographed in one exposure and is included in reduced form at the back of the book.

Photographs included in the original manuscript have been reproduced xerographically in this copy. Higher quality 6" x 9" black and white photographic prints are available for any photographs or illustrations appearing in this copy for an additional charge. Contact UMI directly to order.

U·M·I

University Microfilms International
A Bell & Howell Information Company
300 North Zeeb Road, Ann Arbor, MI 48106-1346 USA
313.761-4700 800.521-0600

Order Number 1354031

**Numerical simulation of groundwater in the Umm Er Radhuma
aquifer at SHADCO project - eastern province**

Al-Assar, Rajai Samih, M.S.

King Fahd University of Petroleum and Minerals (Saudi Arabia), 1992

**NUMERICAL SIMULATION OF GROUNDWATER
IN THE UMM ER RADHUMA AQUIFER AT
SHADCO PROJECT - EASTERN PROVINCE**

BY

RAJAI SAMIH AL ASSAR

A Thesis Presented to the
FACULTY OF THE COLLEGE OF GRADUATE STUDIES
KING FAHD UNIVERSITY OF PETROLEUM & MINERALS
DHAHRAN, SAUDI ARABIA

In Partial Fulfillment of the
Requirements for the Degree of

MASTER OF SCIENCE

In

CIVIL ENGINEERING

JANUARY, 1992

KING FAHD UNIVERSITY OF PETROLEUM & MINERALS

DHAHRAN, SAUDI ARABIA

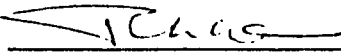
This thesis, written by

RAJAI SAMIH ALASSAR

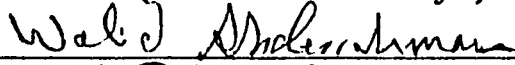
under the direction of his Thesis Advisor, and approved by his Thesis Committee, has been presented to and accepted by the Dean of the College of Graduate Studies, in partial fulfillment of the requirements for the degree of

MASTER OF SCIENCE IN CIVIL ENGINEERING

Thesis Committee



Chairman (Dr. Rasheed I. Allayla)



Co-Chairman (Dr. Walid Abderrahman)



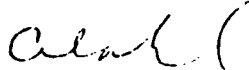
Member (Dr. Achi M. Ishaq)



Member (Dr. M. A. Marhoun)



**Dr. Ghazi J. Al-Sulaimani
Department Chairman**



**Dr. Ala H. Al-Rabeh, Dean,
College of Graduate Studies**

Date : 19-7-92



Dedicated To
My Parents, J.R., and all
faithful Muslims

ACKNOWLEDGEMENT

First of all I thank "ALLAH" The Almighty for the knowledge, help and guidance HE has showered on me. Thanks are also to our Prophet Mohammad (pbuh) who encouraged us as Muslims to seek knowledge and stressed that science and Islam are never separable.

My sincere appreciations are due to Dr. Rashid I. Allayla, my main advisor, for his help, support and encouragement in making this work possible. I deeply thank Dr. Walid Abderrahman, Dr. Achi M. Ishaq and Dr. Mohammad Al-Marhoun, my thesis committee members, for their valuable suggestions during this study.

Acknowledgement is due to Dr. Ghazi Al-Sulaiman who lent considerable help as the Chairman of the Civil Engineering Department.

Thanks are to Dr. F. M. Mohsen, who made the science of water resources loveable. The gap he left in the Water Resources Division is hard to fill.

Special thanks are due to Al-Sharqia Agricultural Company (SHADCO) for the valuable information provided through its engineers.

Gratitudes are due to Mr. Mumtaz Ali Khan and to Mr.

Ishtiaq Khan and Mr. Amla Ghalib of the Data Processing Center for their continuous help.

I wish to thank my friends and colleagues at KFUPM for their moral support and understanding. Special thanks and appreciations are due to Ala' Abduldayem, Adnan Blaibel, Isa Al-Buraim, Wail Al-Khatib, Mohammed Baymout, Hosam Abo-Younis and Hasan Al-Drainly. I should never forget the support of all graduate students in the water resources and environmental division at the civil engineering department.

I wish to express wholehearted gratitudes for my parents, brothers and sisters, for their love, encouragement and support. Thanks and appreciations are due to J.R. whose encouragement, support and patience have been limitless.

TABLE OF CONTENTS

	<i>Page</i>
Acknowledgement	I
Table of Contents	III
List of Figures	VI
List of Tables	X
List of Appendices	XI
Abstract(Arabic)	XII
Abstract	XIII
1. INTRODUCTION	
1.1 General	1
1.2 Objectives	3
2. LITERATURE REVIEW	
3. HYDROGEOLOGICAL SETTING OF THE STUDY AREA	
3.1 The Study Area	14
3.2 Topography	17
3.3 Climate	21
3.4 Physical & Chemical Water Analysis	24
3.4.1 General	24
3.4.2 Water Quality in the Study Area	25
3.5 Cultivation in the Study Area	28
3.6 Geology	30

3.6.1	<i>General</i>	30
3.6.2	<i>Umm er Rhoduma (UER)</i>	36
3.7	Hydrogeology	38
3.7.1	<i>Wasia Aquifer</i>	38
3.7.2	<i>Aruma Aquifer</i>	39
3.7.3	<i>UER Aquifer</i>	39
3.7.4	<i>Khobar Aquifer</i>	40
3.7.5	<i>Alat Aquifer</i>	40
3.7.6	<i>Neogene Aquifer</i>	44
4.	MODELLING TECHNIQUE	
4.1	Introduction	45
4.1.1	<i>Flow Equation of Flow Through Porous Media</i>	45
4.1.2	<i>The Finite Difference Technique</i>	47
4.1.3	<i>The U.S.G.S. Model</i>	53
4.2	Input Variables	56
4.2.1	<i>Transmissivity</i>	58
4.2.2	<i>Storativity</i>	61
4.2.3	<i>Initial Piezometric Surface</i>	63
4.2.4	<i>Extraction Rates</i>	65
4.3	Boundary Conditions and Discretization	68
4.4	Calibration	71
4.4.1	<i>General</i>	71
4.4.2	<i>Steady-State Calibration</i>	73
4.4.3	<i>Transient Calibration</i>	79

4.5	Sensitivity Analysis	86
	4.5.1 <i>General</i>	86
	4.5.2 <i>Transmissivity</i>	87
	4.5.3 <i>Head-Dependent Boundary</i>	87
5.	MANAGEMENT ALTERNATIVES	
	5.1 General	91
	5.2 Alternative I	94
	5.3 Alternative II	99
	5.4 Alternative III	112
6.	CONCLUSIONS AND RECOMMENDATIONS	129
	6.1 Conclusions	129
	6.2 Recommendations	130
	REFERENCES	133
	APPENDICES	
	<i>Appendix A-1</i>	140
	<i>Appendix A-2</i>	166
	<i>Appendix B</i>	182

LIST OF FIGURES

<i>Figures</i>	<i>Page</i>
3.1 The Study Area	15
3.2 Distribution of Fields in the Study Area	18
3.3 Aerial Camera (after Moffit and Bouchard 1982) ..	19
3.4 A Typical Aerial Photograph	20
3.5 Topographic Map of the Study Area.....	22
3.6 Classification of Irrigation Water Based on SAR and Conductivity	26
3.7 Chemical Analysis of Groundwater	29
3.8 Percentage of Crops Grown in Fields.....	33
3.9 Lithostratigraphic Generalized Sequence of Area IV (after Italconsult 1969)	35
3.10 A Lithostratigraphic Section along the C-wells in the Study Area.....	37
3.11 Contour Map of the Top of the UER Aquifer	41
3.11-1 Three-Dimensional Plot of the Top of the UER Aquifer.....	42
3.12 Depth to the Top of the UER Aquifer.....	43
4.1 Typical Block-centered Mesh	47
4.2 The Derivative of a Function	49
4.3 Schematic Diagram of Recovery Test	59
4.4 Spatial Distribution of Transmissivity Values Obtained from Pumping Tests	62
4.5 Map of Initial Piezometric Heads.....	64
4.6 Volume of Water Extracted Since 1984	66
4.7 Percentage of Water Extracted in Each Stress	

	Period	67
4.8	Head-Dependent Boundary (McDonald and Har- bough 1984)	70
4.9	The Discretized Area with Boundary Conditions ..	72
4.10	Map of Simulated Steady-State Piezometric Heads .	74
4.11	Map of the Difference Between Observed and Simulated Steady-State Piezometric Heads	77
4.12	Map of the Calibrated Transmissivity Values	78
4.13	Map of the Calibrated Storativity Values	81
4.14	Location of Observation Wells in the Study Area .	82
4.15-1	Simulated vs. Observed Heads at Observation Well B1	83
4.15-2	Simulated vs. Observed Heads at Observation Well F3	84
4.15-3	Simulated vs. Observed Heads at Observation Well I4	85
4.16	Sensitivity to Transmissivity	88
4.17	Sensitivity to Conductance of Head-Dependent Boundaries	90
5.1	Location of Observation Wells for the Prediction Period	95
5.2	Simulated Heads for the Period 1991/1998 Alter- native I	96
5.3	Piezometric Head Map at the End of Prediction Period - Alternative I	97
5.4	Drawdown Map at the End of Prediction Period - Alternative I	98
5.5	The Effect of Reducing Irrigation Water on the Piezometric Head at Well B1	101
5.6	The Effect of Reducing Irrigation Water on the Piezometric Head at Well F3	102

5.7	The Effect of Reducing Irrigation Water on the Piezometric Head at Well I4	103
5.8	The Effect of Reducing Irrigation Water on the Piezometric Head at Well D6	104
5.9	Heads at the End of Prediction Period vs. the Percentage of Reduction in Irrigation Water	105
5.M	Master Map for Figures 5.10-5.19	106
5.10	Piezometric Head Map at the End of Prediction Period - Alternative II - 10% Reduction in Irrigation Water	107
5.11	Piezometric Head Map at the End of Prediction Period - Alternative II - 20% Reduction in Irrigation Water	108
5.12	Piezometric Head Map at the End of Prediction Period - Alternative II - 30% Reduction in Irrigation Water	109
5.13	Piezometric Head Map at the End of Prediction Period - Alternative II - 40% Reduction in Irrigation Water	110
5.14	Piezometric Head Map at the End of Prediction Period - Alternative II - 50% Reduction in Irrigation Water	111
5.15	Drawdown Map at the End of Prediction Period Alternative II - 10% Reduction in Irrigation Water	113
5.16	Drawdown Map at the End of Prediction Period Alternative II - 20% Reduction in Irrigation Water	114
5.17	Drawdown Map at the End of Prediction Period Alternative II - 30% Reduction in Irrigation Water	115
5.18	Drawdown Map at the End of Prediction Period Alternative II - 40% Reduction in Irrigation Water	116
5.19	Drawdown Map at the End of Prediction Period Alternative II - 50% Reduction in Irrigation Water	117
5.20	Location of Heavily Irrigated Crops - Alt 3-1	119
5.21	Location of Heavily Irrigated Crops - Alt 3-2	120

5.22	Piezometric Head Map at the End of Prediction Period - Alt.III-1.....	121
5.23	Piezometric Head Map at the End of Prediction Period - Alt.III-2.....	122
5.24	Drawdown Map at the End of Prediction Period - Alt.III-1.....	123
5.25	Drawdown Map at the End of Prediction Period - Alt.III-2.....	124
5.26	The Difference Between the Heads in Alt.III-2 and the Heads in Alt.III-1.....	125
5.27	Simulated Heads for the Period 1991-1998 Alternative III-1.....	127
5.28	Simulated Heads for the Period 1991-1998 Alternative III-2.....	128

LIST OF TABLES

<i>Tables</i>		<i>Page</i>
3.1	Study Area Dimensions	16
3.2	Physical and Chemical Water Analysis	27
3.3	Crops Grown in the Fields since 1984	31
4.1	The Values of RMSE at Selected Runs.....	76
5.1	Total Number of Each Crop Grown in Each Year .	92

LIST OF APPENDICES

- Appendix A1: Pumping Test Graphs (Jacob Method)	140
- Appendix A2: Pumping Test Graphs (Recovery Method)	166
- Appendix B : Heads at the End of Stress Periods	182

خلاصة الرسالة

- اسم الطالب : رجائي سميح موسى العصار .
عنوان الدراسة : المحاكاة العددية للمياه الجوفية للخزان المائي أم الرضمة في منطقة مشروع شادكو .
التخصص : هندسة موارد المياه .

في هذه الدراسة تم استخدام نموذج رقمي ثنائي الأبعاد لتدفق المياه الجوفية في خزان أم الرضمة المحصور . ولقد أختيرت المزرعة المملوكة للشركة الشرقية للتنمية الزراعية والتي بها خمسة وسبعون بئراً محفورة في مساحة تقدر بتسعين كيلو متر مربع تستخدم لري المحاصيل الموسمية باستخدام نظام ري محوري لتكون موقعاً للدراسة . ولقد تم ربط ارتفاعات الآبار بالنسبة لبعضها البعض عن طريق تطوير خريطة طبوغرافية باستخدام الصور المأخوذة من الجو عن طريق الطائرات . وتم تحليل عينات من المياه الجوفية للتعرف على الخصائص الفيزيائية والكيميائية لها . ولقد دلت التجارب على أن المياه الجوفية المستخرجة متوافقة مع مواصفات الجودة للمياه المستخدمة في الزراعة . وقد تم تغيير الخواص الفيزيائية للخزان خلال حالات التدفق المنتظم وغير المنتظم للحصول على توافق بين مستويات المياه المتوقعة عن طريق النظام وتلك التي سجلت في المزرعة . وقد دلت قيم النفاذية على أن الخزان ذو إنتاجية عالية . عندئذ تم استخدام النموذج المعيار في توقع مستوى الماء ودرجة إستجابة الخزان عبر فترة زمنية مقدارها سبعة أعوام وذلك من خلال عدة بدائى . وقد دلت الدراسة على أن البديل الأفضل يكون في الاقتصاد وزرع المحاصيل التي تتطلب فترة ري طويلة في المنطقة الغربية من المزرعة .

Abstract

Full Name: Rajai Samih AlAssar
Title of Study: Numerical Simulation of Groundwater
in the Umm Er Radhuma Aquifer at
SHADCO Project Area-Eastern Province
Major Field: Water Resources Engineering

A Numerical two-dimensional model was used to model groundwater flow in the Umm Er Radhuma confined aquifer. The study area was chosen to be the farm of Al-Sharqiya Agricultural Company where 75 wells were drilled in an area of about 90 square kilometers to irrigate serial crops using central-pivoted irrigation system.

A topographic contour map of the area was made using aerial photogrammetry. Chemical and physical water analysis showed that water extracted from the aquifer was in agreement with irrigation water quality standards.

The calibrated physical parameters of the UER aquifer indicated that the aquifer is highly productive. The calibrated model was used to predict the aquifer's response for a 7-year planning period where different management alternatives were evaluated. The study showed the best alternative is to conserve water in addition to relocation of continuously irrigated crops to the western part of the study area.

Chapter 1

INTRODUCTION

1.1 GENERAL

Water is one of the most fundamental resources and the most unusual. This substance once referred to as "a great drink, but one that will never sell", can be truly called the elixir of life. The value of water is more pronounced especially in places where resources are finite and limited. For years nearly everybody took water for granted. Few people, however, realized its finite limits.

Saudi Arabia is a country where fresh water is not available in sufficient quantities. This is due to the arid nature of the environment and the scarcity of surface water such as rivers and streams. The rapid development in agriculture and social standards has accelerated the need for fresh water. Desalination as an alternative has been costly which made groundwater even more important economically as an alternative. Saudi Arabia in general and the Eastern Province in particular, have low precipitation and high evaporation rates. This means that water taken out of the ground aquifers may not be replenished. Groundwater from all aquifers have been used for agricultural, industrial, municipal purposes and have been mixed with desalination water for domestic use. This has resulted in excessive drawdowns, low well yields,

and a gradual decline in water quality due to contamination by irrigation and salt water intrusion from the sea. Therefore, the obvious challenging problem is how to utilize this resource as effectively as possible.

Modelling has been a very useful tool in solving many engineering problems. In its broad definition, a model is a tool designed to represent a simplified version of life. In fact, models are used in everyday's life. A map, for example, is a way to represent reality in a simplified form. Models have been used to study groundwater flow systems. The goal of modelling is to predict the value of the unknown variable such as groundwater head or concentration of a contaminant. Three types of models have been used in groundwater engineering namely; sand tank models, analog models, and mathematical models. Sand tanks have been used to scale down a complex field situation. Electrical analog models were widely used in the pre-high speed digital computer era. They work according to the principle that groundwater flow is analogous to the flow of electricity. A major drawback of the electrical analog models is that they are only useful to study steady-state flow problems. A mathematical model is a representation of a real-life situation by a set of differential equations. Because field situations are too complicated to be solved analytically, simplifying assumptions have always been made. The reliability of predictions using a groundwater model depends on how

well the model approximates the field situation. Unfortunately, most of groundwater flow problems arising in real life do not have the ideal solutions which one encounters most often with textbook problems. For example, many analytical solutions require that the medium be homogenous and isotropic. In order to get realistic solutions, it is usually necessary to use numerical techniques. Two types of numerical models have been widely used. These are the finite difference and the finite element models. With the development of high-speed digital computers, many problems previously beyond our capabilities can now be solved approximately to a high degree of accuracy.

1.2 OBJECTIVES

The following is a list of the objectives of this study:

1. To define the geological and hydrogeological settings of the project area of Al-Sharqiya Agricultural Company (SHADCO). This includes the hydraulic parameters of the Umm er Radhuma (UER) aquifer within the project area from previous pumping tests and the water quality in the study area.
2. To define the groundwater flow characteristics in the UER aquifer using numerical modelling techniques under steady and unsteady flow conditions.

3. To forecast the hydraulic responses of the aquifer system under different discharge patterns and to define the groundwater flow conditions under different water stress alternatives.

Chapter 2

LITERATURE REVIEW

Sand tank models are the oldest models used to study groundwater flow. Conclusions drawn from such models may need to be qualified when translated to a field situation. This is because phenomena measured at the scale of a sand tank model are often different from conditions observed in the field. Hubbart (1937) may be one of the earliest people to scientifically study geologic structures using scale models. Stallworth (1950) pointed out that quickly constructed models (scale models) facilitate seepage studies. Dry and Luthin (1954) experimented with sand models to study the distribution of water pressure under canals. Todd (1956) conducted a laboratory research on groundwater models including scaled models. Krayenhoff (1962) studied some effects of the unsaturated zone on non-steady free-surface groundwater flow using a scaled granular media.

Analog models are grouped into two categories namely, viscous fluid, and electrical models. Viscous models are known as Hele-Shaw or parallel plate models because a fluid more viscous than water is made to flow between two closely spaced parallel plates. Hele-Shaw was the first to experiment with the viscous models in (1887). He conducted experiments to find out the nature

of the surface resistance in pipes and ships. This technique, then, became popular in groundwater problems. Hanson (1952) solved complicated well problems using this technique. The Hele-Shaw viscous fluid model was used by Todd (1954, 1955) to study the unsteady flow in porous media. Zee (1955) studied the flow into wells using analog models. A horizontal scale model based on the viscous flow analogy was constructed by Santing (1957) to study groundwater flow aquifers having storage. Bear (1960) proposed the scales of viscous analogy models for groundwater studies. DeJong (1961) applied the technique to multiple fluid flow. Sternberg and Scott (1963) used the Hele-Shaw model as a tool in groundwater research. The wedge-shaped aquifers were investigated by means of viscous models by Williams (1966).

Electrical analog models work according to the principle that groundwater flow is analogous to the flow of electricity. These models consist of boards wired with electrical networks of resistors and capacitors. The analogy is expressed in the mathematical similarity between Darcy's law for groundwater flow and Ohm's law for the flow of electricity. The model was used to solve water seepage problems by Wyckoff and Reed (1935). Varendenburgh and Stevens (1936) electrically investigated underground water flow nets. Visualizing flow in condensate reservoirs was aided by the use of electrical models by Hurst (1941). The technique helped Botset (1946) and Wolf (1948) to study recovery

problems. Kuthin (1953) solved drainage problems by means of an electrical resistance network. Two- and three-dimensional groundwater flow was analyzed by Opsal (1955) using electrical analogy.

The extensive use of mathematical models at present time supports Lehr's statement in 1979 "Mathematical groundwater models may be intellectual toys today, but they should be useful tools tomorrow". Mathematical models can be grouped into three categories, namely; statistical, analytical, and numerical.

The science of statistics is the backbone in statistical models. These models mainly depend on historical records. Baker (1978) presents a stochastic analysis of spatial variability in subsurface hydrology. Cooley (1979) applies statistical models to assess groundwater steady-state flow. Macro dispersion in a stratified aquifer was stochastically analyzed by Gelhar (1979). Finite and infinite groundwater domains were treated by Gutjahr (1981). Neuman (1980) presented a statistical approach to the inverse problem of aquifer hydrology.

Analytical and numerical models are the most useful tools in groundwater studies. Freeze (1971) presented an analytical model to solve groundwater flow equations. Karanjac (1977) proposed a mathematical model of Uluova Plain in Turkey. An overview of groundwater modeling is presented by Mercer (1980). The area where analytical models have been widely used is the field of

well hydraulics. Thiem (1906) was one of the first to present an analytical model by which the hydraulic conductivity of an aquifer at steady-state can be determined. DeGlee (1930) presented a model for the steady-state drawdown in an aquifer with leakage from a semi-pervious covering layer. Hantush and Jacob (1955) presented the same model with some modifications. Dupuit (1863) and Thiem (1906) modified Thiem's method to suit the steady-state flow in unconfined aquifers. The unsteady-state flow problem has also been analytically treated. Theis (1935) analytically solved the problem of unsteady-state flow in confined aquifers. Chow (1952) developed a method which has the advantage of avoiding the curve fitting of the Theis method. Jacob and Cooper (1946) gave a simplified solution to the Theis formula by restricting some conditions for the application of the model. Theis (1935) proposed a recovery test of aquifers for which an analytical solution was recommended. The unsteady-state flow in semi-confined aquifers was treated by Walton (1962). Hantush (1956) developed three methods of analyzing the data from pumping tests in semi-confined aquifers. Boulton (1963) introduced a method of analyzing pumping test data from unconfined aquifers, in which allowance is made for the delayed yield from storage due to gravity drainage. Boulton (1963) similarly treated the unsteady-state flow in semi-confined aquifers. The complexity of groundwater flow problems makes analytical models of limited use. This is due to the many simplifications attempted to overcome the mathematical obstacles. The

literature is full of analytical models. The use of these models, however, is limited to simple problems.

The rise of numerical techniques such as finite difference and finite element methods and the rapid advancing technology in digital computers have made it possible for complex groundwater systems to be studied. The literature is full of papers published on numerical techniques. The technique has been applied successfully in many fields. This is supported by the use of the finite difference technique in petroleum engineering by Crichtlow and Peaceman (1977). The use of numerical models in groundwater management was discussed by Bachmat (1980). A numerical method of estimating parameters in groundwater flow was presented by Cooley (1977). Faust (1980) discussed the use of numerical models in groundwater flow. Gillham (1974) carried out a sensitivity analysis of input parameters in numerical modeling of steady state groundwater flow. The transport equation was numerically analyzed by Gray and Pinder (1976). Pinder (1977) presented a numerical technique for calculating the transient position of the salt water front. Apple (1976) wrote a note on computing finite difference interblock transmissivities. Finnemore (1968) used the finite difference technique to assess seepage through an earth dam. Huntoon (1974) used the finite difference technique to solve problems in groundwater flow. Prickett and Lonquist (1971) and Trescott (1976) constructed two-dimensional finite difference

groundwater flow models. Three-dimensional models were also developed by Trescott (1975) and Freeze (1971). The United States Geological Survey (U.S.G.S.) developed a three-dimensional finite difference groundwater flow model in 1984 which is successfully replacing its widely used predecessors, USGS2D (Trescott, Pinder and Larson, 1976) and USGS3D (Trescott 1975). The finite element numerical technique was also used by groundwater engineers. Chen (1978) modeled hydraulic systems by the finite element method. Gary (1976) discussed the method as applied to groundwater transport. Pinder (1977) discussed the method in surface and subsurface hydrology. Salt water front was simulated by the finite element technique by Segol and Gary (1975).

The area under investigation is a part of the Eastern Province of Saudi Arabia where several studies have been carried out. Naimi (1965), for example published the first report on the groundwater picture of northeastern Saudi Arabia. The report was descriptive where no modelling was conducted. In a detailed study, Italconsult (1969), conducted the characteristics of the aquifers in Area IV were investigated. A regional study in Al-Hassa area by the Bureau de Recherches Geologiques et Minieres (BRGM, 1977) provided data on the transmissivities, storage coefficients and vertical leakances in the area. A three-dimensional model was used in the study, where twelve production alternatives were simulated. In another study BRGM (1976) developed a simu-

lation model for Al-Wasia aquifer. A multi-aquifer simulation model was developed by Groundwater Development Consultants (GDC, 1980). GDC studied the UER, Khobar, Alat and Neogene aquifers with the concentration given to Bahrain area. A comprehensive study by Al-Layla, et al., (1986) in the Eastern Province of Saudi Arabia led to the development of a two-dimensional simulation model, a modified version of the United States Geological Survey Model (Konikow and Bredehoeft, 1978) was used to simulate solute transport in Dammam aquifer. The aquifers of UER, Alat and Khobar were also studied by Rasheeduddin, et al., (1989) using the USGS model (McDonald and Harbaugh 1984).

The previous studies were conducted on a regional basis where the grid spacing was large. It is believed that adopting the results of the previous studies to SHADCO project will not be suitable, especially due to the relatively small area of the project in addition to the high discharge rates. During peak demand periods, drawdowns in the wells, especially those located in the middle and eastern parts of the area, were observed. This is due to the additional drawdown which resulted from the interference of pumping effects of the surrounding wells. Therefore, the groundwater flow characteristics under different pumping scenarios from different wells in the area is important to develop a proper groundwater management scheme. The use of numerical techniques to simulate groundwater flow in the area becomes essential. Previous hydro-

logical studies by Italconult (1969) indicated that the UER aquifer exists in the Eastern Province of Saudi Arabia as part of a multi-layered aquifer system where the confining beds are leaky aquitards and vertical flow between aquifers occurs with change in head and vertical gradient in the aquifer system. Consequently, the groundwater flow in the area is best studied by a three-dimensional groundwater flow model. Unfortunately, due to the lack of data on water heads in the overlying aquifers, the groundwater flow in the UER aquifer is going to be simulated in two dimensions using a block-centered finite difference approach. The United States Geological Survey (USGS) numerical three-dimensional finite difference groundwater flow model developed by McDonald and Harbough (1984) is selected. It is selected because it has histories of high confidence and well established codes. The model makes use of a numerical technique to solve the partial differential equation:

$$\frac{\partial (K_{xx} \frac{\partial h}{\partial x})}{\partial x} + \frac{\partial (K_{yy} \frac{\partial h}{\partial y})}{\partial y} + \frac{\partial (K_{zz} \frac{\partial h}{\partial z})}{\partial z} + R = S_s \frac{\partial h}{\partial t}$$

where

K_{xx} = hydraulic conductivity in the x-direction

K_{yy} = hydraulic conductivity in the y-direction

K_{zz} = hydraulic conductivity in the z-direction

S_s = The specific storage

R = is the volumetric injection rate

t = time

Chapter 3

HYDROGEOLOGICAL SETTING OF THE STUDY AREA

3.1 THE STUDY AREA

The study area located in the Eastern Province of Saudi Arabia is part of a larger area owned by Al-Sharqiya Agricultural Company (SHADCO). The whole area owned by SHADCO is bounded on the north by a latitude $26^{\circ} 50' 31.15''$ N, on the south by latitude $26^{\circ} 34' 34.91''$ N, on the east by longitude $49^{\circ} 16' 15.39''$ E, and on the west by longitude $48^{\circ} 59' 58.23''$ E (Fig. 3.1). From these coordinates, the lengths of the polygon sides enclosing the area can be computed as shown in Table (3.1). The area covers more than 600 square kilometers. The study area is located in the upper right quarter of the area shown in Fig. (3.1). The study area ranges around 10 kilometers from west to east and 9 kilometers from north to south. The area chosen for modelling includes the only 75 wells drilled in the area owned by SHADCO. These wells are entirely devoted for agricultural purposes.

The wells located in the study area extract water from the Umm er Radhuma aquifer (UER). The water extracted is used to irrigate the surrounding fields using a central-pivoted irrigation system. The fields are of two types: the first type has an area

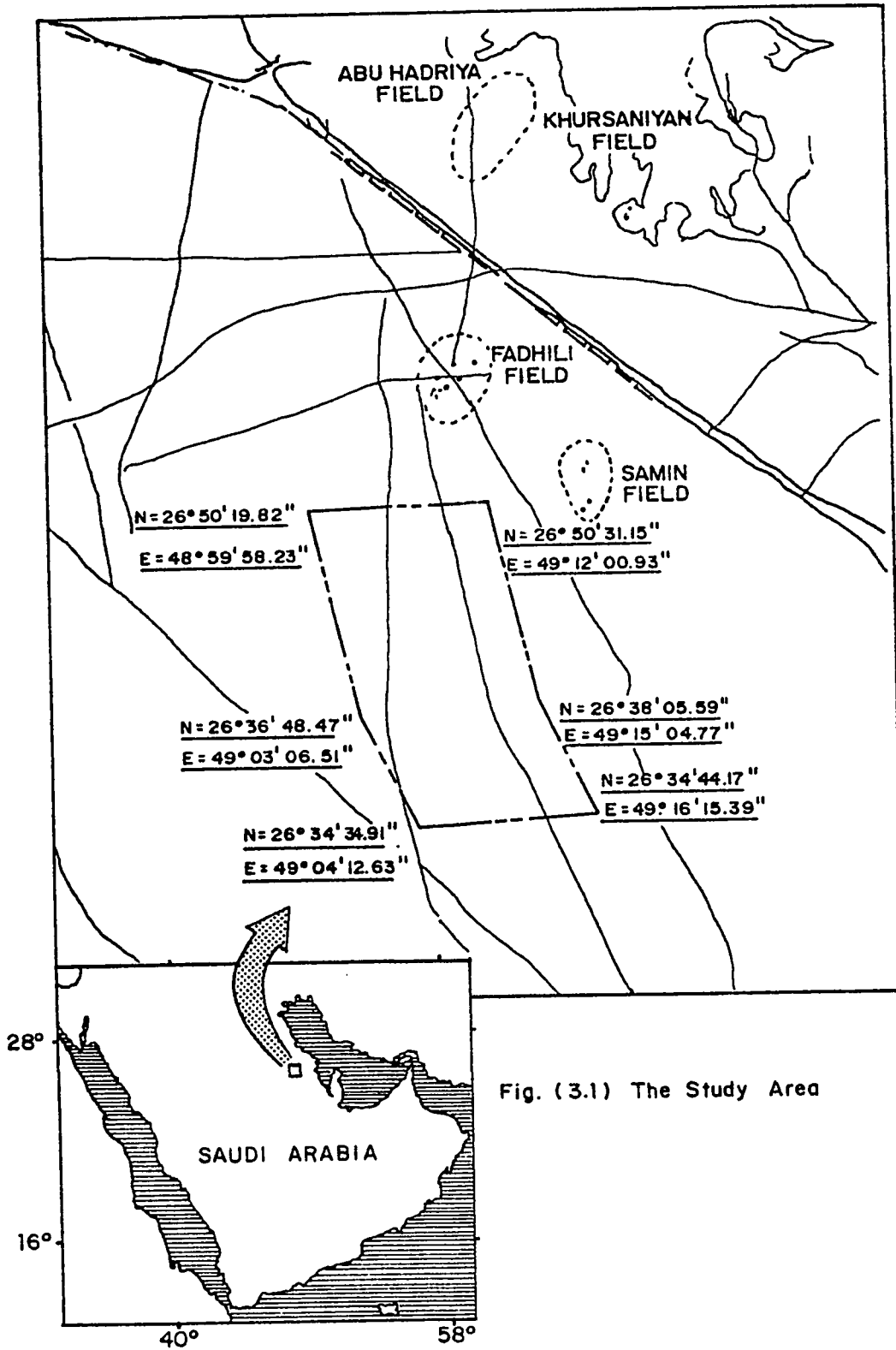


Fig. (3.1) The Study Area

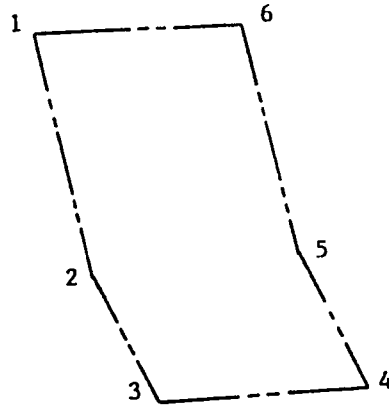


Table 3.1: Study Area Dimensions

Point	Bearing	Distance (meters)	North Coordinate	East Coordinate
1	S 10 52 58.190 E	25510.2361	2970193.7430	301206.1920
2	S 23 07 27.366 E	4499.6811	2943112.3070	306022.5910
3	S 89 59 51.319 E	20004.0560	2941004.1490	307789.7370
4	N 16 12 52.871 E	6400.6552	2941003.3100	327793.7930
5	N 11 11 07.881 W	23502.3268	2947228.3470	325924.4530
6	S 89 51 25.096 W	19958.1652	2970213.5650	321164.2930
1			2970193.7430	301206.1920

of 78 hectares and the second type has an area of 85 hectares. The first set of fields include those surrounding the wells F1, G1, H1, F2, G2, and H2. All the other fields are 85 hectares in area Fig. (3.2).

3.2 TOPOGRAPHY

Water levels in the SHADCO wells have been documented as the distance from the ground surface to the water surface. There had been no mention of how these wells are topographically related to each other. The heads used in the governing differential equation of groundwater flow represent the pressure head as well as the elevation head. Therefore, it is necessary to relate the wells to a common datum so that the hydraulic head at each well is known. A topographic contour map, then becomes essential. Due to the large area covered by the study (90 squared kilometers), classical surveying techniques would be impractical and time consuming. The aerial photogrammetry technique is most suitable.

Aerial photogrammetry is the science of making measurements on photographs taken from the air. Photographs are taken by aerial cameras similar to the one schematically shown in Fig. (3.3). The camera is fixed in a camera mount which is secured over an opening in the bottom of the airplane. Photographs such as the one shown in Fig. (3.4), are then taken. If the focal

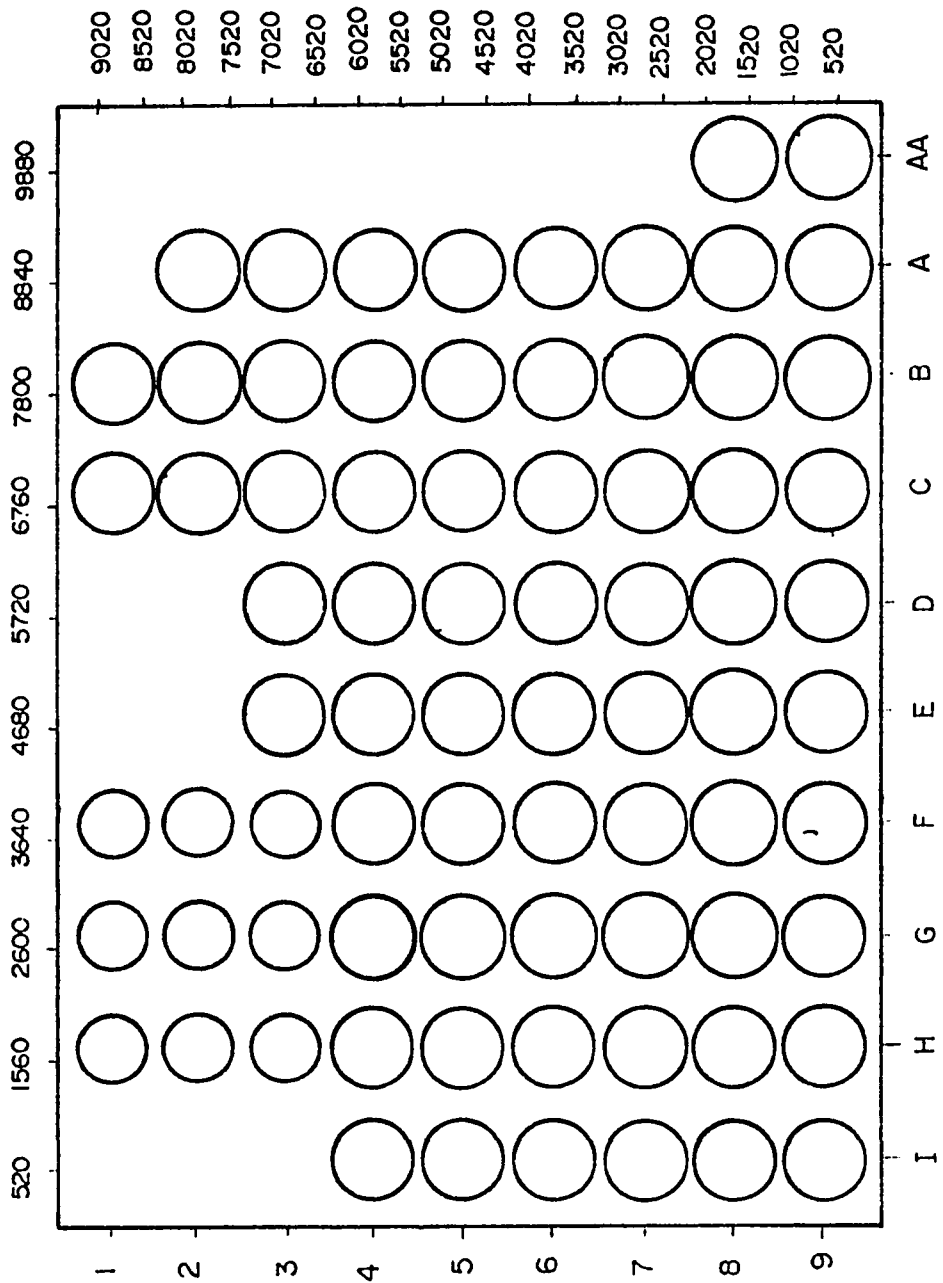
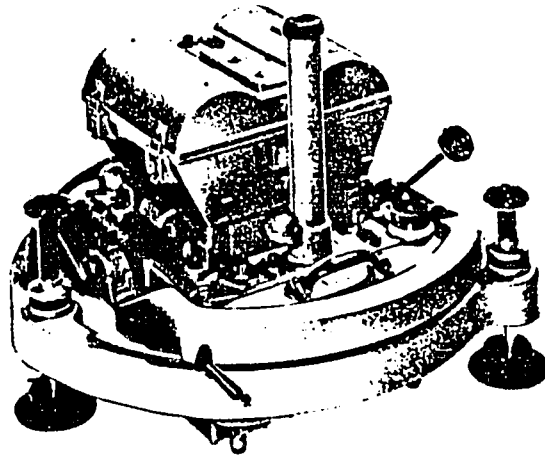
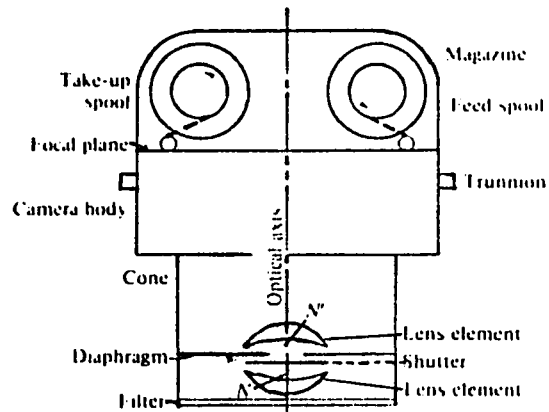


Fig. 3.2: Distribution of fields in the study area.





Aerial camera installed in mount



Component parts of aerial camera

Fig. 3.3: Aerial camera (after Moffit and Bouchard 1982).

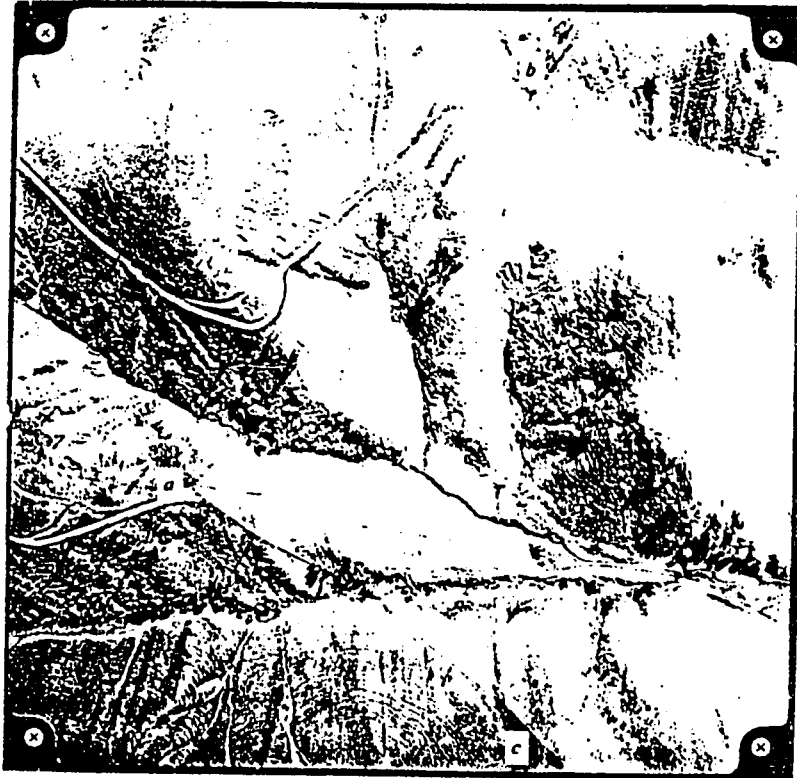


Fig. 3.4: A typical aerial photograph

63

length of the camera and the elevation of any point is known, all the other points can be related to the known point. A topographic contour map can then be constructed.

The locations of the wells were marked on the corresponding aerial photographs of the Saudi Aramco. The floating point technique was used to obtain the map shown in Fig. (3.5). It is noted that the area is generally level with maximum elevation difference of around 20 meters. Higher elevations are noted north and east of the area. Few low points are present locally at the northeast of the area.

3.3 CLIMATE

The following is extracted from a report on water of Saudi Arabia published by the Ministry of Agriculture and Water.

The Eastern Province of Saudi Arabia is generally a tropical and a sub-tropical desert linked climatically to the eastern Mediterranean and adjacent lands. The area is generally hot and humid in summer and cool in winter. The study area, as part of the northeastern region of Saudi Arabia, is in the desert belt but experiences relatively more rainfall than areas further west. Rainfall of 70 to 100 millimeters usually occurs in the area. These rains take place primarily in the winter when they are associated with irregular incursions of polar air modified along the coast by

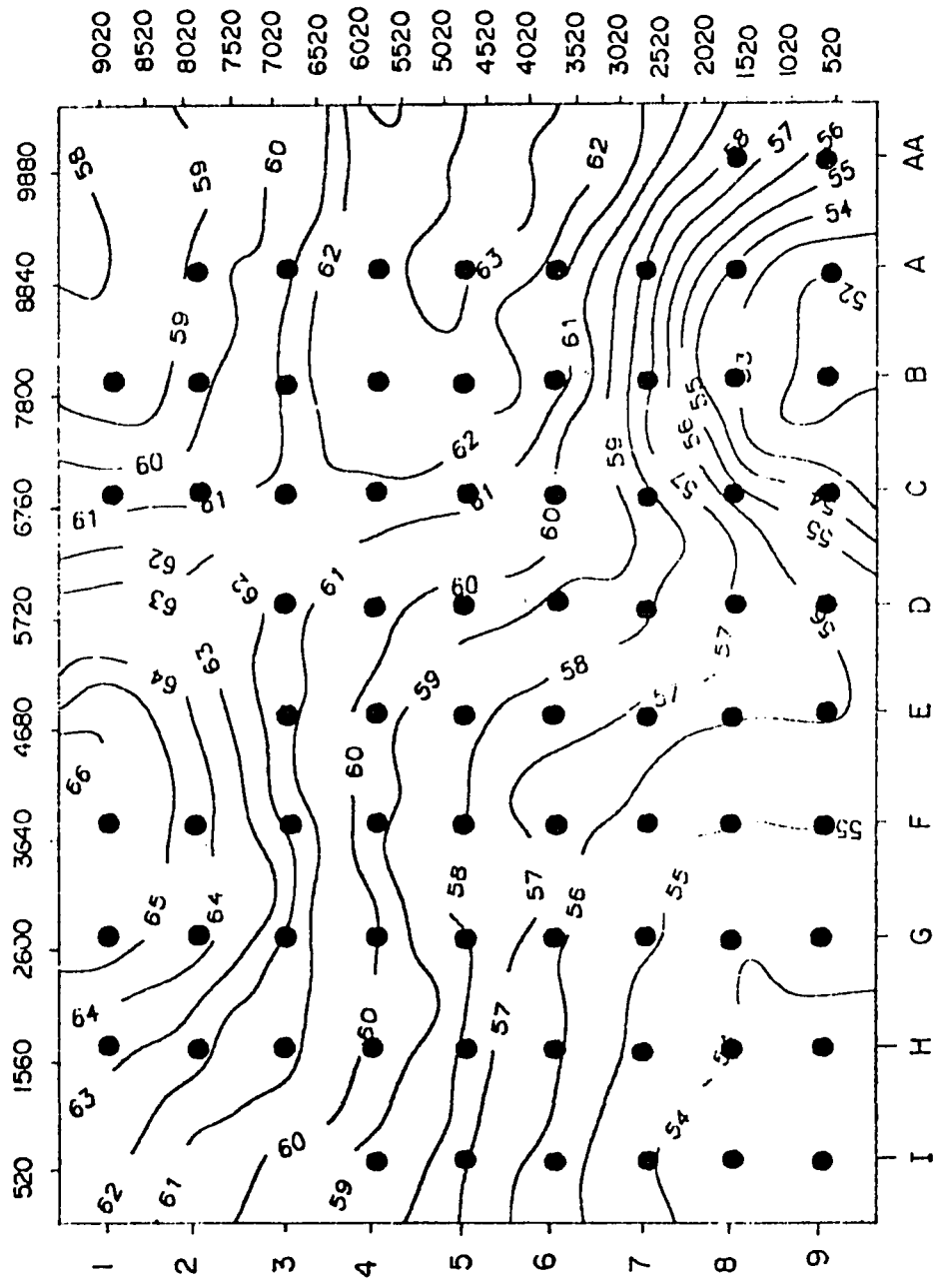


Fig. 3.5: Topographic map of the study area
 -Values given in meters
 ● Wells

the Arabian Gulf. The ambient air temperature of the Eastern Province varies from season to season and from region to region. During winter (December, January, February), temperatures below freezing are not uncommon in the northeastern part of Saudi Arabia. The winter temperatures of the coastal area are higher than those recorded inland. The summer temperatures are around 48°C. The lowest relative humidity is generally noted during June and July whereas December and January are the months of maximum relative humidity. The difference between the minimum and maximum relative humidity is generally minor. The continuous humidity in the Eastern Province can be attributed to the combined effect of the Gulf and the evapotranspiration from irrigation areas. The relative humidity ranges from 60 to 90 percent. The range of seasonal sunshine hours in the area is between 6 hours during winter and 12 hours during summer. The mean monthly solar radiation has been estimated to be from 300-600 langley's per day (a langley is a unit of solar radiation equivalent to 1 gm calorie per square centimeter). The mean monthly pan evaporation has been estimated as 150 millimeters in December and January and 350 millimeters in June and July.

3.4 PHYSICAL AND CHEMICAL WATER ANALYSIS

3.4.1 General

The volume of water that can be extracted from an aquifer is a very important factor in determining the suitability of that aquifer. In many areas, however, the physical or chemical nature of the groundwater may be more of interest. Several water quality regulations have been set to insure the suitability of water for a given purpose. These include drinking, agricultural, and municipal water quality standards. If a successful irrigation is to be achieved, not only the soil types and cropping practices should be investigated, water should also be acceptable in quality. For example, the concentration of salt in top soils, due to irrigation with saline water, makes it difficult for crop roots to extract enough water and nutrients. Toxicity is also a problem in maintaining good yields. The ratio of sodium to calcium and magnesium is of particular importance in irrigation. Clay present in soils takes up sodium from sodium-rich water. The soil, in exchange, gives up calcium and magnesium. The sodium can greatly affect the soil properties because it makes clay sticky and slick leading to low permeability. When soil is dry, clay shrinks and the land becomes difficult to cultivate. The low permeability as a result of adsorbing sodium can lead to growth retardation. The existence of calcium and magnesium ions in water sufficient to equal or exceed the sodium ions maintains good permeability and discourages

growth retardation. The sodium adsorption ratio (SAR) method has been set by the United States Salinity Laboratory (U.S.S.L.) to insure adequate sodium quality. The SAR is defined as:

$$\text{SAR} = \frac{\text{Na}^+}{\frac{\sqrt{\text{Ca}^{++} + \text{Mg}^{++}}}{2}}$$

The United States Department of Agriculture (USDA) has constructed classification nomographs of irrigation water depending on the electrical conductivity and SAR, (Fig. 3.6).

Several other important physical and chemical parameters have to be tested. These include color, odor, taste, turbidity, temperature, and electrical conductivity on the physical side. The chemical parameters include pH, potassium, bicarbonate, chloride, sulphate, nitrate, boron, fluoride, hydrogen sulphide, and iron.

3.4.2 Water Quality in the Study Area

Analysis of water samples taken from the wells is shown in Table (3.2). When comparing the results of the analysis to the recommended maximum concentrations of irrigation water, it is noted that the SAR value of 2.2 obtained is far below the maximum. This indicates that sodium is low enough for use in irrigation. Boron, fluoride, and iron concentrations, also fall within the allowable limits. A graphical representation of the cations and

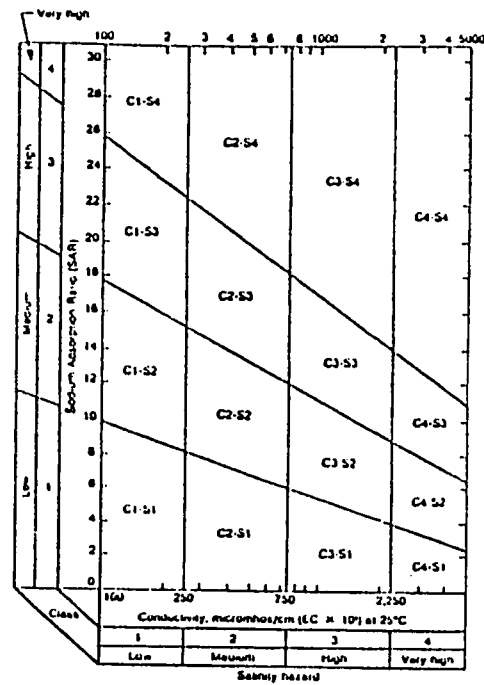


Fig. 3.6: Classification of irrigation waters based on SAR and conductivity (U.S. Department of Agriculture).

Table 3.2: Physical & Chemical Water Analysis

Type of Analysis	Tests	Irrigation Standards
Color	Colorless	
Odor	Odorless	
Appearance	Clear	
Taste	Unobjectionable	
Turbidity	0	
Temperature	36°C	
Electric Conductivity	1950 mhoms/cm	
pH	7.9	
Calcium	9.3 meq/l	SAR < 10
Magnesium	6.6 meq/l	SAR < 10
Sodium	6.2 meq/l	SAR < 10
Potassium	0.2 meq/l	
Bicarbonate	2.0 meq/l	
Chloride	6.6 meq/l	
Sulphate	12.0 meq/l	
Nitrate	0	
Boron	0.3 mg/l	0.7 mg/l
Fluoride	0.9 mg/l	1.0 mg/l
Hydrogen Sulphide	0	
Iron	0	5.0 mg/l
Total Dissolved Solids	1280 mg/l	

anions of water is given in Fig. (3.7). According to the USDA classification (Fig. 3.6), groundwater in the area can be classified as C3-S1. The C3-classification can be interpreted as high-salinity water. According to the USDA, this type of water can not be used on soils that have restricted drainage. With adequate drainage, special management for salinity control may be required and plants with good salt tolerance should be selected. The S1-classification can be interpreted as low-Sodium water which can be used with little danger on nearly all soils. Sodium sensitive crops such as stone-fruit trees and avocades may accumulate injurious concentration Sodium. Since the soil in the study area is mostly sand, there is clearly no potential problem associated with the water extracted from the UER aquifer.

3.5 CULTIVATION IN THE STUDY AREA

The wells drilled in the UER aquifer extract water for the use of irrigation. Several crops are cultivated in the fields. These include wheat, barley, alf-alf, and rhodas. The land owned by SHADCO is representative of the type of land in Saudi Arabia. Sand is 90% of the soil's constituents. Therefore, frequent irrigation is needed to overcome the low water-retaining property of sand. Organic contents of the soil are very low increasing the demand on fertilizers. Preseason irrigation has been used to encourage the growth of seeds which are helpful in increasing the

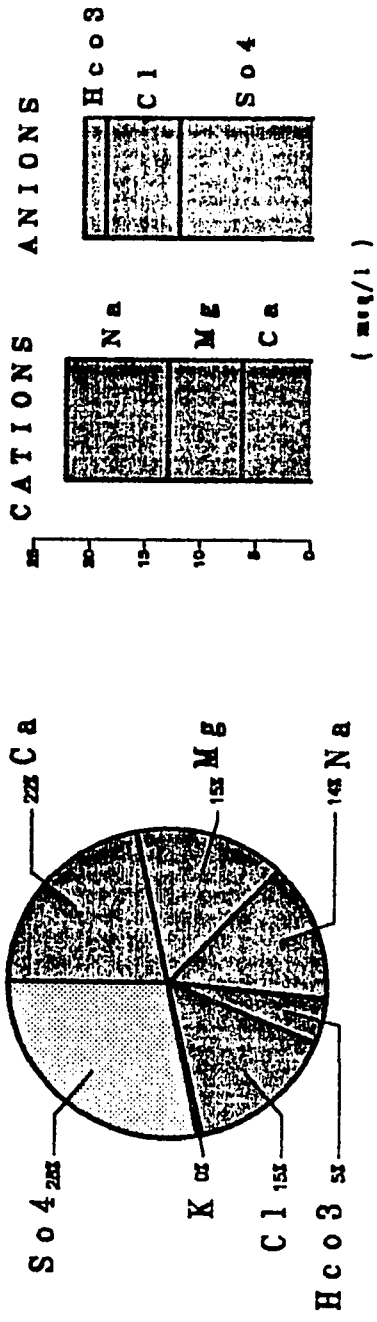


Figure (3.7) Chemical Analysis of Groundwater

organic contents of the soil. The irrigation routine starts early November for barley and wheat. The harvest is early April. Alfalf is irrigated continuously throughout the year. Rhodas is irrigated for the whole year except in December, January and February. The irrigation practice is almost the same in all fields. Crops receive water 24 hours aday at the rate of 1000-1800 gallons per minute. The field F2 is used to grow vegetables that require little water. The three fields B1, F3 and I4 have not been cultivated. They are mainly used to monitor water levels. Table (3.3) lists the crops grown in the fields since 1984. It is noted that the amount of water used for irrigating the crops is independent of the type of crop. The discharge rates are all equal. The percentage of each crop cultivated in the area is shown in Fig. (3.8).

3.6 GEOLOGY

3.6.1 General

The following discussion is extracted from a report by Italconsult (1969) where the geology of area IV in the Eastern Province of Saudi Arabia was studied. The area is located between 24° 00' to 28° 00' N and longitude of 48° 00' to 51° 00' E.

The stratigraphic sequence outcropping in area IV of Saudi Arabia ranges from Cretaceous to Quaternary and Recent. On the whole, the entire sedimentary succession consists of an

Table 3.3: Crops Grown In The Fields Since 1984

Field/ Season	1984-85	1985/86	1986-87	1987/88	1988/89	1989/90	1990/91
A2	---	---	---	---	---	---	---
A3	---	---	---	R	R	R	B
A4	---	---	---	R	R	R	B
A5	---	---	---	B	R	R	B
A6	---	---	---	B	B	B	B
A7	---	---	A	A	B	B	B
A8	---	---	B	B	B	B	B
A9	---	---	W	W	W	W	W
B1	---	---	---	---	---	---	---
B2	---	---	---	R	R	R	R
B3	---	---	---	R	R	R	B
B4	---	---	---	R	R	R	R
B5	---	---	---	B	R	R	B
B6	---	---	A	A	B	B	B
B7	---	---	A	A	B	B	B
B8	---	---	---	B	B	B	B
B9	---	---	W	W	W	W	W
C1	---	---	---	---	---	---	---
C2	---	---	---	R	R	R	R
C3	---	---	---	R	R	R	B
C4	---	---	---	R	R	R	R
C5	---	---	---	R	R	R	B
C6	---	---	---	B	B	B	B
C7	---	---	---	W	W	B	B
C8	---	---	B	B	B	B	B
C9	---	---	W	W	W	W	W
D3	---	W	W	W	W	A	A
D4	---	W	W	W	W	W	W
D5	---	W	W	W	W	W	W
D6	---	A	A	R	R	R	B
D7	---	R	R	R	R	R	B
D8	---	W	W	W	W	W	W
D9	---	---	W	W	W	W	W
E3	---	W	W	W	W	W	W
E4	---	W	W	B	B	B	B
E5	---	W	W	W	W	W	W
E6	---	W	W	W	W	W	W
E7	---	W	W	W	W	W	W
E8	---	W	W	W	W	W	W
E9	---	---	W	W	W	W	W

W: Wheat
 B: Barley
 A: Alf-Alf
 R: Rhodus

(Contd.)

Field/ Season	1984-85	1985/86	1986-87	1987/88	1988/89	1989/90	1990/91
F1	W	W	W	A	B	B	B
F2	-----GREEN HOUSE-----						
F3	---	---	---	---	---	---	---
F4	---	---	---	B	B	B	B
F5	---	---	---	B	B	B	B
F6	---	W	W	W	W	W	W
F7	---	---	---	---	---	---	---
F8	---	---	W	W	W	W	W
F9	---	---	W	W	A	A	A
G1	---	W	W	A	B	B	B
G2	---	---	A	A	B	B	B
G3	---	---	---	---	---	---	---
G4	---	W	W	A	W	W	W
G5	---	---	B	B	B	B	B
G6	---	W	W	W	W	W	W
G7	---	W	W	W	W	W	W
G8	---	W	W	W	W	W	W
G9	---	---	B	B	B	B	B
H1	W	W	W	A	B	B	B
H2	---	W	W	W	A	A	A
H3	---	---	---	A	B	B	B
H4	---	---	---	B	B	B	B
H5	---	W	W	W	W	W	W
H6	---	W	W	W	W	W	W
H7	---	W	W	W	W	W	W
H8	---	---	---	---	---	---	---
H9	---	---	B	B	B	B	B
I4	---	---	---	---	---	---	---
I5	---	W	W	W	W	W	B
I6	---	W	W	W	W	W	B
I7	---	W	W	W	W	W	B
I8	---	---	W	W	W	W	B
I9	---	---	B	B	B	B	B
AA-8	---	---	B	B	B	---	---
AA-9	---	---	W	W	W	W	W

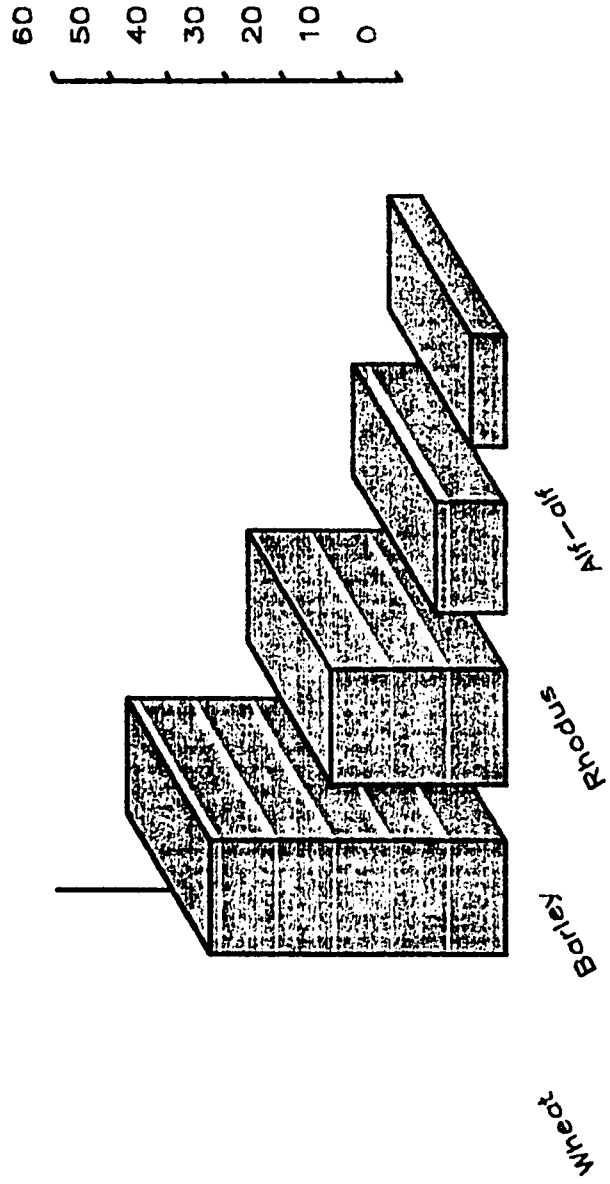


Figure (3.8) Percentage of Crops Grown in Fields

alternation of marine and continental phases which may be subdivided into three sedimentary cycles. The first cycle is represented by Al-Wasia which outcrops in a belt running along the edge of the Arabian Shield. This consists mainly of a sequence of sandstones of continental environment alternating in the upper part with fine clastics of transitional and marine environment. The second cycle starts with the Wasia-Aruma unconformity and is mainly represented by marine carbonate sequence with the intercalation of fine clastics and evaporites which are particularly well developed and frequent in the upper part of the Paleocene and lower Eocene. The third cycle, represented by a Miocene-Quaternary series that unconformably overlies Cretaceous and Eocene formations, is mainly formed by continental clastics with marine and transitional deposits interbedded in the lower and middle part. The lithographic sequence and the relationships between the various formations are shown schematically in Fig. (3.9). On the basis of the water-bearing properties of the various lithologic units, the entire succession has been divided into aquifers and aquicludes. From the regional point of view, except for the local facies variations, the major water-bearing units of the area are the sandstones of the Wasia formation, the limestones of the Aruma formation, the limestones and dolomites of the UER formation, the limestones and dolomites of the Khobar and Alat member, the clastics of the Neogene complex and the limestones of the Dammam formation. The aquicludes are represented by the shales and marls of the upper

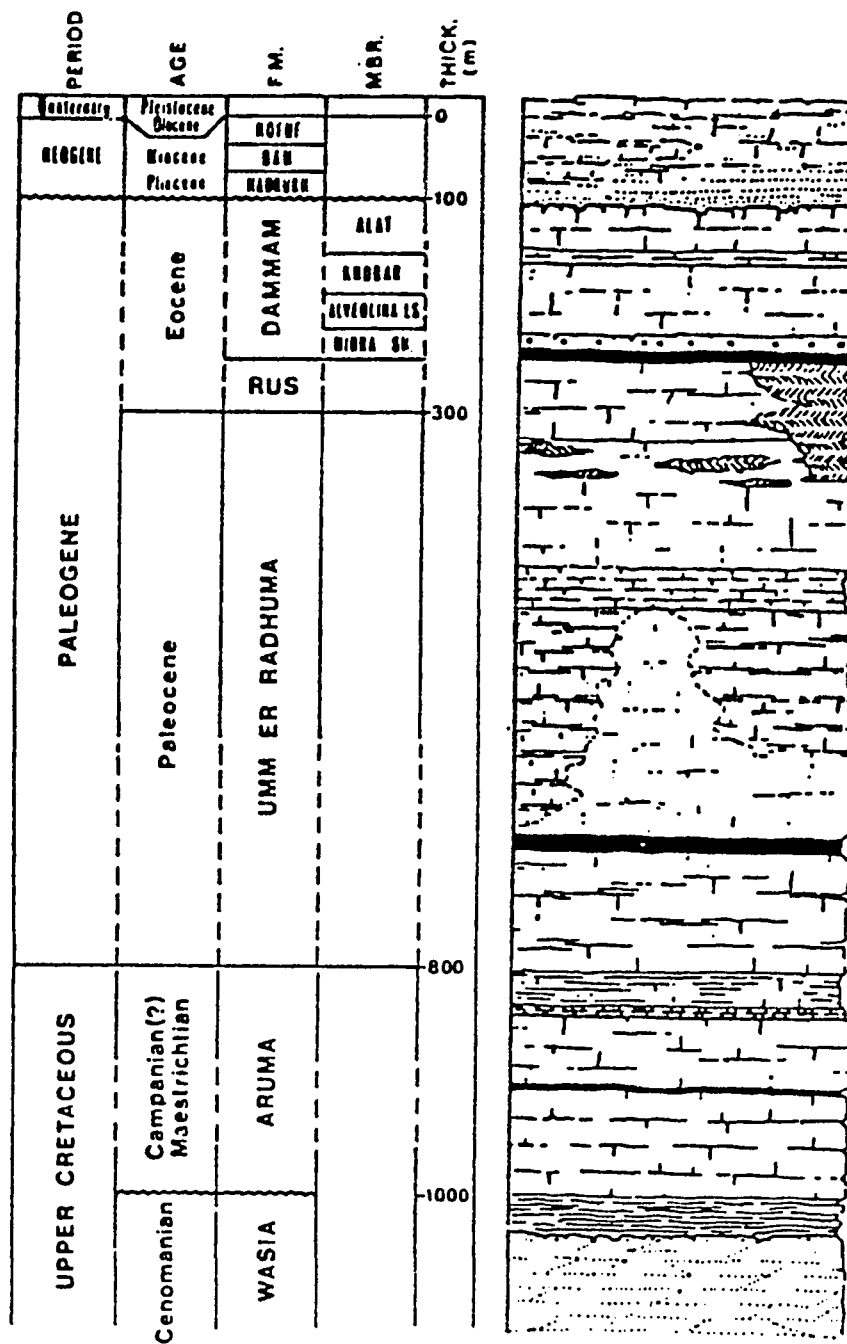


Fig. 3.9: Lithostratigraphic Generalized Sequence of Area IV (after Italconsult 1969).

part of the Wasia formation, the varicolored shales and marls of the top of the Aruma, the fine clastics and evaporites of the Rus formation and Midra and Salla shale at the top of the UER aquifer, the marls and shales (orange marls) of the base of the Alat member, and the shales of the Hadruk formation and marks of the Damman formation, Fig. (3.9).

3.6.2 Umm er Radhuma (UER)

The UER formation overlies the Aruma formation without any apparent break in the sedimentation. UER is bounded at the bottom by the marls and varicolored shale of the upper unit of the Aruma formation and at the top by the soft chalky limestones of the Rus formation.

The analysis of the well logs in SHADCO area reveals the characteristics of the geology of the area. Fig. (3.10) shows a section running north to south along the C-wells. It can be clearly noted that limestone and dolomite are the main constituents of UER formation. Except for the UER aquifer, it is extremely difficult to indicate the boundaries of the other aquifers. The sequence of the rocks are quite variable due to the large area (90 square kilometers) covered by the project. A sequence, however, may be noted. Sand and sandstones constitute the upper part of the columns. Limestone followed by clay is common beneath the

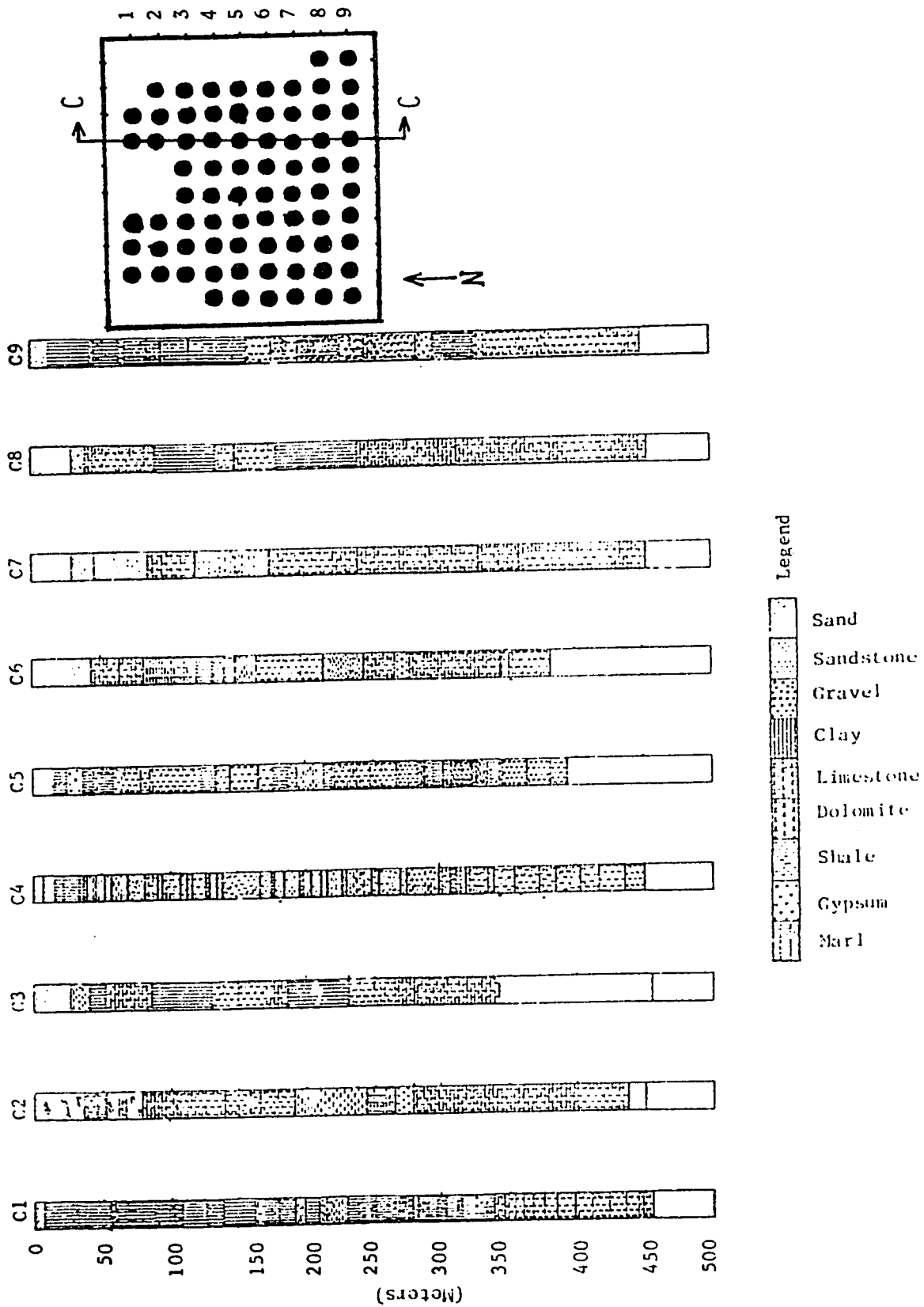


Fig. 3.10: A Lithostratigraphic section along the C-wells in the study area.

sandstones. Marl appears next which overlays the main constituents of the Khobar and UER aquifer namely; limestone and dolomite.

The variability and inconsistency of the formation sequence may also be due to the fact that the wells were drilled by several contractors. Therefore, the number of the specimens taken for testing from the logs and the judgement of the analyst may be of considerable variability. This becomes more affirmative by comparing the logs of the wells C4 and C9 which were drilled by the same contractor to the log of the well C7 which was drilled by a different contractor.

3.7 HYDROGEOLOGY

The lithostratigraphic units discussed earlier have been divided on the basis of their water-bearing properties. The following is a brief discussion on each unit extracted from Italconsult (1969). Except for the UER aquifer, none of the aquifers are investigated in this study.

3.7.1 Wasia Aquifer

The Wasia aquifer productivity was investigated by three companies. Italconsult drilled a well from which a transmissivity value of 10^{-5} square meters per second was reported. Aramco

reported the highest transmissivity value of this aquifer (0.2 square meters per second). Astals Company reported a transmissivity of $5 * 10^{-3}$ meters square per day. It is believed that the high costs, due to the depth of the aquifer, limits its use as an aquifer with a high potential productivity.

3.7.2 Aruma Aquifer

This aquifer is of limited importance. The low transmissivity values obtained from the pumping tests performed on the wells drilled in this aquifer (close to zero) suggests an aquiclude type of behavior.

3.7.3 Umm er Raduma Aquifer

The Umm er Raduma aquifer is the most important of the aquifers that can be exploited in the Eastern Province of Saudi Arabia. Many wells have been drilled by Aramco in the UER aquifer in order to insure water supplies to the Dhahran and Abqaiq centers. Italconsult (1969) has drilled and tested five wells in this aquifer. Italconsult reports very high transmissivities of the aquifer ranging from 10,000 to 30,000 square meters per day. All studies conducted on the aquifer have shown that the UER aquifer has the highest potential of the post-Cretaceous aquifers. Storativities computed by Italconsult range from 0.015 to 0.0005 indicating the large variability in the aquifer's parameters. The top of

the UER aquifer map shows the general dip of the aquifer towards northeast, Figs. (3.11, 3.11-1). The depth from the ground surface to the top of the aquifer is also shown in Fig. (3.12). The depth to the top of the aquifer ranges from 330 to 355 meters. Quantitative tests have been performed in the area. These tests are discussed in details in Chapter 3.

3.7.4 Khobar Aquifer

Many wells have been drilled in this aquifer. High transmissivity values ranging from 0.009 to 0.29 square meters per second were reported near the Qatif oasis. In Al-Hassa area, tests gave low transmissivity values ranging from a minimum of $5.7 * 10^{-6}$ square meters per second to a maximum of $5 * 10^{-4}$ square meters per second. On the island of Bahrain, the aquifer gave transmissivities between 0.014 to 0.072 square meters per second. It is obvious that this aquifer has very variable transmissivity from place to place.

3.7.5 Alat Aquifer

This aquifer is of no interest to irrigation. Many wells were drilled in this aquifer by Aramco. Other wells were hand-dug. Most of the wells are used for providing drinking water supplies. The transmissivity values ranged from $3.1 * 10^{-4}$ to a maximum of 0.079 square meters per second.

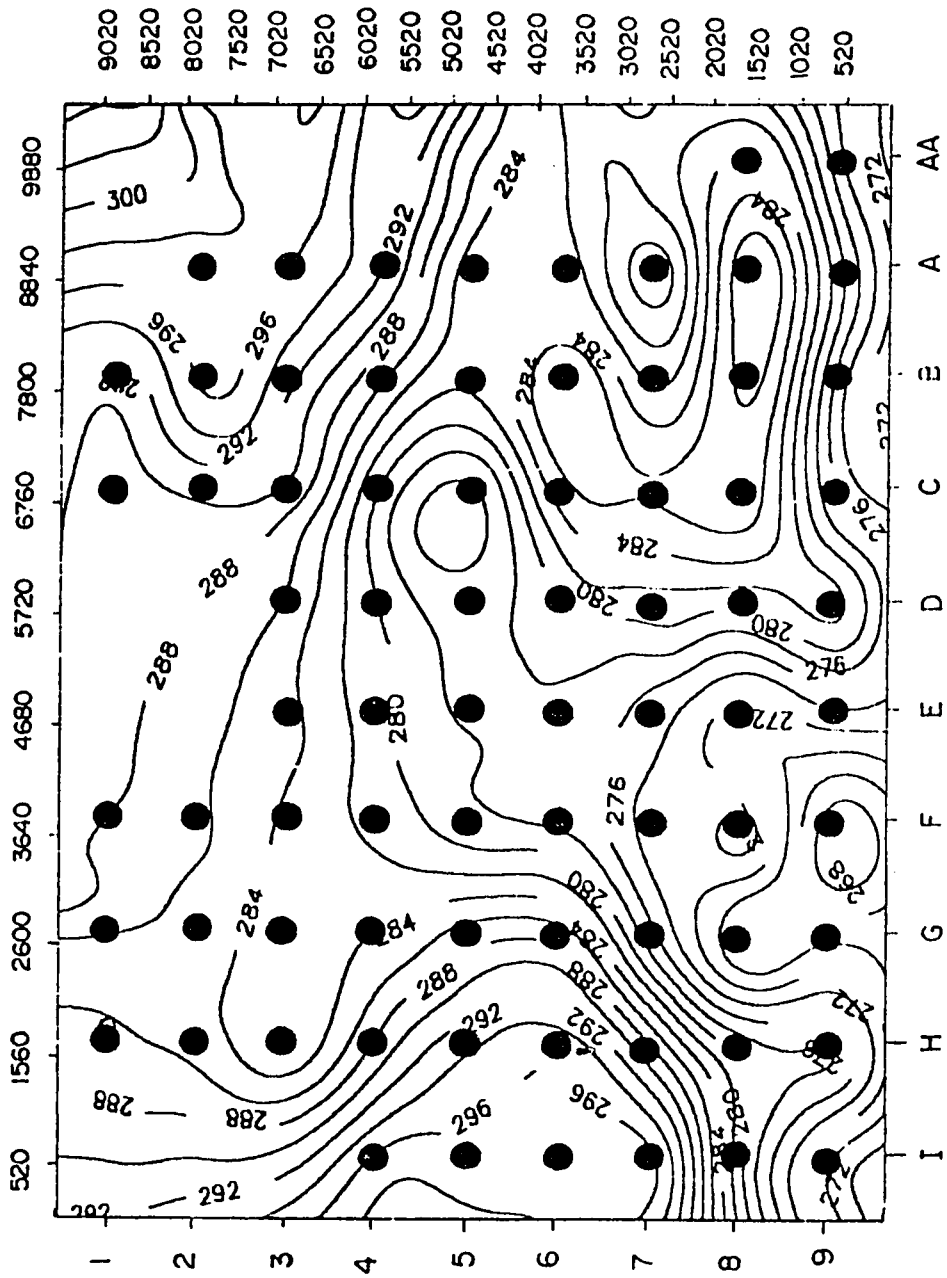


Fig. 3.11: - Contour map of top of the UER aquifer;
 - All values are below MSL. (meters)
 ● Wells



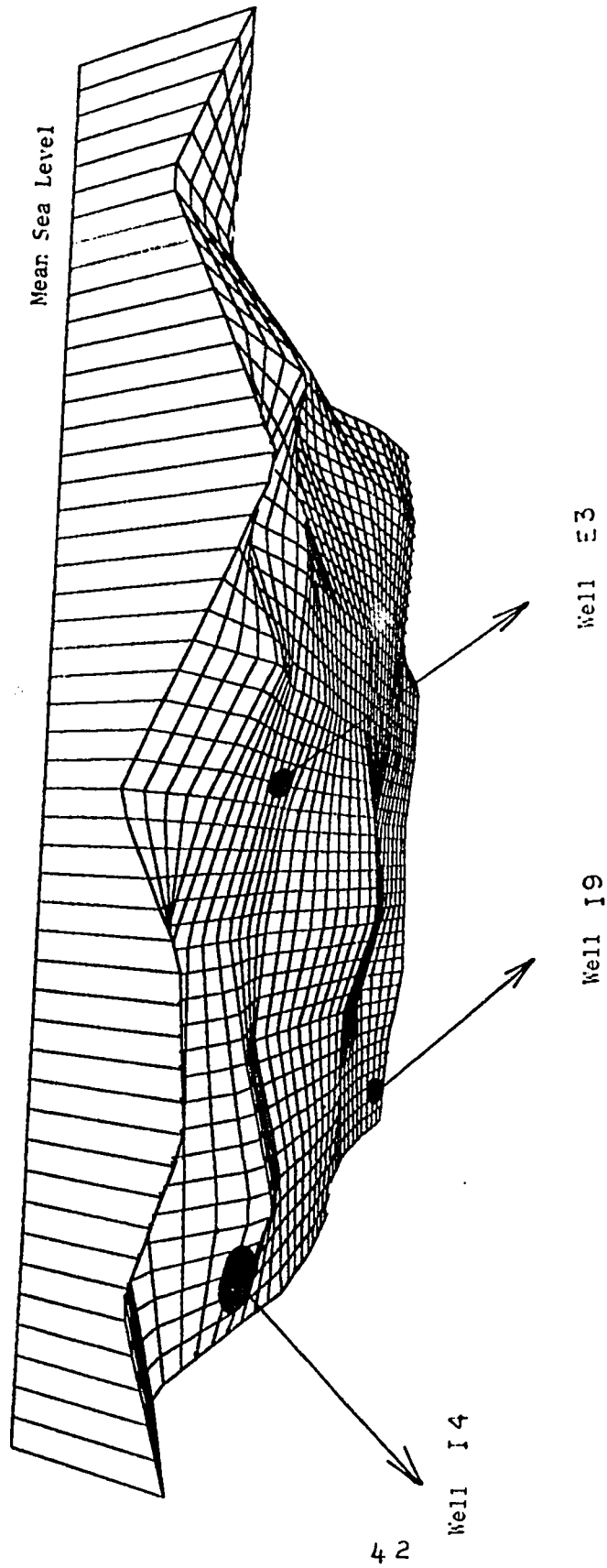


Fig. 3.11-1: Three-dimensional plot of top of the UER aquifer.

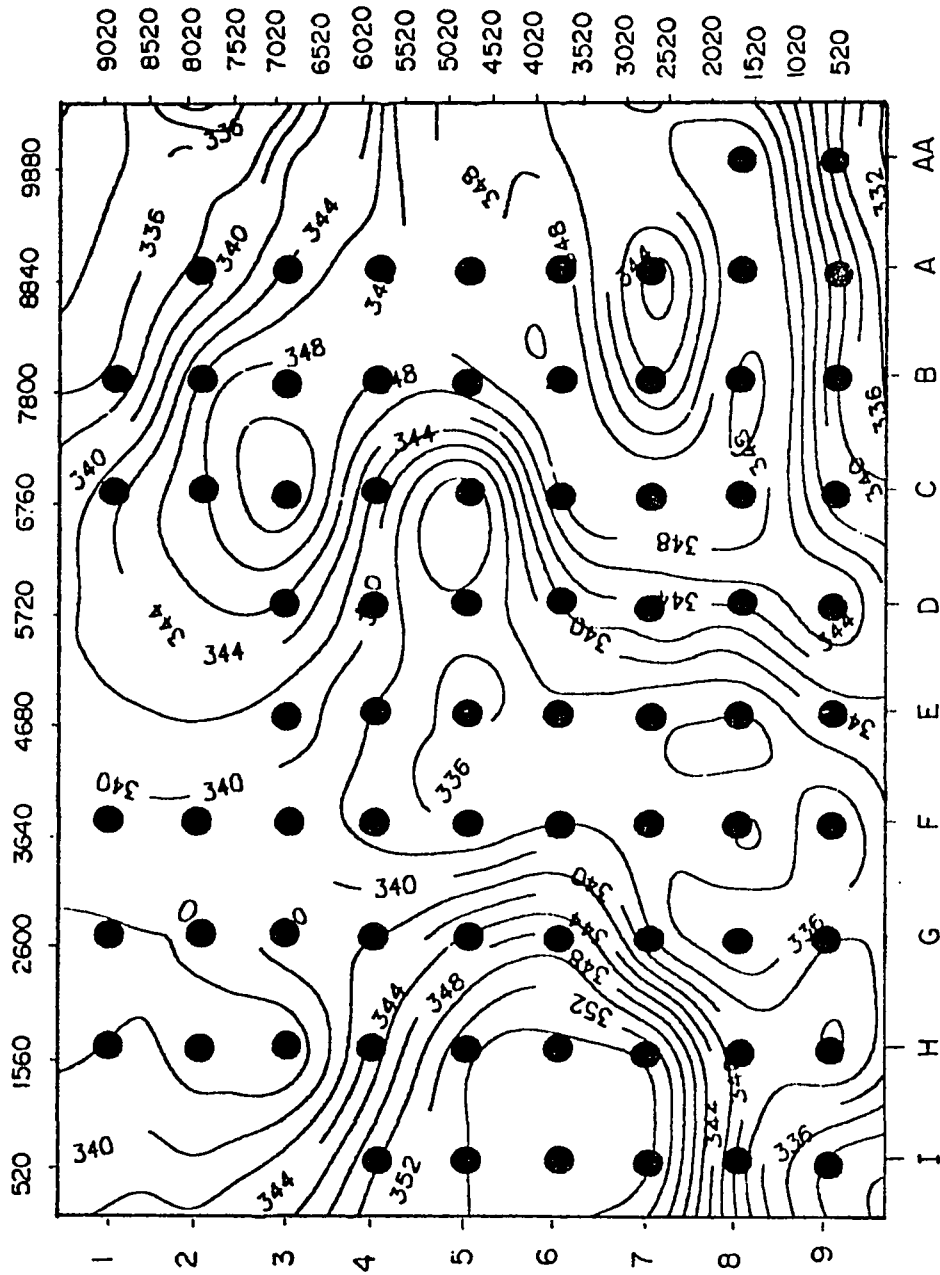


Fig. 3.12: Depth to the top of the UER aquifer (meters)

● Wells

3.7.6 Neogene Aquifer

This aquifer is not productive except in Al-Hassa where most of the springs and wells supply irrigation water to the largest oasis in Saudi Arabia. Transmissivity ranged from $5 * 10^{-5}$ to a larger value of 0.2 square meters per second.

Chapter 4

MODELING TECHNIQUE

4.1 INTRODUCTION

4.1.1 Flow Equation of Flow Through Porous Media

The most general groundwater flow equation is derived by combining the continuity equation and the flux equation prescribed by Darcy's equation. Darcy's equation can be expressed as:

$$\bar{q} = -\bar{K} \cdot \nabla h \quad (4.1)$$

where:

q = is the volume of water passing per unit time per unit cross-sectional area.

K = is the proportionality constant called the hydraulic conductivity (in the most general form, it is a second rank tensor).

h = is the hydraulic head

The hydraulic head is a combination of gravitational head and pressure head. With the assumption that the hydraulic conductivity tensor is symmetric and that the axes can be rotated such that off-diagonal terms in the tensor are zero, equation (4.1) reduces to:

$$q_x = -K_{xx} \frac{\partial h}{\partial x} \quad (4.2)$$

with the other y , z components similar.

The continuity equation is reached at by means of mass balance in a small volume element in a porous media over a small time interval. It can be expressed as:

$$-\frac{\partial (\rho q_x)}{\partial x} - \frac{\partial (\rho q_y)}{\partial y} - \frac{\partial (\rho q_z)}{\partial z} + R = \frac{\partial (\phi \rho)}{\partial t} \quad (4.3)$$

where:

R = is the volumetric injection rate

ϕ = is the porosity

t = is time

The time derivative can be related to the hydraulic head (Jacob 1950). With the assumption that water is incompressible, combining the continuity equation with the flux equation, we get the most general groundwater flow equation expressed as:

$$\frac{\partial (K_{xx} \frac{\partial h}{\partial x})}{\partial x} + \frac{\partial (K_{yy} \frac{\partial h}{\partial y})}{\partial y} + \frac{\partial (K_{zz} \frac{\partial h}{\partial z})}{\partial z} + R = S_s \frac{\partial h}{\partial t} \quad (4.4)$$

where:

S_g = is the specific storage for confined aquifers.

4.1.2 The Finite Difference Technique

Equation 4.4 is a boundary value problem, which except for few limited situations having analytical solutions, requires approximate solutions. One such approach is the finite difference technique. The technique provides a rationale for operating on the differential equation 4.6 and for transforming it into a set of algebraic equations. The finite difference technique, as a typical numerical technique, yields values for only a predetermined, finite number of points in the problem domain. For simplicity, two-dimensional plane flow is used rather than the three-dimensional. This is due to the lack of head readings along the vertical direction. Usually a grid system similar to that shown in Figure (4.1) is overlain on a map view of the aquifer. Two types of grids are commonly used: mesh-centered, and block-centered. The block-centered grid is advantageous where the flow is specified on the boundary.

A function $y = f(x)$ whose values and derivatives are continuous in the vicinity of a point 'a' may be expanded around point 'a' by Taylor's series:

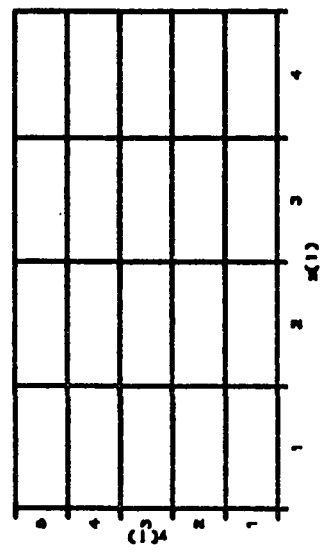
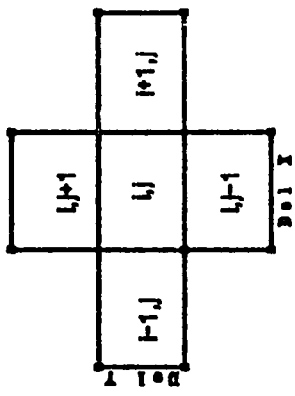


Figure (4.1) Typical Block-Centered Mesh

$$f(x) = \sum_{n=0}^{\infty} \frac{f^{(n)}(a)}{n!} (x - a)^n \quad (4.5)$$

where:

$f^{(n)}(a)$ = is the nth derivative evaluated at point a.

From Figure 4.2, the Taylor's series expansion of $f(x)$ becomes:

$$\begin{aligned} f(x_2 + \Delta x) = & f(x_2) + \frac{f'(x_2)}{1!} \Delta x + \frac{f''(x_2)}{2!} (\Delta x)^2 \\ & + \dots + \frac{f^{(n)}(x_2)}{n!} (\Delta x)^n + \dots \end{aligned} \quad (4.6)$$

where:

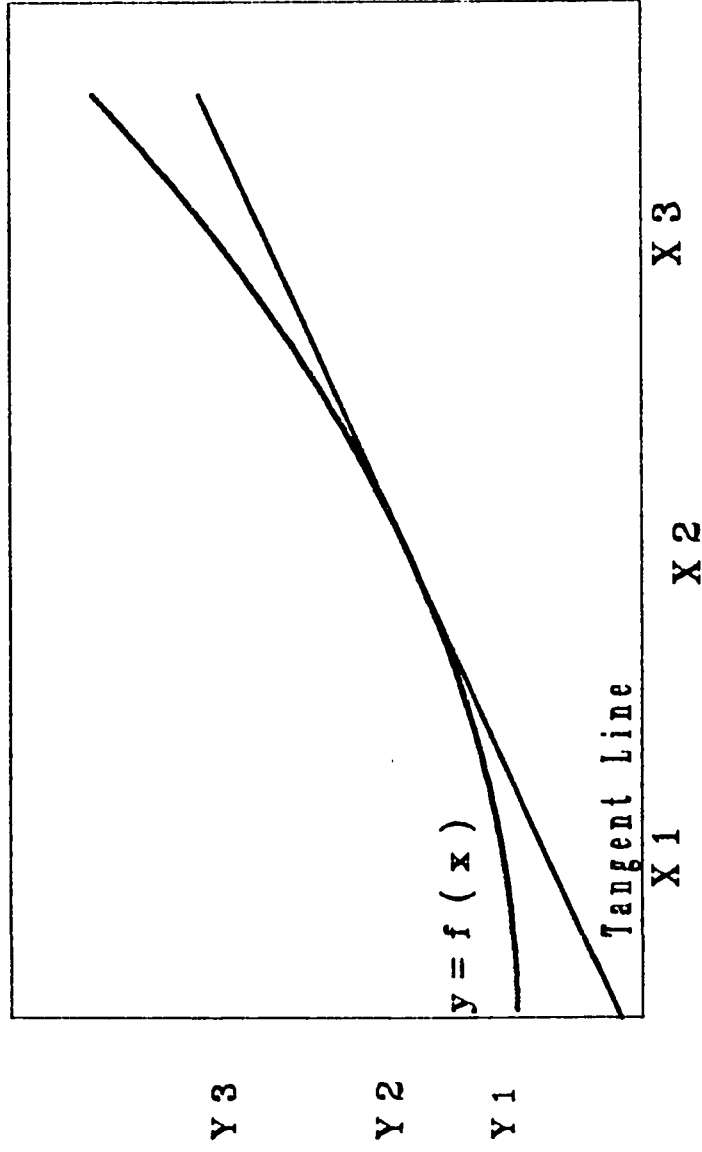
$$x_2 + \Delta x = x_3$$

$$f(x_2 + \Delta x) = y_3$$

Therefore, the forward difference gives,

$$y_3 = y_2 + f'(x_2) \Delta x + \frac{f''(x_2) (\Delta x)^2}{2!} + \dots \quad (4.7)$$

Considering Figure (4.2) again, x can be treated in a backward direction. Letting $x = x_2 - \Delta x$, equation 4.5 becomes:



Figure(4.2) The Derivative of a Function

$$\begin{aligned}
 f(x_2 - \Delta x) = f(x_2) - \frac{f'(x_2)}{1!} \Delta x + \frac{f''(x_2) (\Delta x)^2}{2!} \\
 - \dots \pm \frac{f^{(n)}(x_2) (\Delta x)^n}{n!} \pm \dots
 \end{aligned}
 \tag{4.8}$$

where:

$$x_1 = x_2 - \Delta x$$

$$f(x_2 - \Delta x) = y_1$$

Therefore, the backward difference gives,

$$\begin{aligned}
 y_1 = y_2 - f'(x_2) \Delta x + \frac{f''(x_2)}{2!} (\Delta x)^2 - \dots \\
 \pm \frac{f^{(n)}(x_2)}{2!} (\Delta x)^n \pm
 \end{aligned}
 \tag{4.9}$$

By subtracting equation 4.9 from equation 4.7, an improved analog for the first derivative may be obtained:

$$y_3 - y_1 = 2f'(x_2) (\Delta x) + 2 \frac{f'''(x_2)}{3!} (\Delta x)^3 + \dots$$

Solving for the first derivative gives:

$$f'(x_2) = \frac{y_3 - y_1}{2\Delta x} - \frac{f'''(x_2)}{3!} (\Delta x)^2 - \dots \tag{4.10}$$

Truncating all higher derivatives yields the central finite difference analog for the first derivative at x_2 :

$$f'(x_2) = \frac{y_3 - y_1}{2\Delta x} - O(\Delta x)^2 \quad (4.11)$$

The x-derivative at node (1,j) (Figure 4.1) in terms of the mid-points and a spacing of $\frac{1}{2} \Delta x_1$ can be expressed as:

$$\frac{\partial h}{\partial x} \Big|_{1,j} = \frac{h_{1, \frac{1}{2}, j} - h_{1, \frac{3}{2}, j}}{\Delta x_1} - O(\Delta x)^2 \quad (4.12)$$

Equation 4.4 can be rewritten in two-dimensions as:

$$\frac{\partial \left(T_{xx} \frac{\partial h}{\partial x} \right)}{\partial x} + \frac{\partial \left(T_{yy} \frac{\partial h}{\partial y} \right)}{\partial y} + W = S \frac{\partial h}{\partial t} \quad (4.13)$$

where:

T = is the transmissivity

S = is the storage coefficient

Equation 4.12 can be used to evaluate the first term in equation 4.13:

$$\frac{\partial \left(T_{xx} \frac{\partial h}{\partial x} \right)}{\partial x} = \frac{1}{\Delta x_1} \left\{ \left(T_{xx} \frac{\partial h}{\partial x} \right)_{1, \frac{1}{2}, j} - \left(T_{xx} \frac{\partial h}{\partial x} \right)_{1, \frac{3}{2}, j} \right\} \quad (4.14)$$

The first derivatives on the right side of equation 4.14 can be evaluated using equation 4.12. Therefore:

$$\begin{aligned} \frac{\partial(T_{xx} \frac{\partial h}{\partial x})}{\partial x} &= \frac{1}{\Delta x_1} \left\{ T_{xx_{1, \frac{1}{2}, j}} \frac{(h_{1,1,j} - h_{1,j})}{\Delta x_{1, \frac{1}{2}}} \right. \\ &\quad \left. - T_{xx_{1, \frac{1}{2}, j}} \frac{(h_{1,j} - h_{1-1,j})}{\Delta x_{1, \frac{1}{2}}} \right\} \end{aligned} \quad (4.15)$$

The y-derivative is similarly analyzed to give:

$$\begin{aligned} \frac{\partial(T_{yy} \frac{\partial h}{\partial y})}{\partial y} &= \frac{1}{\Delta y_j} \left\{ (T_{yy_{1,j, \frac{1}{2}}} \frac{(h_{1,j+1} - h_{1,j})}{\Delta y_{j, \frac{1}{2}}} \right. \\ &\quad \left. - T_{yy_{1,j, \frac{1}{2}}} \frac{(h_{1,j} - h_{1,j+1})}{\Delta y_{j, \frac{1}{2}}} \right\} \end{aligned} \quad (4.16)$$

Using a backward difference in evaluating the time derivative:

$$\frac{\partial h}{\partial t} = \frac{h_{1,j}^n - h_{1,j}^{n-1}}{\Delta t} \quad (4.17)$$

where:

n = is the time level.

Combining equation 4.17 with equations 4.16 and 4.15 yields:

$$\begin{aligned}
& \frac{1}{\Delta x_1} \left\{ T_{xx_{1, \frac{1}{2}, j}} \frac{(h_{i+1, j}^n - h_{i, j}^n)}{\Delta x_{1, \frac{1}{2}}} - T_{xx_{1, \frac{1}{2}, j}} \frac{(h_{i, j}^n - h_{i-1, j}^n)}{\Delta x_{1, \frac{1}{2}}} \right\} \\
& + \frac{1}{\Delta y_j} \left\{ T_{yy_{1, j, \frac{1}{2}}} \frac{(h_{i, j, 1}^n - h_{i, j}^n)}{\Delta y_{j, \frac{1}{2}}} - T_{yy_{1, j, \frac{1}{2}}} \frac{(h_{i, j}^n - h_{i, j-1}^n)}{\Delta y_{j, \frac{1}{2}}} \right\} \\
& + W^n \approx S_{i, j} \frac{h_{i, j}^n - h_{i, j}^{n-1}}{\Delta t} \tag{4.18}
\end{aligned}$$

Equation 4.18 represents an algebraic equation which can be evaluated at each node. Solving the algebraic equations simultaneously using any of the techniques yields values of head at the predetermined nodes.

4.1.3 The U.S.G.S. Model

The United States Geological Survey (U.S.G.S) developed a model for groundwater flow which successfully replaced its widely used predecessors USGS2D (Trescott, Pinder and Larson, 1976) and USGS3D (Trescott, 1975). The new code may be used for either two or quasi three-dimensional applications. The new model is simple to use and maintain and can be executed on a variety of computers with minimal changes. The program is written in Fortran 66 and can be run on any Fortran 77 compilers. The program is efficient with respect to computer memory and execution time

because it utilizes modular structure wherein similar programming functions are grouped together. Specific computational and hydrological options are constructed in such a way that each option is independent of the others. The model program is divided into a main program and a series of highly independent subroutines called modules. The modules are grouped into packages that deal with single aspects of simulation. The main program controls the order in which the modules are executed and serves as a switching system for information. The main program does not interfere in the finite difference equation but regulates the work of other packages which add specified terms to the finite difference equation. Packages which are completely independent of each other can be added or removed without affecting other packages. The model contains the following packages:

1. The BASIC package discretizes space and time into cells and time steps. It specifies the initial and boundary conditions and heads at the beginning and end of time steps. The package specifies the program options to be used and controls the output results. It also gives a summary of the volumetric budget.
2. The WELL package simulates recharging and discharging wells.
3. The DRAIN package simulates leakage of an aquifer through a barred drain.

4. The RIVER package simulates infiltration of water through river beds.
5. The GENERAL HEAD BOUNDARY (GHB) package simulates special types of boundaries other than those simulated by the BASIC package.
6. The RECHARGE package simulates areal recharge from either surface waters or rainfall.
7. The EVAPOTRANSPIRATION (ET) package simulates evaporation and transpiration of both surface and subsurface waters.
8. The BLOCK CENTERED FLOW (BCF) package computes the conductance components of the finite difference equation which determines flow between adjacent cells. It also computes the terms that represent the rate of movement of water to and from storage.
9. The STRONGLY IMPLICIT PROCEDURE (SIP) package solves the set of equations to a predetermined accuracy.
10. The SUCCESSIVE OVER RELAXATION (SOR) package is an alternative package to solve the set of equations.

The model output usually consists of heads at various cells, and a volumetric budget. A more detailed output can be obtained by using the output control option.

The model has gained respect through its ability to simulate groundwater flow in all known aquifers. Flow can be simulated both at steady and at transient states. The model has a history of high confidence. The approach taken by McDonald and Harbaugh (1984) makes use of physical concepts regarding the flow system rather than sophisticated calculus techniques.

4.2 INPUT VARIABLES

4.2.1 Transmissivity

Transmissivity of the UER aquifer has been tested by Italconsult (1969) and GDC (1980). The values obtained cover a long range which indicates the variability of the transmissivity in this aquifer. Therefore, the findings of the previous studies can not be extended to this study.

Pumping tests have been conducted on the 75 wells in the study area. No knowledge of how these tests were conducted is available. The data from pumping tests have been analysed using two techniques namely; Jacob Straight Line Method, and the Recovery Method.

The Jacob straight line technique assumes that higher order terms of the infinite series of the well function become very small, and the non-equilibrium equation formula could be approxi-

mated by:

$$h_o - h = \frac{2.3Q}{4\pi T} \log \left(\frac{2.25 Tt}{Sr^2} \right) \quad (4.19)$$

where:

$h_o - h$ = is the drawdown

Q = is the discharge rate

T = is the transmissivity

t = is the time since pumping began

r = is the distance from the observation well to the pumping well

S = is the aquifer storativity

When plotting the equation on a semi-log paper with consistent units for the parameters, the value of transmissivity may be found from the equation:

$$T = \frac{2.3 Q}{4\pi \Delta(h_o - h)} \quad (4.20)$$

where

$\Delta(h_o - h)$ = is the drawdown per log cycle of time.

The graphs of the Jacob straight line pumping tests are presented in Appendix A-1.

The recovery test is used when turbulence in wells makes it difficult to record drawdowns accurately. The test is started by a constant discharge rate for some time. The pumping is then suddenly stopped allowing the water level in the well to recover. Drawdowns in the recovery stage are recorded. Figure (4.3) shows the graphical representation of the test. The discharging rate is assumed to continue to a time interval equal to the discharging time interval. A hypothetical recharging rate, equal to the discharge rate, is assumed to start at the time where the discharging process stopped. From the Jacob straight line formula:

$$s_1 = \frac{2.3Q}{4\pi T} \log \left(\frac{2.25 Tt}{Sr^2} \right) \quad (4.21)$$

where:

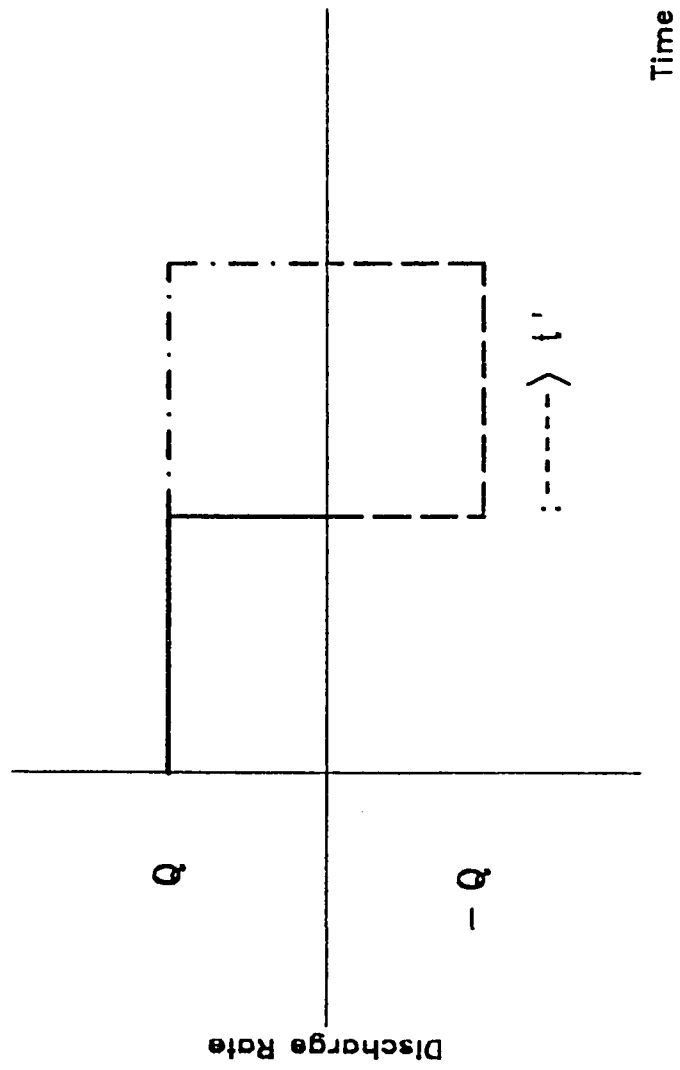
t = represents any time in the whole process

s_1 = is the drawdown due to the discharging effect

The recharging effect can be formulated as:

$$s_2 = \frac{2.3Q}{4\pi T} \log \left(\frac{2.25 Tt'}{Sr^2} \right) \quad (4.22)$$

where:



Figure(4.3) Schematic Diagram of Recovery Test

s_2 = is the drawdown due to the recharging effect

t' = time since pumping stopped

The actual drawdown is found by the superposition principle:

$$s = s_1 + s_2 = \frac{2.3Q}{4\pi T} \log \frac{t}{t'} \quad (4.23)$$

If equation 4.23 is plotted on a semi-log graph paper, the transmissivity can be computed as:

$$T = \frac{2.3 Q}{4\pi \Delta s} \quad (4.24)$$

where:

Δs = the drawdown per log cycle of t/t' .

Appendix A-2 contains the recovery pumping tests graphs.

Because the tests ,both Jacob straight line and the recovery, are of short durations (two-three days), they are subject to criticism. The discharging rates are low resulting in low observable drawdowns. Upon investigating the graphs in Appendix A, it is noted that, except for few tests, the data do not follow any of the known behavior of wells. Negative drawdowns are sometimes observed upon pumping!. Sudden increases in drawdown values are observed (Well No. B2). This kind of behavior may be due to the clogging of the well screen which creates pressure on the out-

side of the screen until a point where the high pressure washes out the clogging rock fragments resulting in sudden increases in heads or negative drawdowns. Another reason can be the behavior of the geological formation itself. Along its path, water may be exposed to different degrees of resistance resulting in flow retardation followed by an easy flow. This may explain the sudden drops in heads observed at well B2. Since these values are going to be calibrated, the values obtained from pumping tests become less important, Figure (4.4). The values from pumping tests range from as low as 700 square meters per day to as high as 30,000 square meters per day. This indicates the large variability of the transmissivity in this area. It is noted that the UER aquifer has very high transmissivity values validating the reasons why it is heavily used.

4.2.2 Storativity

The uncertainty of the transmissivity values obtained from pumping tests, makes it more difficult to rely on these tests to determine the storativity values at each cell of the model. Storativity values determined by Italconsult (1969) were in the range of 3.0×10^{-4} to 5.0×10^{-4} . Rasheduddin, et.al., (1989) calibrated these values in an area located southeast of the study area. A constant value of 4.0×10^{-4} was reached at for more than 90 percent of the cells in the area of 9400 square kilometers! The stora-

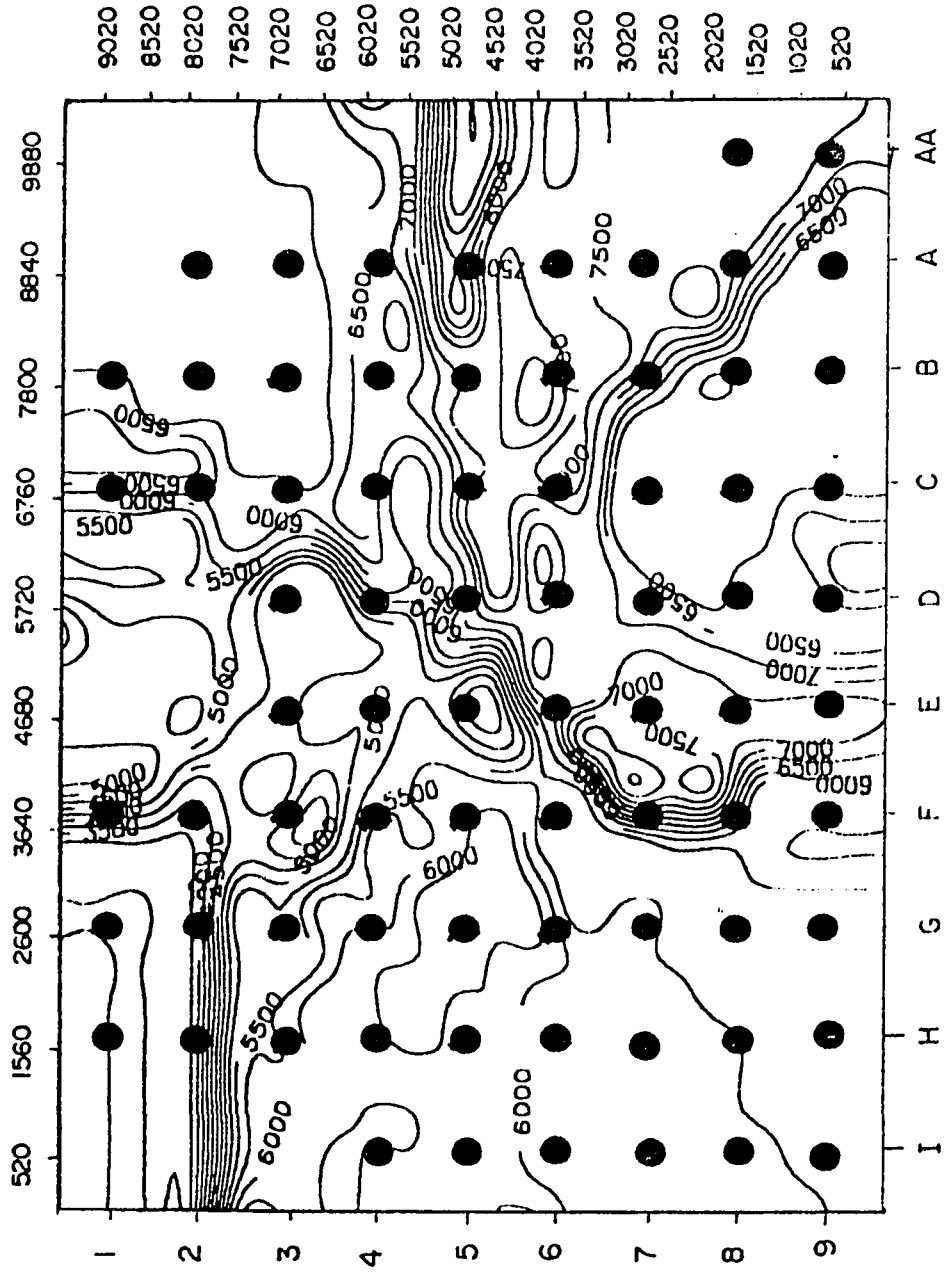


Fig. 4.4: Spatial distribution of transmissivity values obtained from pumping tests (square meters per day).
 ● Wells

↑ N

tivity values can be computed from pumping tests by the equation:

$$S = \frac{2.25 T t_o}{r^2} \quad (4.25)$$

where:

S = is the storativity

T = is the transmissivity

t_o = is the time at zero drawdown

r = is the radius of the well or the distance from the observation well to the discharging well.

The tests gave unrealistic results. Some tests gave values more than 60 whereas others gave values of as low as 1×10^{-6} . It is obvious that these values can not be used in this study. Therefore, the values calibrated by Rasheeduddin are going to be used during simulation.

4.2.3 Initial Piezometric Surface

The development of the topographic map of the study area made it possible to construct an initial piezometric surface map of the study area. The water levels in the wells were recorded as the distance from the ground to the water surface. Figure (4.5) shows the initial piezometric surface map of the study area. The map reveals the general flow pattern from west and southwest to

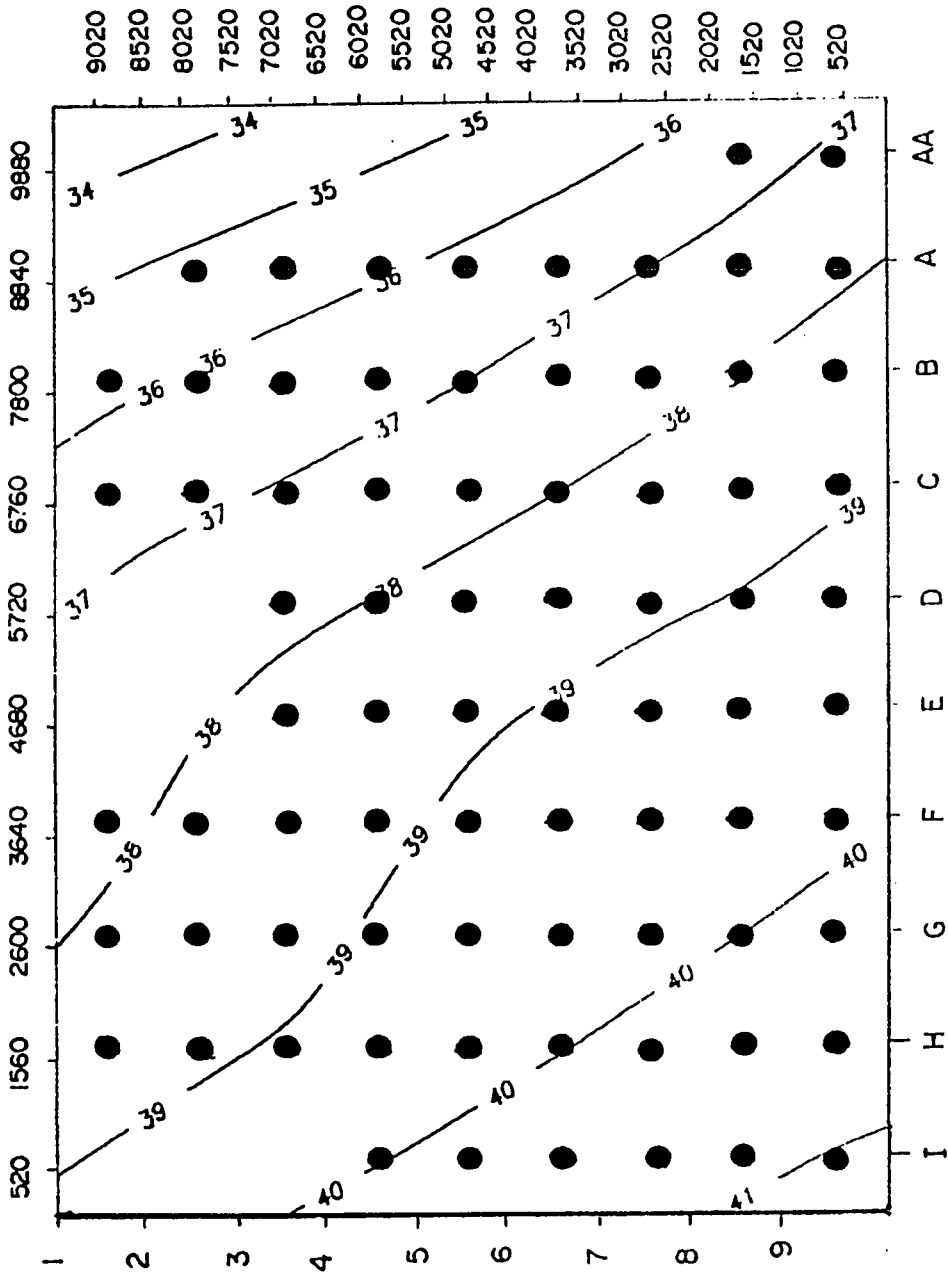


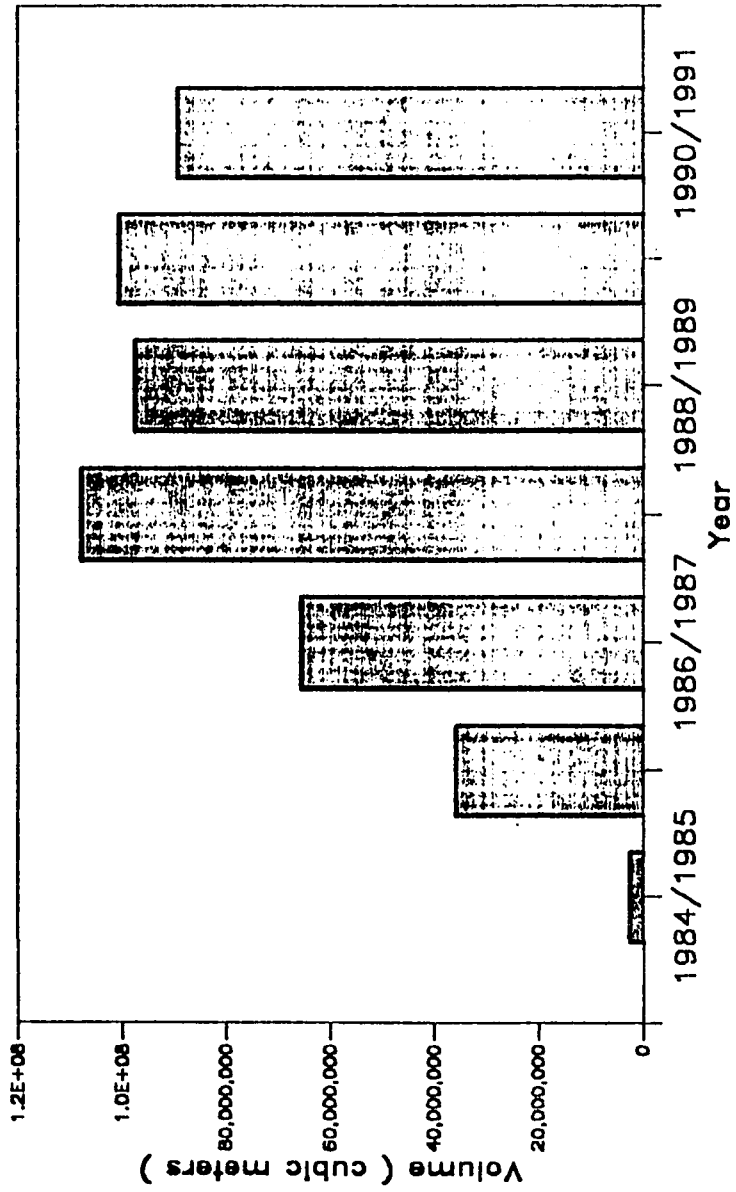
Fig. 4.5: Map of Initial Piezometric Heads (meters)

● Wells

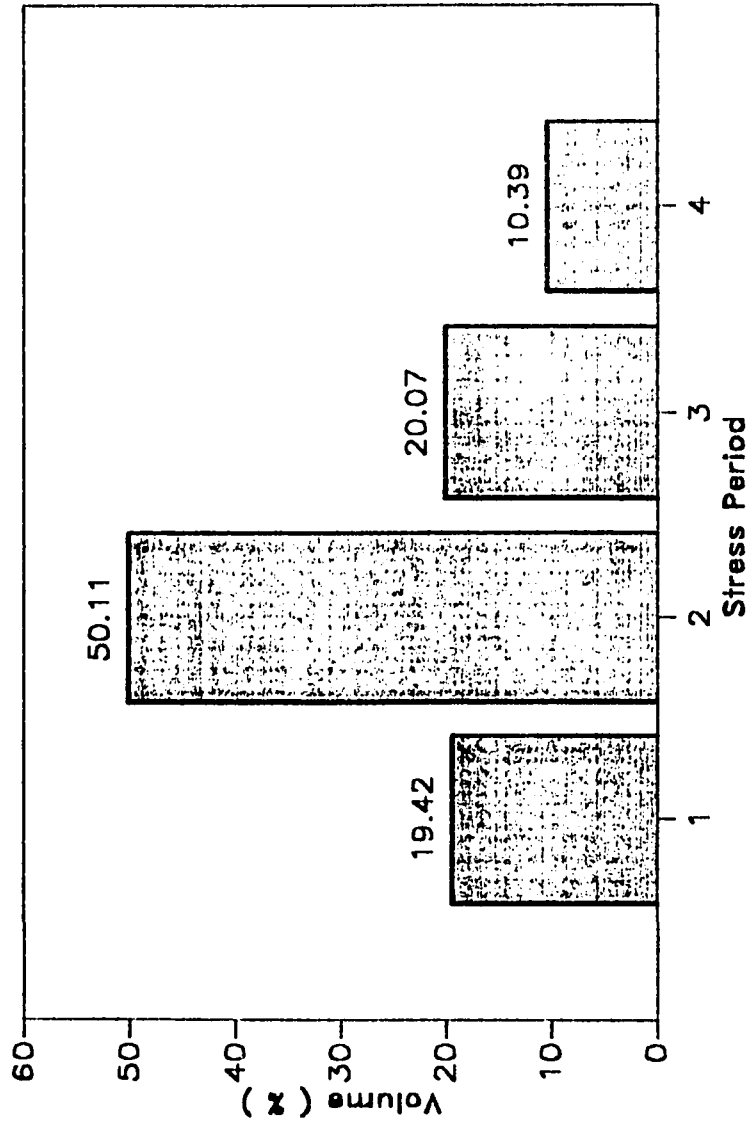
east and northeast towards the Arabian Gulf. The hydraulic gradient is found to be 5.0×10^{-4} . The bend in the contour lines may be due to high transmissivities along the vertical line F.

4.2.4 Extraction Rates

Water extracted from the UER aquifer in the study area is used solely for agricultural purposes. The wells in the study area were drilled at different times from 1984 to 1989. The discharge rates from the wells range from 1000 to 1800 gallons per minute. The year has been divided into four stress periods. The first period includes November only. The second stress period is from the first of December until the end of February. The third period includes March only. The last stress period starts from the first of April until the end of October. This division into four stress periods is dictated by the irrigation practice used by SHADCO. Rhodus irrigation stops during December, January and February. Wheat and barley are harvested in April whereas alf-alf is irrigated continuously throughout the year. Figure (4.6) shows the volume of water extracted since 1984. The percentage of extracted water in each stress period is shown in Figure (4.7). It can be seen that the second stress period has the highest percentage of water consumption. This is due to the length of the period (3 months). The fourth stress period has the lowest percentage of water con-



Figure(4.6) Volume of Water Extracted Since 1984



Figure(4.7) Percentage of Water Extracted in Each Stress Period

sumption because irrigation stops for all crops except alf-alf which is grown in few fields. However, the second stress period is ranked the second lowest in terms of daily water consumption because the irrigation of Rhodus stops at this stage.

4.3 BOUNDARY CONDITIONS & DISCRITIZATION OF THE STUDY AREA

Except for the direction of flow, little is known about boundary conditions in the study area. Since for isotropic soil the direction of flow is perpendicular to the equipotential lines. It would seem reasonable that a no-flow boundary be set perpendicular to the equipotential lines. This boundary has been set as far as 50000 meters at a slope perpendicular to the equipotential lines. The eastern and western boundaries have been modelled as head-dependent boundaries. By the head-dependent cell, it is meant that flow into or out of a cell from an external source is provided in proportion to the difference between the head in the cell and the head assigned to the external source. Therefore, a linear relationship between flow into the cell and head in the cell is established, i.e.

$$Q_b = C_b (h_b - h) \quad (4.26)$$

where:

Q_b = is the flow into the cell from the source

C_b = is the conductance between the external source and the cell

h_b = is the head assigned to the external source

h = is the head in the cell.

The relationship between the cell and the external source is shown schematically in Figure (4.8). In this study, the external source is considered to be the head in the aquifer outside the modelled area. It is determined 50000 meters away from both sides by the knowledge of the hydraulic gradient in the area to insure that the source cells do not affect the modeled area. The conductance which is the proportionality constant in equation 4.26 is computed by:

$$C_b = \frac{TW}{L} \quad (4.27)$$

where:

T = is the transmissivity of the aquifer between the external source and the model boundary

W = width of the cell

L = is the distance between the external source and the model boundary

The heads at the source boundaries were calculated based on the hydraulic gradient in the area. The conductance terms were calculated based on the average transmissivity values and the distance to the source boundaries. The head dependent boundaries

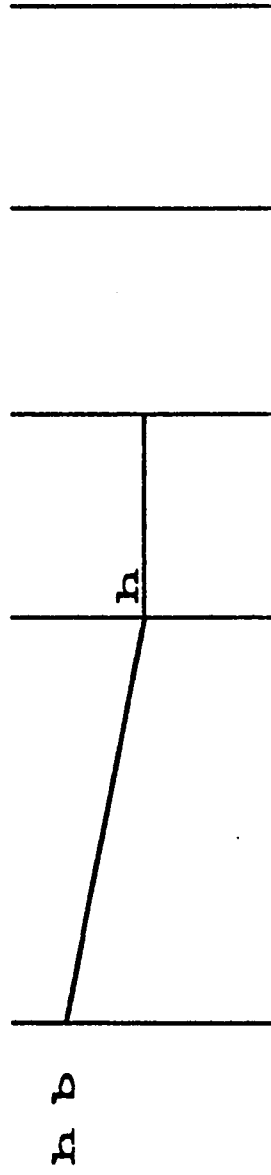


Figure (4.8) Head-Dependent Boundary (McDonald and Harbough 1984)

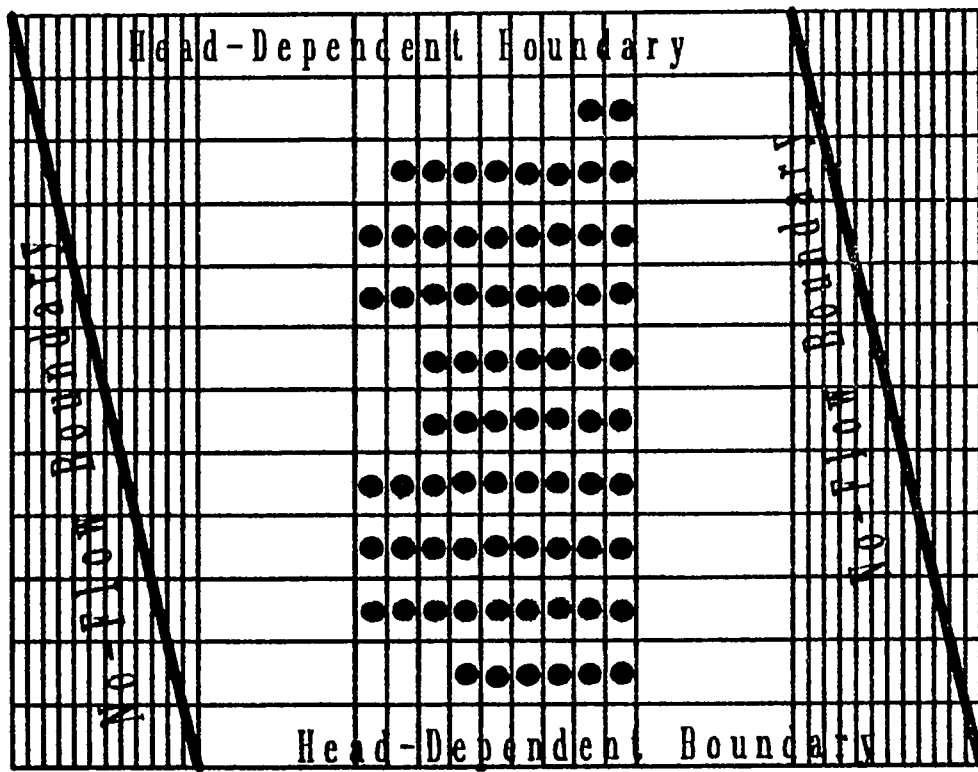
are handled by the General Head Boundary package of the model. Figure (4.9) shows the discretized study area with the boundary conditions. The spacing of the grid system was chosen carefully to exactly center the wells at the middle of cells. The total number of cells is 420 from which 264 cells are active and the remaining 156 cells are inactive. The grid spacing was found to meet the computational time requirements.

4.4 CALIBRATION

4.4.1 General

The goal of most computer simulations is to predict the effects of some proposed management schemes on a particular groundwater system. The final test of a numerical model is to determine whether it successfully simulates field observations. Such a model is said to be calibrated and verified. The process of calibration generally requires adjustment of model parameters. In general, the first step in model calibration is to design a steady-state model to solve for the head distribution to be used as the initial conditions in a later transient simulation.

The trial and error procedure has been adopted in the present study to calibrate the model. The model parameters such as transmissivities and storativities have been adjusted to obtain a match between observed and simulated heads. The process was



● Wells

Figure(4.9) The Discretized Area with Boundary Conditions

carried out in two stages namely; steady-state and transient calibration.

4.4.2 Steady-State Calibration

The steady-state calibration process involves the adjustment of transmissivity values in the study area. The storativity values are not adjusted at this stage because they are not part of the differential equation describing the steady-state condition. The model has been calibrated against the initial piezometric heads shown in Fig. (4.5). Boundary conditions have not been altered at this stage. No discharge from wells was considered. The aquifer was judged confined and modelled as a layer type 'O' (McDonald and Harbough 1984). The calibration process was terminated after 73 runs where a satisfactory match was reached at. At this stage the simulated heads were reasonably in accordance with the initial heads shown in Fig. (4.5). It is noted that the two maps (Fig. 4.5 and Fig. 4.10) are in good accordance. A statistical measure to the goodness of calibration is the root mean square error defined by:

$$RMSE = \frac{\sqrt{\sum_{i=1}^r \sum_{j=1}^c (h_{i,j}^n - h_{i,j}^o)^2}}{r \times c}$$

where:

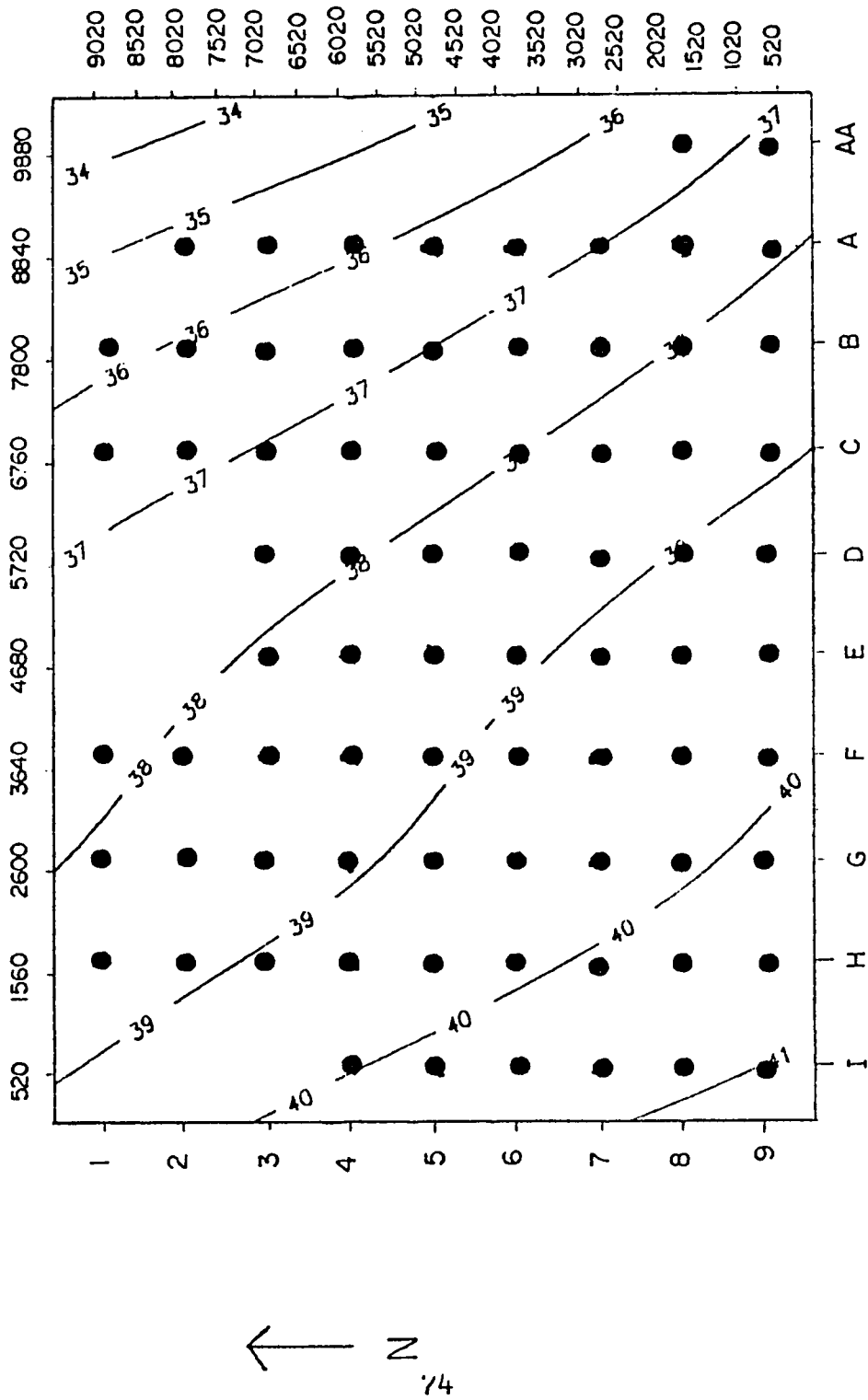


Fig. 4.10: Map of simulated steady-state Piezometric heads (meters)

● Wells

r = is the number of rows

c = is the number of columns

$h_{i,j}^n$ = is the simulated head at run number n at cell i,j .

$h_{i,j}^o$ = is the observed head at cell i,j .

The values of RMSE at selected runs are shown in Table (4.1). The difference of (20.2) in the RMSE between the first and final run indicates the significant improvement in the transmissivity distribution over the study area. The high RMSE at the first run is probably due to the poor assessment of the initial input transmissivity values obtained from pumping tests. Fig. (4.11) shows the difference between observed and simulated heads. The calibrated transmissivity distribution is shown in Fig. (4.12). It is noted that these transmissivity values are different from those obtained from pumping tests which supports the assumption that pumping tests were conducted in an improper way. It can also be noticed that the transmissivity values are very high along the wells running along the F-line. It is believed that these high transmissivity values cause the bend in the piezometric head contour lines shown in Figure (4.10).

**Table 4.1: The Values of RMSE
at Selected Runs**

Run No.	RMSE
1(initial)	21.080
2	11.595
10	5.270
15	3.162
20	2.635
50	1.312
72	0.887
73(final)	0.886

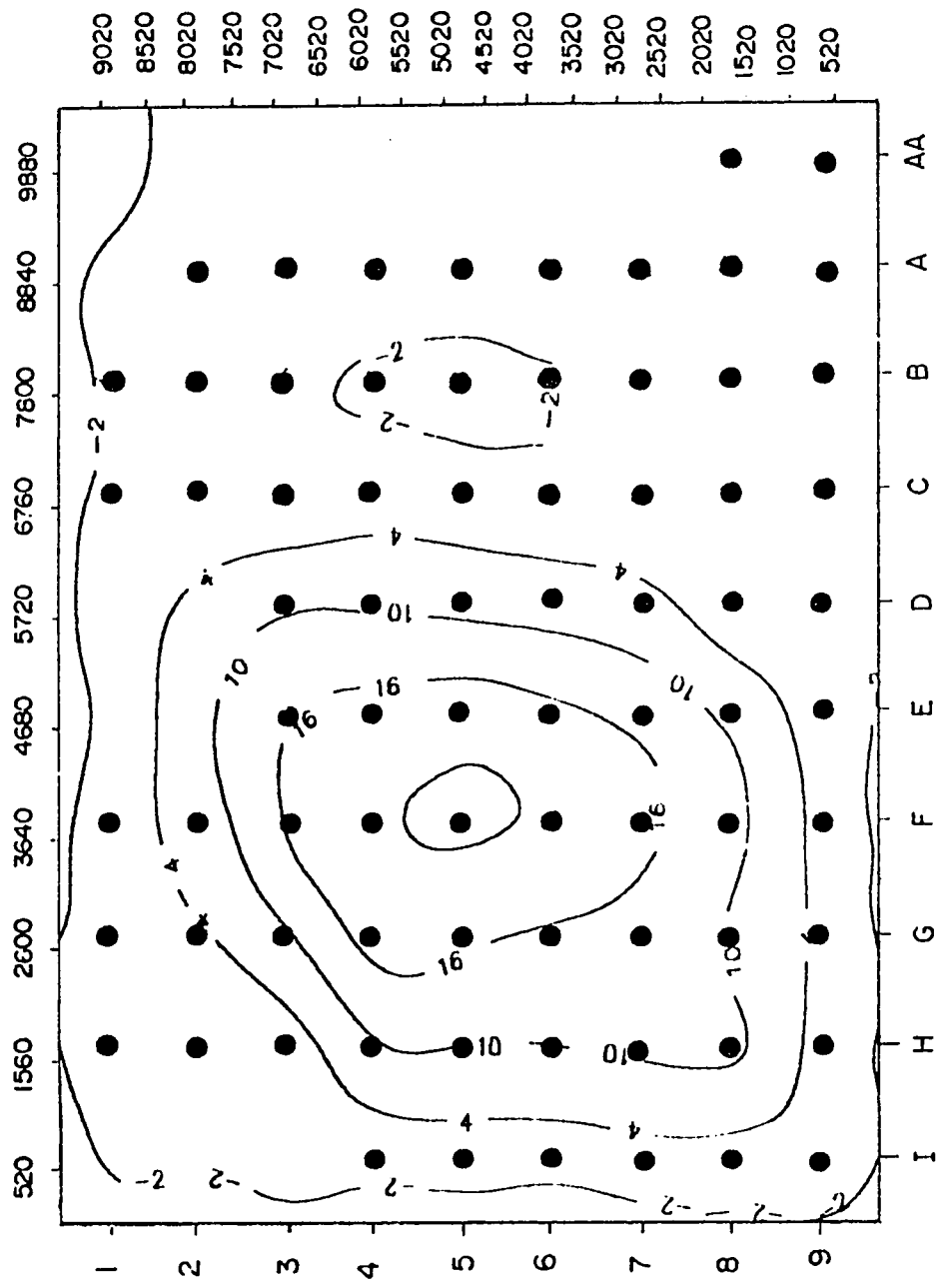


Fig. 4.11: Map of the difference between observed and simulated steady-state Piezometric heads (cm)
 ● Wells

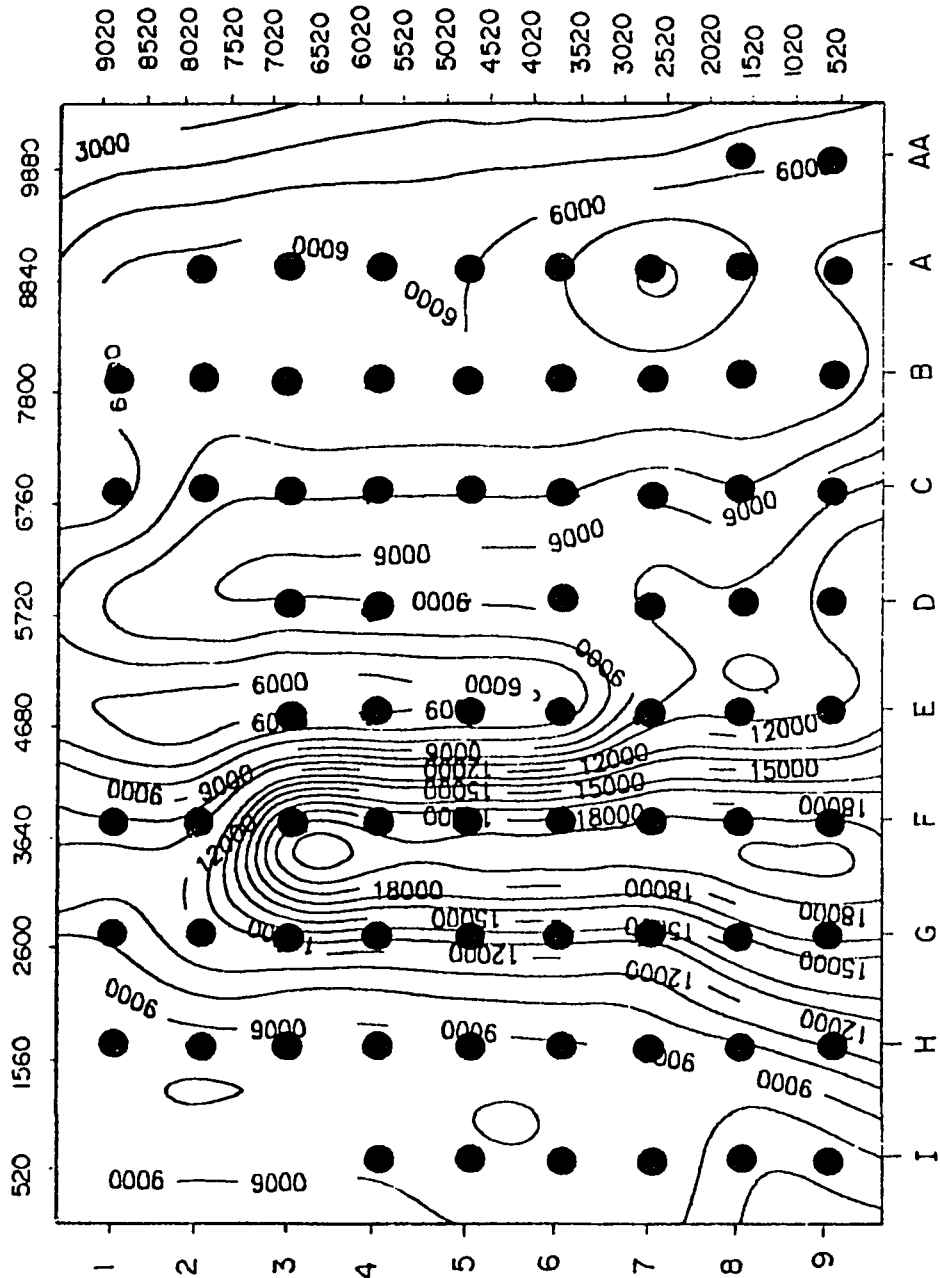


Fig. 4.12: Map of the calibrated transmissivity values (square meters per day).
 ● Wells

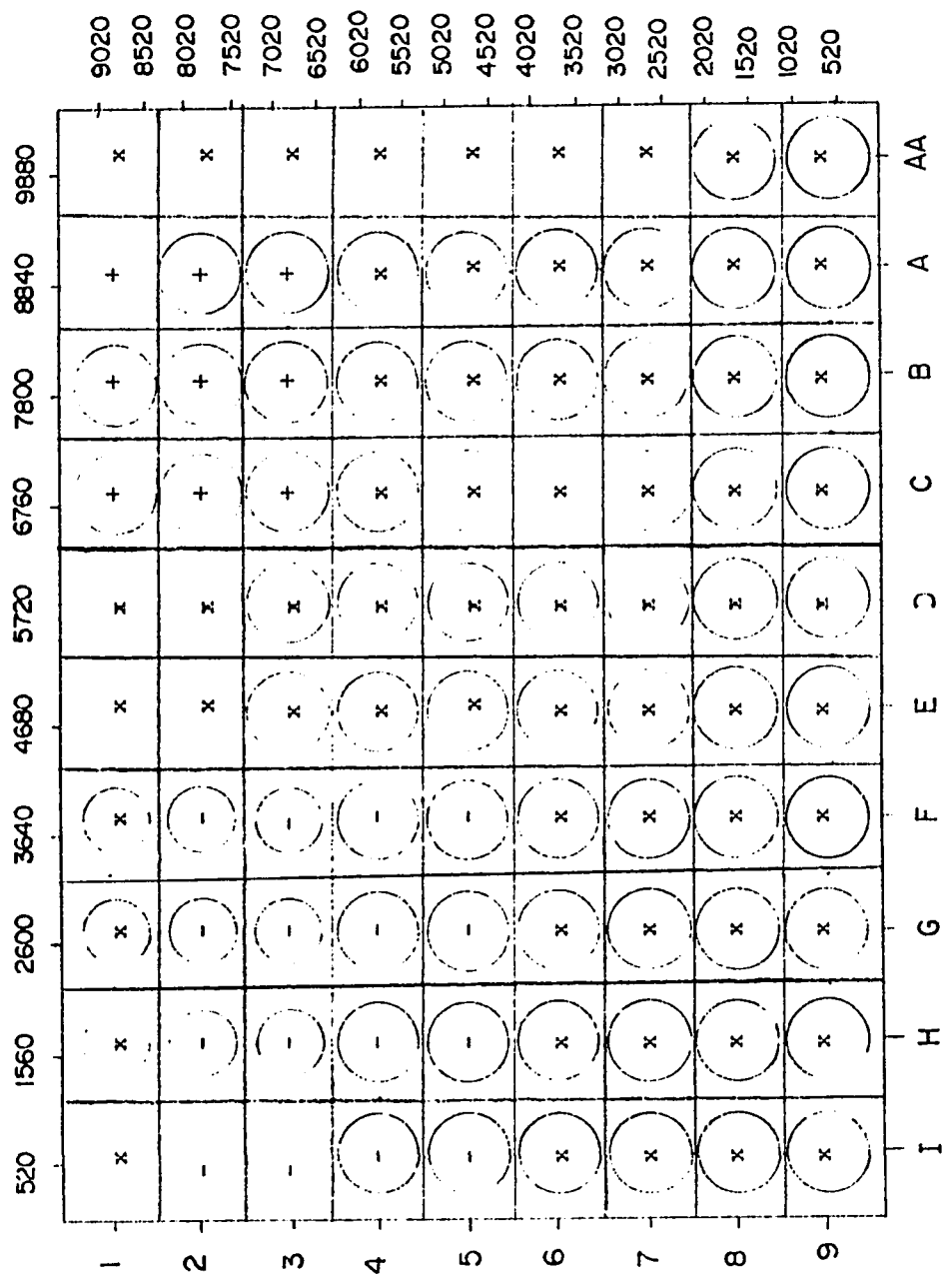
4.4.3 Transient Calibration

Not only the spatial variations in piezometric heads are important, but also the temporal variations are of concern. Transient calibration is carried out to adequately describe the hydraulic changes in the aquifer with time. Transient calibration involves the change of aquifer parameters so that the historical records of heads match those obtained from the simulation. In this regard, the model has been calibrated from 1984 to 1990.

The simulation period has been divided into 28 stress periods to match the irrigation practice adopted by SHADCO. Every single year has been divided into four stress periods. The first stress period includes November, the second includes December, January and February, the third includes March and the fourth period includes April, May, June, July, August, September and October. Each stress period has been divided into non-uniform time steps to avoid oscillations in the solution of the flow equation. Starting heads were those obtained in the final run of the steady state stage. No changes in transmissivity values or boundary conditions have been attempted at this stage. With the extraction rates discussed in Section (4.2.4), the transient calibration of the storativity values was conducted. The storativity calibrated seems to be of little spatial variations. Rasheeduddin (1989) supports this fact by reaching to a constant storativity of 4×10^{-4} in an

area of 9400 squared kilometers. Fig. (4.13) shows the distribution of storativity in the study area. Appendix B contains the graphs of the piezometric heads at the end of each stress period. To verify the accuracy of the predicted heads, the measured heads from the three observation wells shown in Fig. (4.14) obtained from a report submitted to SHADCO by King Fahd University of Petroleum and Minerals (KFUPM) research team have been compared to the simulated heads. The hydrographs of the water levels in wells B1, F3, and I4 are shown in Figs. (4.15-1,4.15-2,4.15-3).

The hydrographs show the simulated and the observed heads at the three observation wells. It can be noticed that the model predicts increase in drawdowns until the end of March which is the third stress period. The heads, then, start to increase during the fourth stress period as a result of harvesting all crops except Alf-alf and Rhodus. This period is important for recovery from the heavy pumping during the first three stress periods. Comparing the simulated and the observed heads, it can be noticed that the model agrees to a very good extent with the observed heads in the first three stress periods and underestimates the rate at which recovery takes place at wells B1 and F3 while overpredicting the recovery rate at well I4. It is, however, noticed that the model agrees well with the observed heads with the difference hardly exceeding one meter at all times. It is noted that the



Legend: + = 7×10^{-5}
 x = 5×10^{-4}
 - = 4×10^{-3}

Fig. 4.13: Map of the Calibrated Storativity Values

↑ N
 1

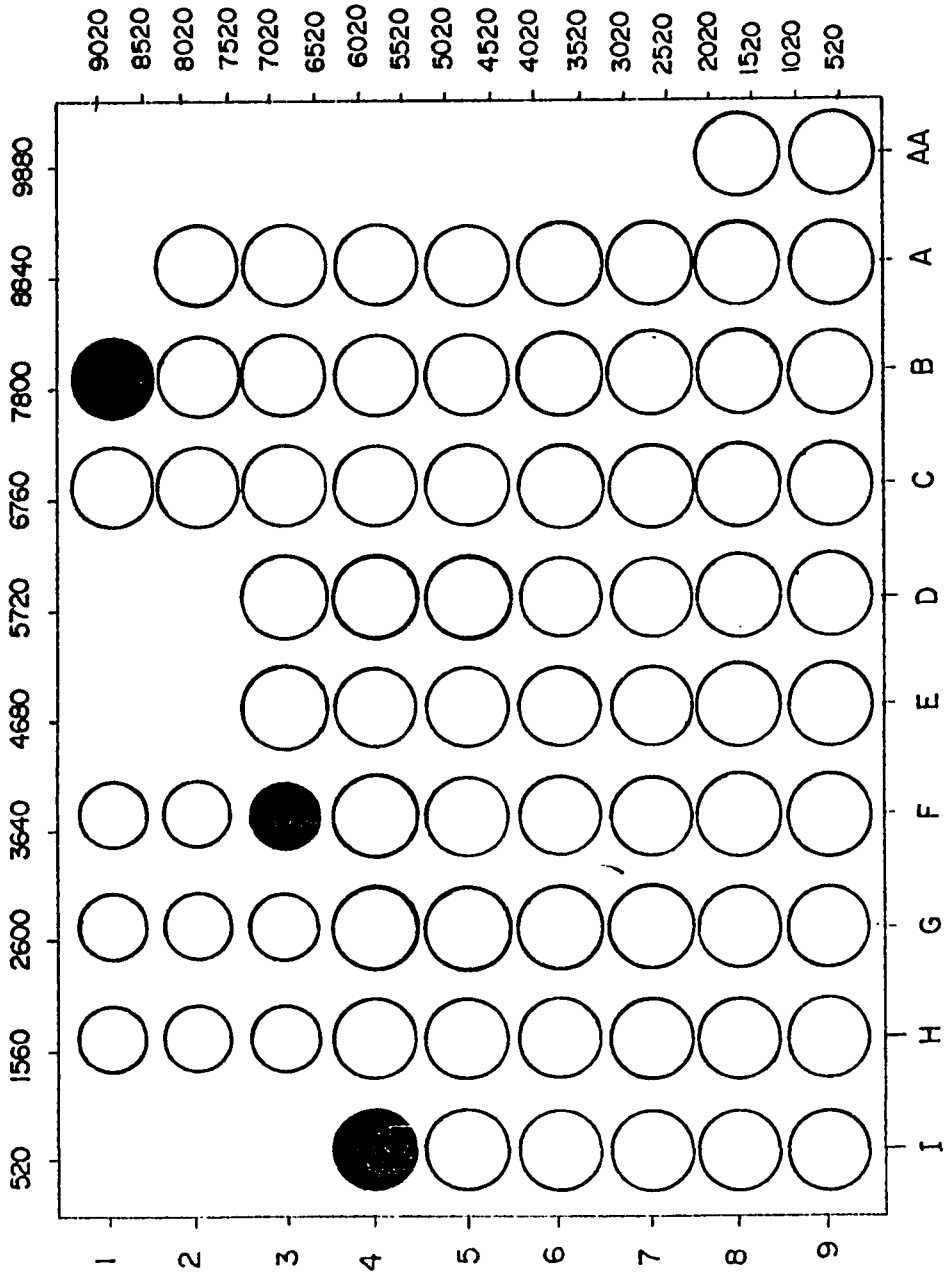


Fig. 4.14: Location of observation wells in the study area.

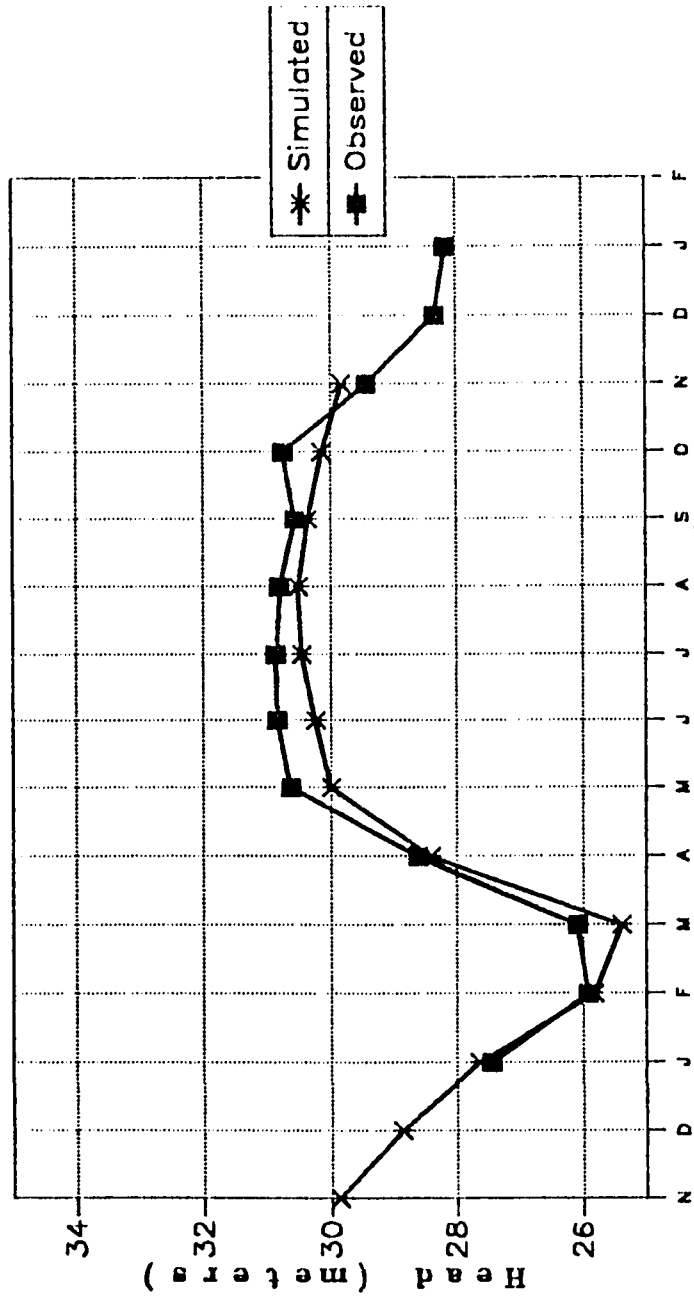
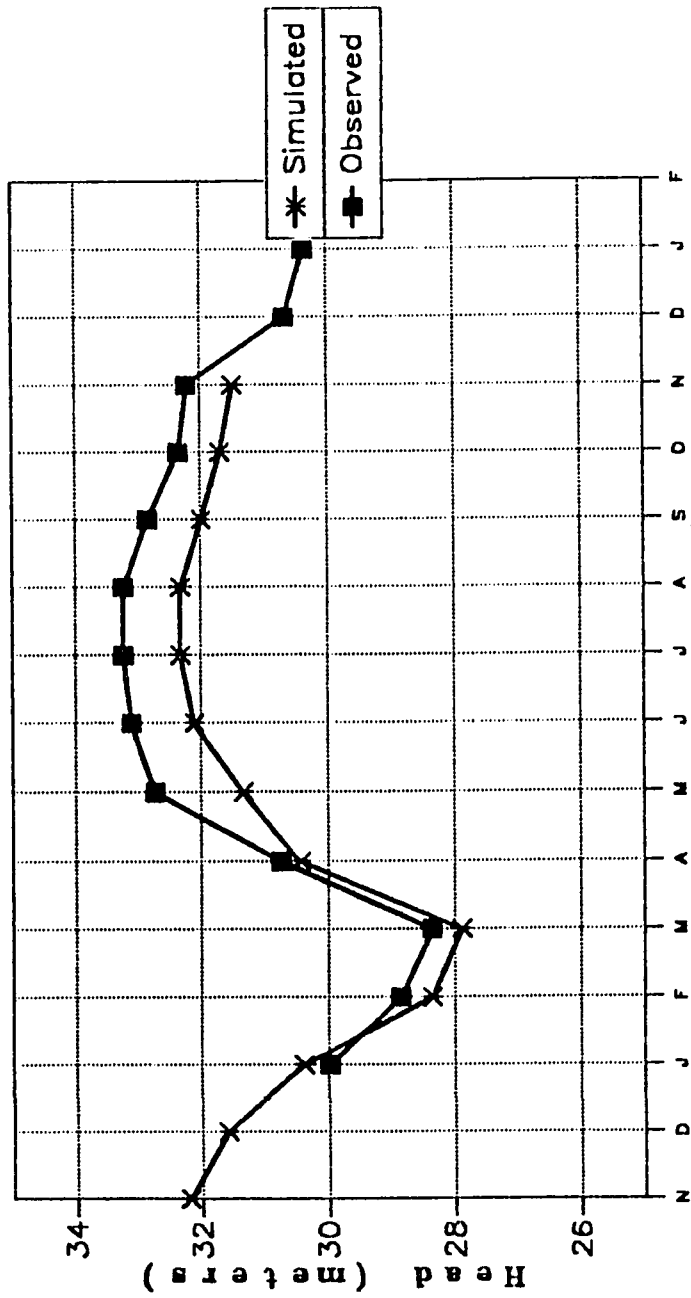


Figure (4.15-1) Observed vs. Simulated Heads at Well B1
Season 80-91



Figure(4.15-2) Observed vs. Simulated Heads at Well F3
Season 90-91

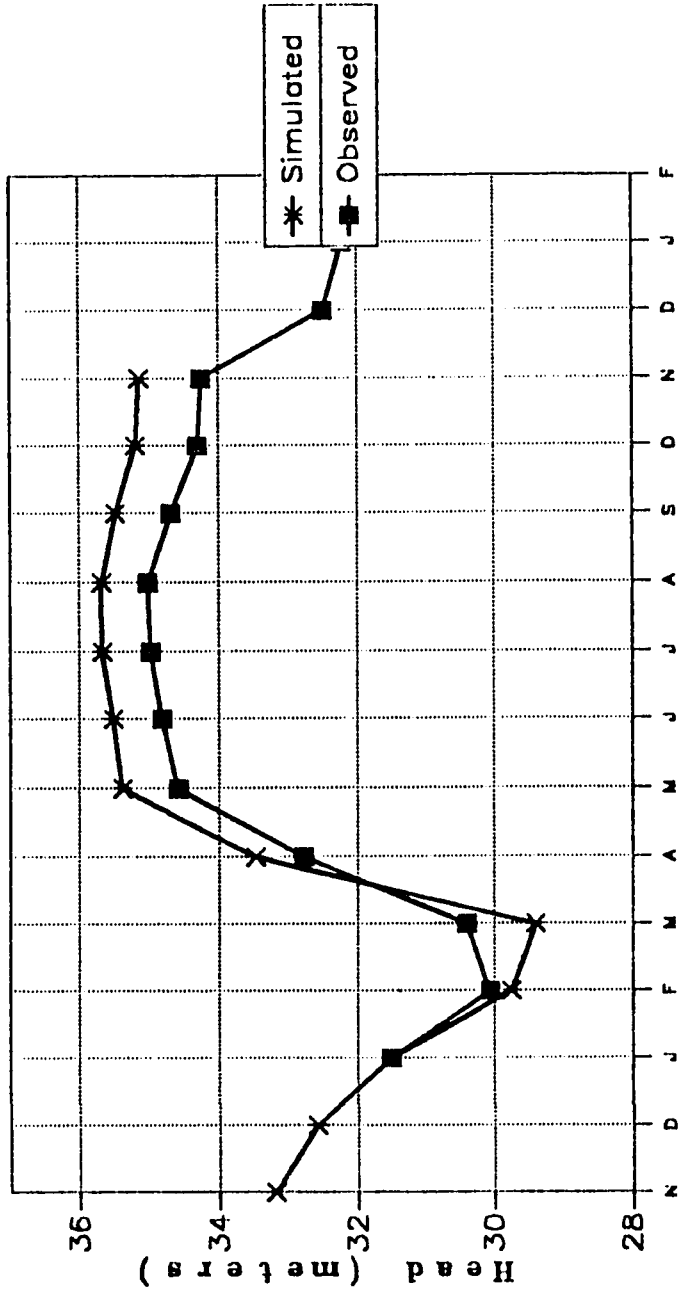


Figure (4.15-3) Observed vs. Simulated Heads at Well 14 Season 90-91

observation wells almost lie on a straight line. The location of these wells does not reflect the effects on the whole study area. The observation wells should have been located so as full picture of the heads on the whole study area can be attained.

4.5 SENSITIVITY ANALYSIS

4.5.1 General

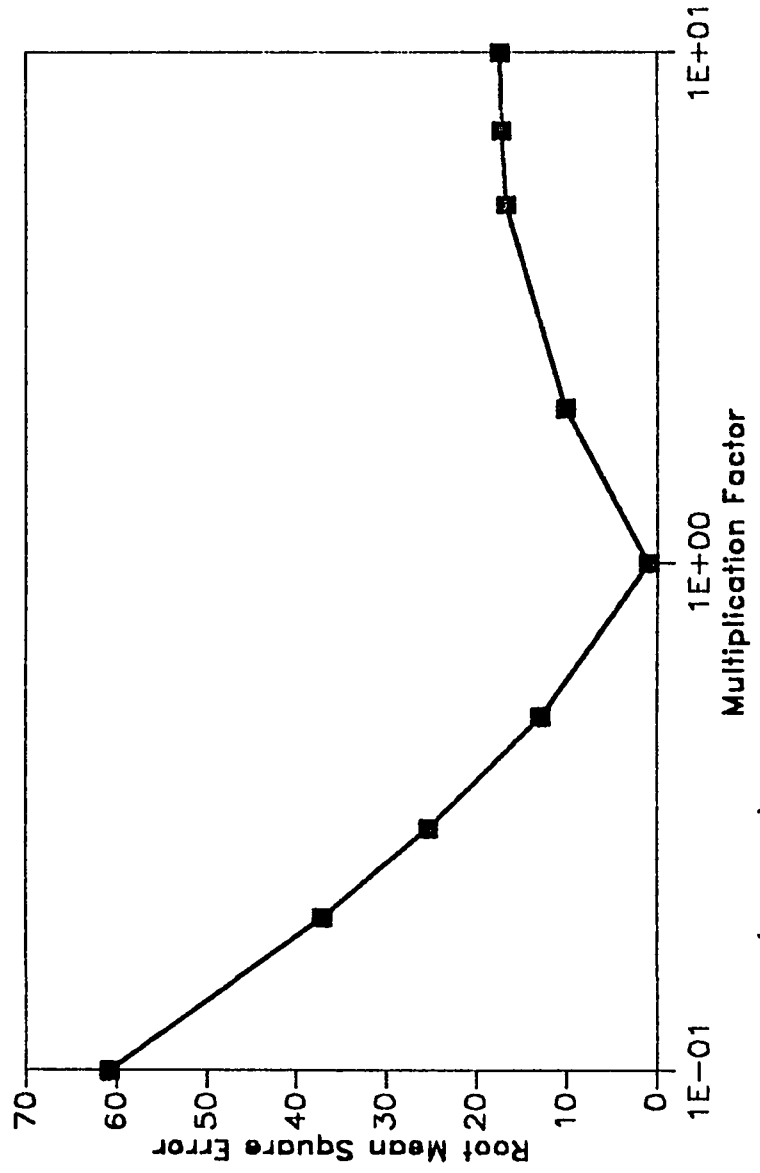
The need for a sensitivity analysis is dictated by the uncertainty and inaccuracy of the physical parameters of the aquifer. Sensitivity analysis is performed by studying the changes in the aquifer response corresponding to changes in certain input parameters. A sensitivity analysis has been performed on the calibrated transmissivity of the aquifer. Sensitivity to boundary conditions by changing the conductance values of the head-dependent boundaries. Sensitivity to storativity values change has not been conducted because of the inadequate locations of the observed heads and consequently the poor assessment of the spatial variations of the hydraulic heads. Perhaps the most reasonable quantity to use in the sensitivity analysis is the change in head. By relating the changes in heads to the observed heads, the effects of the parameters can be clearly noticed. To quantify the effects, the root mean square error (RMSE) has been used.

4.5.2 Transmissivity

The sensitivity to transmissivity study has been carried out at the steady-state. Fig. (4.16) shows the relation between the change in transmissivity values and the corresponding change in RMSE. It can be noticed that transmissivity has a major impact as an input parameter. Decreasing the transmissivity values by 10 times causes a corresponding jump in the RMSE value of more than 60 times. On the other hand, increasing the transmissivity also, tends to increase the RMSE value. The increase in the RMSE value, however, stops at a certain level (Fig. 4.16). At this level, the transmissivity values which reflect the ease with which water flows, become excessively high. The easy passing of water resembles the water running in pipes. At this stage, it does not matter what the transmissivity value is. All values of transmissivity give the same result. This reasoning is the same as mathematically adding one to infinity. This effect can be noticed at the right portion of Fig. (4.16).

4.5.3 Head-Dependent Boundary

The sensitivity to the conductance of the head-dependent boundaries has been carried out by changing the conductance values and examining the corresponding change in the RMSE value. Fig. (4.17) demonstrates the relation between the RMSE and the



Figure(4.16) Sensitivity to Transmissivity

change of conductance. It can be noticed that an increase of 10 times in the conductance values results in an increase of more than 60 times in the RMSE value. Decreasing the conductance values, however, results in decreasing the RMSE to a certain level. At this level, the RMSE value is maintained no matter what the decrease in the conductance values is. When the conductance values are very low, the volume of water entering from or leaving to the constant head boundaries drops to a very minor amount (Equation 4.28). At this stage, the constant head boundaries act as no-flow boundaries. Since there is no discharge from the wells, steady-states are reached quickly. Fig. (4.17) supports this reasoning by displaying the horizontal left branch of the graph.

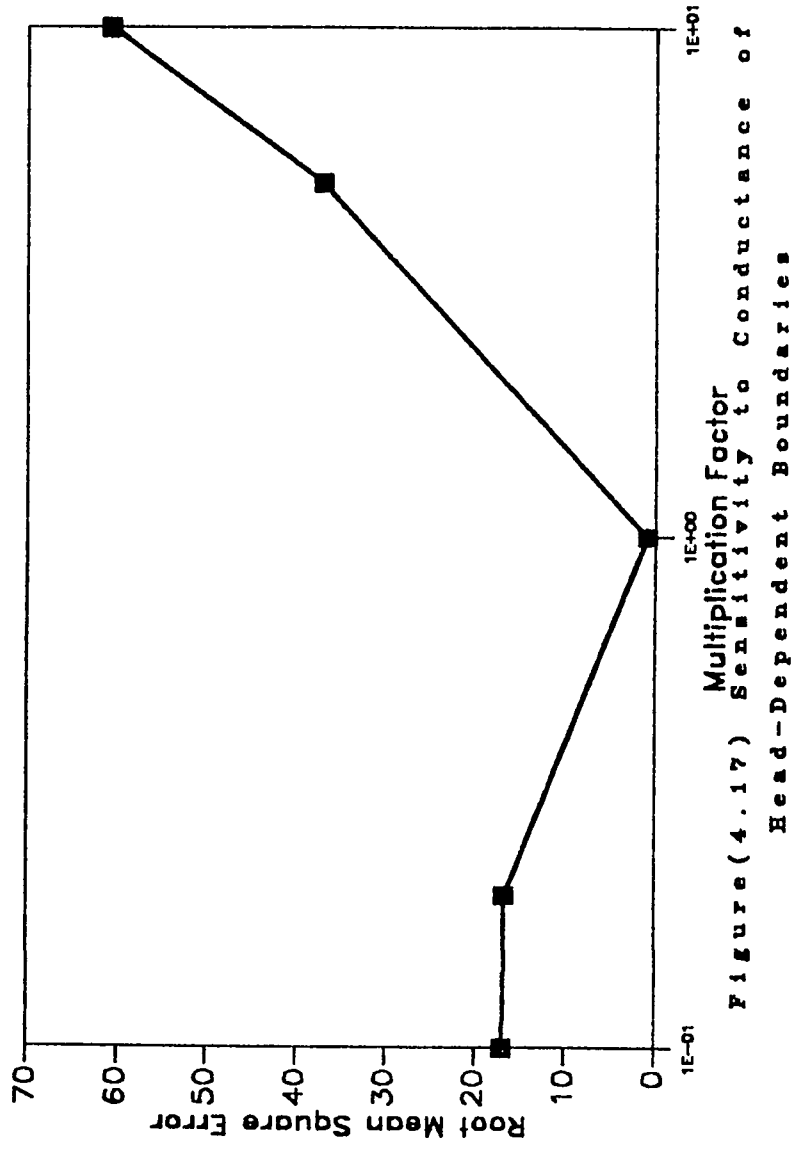


Figure (4.17) Multiplication Factor Sensitivity to Conductance of Head-Dependent Boundaries

Chapter 5

MANAGEMENT ALTERNATIVES

5.1 GENERAL

The goal of most computer simulations is to predict the effects of some proposed management scheme on a particular groundwater system. The prediction stage gives an early look into the future as to select the best management alternative where several factors such as cost and environmental aspects are considered. There are many alternatives that can be considered at this stage. However, few of these alternatives are feasible. The important task is to formulate the alternatives based on realistic operational practices.

The time span of historical data and the relatively short period for which the project has been operated (7 years), limits the prediction period to a length of time equal to the simulation period (7 years). The alternatives have been chosen based on the cropping practice adopted by SHADCO. Table (5.1) lists the types of crops grown in each year since 1984/85. The table reveals the trends in cropping practice in the last few years. Although the daily irrigation is the same for all crops (1686 gallons per minute), certain crops are not irrigated at certain times of the year. Referring to Fig. (4.6), it is noted that water consumption

Table 5.1: Total Number of Each Crop Grown in Each Year

Crop/Season	84/85	85/86	86/87	87/88	88/89	89/90	90/91	91/92 (Current)
Wheat	2	25	34	30	29	29	25	31
Barley	-	--	7	16	22	22	35	31
Rhodus	-	1	1	11	13	13	4	1
Alf-alf	-	1	5	9	2	3	3	3
Total	2	27	47	66	66	67	67	66

in the year 1987/1988 was maximum. This can be explained by the relatively large number of Rhodus and Alf-alf fields (20 fields) compared to only 5 fields in the last simulation year. Because Alf-alf is irrigated continuously for the whole year and Rhodus is irrigated for 9 months (irrigation stops in December, January, February), a considerable amount of water was used in 1987/1988 in excess to that used in the last simulation year 1990/1991. Table (5.1) also reveals the trends in increasing the cropping of Barley in the last three years. The types of crops and their spatial distribution is believed to have significant impacts on the distribution of piezometric heads in the study area. An experiment carried out last year by KFUPM research institute indicated that the reduction of 50% in irrigation water had minor impact on the yield of fields.

Based on the above-mentioned discussion, three alternatives can be set. The first alternative assumes that the trends of the last simulation year would continue. The second alternative takes into account the effects resulting from reducing irrigation water by different percentages. According to SHADCO engineers, a plan for cropping the area that was set in 1990 for the season 1991/92 was suddenly changed. It is understood that many factors play roles in determining which crops are to be grown in each season. There are no indications of any kind of expansion on the project. Consequently, a third alternative can be set in which spatial distributions of the crops are considered.

To quantify the effects of the alternatives, four observation cells have been selected. These are the wells numbered B1, F3, I4 and D6. The last has been chosen to reflect the spatial changes in heads, Fig. (5.1). The heads in these wells will be displayed throughout the prediction period for each alternative. Drawdown and head maps for the whole study area will be shown for each alternative at the end of the prediction period.

5.2 ALTERNATIVE I

The existing trends in the year 1990/1991 are assumed to continue for the 7-year prediction time. The prediction period has been divided into 28 stress periods based on the same reasoning for dividing the simulation period. Fig. (5.2) shows the heads at the observation wells for the period from 1991/1992 to 1997/1998. The general decrease in heads is noticed for all observation wells. The spring-shaped graph indicates the recovery stages in the period from April to October in each year. The head distribution at the end of the prediction period is shown in Fig. (5.3). Drawdowns are shown in Fig. (5.4). The cone of depression is clearly noticed. The area at the east part of the area suffers low heads. The central area exhibits excessive drawdowns due to the accumulation of drawdowns from each well. Although the wells are allowed to recover during a long period of time, the excessive discharge rates and the close spacing of wells make it difficult to

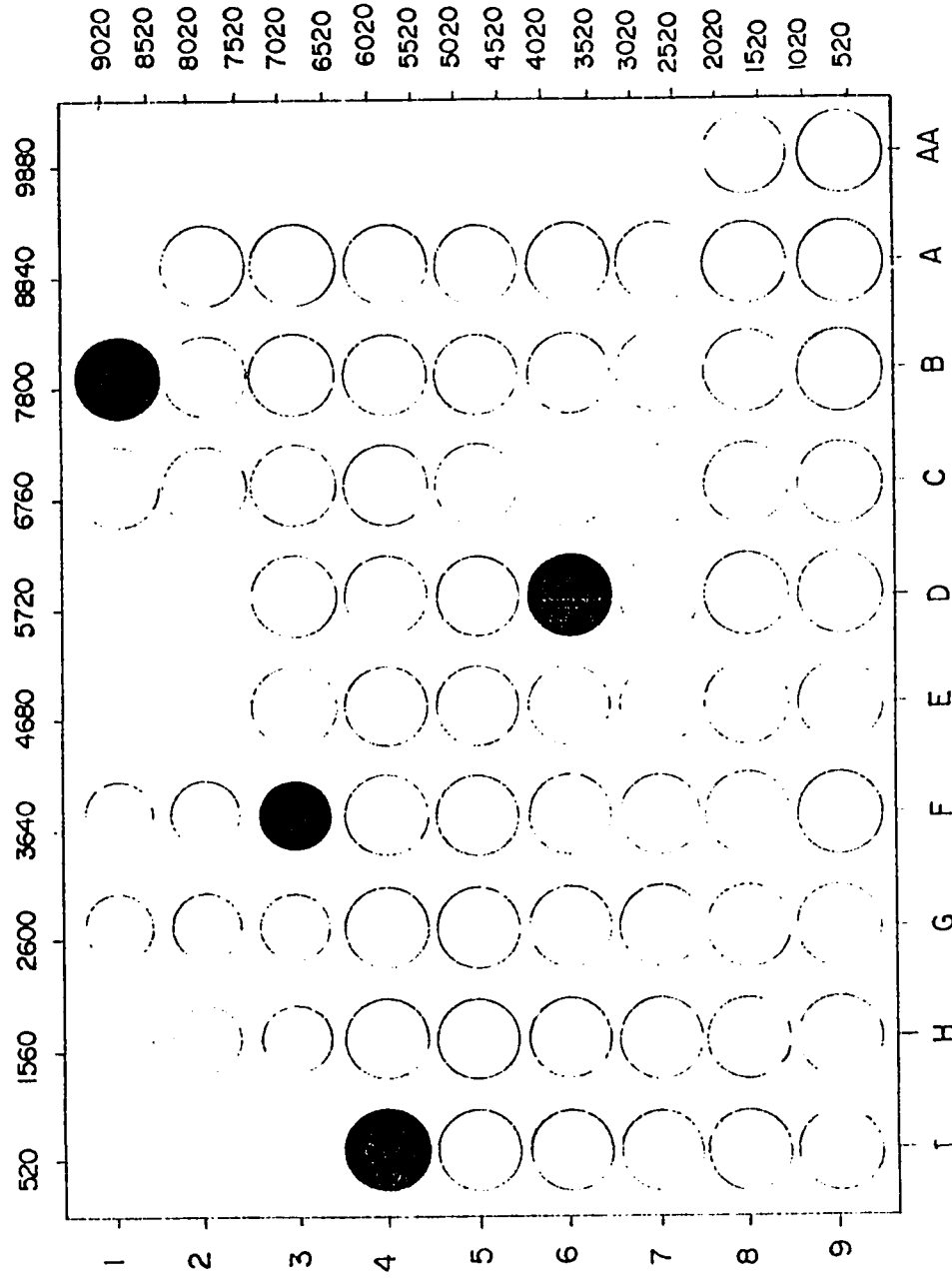


Fig. 5.1: Location of Observation Wells for the Prediction period.

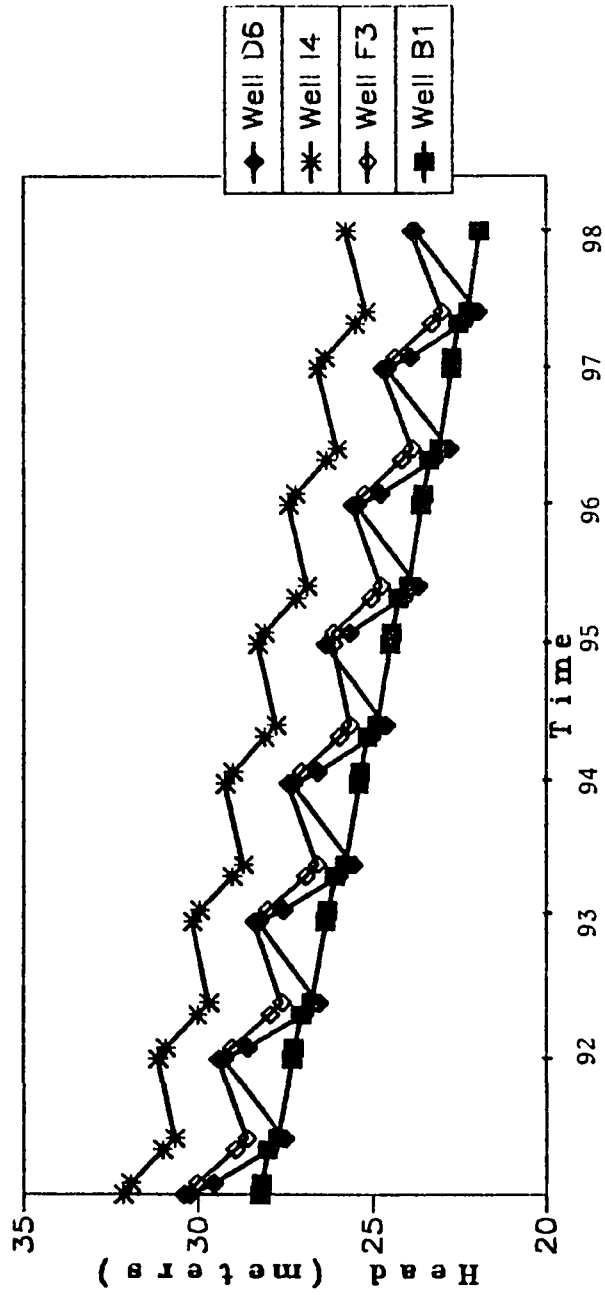


Figure (5.2) Simulated Heads for the Period 1991-1998

Att. I

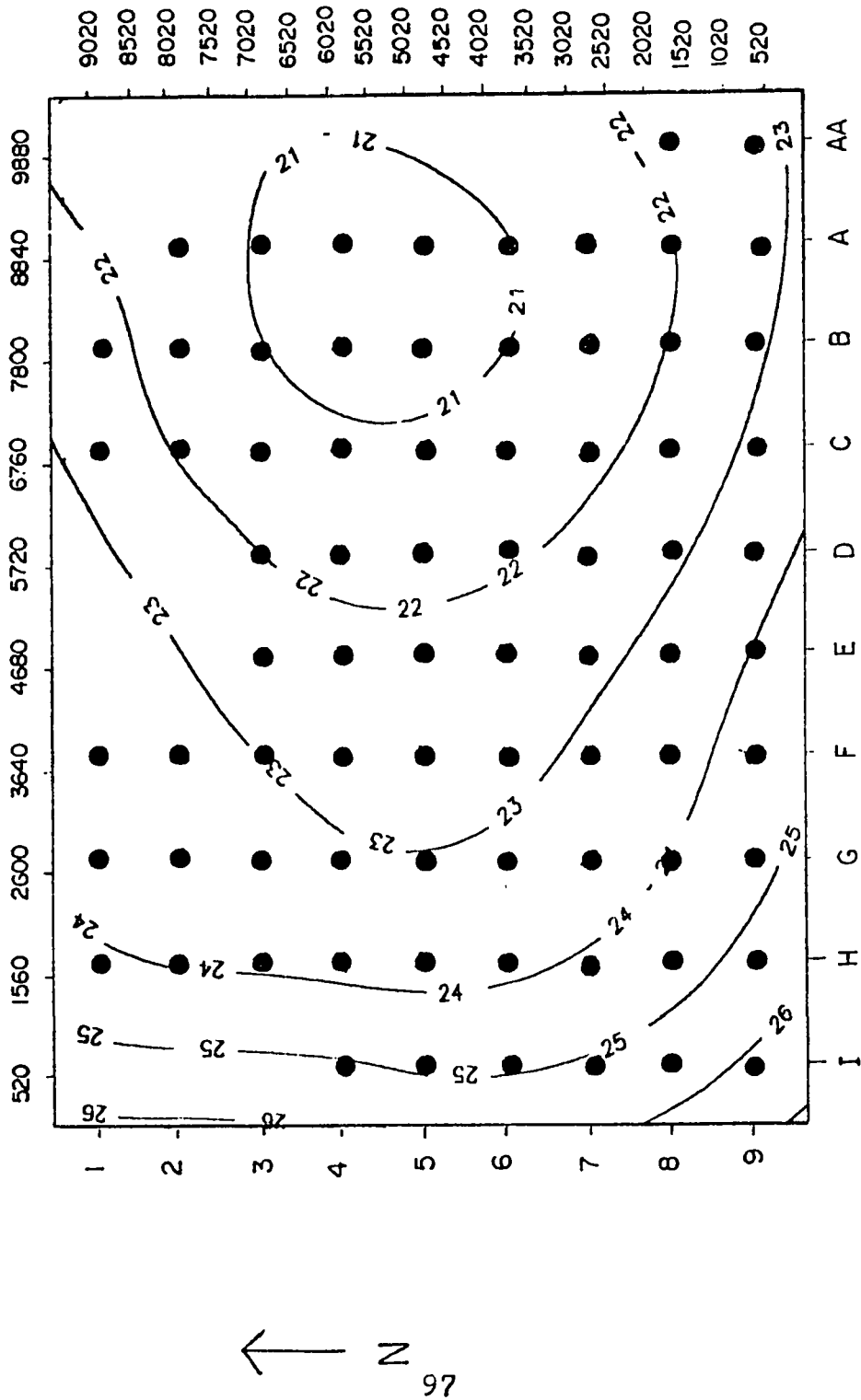


Fig. 5.3: Piezometric head map at the end of prediction period
(Alt. I) (meters)
● Wells

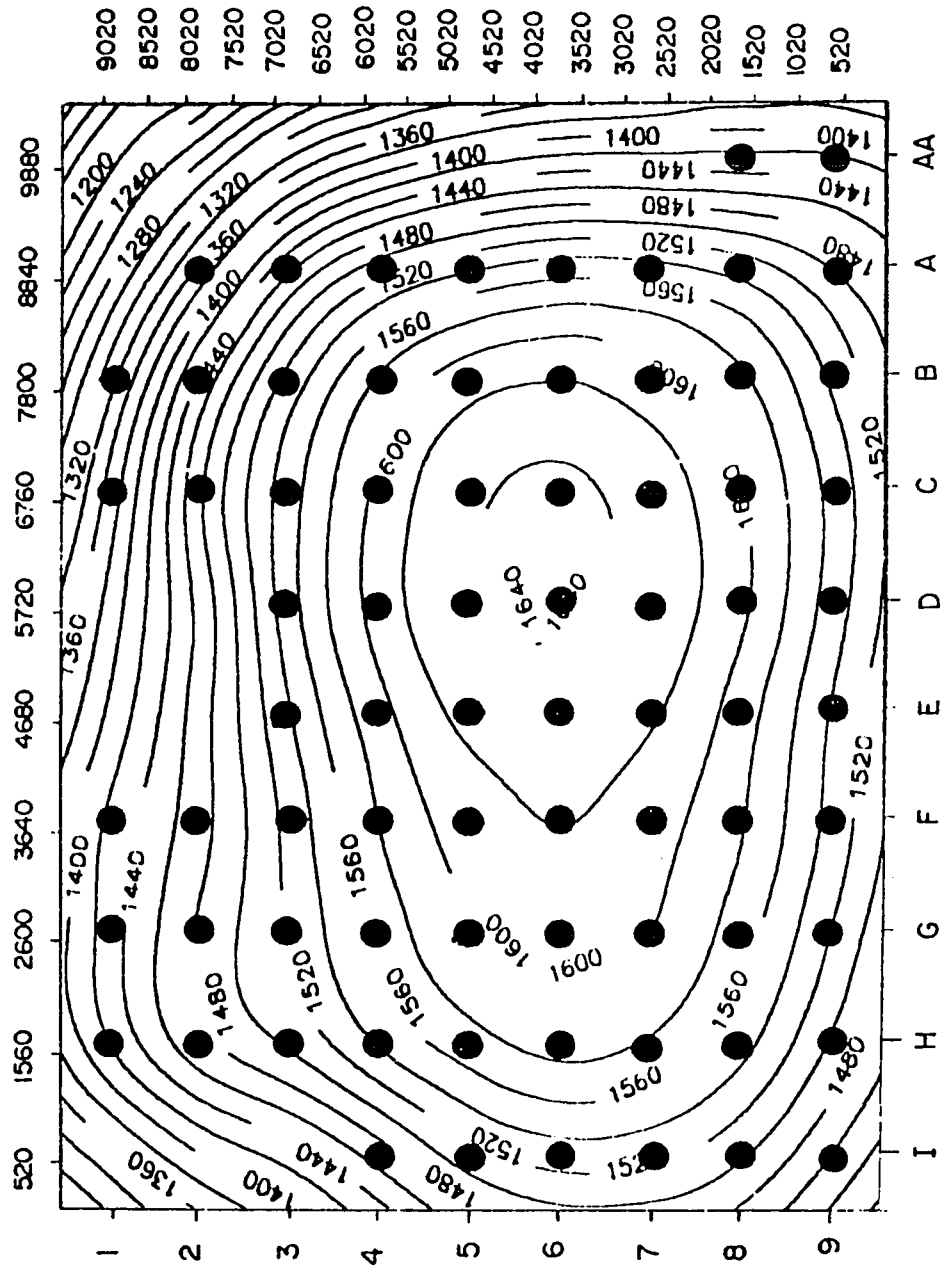


Fig. 5.4: Drawdown map at the end of prediction period (Alt.I) (cm)

● Wells

recover the relatively large losses in heads (Fig. 5.3).

It is interesting to notice the importance of the relaxation period from April to October. During the first three stress periods in every year, the aquifer water is exposed to heavy pumping. The rate at which the water level falls in the wells can be computed from Fig. (5.2). If there were no relaxation period the estimated head drop would be 4 to 5 times greater.

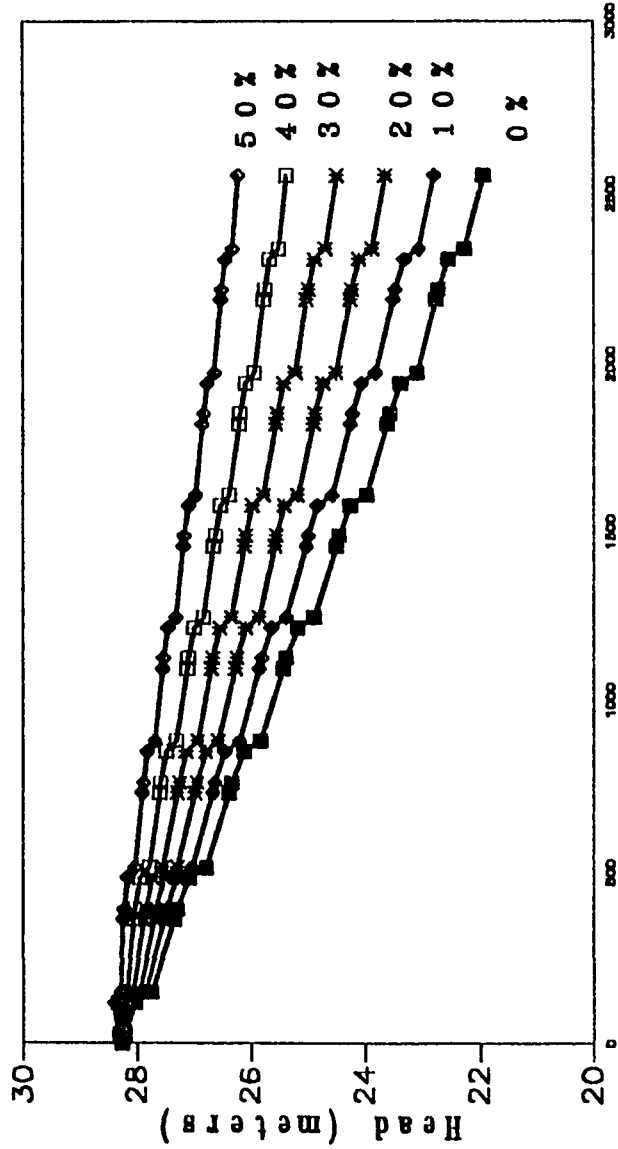
5.3 ALTERNATIVE II

The experiment demonstrated that reducing the amount of irrigation water by 50% had minor impacts on the yields of the fields, was conducted on three fields. It is not possible to generalize this result to all the other fields because of the many variables involved. These include type of crop, environmental and geological factors. To insure maximum yields of fields, the crop water requirements have to be met. To get maximum yields, it is not necessary that excess water has to be provided. Instead, maximum yields are obtained at certain applied water (Linsley and Franzini 1979). The best way to estimate the crop water requirements is through experiments. The research institute team at KFUPM has developed a computer program that calculates the crop water requirements depending on many factors such as weather and soil moisture content. The rates at which crops are irrigated

change from day to day. Consequently, it is difficult to predict the head changes within the next 7 years for every little change in the irrigation practise. Therefore, fixed reduction percentages are set to evaluate the head changes.

Assuming that it is possible to reduce irrigation water by a certain percentage, the expected heads at the end of the prediction period are certainly higher than those obtained in Alternative I. However, the relative changes in heads are worth investigating. Alternative II is, therefore, to reduce the irrigation water by 10, 20, 30, 40 and 50 per cent and evaluate the increase in heads.

The results of reducing irrigation water by different percentages at each observation well are shown in Figs. (5.5, 5.6, 5.7 and 5.8). It can be noticed that reducing irrigation water by 50% results in increase in heads by 5-6 meters at the observation wells. This amount of head increase is considered to be large especially in a confined aquifer such as the UER. Fig.5.9 shows the heads at the last stress period with respect to different water reduction values. It is noticed that the slope of the line at well D6 is higher than the other lines. This may be due to higher transmissivity value at the well and to its location near the cone of depression. The location of well D6 makes it exposed to the effects of the surrounding wells more than the other observation wells. Figs. 5.10 to 5.14 show the head distribution in the study



Figure(5.5) The Effect of Reducing Irrigation Water on the Piezometric Head at Well B1 (From Nov. 1991 untill Oct. 1996)

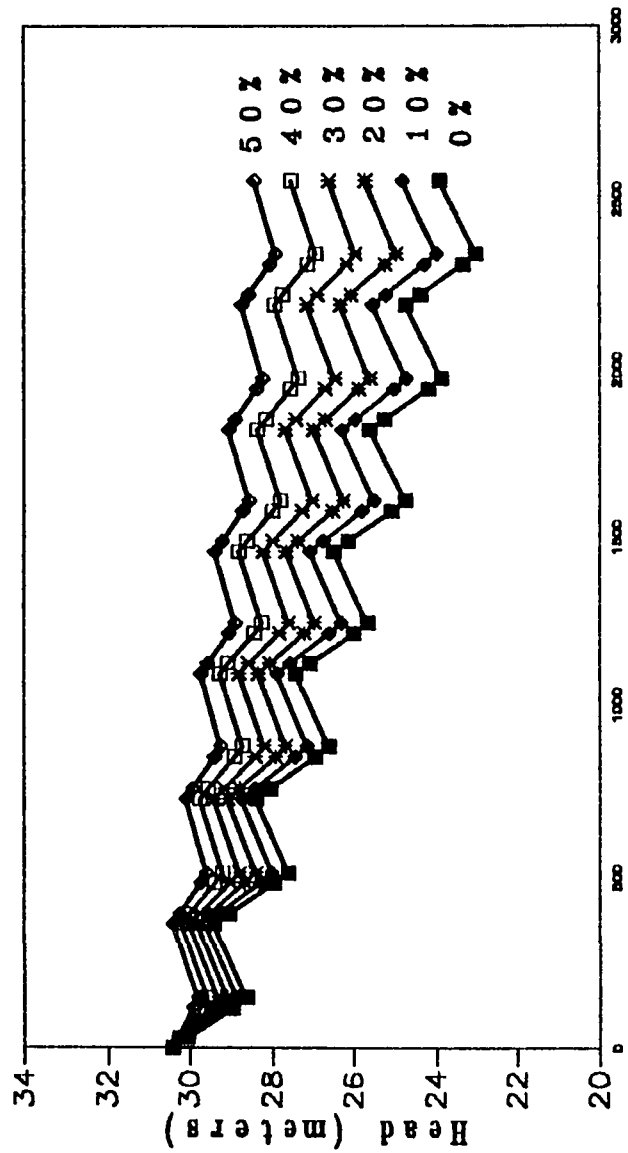
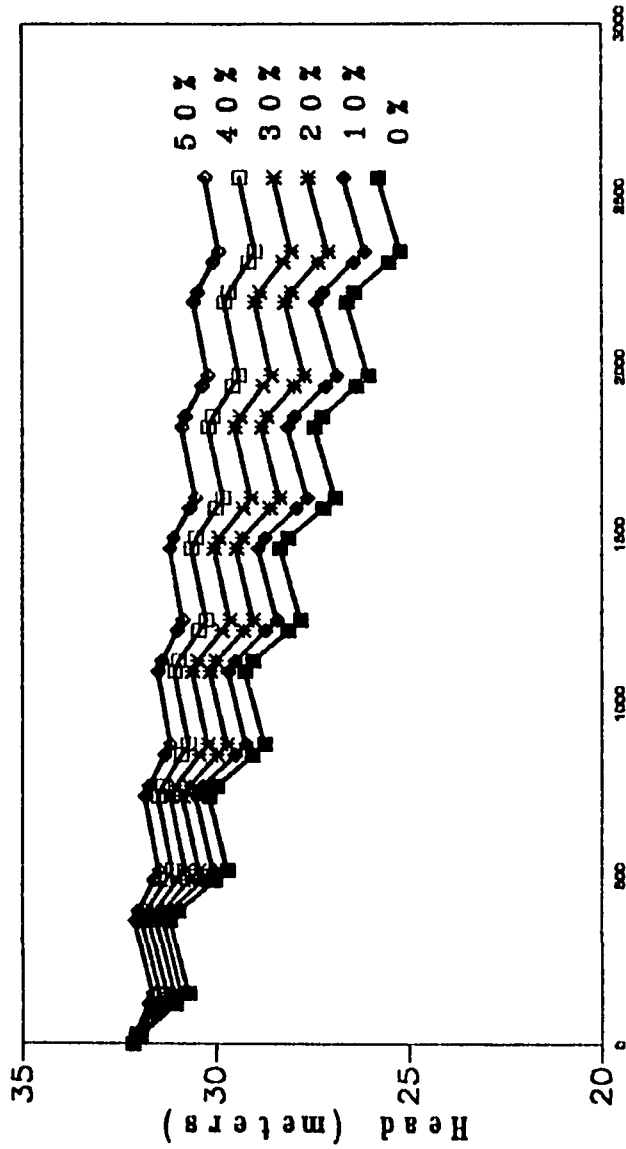
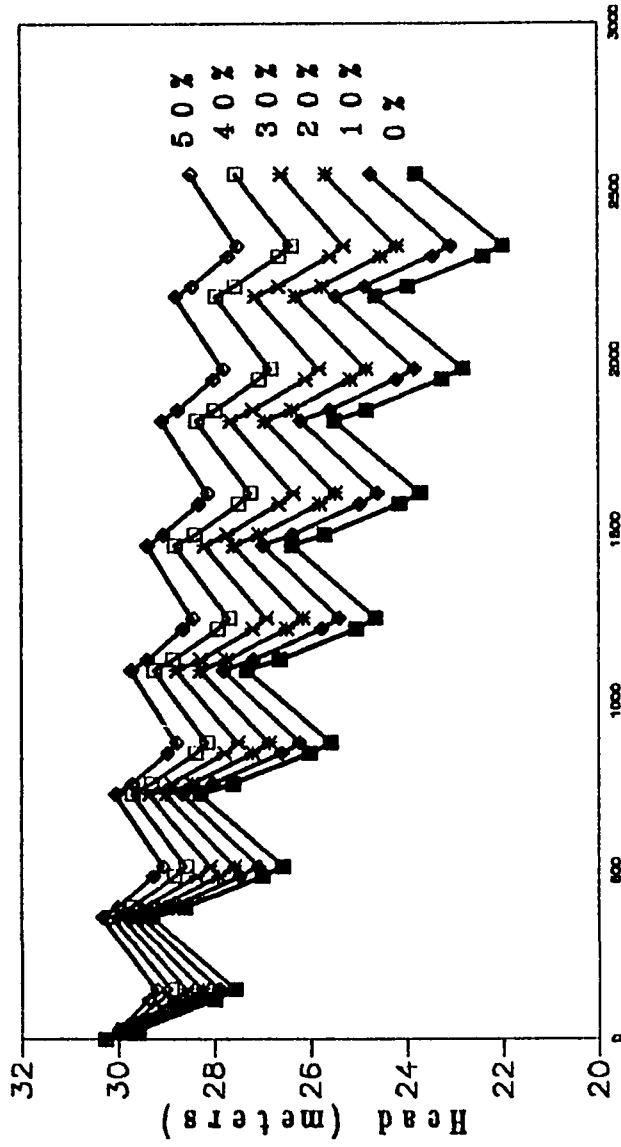


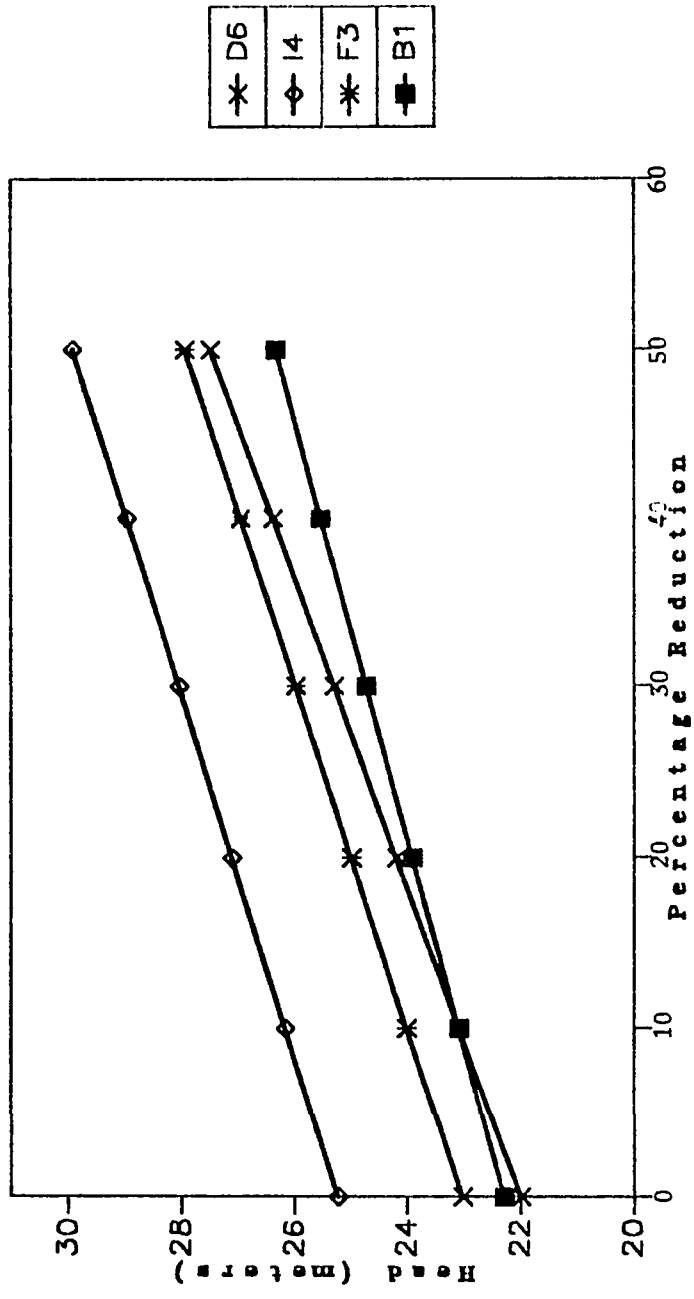
Figure (5.6) The Effect of Reducing Irrigation Water on the Piezometric Head at Well FS (From Nov. 1991 until Oct. 1998)



Figure(5.7)The Effect of Reducing Irrigation Water on the Peizometric Head at Well I4 (From Nov. 1991 untill Oct. 1998)



Figure(5.8)The Effect of Reducing Irrigation Water on the Peizometric Head at Well D6 (From Nov. 1991 untill Oct. 1998)



Figure(5.9) Heads at the End of Prediction Period versus Percentage of Reduction in Irrigation Water

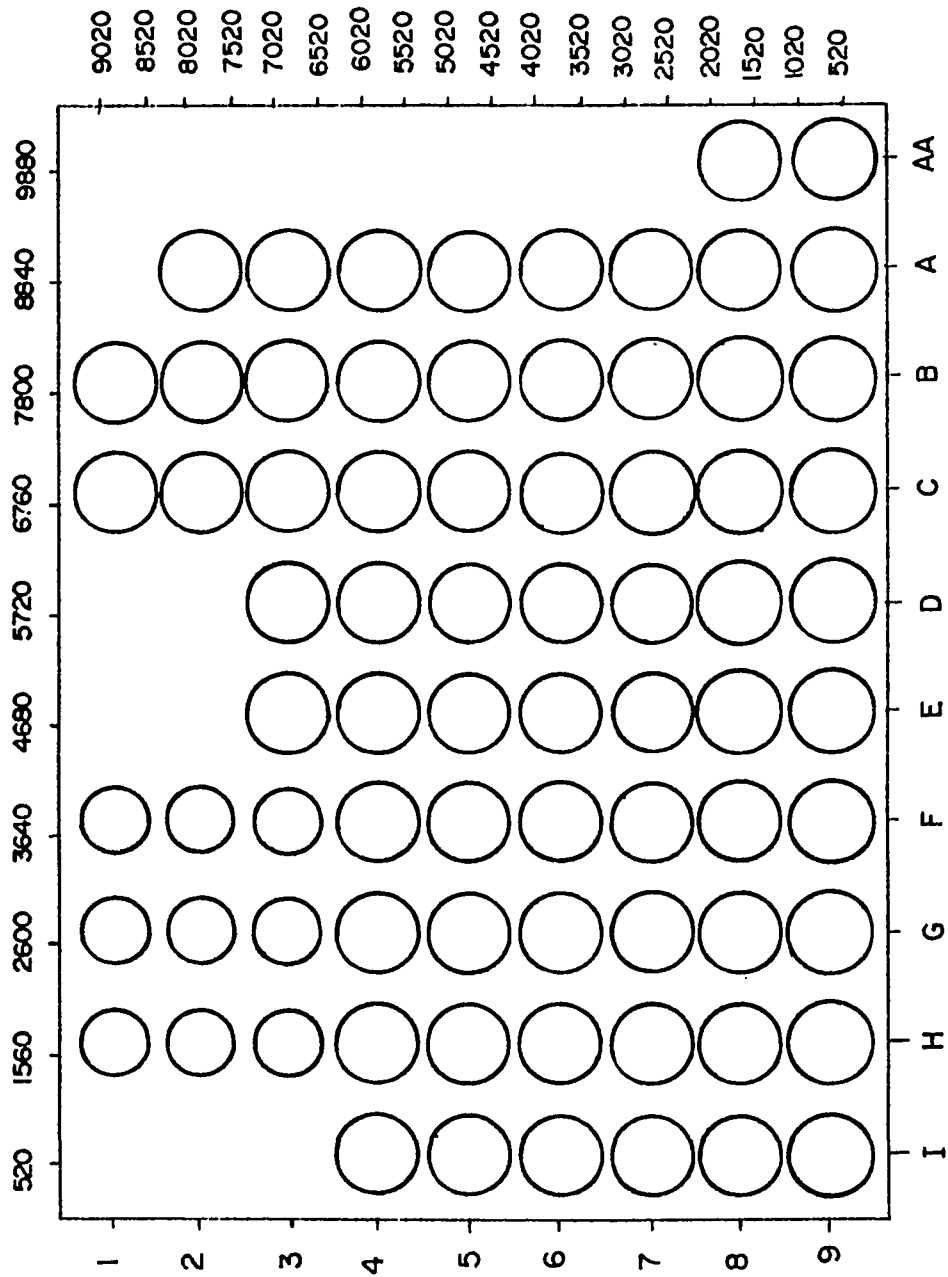


Fig. 5. N: Master Map for Figures 5.10 - 5.19.



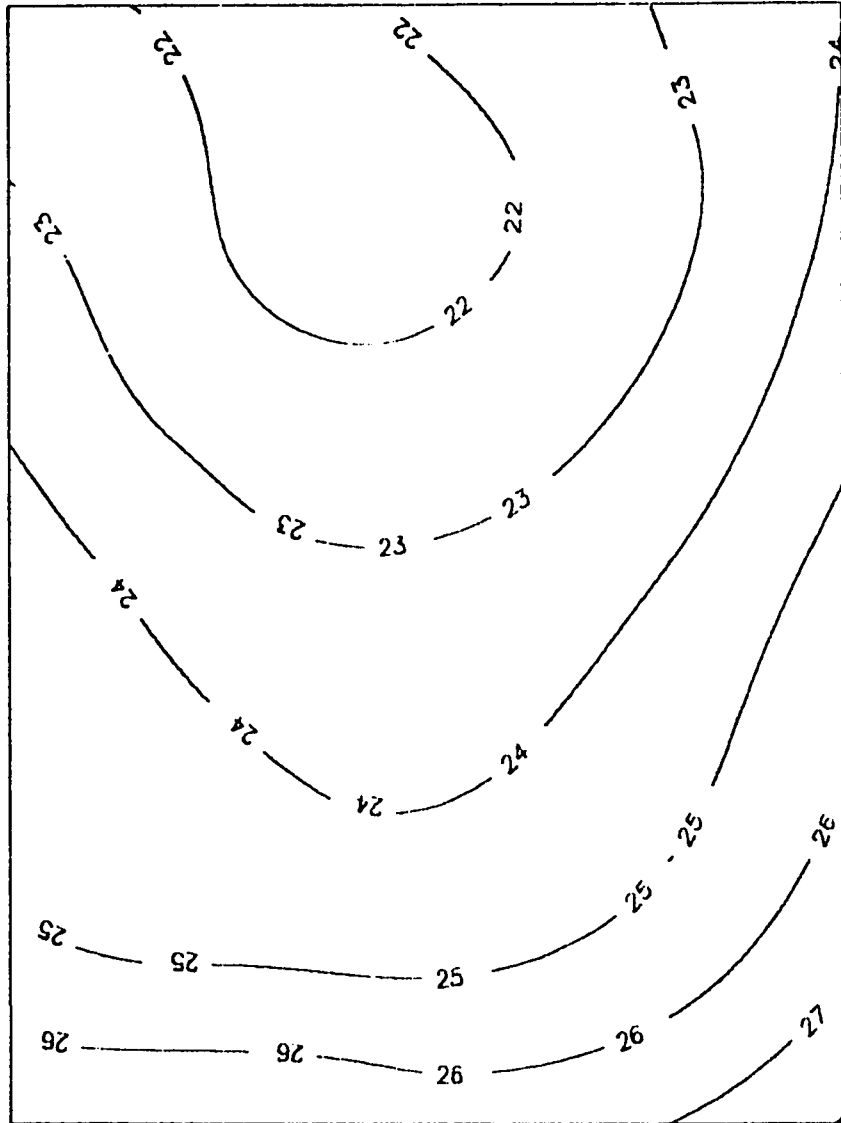


Fig. 5.10: Piezometric head map at the end of prediction period
 Alt. II - 10% Reduction in Irrigation water (meters).

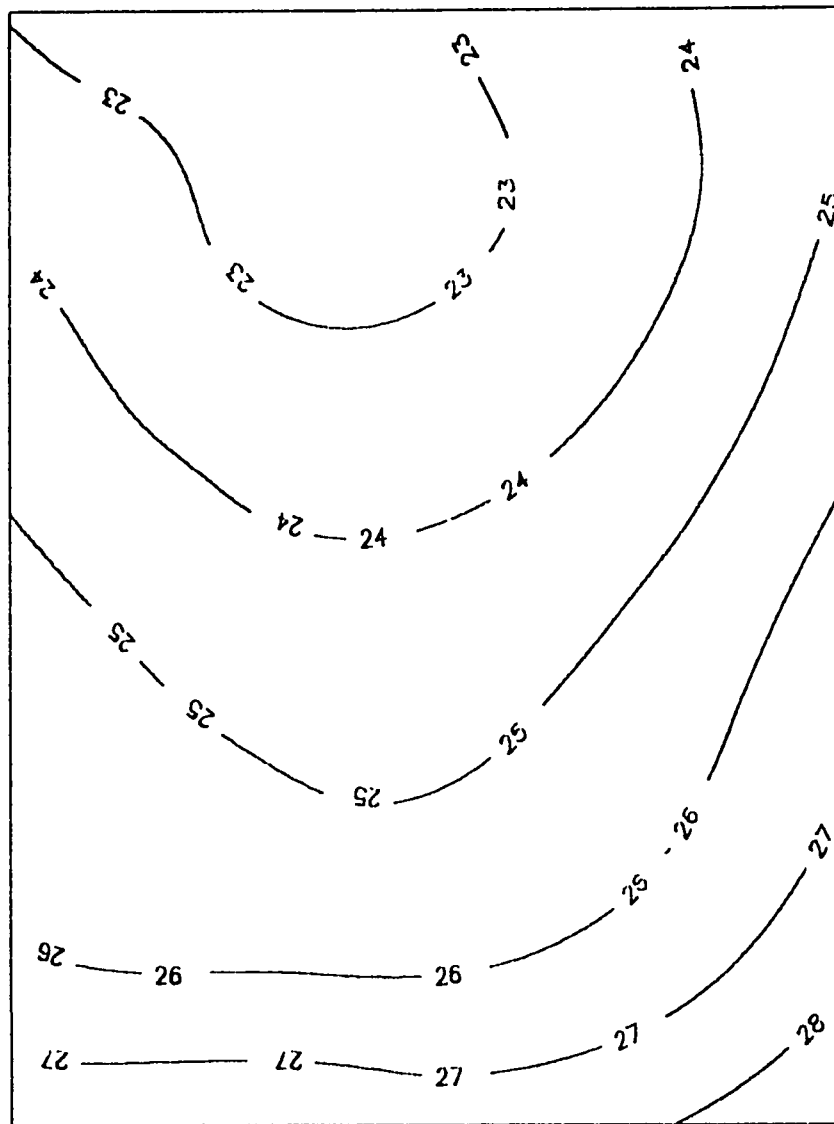


Fig. 5.11: Piezometric head map at the end of prediction period
 Alt.II - 20% Reduction in Irrigation water (meters)

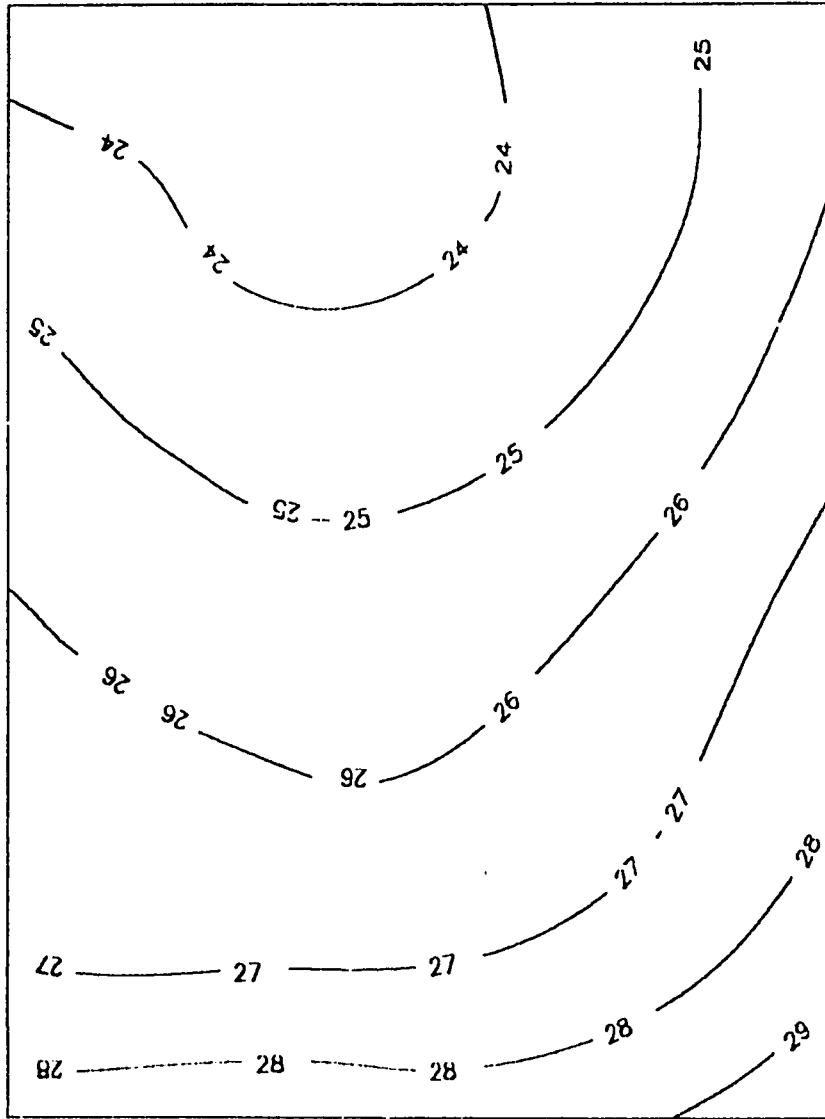


Fig. 5.12: Piezometric head map at the end of prediction period
 Alt.II - 30% Reduction in Irrigation water (meters)

(7)

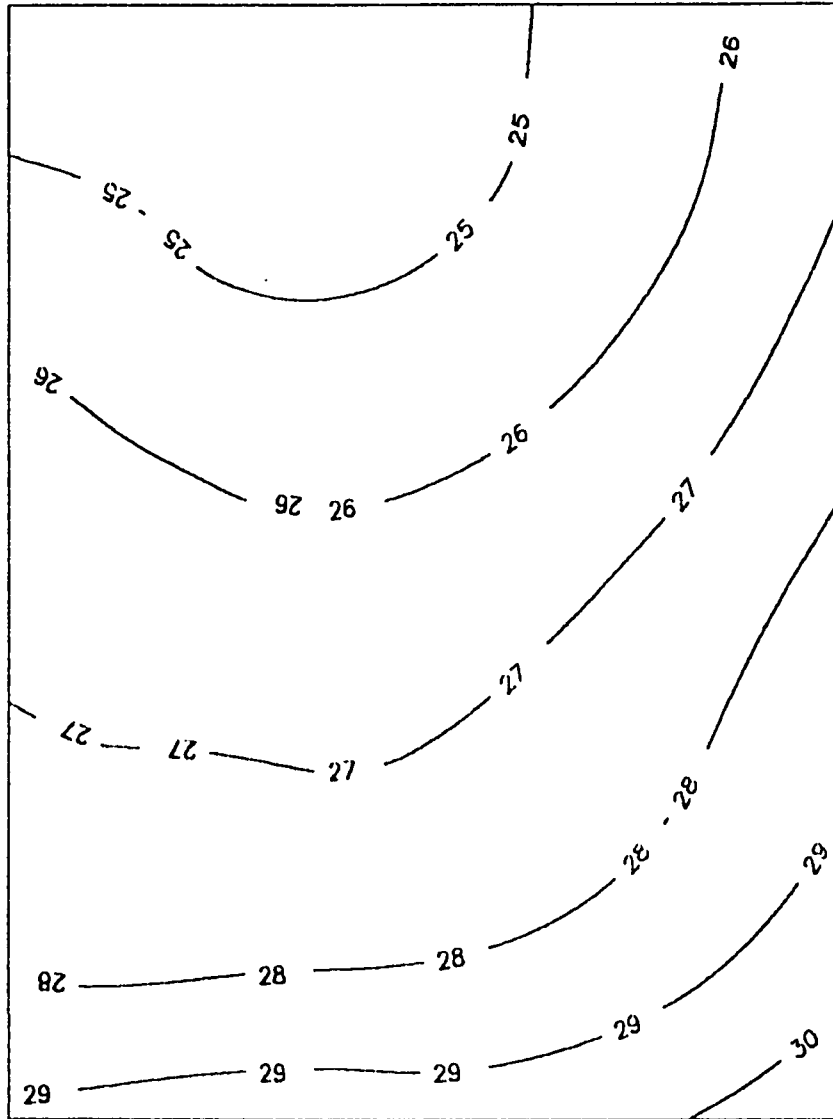


Fig. 5.12: Piezometric head map at the end of prediction period
 Alt.II - 40% Reduction in Irrigation water (meters)

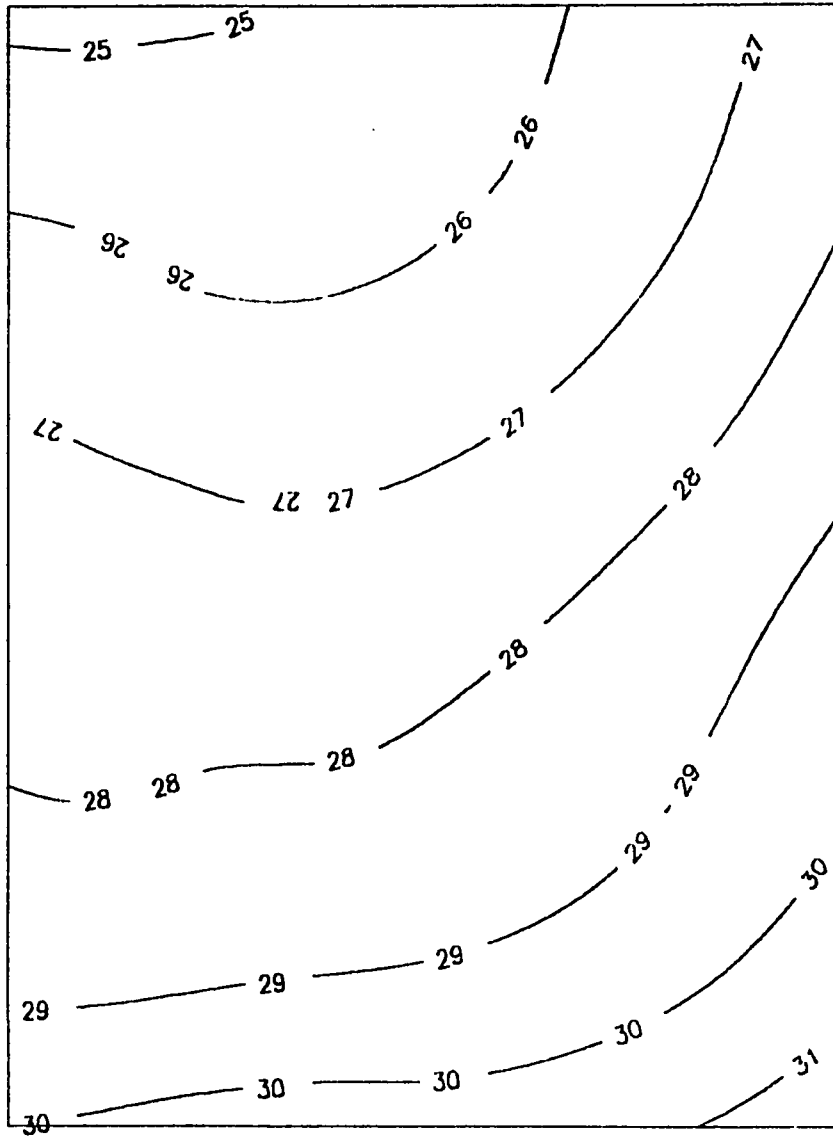


Fig. 5.14: Piezometric head map at the end of prediction period
 Alt.II - 50% Reduction in Irrigation water (meters)

area for each water reduction value. Figs. (5.15 to 5.19) show the corresponding drawdowns.

The graphs presented are important for the given percentage reductions in irrigation water. If a different percentage is reached at, one can always interpolate the graphs to determine the projected heads for that given value. Because the soil is more than 90% sand, higher reductions in irrigation waters are not expected.

5.4 ALTERNATIVE III

Upon investigating the heads predicted for Alternative I, one can conclude that the eastern part of the study area suffers low heads. It is logical to avoid stressing the eastern part by locating crops which are irrigated for a long period of time in that area. According to the management of SHADCO, the plans for choosing crops each season is made on yearly basis. The management, however, assures that the crops displayed in Table 5.1 for the season 1991/1992 will be exposed to $\pm 10\%$ maximum changes.

Assuming that the statement made by SHADCO management is true, Alternative I covers the prediction of the heads for the next 7 years. However, it is always wise to expect the worst. The same reasons that made SHADCO grow 11 Rhodus fields and 9 Alf-alf fields in the season 1987/1988 can show up again.

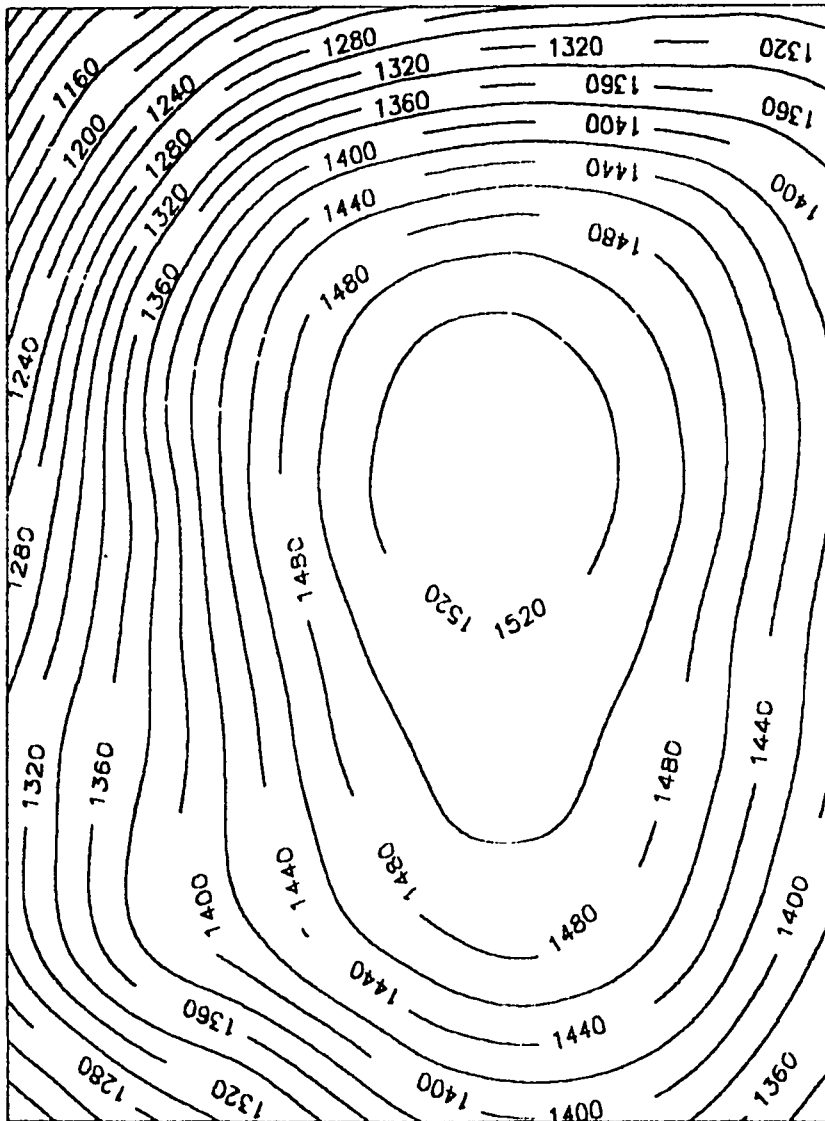


Fig. 5.15: Drawdown map at the end of prediction period
 Alt.II - 10% Reduction in Irrigation water (cm).

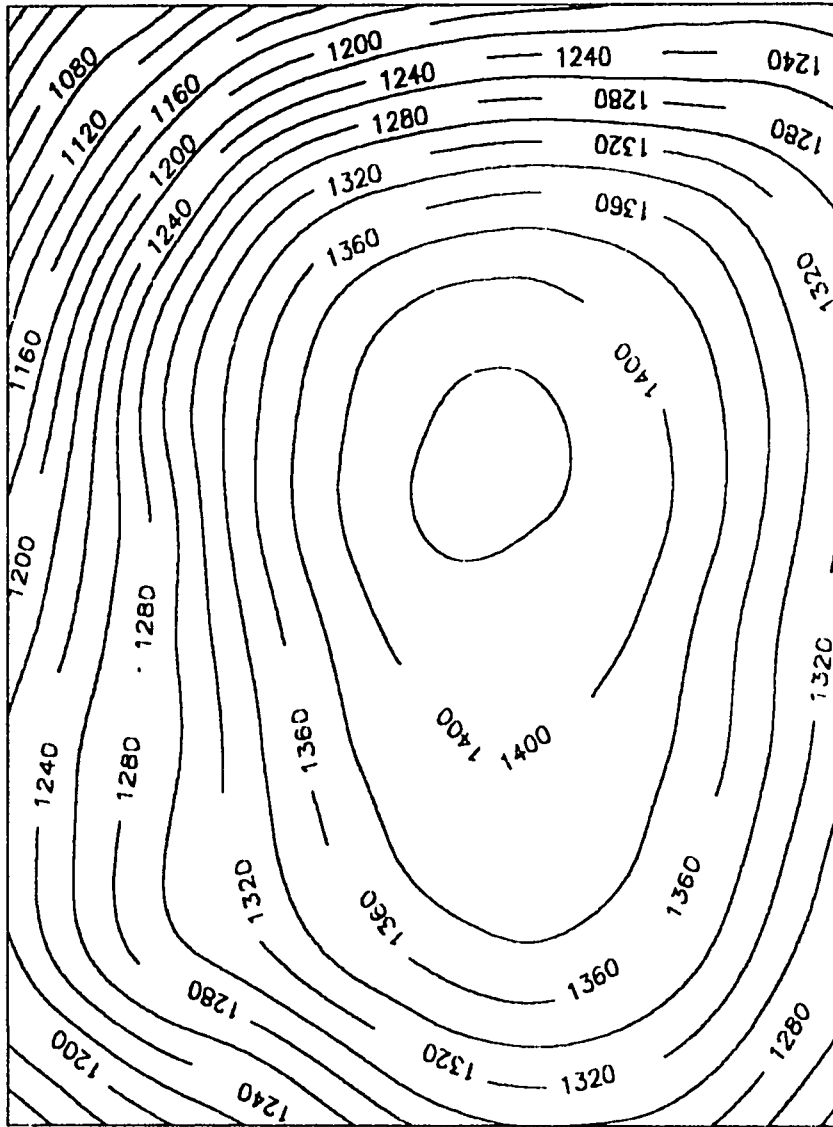


Fig. 5.16: Drawdown map at the end of prediction period
 Alt.II - 20% Reduction in Irrigation water (cm).

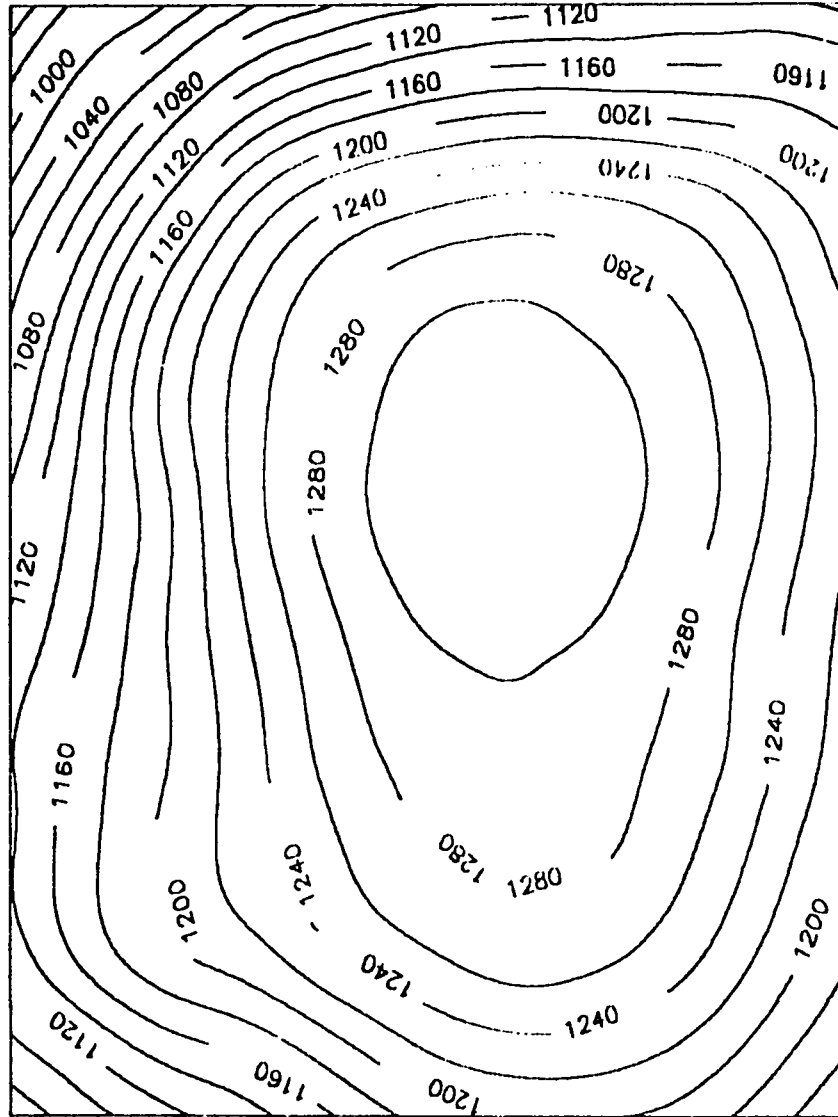


Fig. 5.17: Drawdown map at the end of prediction period
Alt.II - 30% Reduction in Irrigation water (cm).

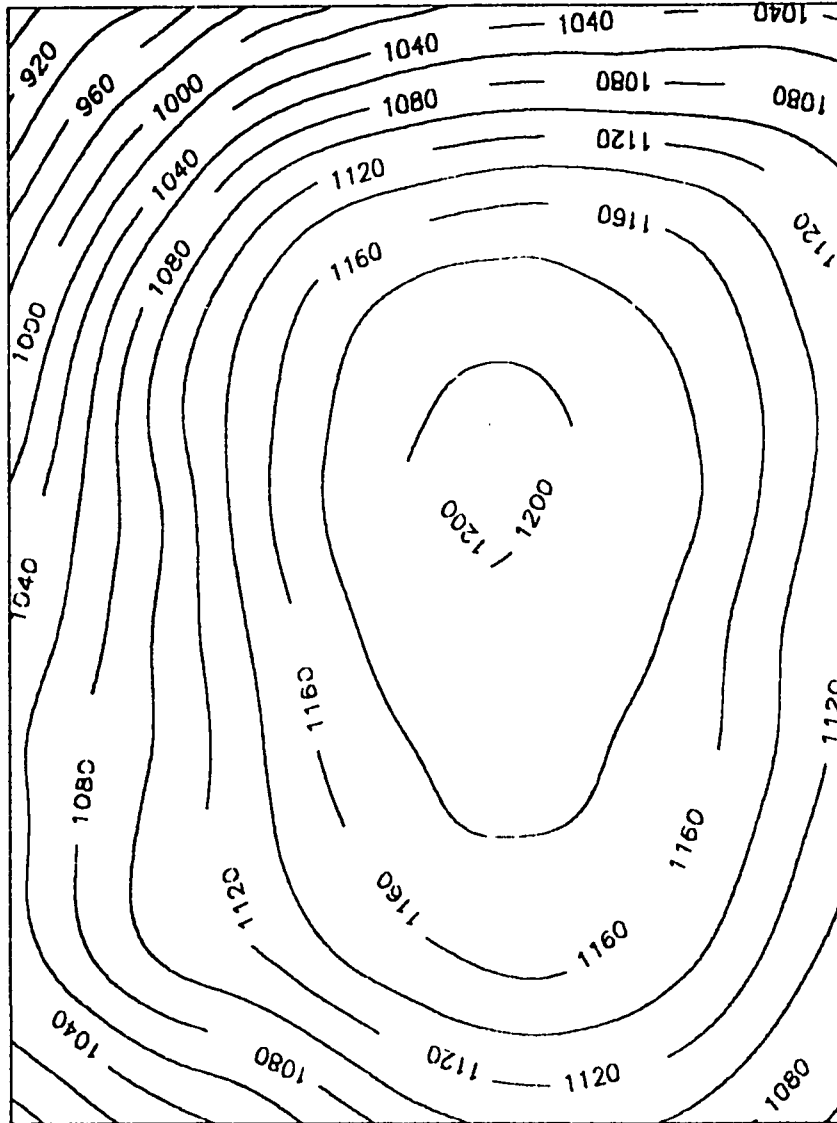


Fig. 5.18: Drawdown map at the end of prediction period
 Alt.II - 40; Reduction in Irrigation water (cm).

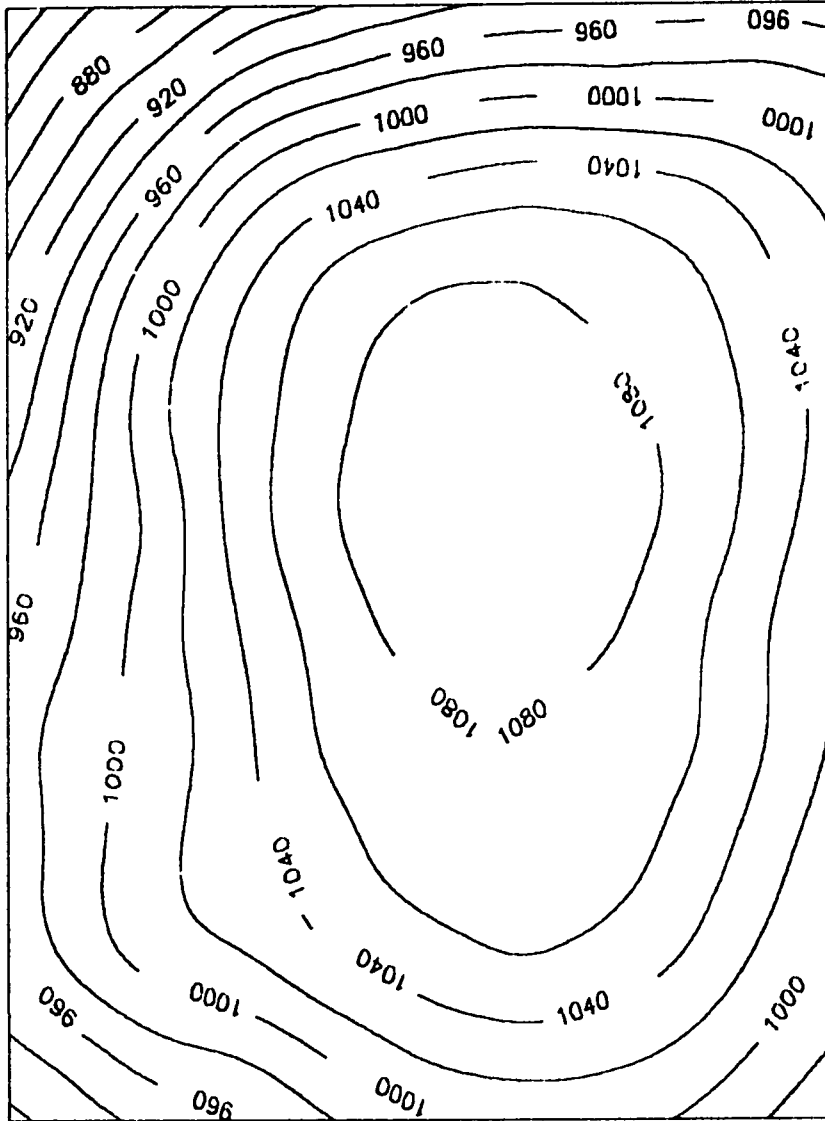


Fig. 5.19: Drawdown map at the end of prediction period
 Alt.II - 50% Reduction in Irrigation water (cm).

Therefore, Alternative III is to consider the cropping practise of the season 1987/1988 would be continued for the next 6 years. This is because the season 1991/1992 has already been decided on. The crops in season 1987/1988 were chosen for the prediction period due to the excess amount of water used to irrigate Rhodus (9 months) and Alf-alf (12 months).

At this stage, the low heads at the eastern part of the study area indicate the need for a crop distribution plan as to minimize the losses in heads at that part. Two distributions have been selected. In the first distribution, the crops that need long irrigation time (Rhodus and Alf-alf) are located within the cone of depression Fig. (5.20). The second distribution locates the same crops at the highest head lines in the study area (the western part) Fig. (5.21). The heads at the end of the prediction periods for Alt. 3-1 and Alt. 3-2 are shown in Figs. (5.22, 5.23). The corresponding drawdowns are shown in Figs. (5.24, 5.25).

the cone of depression is obviously located at the eastern part of the study area Fig. (5.24). It is also, obvious that this cone of depression has been effectively distorted by the relocation of the crops to the west of the study area Fig. (5.23). This fact is supported by the shift in the drawdown cone to the west of the study area. Fig. (5.26) shows the difference between the heads resulting from locating the heavily irrigated crops at the west part and the heads resulting from locating them at the east part of the

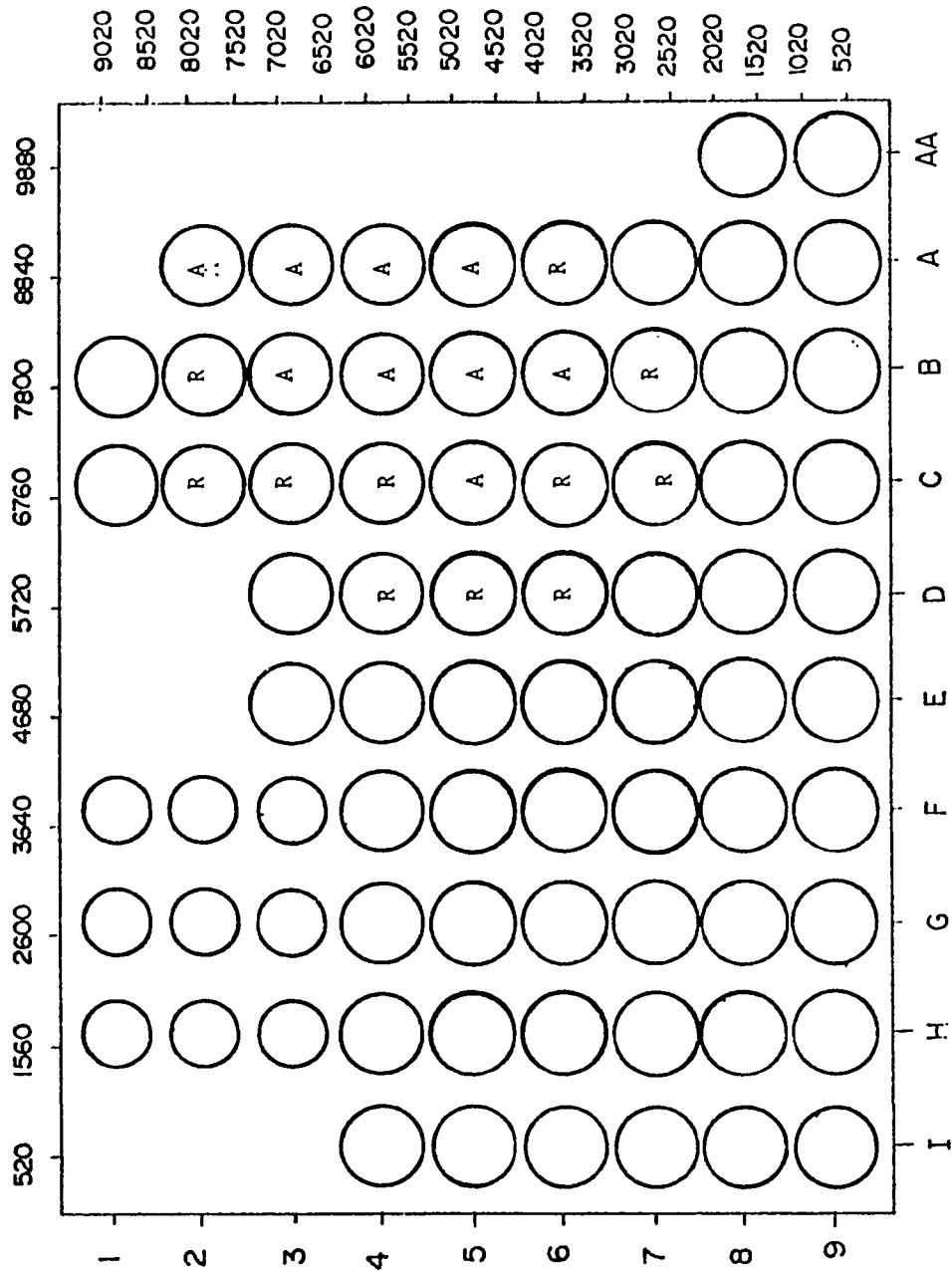
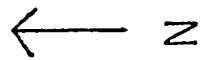


Fig. 5.20: Location of heavily irrigated crops - Alt.3-1.

R: Rhodus
A: Alf-alf



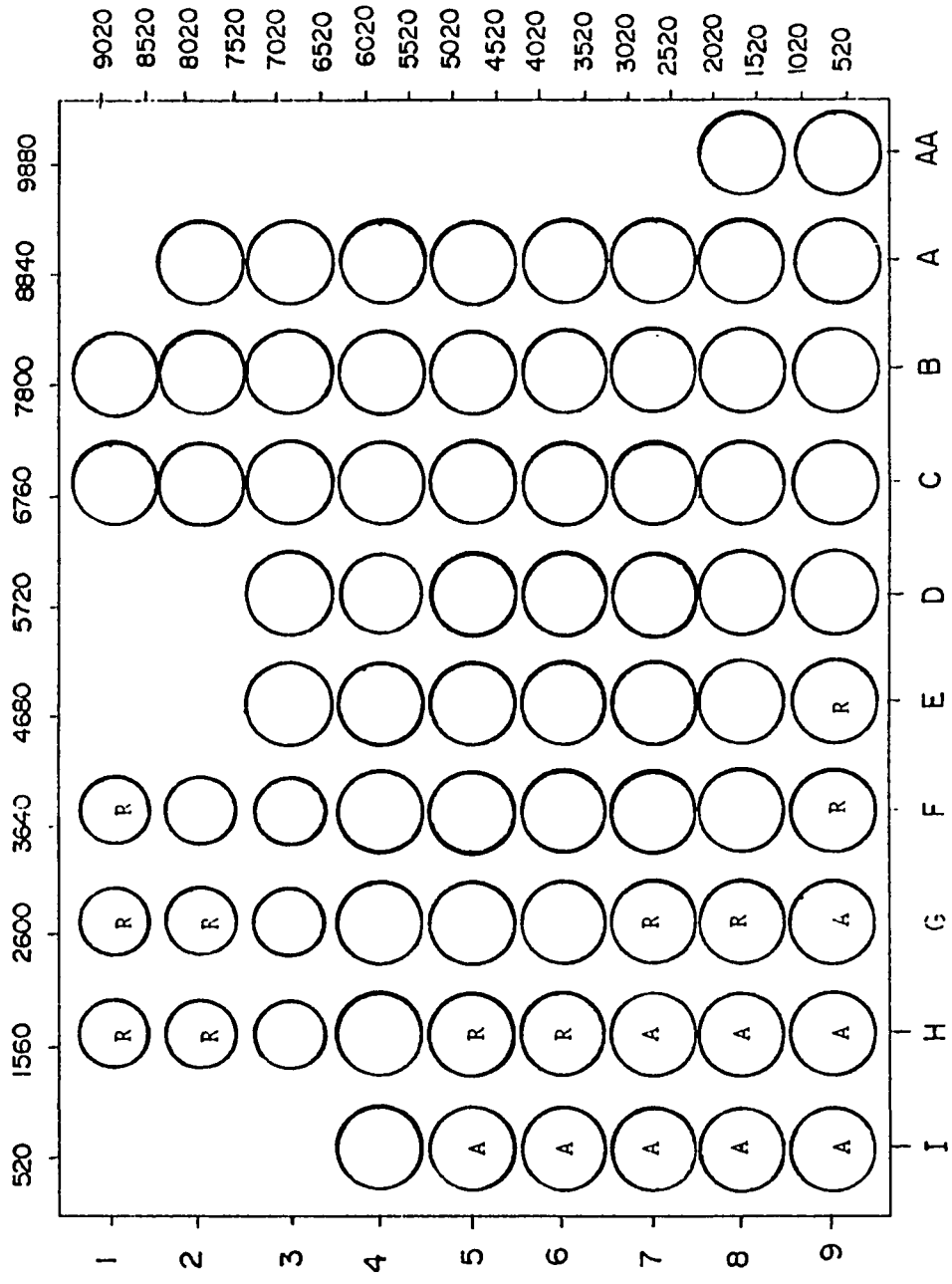


Fig. 5.21: Location of heavily irrigated crops, Alt.3-2.

R: Rhodus

A: Alf-alf



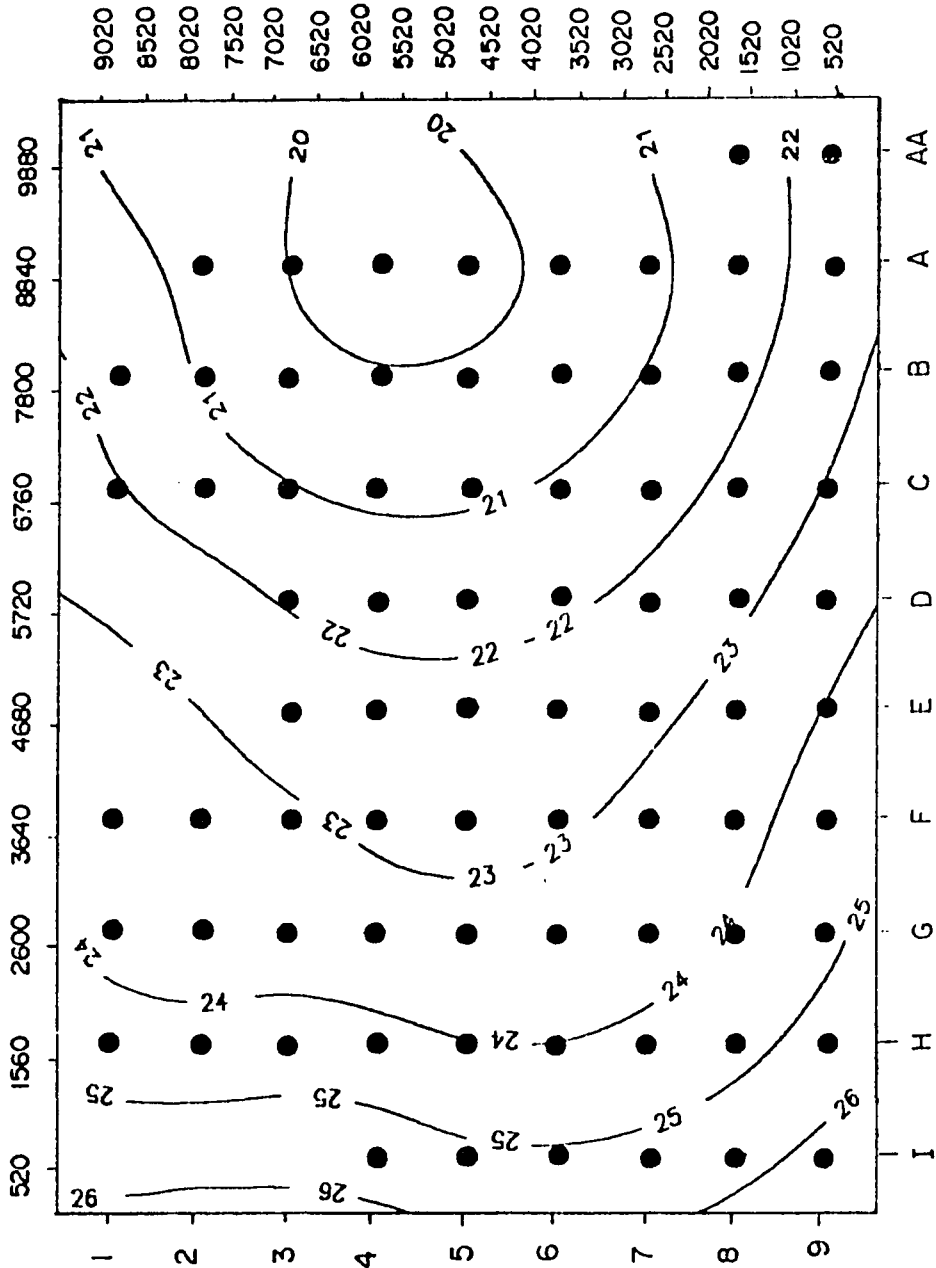


Fig. 5.22: - Piezometric head map at the end of prediction period
 - Alt. III-1. (meters)
 ● Wells

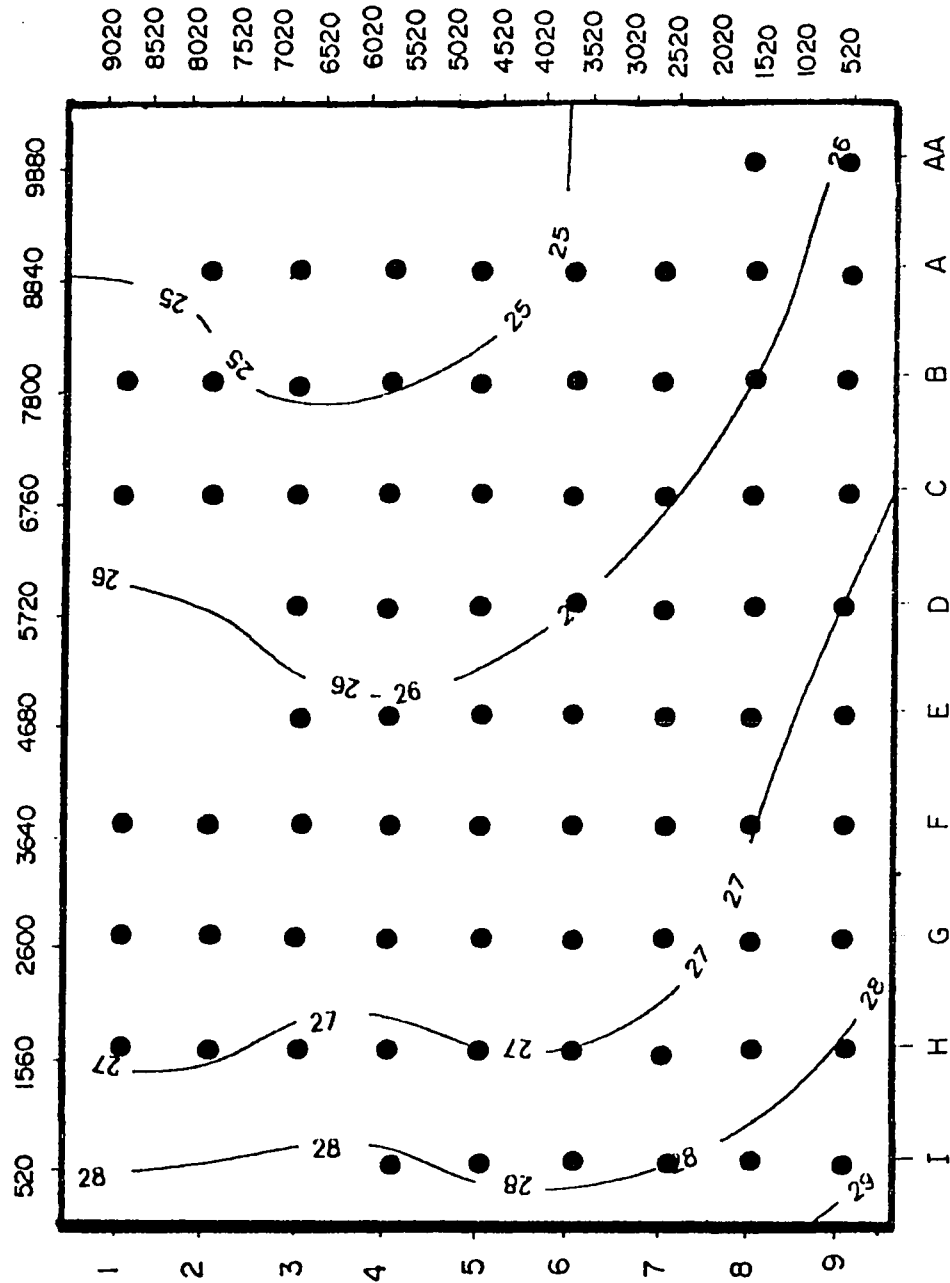


Fig. 5.23: - Piezometric head map at the end of prediction period
 - Alt. III-2. (meters)
 ● Wells



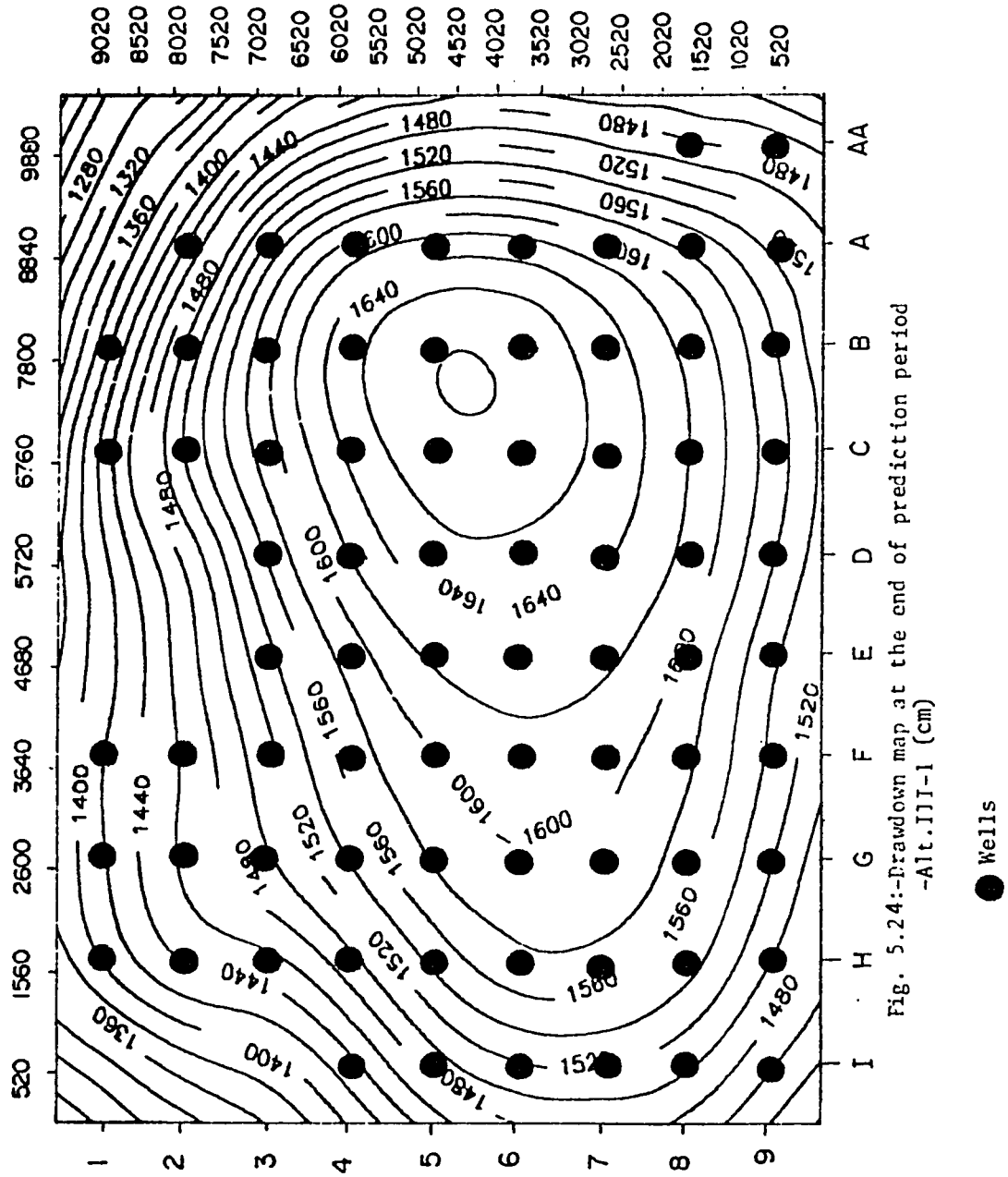


Fig. 5.24:-Drawdown map at the end of prediction period
-Alt.III-1 (cm)

● Wells



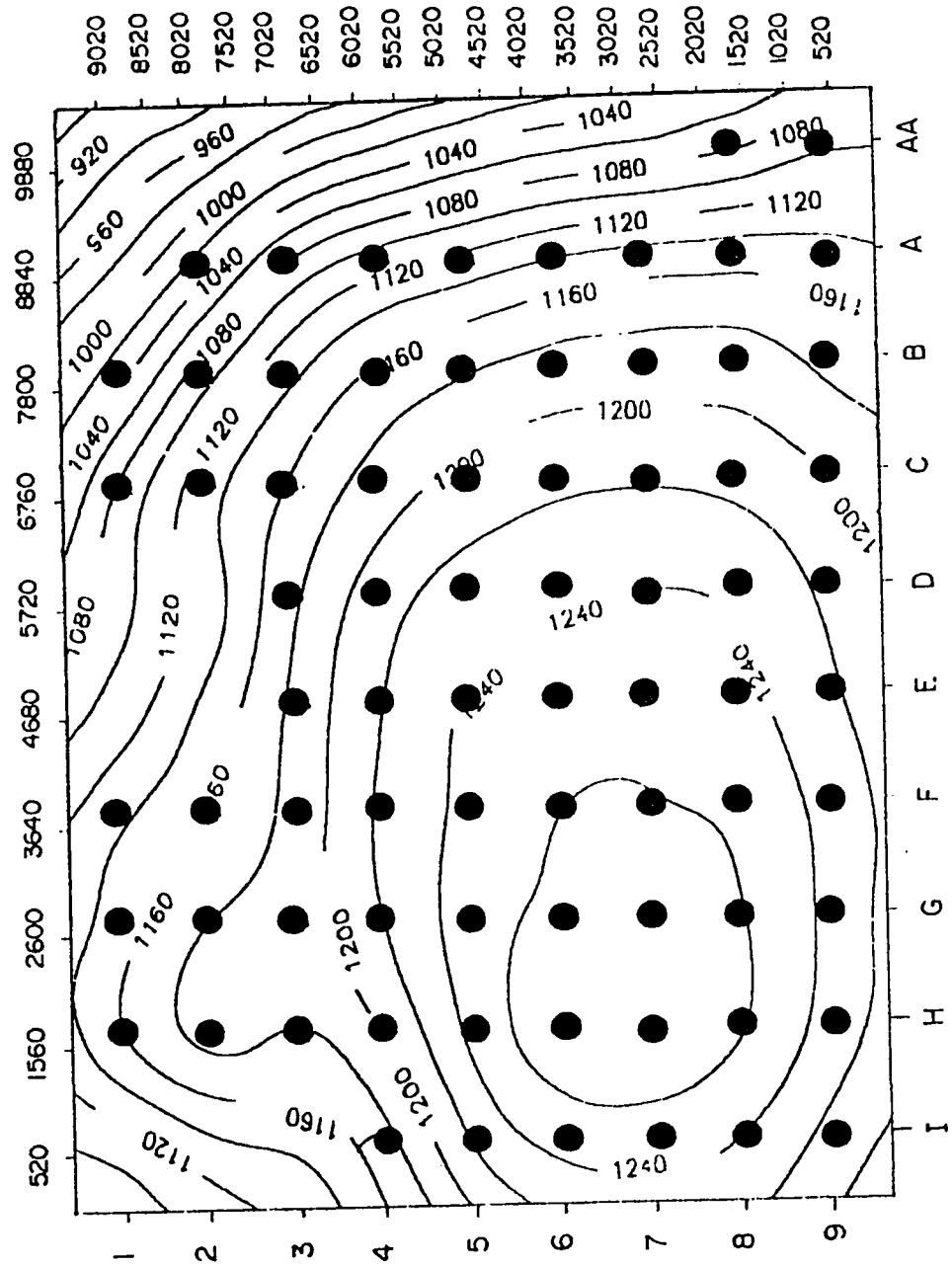


Fig. 5.25: - Drawdown map at the end of prediction period

- Alt. III-2. (cm)

● Wells

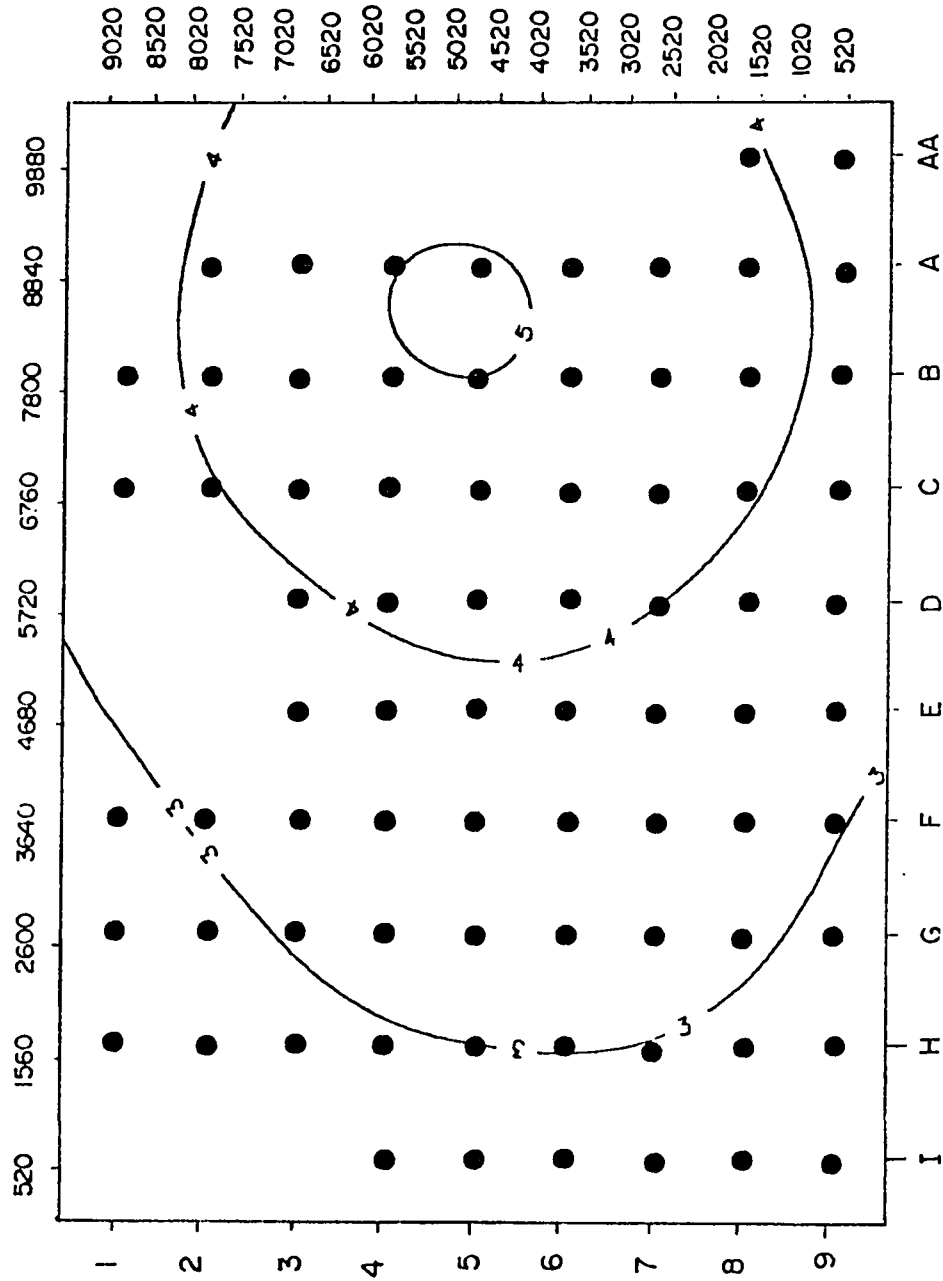


Fig. 5.26: The difference between the heads of Alt. III-2 and the heads in Alt. III-1. (meters)

● Wells



study area. It can be clearly noticed that this relocation has resulted in an increase in heads. The increase takes maximum values at the east part of the study area. More than 5 meters difference in heads can be noted at that particular place. Consequently, one can conclude that growing such types of crops should take place only at the west part of the study area. Figs. (5.27, 5.28) show the predicted heads at the observation wells B1, F3, I4, and D6. Because there is no relaxation period for the western part of the study area, the spring shape of the head at well I4 shown in Fig. (5.27) disappears in Fig. (5.28). This means that the western area in Alternative II-1 is continuously exposed to head decrease.

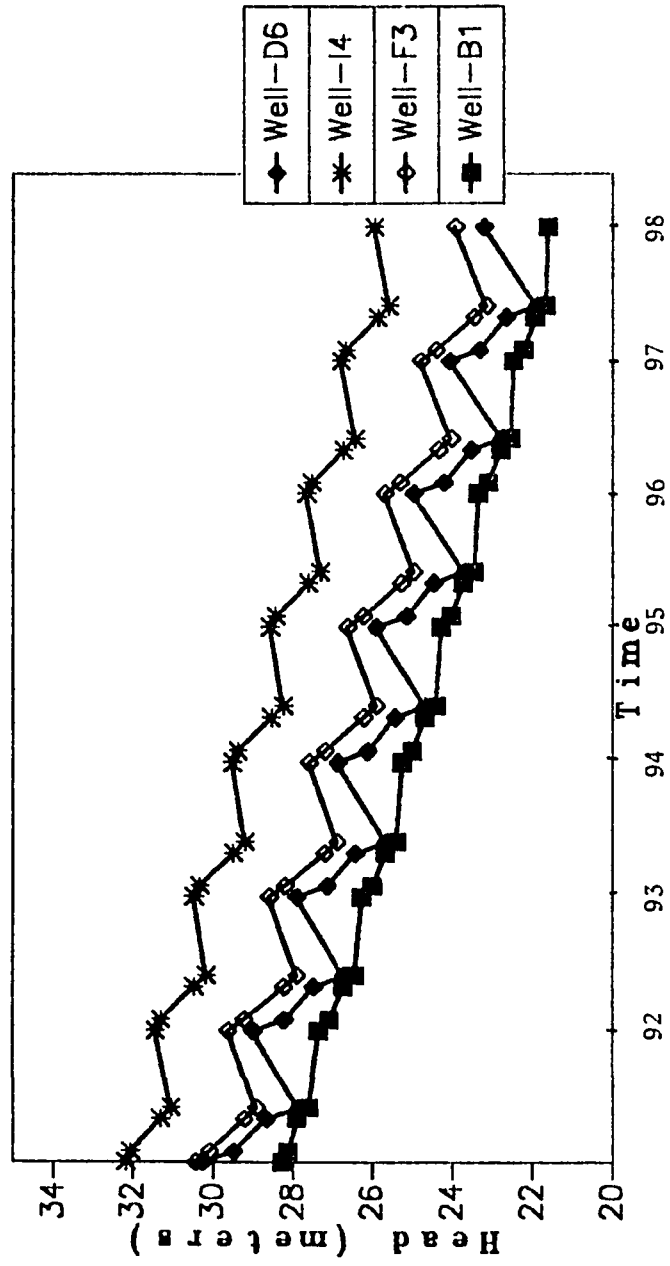


Figure (5.27) Simulated Heads for The Period 1991 untill 1998

Alternative III-1

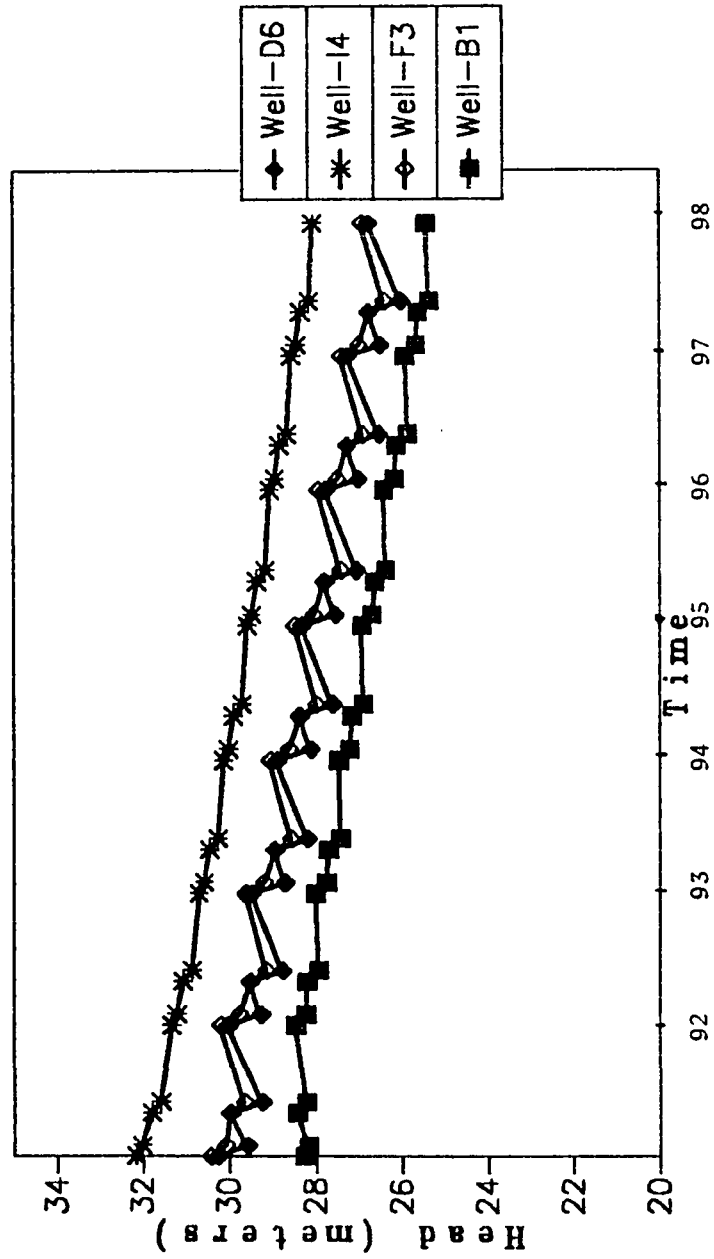


Figure (5.28) Simulated Heads for The Period 1991 untill 1998
Alternative III-2

CONCLUSIONS AND RECOMMENDATIONS

CONCLUSIONS

From the results obtained from this study, the following limited conclusions can be drawn:

- Two-dimensional finite difference model was used to simulate groundwater flow in the study area. Goodness of fit and sensitivity analysis were two measures to evaluate the accuracy of the model. After adjusting the physical parameters of the aquifer, the model showed agreement with the observed steady-state heads. The maximum difference was lower than 30 centimeters. High transmissivity values were generally observed during the steady state calibration stage. The transmissivity was high along the F-line running north to south.
- Transient calibration resulted in almost uniform storativity values.
- The study showed that the model is very sensitive to transmissivity. The model becomes less sensitive to transmissivity at high rather than at low values. At this stage, the flow of water through the geologic formations becomes similar to the flow in open channels at which transmissiv-

ity is of limited importance.

- The study showed that the aquifer is sensitive to changes in the conductance values of the head-dependent boundaries up to a limit where further decreases in the conductance values result in converting the head-dependent cells to no-flow boundaries.
- Piezometric heads are expected to be higher than those predicted by Alternative I if irrigation water is reduced. Five to six meters are expected to be saved if 30-50% of irrigation water is reduced.
- Piezometric heads are expected to be higher than those obtained from Alternative I by simply relocating heavily irrigated crops to the western part of the study area.

RECOMMENDATIONS

- Pumping tests should be performed on the wells during the relaxation period (April to October) so as to obtain better transmissivity and storativity values.
- The location of the observation wells is not suitable for monitoring water levels because all three wells lie on a straight line. The observation wells should be well

distributed so that full picture of the water levels in the study area can be obtained. The observation wells are best located according to a log scale.

- The crop water requirements should be determined. This is useful in determining the amount of water that can be reduced without affecting the quality and amount of the crop yields. The expected falls in the piezometric heads can be interpolated from the given graphs.
- The study showed that three to five meters of piezometric head can be saved during the next seven years by simply relocating heavily irrigated crops at the western part of the study area where the heads are high compared to the heads at the eastern part. Therefore , these crops should be located as far away from the low-head areas as possible.
- The study showed the importance of the relaxation period (April to October) in giving the water levels in the wells enough time to partly recover from the heavy pumping during the irrigation season. Crops such as Rhodus and Alf-alf are irrigated continuously throughout the year which eliminates the recovery period. Therefore , if economical factors are of limited importance , these crops should always be kept minimum.

- Three alternatives have been evaluated in this study. In alternative II, irrigation water is reduced while in alternative III, physical relocation of crops resulted in significant saving in piezometric heads. Consequently, a combination of these two alternatives would seem reasonable. Once the crop water requirements are determined and continuously irrigated crops are grown at the western part of the study area, better results can be obtained. However, in order to get best results, optimization techniques should be used.

REFERENCES

- 1) Allayla, R. I., Yazicigil, H. and DeJong, R. L., "Optimum Development of Groundwater Resources in Eastern Province", Unpublished Report to King Abdul Aziz City for Science and Technology (KACST), Saudi Arabia, 1986.
- 2) Allayla, R. I., DeJong, R. L. and Selen, W. J., "Alternative Strategies in Water Resources Development", General Directorate of Research Grants Programs - King Abdul Aziz City for Science and Technology (KACST), Saudi Arabia, 1991.
- 3) Bakiewicz, W., Mline, D. M. and Noori, M., "Hydrogeology of Umm Er Radhuma Aquifer, Saudi Arabia with Reference to Fossil Gradients", Quarterly Journal of Engineering Geology, London, Vol. 15, pp. 105-126, 1982.
- 4) Baturic-Rubicic, J., "The Study of Nonlinear Flow Through Porous Media by Means of Electrical Models", J. of Hydraulic Res., Vol. 7, No. 1, Delft, The Netherlands, 1969.
- 5) Bear, J. "Hydraulics of Groundwater", McGraw-Hill Book Co. Inc., New York, N.Y., 1979.
- 6) Bear, J. "Scales of Viscous Analogy Models for Ground Water Studies", J. Hydraulics Div., Am. Soc. Civil Engrs., pp. 11-23, Feb. 1960.
- 7) Bedinger, M. S. and Others, "Methods and Applications of Electrical Stimulation in Ground Water Studies in the Lower Arkansas and Verdigris River Valleys, Arkansas and Oklahoma", U.S. Geol. Survey Water Supply Paper 1971, 71 pp, 1970.
- 8) Bormes, B. J., "An Electric Analog Model for Use in Quantitative Studies, U.S. Geol. Survey Mimeographed Rept., 1960.
- 9) Boulton, N. S., "Analysis of Data from Non-Equilibrium Pumping Tests Allowing for Delayed Yield from Storage", Proc. Inst. Civ. Engr., Vol. 26, pp. 469-482, 1963.
- 10) Bredehoeft, J. D. and others, "Inertial and Storage Effects in Well-Aquifers Systems, an Analog Investigations", Water Resources Res., Vol. 2, No. 4, pp.697-707, 1966.

- 11) Bredehoeft, J. D., "Digital Analysis of Areal Flow in Multi-aquifer Ground Water Systems: a Quasi Three-Dimensional Model", *Water Resources Res.*, Vol. 6, No. 30, pp.883-888, 1970.
- 12) Bureau De Recherches Geologiques et Mineres (BRGM), "Al-Hassa Development Project: Groundwater Resources Study and Management Program", Unpublished Report to Ministry of Agriculture and Water, Riyadh, Saudi Arabia, 1977.
- 13) Chow, V. T., "On the Determination of Transmissivity and Storage Coefficients from Pumping Test Data", *Am. Geophys. Union Trans.*, Vol. 33, pp. 397-404, 1952.
- 14) Day, P. R. and Luthin, J. N., "Sand-Model Experiments on the Distribution of Water-Pressure under an Unlined Canal", *Proc. Soil Sci. Soc. Am.*, Vol. 18, No. 2, 1954.
- 15) Driscoll, F. G., "Groundwater and Wells", Johnson Division, St. Paul, Minnesota 55112, 1986.
- 16) Fetter, C. W., "Applied Hydrogeology", Merrill Publishing Co., Columbus, Ohio, 1988.
- 17) Freeze, R. A. and Cherry, J. A., "Groundwater", Prentice-Hall, Inc., Englewood Cliffs, New Jersey, N. J. 07632, 1979.
- 18) Groundwater Development Consultants (GDC). "Umm Er Radhuma Study: Bahrain Assignment", Demeter House, Station Road, Cambridge, CB1 2RS, Unpublished Report to Ministry of Agriculture and Water, Riyadh, Saudi Arabia, 1980.
- 19) Hantush, M. S., "Analysis of Data from Pumping Tests in Leaky Aquifers", *Am. Geophys. Union Trans.* Vol. 37, pp. 702-714, 1956.
- 20) Hansen, V. E., "Complicated Well Problems Solved by the Membrane Analogy", *Trans. Am. Geophys. Union*, Vol. 33, pp. 912-916, 1952.
- 21) Hele-Shaw, H.S., "Experiments on the Nature of the Surface Resistance in Pipes and on Ships", *Trans. Inst. Naval Architects*, Vol. 39, pp. 145-156, 1897.
- 22) Herbert, R., "Analyzing Pumping Tests by Resistance Network Analogue", *Ground Water*, Vol. 6, No. 2, pp. 12-19, 1968.
- 23) Hubbert, M. K., "Theory of Scale Models as Applied to the

- Study of Geologic Structures," , Bull. Geol. Soc. Am., Vol. 48, pp. 1456-1520, 1937.
- 24) Hurst, W., "Electrical Models as an Aid in Visualizing Flow in Condensate Reservoirs", The Petroleum Engr., Vol. 12, No. 10, pp. 123-124, 1941.
 - 25) Italconsult, "Water and Agricultural Development Studies for Area IV, Eastern Province, Saudi Arabia", Unpublished Report to Ministry of Agriculture and Water, Riyadh, Saudi Arabia, 1969.
 - 26) Jacob, C. E., "On the Flow of Water in an Elastic Artesian Aquifer", Am. Geophys. Union Trans., Vol. 72, Part II: 574-586, 1940.
 - 27) Karplus, W. J., "Analog Simulation", McGraw-Hill Book Co. Inc., New York, 1958.
 - 28) King Fahd University of Petroleum and Minerals-Research Institute, "Comuterized Irrigation Water Management System for Al-Sharqiya Agricultural and Development Company - Final Report", King Fahd University of Petroleum and Minerals, Dhahran, Saudi Arabia, 1991.
 - 29) Krayenhoff Van De Leur, D. A., "Some Effects of the Unsaturated Zone on Non-Steady Free-Surface Groundwater Flow as Studied In a Scaled Granular Model, J. Geophys. Res., Vol. 67, pp. 4347-4362, Oct. 1962.
 - 30) Liebmann, G., "Solution of Partial Differential Equations with a Resistance Network Analogue", British J. of Applied Physics, Vol. 1, pp. 92-103, 1950.
 - 31) Luthin, J. N., "An Electrical Resistance Network Solving Drainage Problems, Soil Sci., Vol. 75, pp. 259-274, 1953.
 - 32) McDonald, M. G. and Harbaugh, A. W., "A Modular Three-Dimensional Finite-Difference Groundwater Flow Model", Scientific Publications Co., Washington, D. C., 1984.
 - 33) McWhorter, D. and D.K. Sunada, "Groundwater Hydrology and Hydraulics", Water Resources Publications, Fort Collins, U.S.A., 1977.
 - 34) Mein, R. G. and Turner, A. K., "A Study of the Drainage of Irrigated Sand Dunes Using an Electrical Resistance Analogue", J. Hydrology, Vol. 6, No. 1, Jan. 1968.

- 35) Moffit, F. H. and H. Bouchard, "Surveying", Harper & Row, Publishers, Inc., New York, N. Y., 1982.
- 36) Naimi, A. I., "The Groundwater of North Eastern Saudi Arabia", Fifth Arab Petroleum Congress, Cairo, Egypt, 1965.
- 37) Opsal, F. W., "Analysis of Two-and Three-Dimensional Ground-Water Flow by Electrical Analogy", The Trend in Eng. at the Univ. Washington, Vol. 7, No. 2, Seattle, pp. 15-20, 32, 1955.
- 38) Pinder, G. F. and Bredehoeft, J. D., "Ground Water Chemistry and the Transport Equation", Internat. Symp. on Mathematical Models in Hydrology, Internat. Assoc. Sci. Hydrology, Warsaw, July 1971.
- 39) Prickett, T.A. and Lonquist, C. G., "Comparison Between Analog and Digital Simulation Techniques for Aquifer Evaluation", Symp. of Tucson, Arizona, Internat. Assoc. Sci. Hydrology, 1968.
- 40) Prickett, T.A. and Lonquist, C. G., "Selected Digital Computer Techniques for Ground Water Resource Evaluation", Illinois State Water Survey, Bull. 55, Urbana, 62 pp., 1971.
- 41) Rasheedudin, M., H. Yazicigil, and R. Allayla "Numerical Modeling of a Multi-Aquifer System in Eastern Saudi Arabia", Journal of Hydrology, 107:193-222, The Netherlands, 1989.
- 42) Santing, G., "A Horizontal Scale Model, Based on the Viscous Flow Analogy, for Studying Ground-Water Flow on an Aquifer Having Storage", General Assembly of Toronto, Internat. Assoc. Sci. Hydrology, pp. 105-114, 1957.
- 43) Stallworth, T. W., "Quickly Constructed Model Facilities Seepage Studies", Civil Eng., Vol. 20, No. 7, pp. 45-46, 1950.
- 44) Sternberg, Y. and Scott, V., "The Hele-Shaw Model as a Tool in Ground-Water Research, Natl. Water Well Assoc. Conf., San Francisco, Sept. 1963.
- 45) Theis, C. V., "The Relation Between the Lowering of the Piezometric Surface and the Rate and Duration of Discharge of a Well Using Groundwater Storage, Am. Geophys. Union Trans., Vol. 16: 519-524, 1935.
- 46) Thiem, G., "Hydrologische Methoden", Gebhardt, Leipzig, 56

p., 1906.

- 47) Todd, D. K., "Unsteady Flow in Porous Media by Means of a Hele-Shaw Viscous Fluid Model", *Trans. Am. Geophys. Union*, Vol. 35, pp. 905-916, 1954.
- 48) Todd, D. K., "Flow in Porous Media Studied in Hele-Shaw Channel, *Civil Engineering*", Vol. 25, No. 2, p. 85, 1955.
- 49) Todd, D. K., "Laboratory Research with Ground-Water Models", *Symposia Darcy, Internat. Assoc. Sci. Hydrology*, Pub. 41, pp. 199-206, 1956.
- 50) Vreedenburgh, C. G. J. and Stevens, O., "Electric Investigation of Underground Water Flow Nets", *Proc. Internat. Conf. Soil Mech. and Foundation Eng.*, Vol. 1, Harvard Univ., Cambridge, Mass., pp. 219-222, 1936.
- 51) Walton, W. C. and Walker, W. H., "Evaluation of Wells and Aquifers by Analytical Methods", *J. Geophys. Res.* Vol. 66, No. 10, 1961.
- 52) Walton, W. C., "Selected Analytical Methods for Well and Aquifer Evaluation", *Illinois State Water Survey Bull.* No. 49, 81 p., 1962.
- 53) Walton, W. C., "Electric Analog Computers and Hydrogeologic System Analysis in Illinois", *Ground Water*, Vol. 2, No. 4, 1964.
- 54) Wang, H. F. and M. Anderson, "Introduction to Groundwater Modeling", W. H. Freeman and Company, New York, 1982.
- 55) Williams, D. E., "Viscous Model Study of Ground-Water Flow in a Wedge-Shaped Aquifer", *Water Resources, Res.*, Vol. 2, No. 3, pp. 479-495, 1966.
- 56) Yazicigil, H., Allayla, R. I. and DeJong, R. L., "Numerical Modelling of the Damnam Aquifer in Eastern Saudi Arabia", *The Arabian Journal for Science and Engineering*, Vol. 11, No. 4, pp. 349-362, 1986.
- 57) Yazicigil, H., Allayla, R. I. and DeJong, R. L., "Optimal Management of a Regional Aquifer in Eastern Saudi Arabia", *Water Resources Bulletin*, Vol. 23, No. 3, pp. 423-433, 1987.
- 58) Yazicigil, H. and Rasheeduddin, M., "Optimization Model for Groundwater Management in Multi-Aquifer Systems", *Journal of Water Resources Planning and Management*, ASCE, Vol.

113, No. 2, pp. 257-273, 1987.

- 59) Zee, C. H., "Flow into a Well by Electric and Membrane Analogy", Proc. Am. Soc. Civil Engrs., Vol. 81, 817, 21 pp., Sep. 1955.

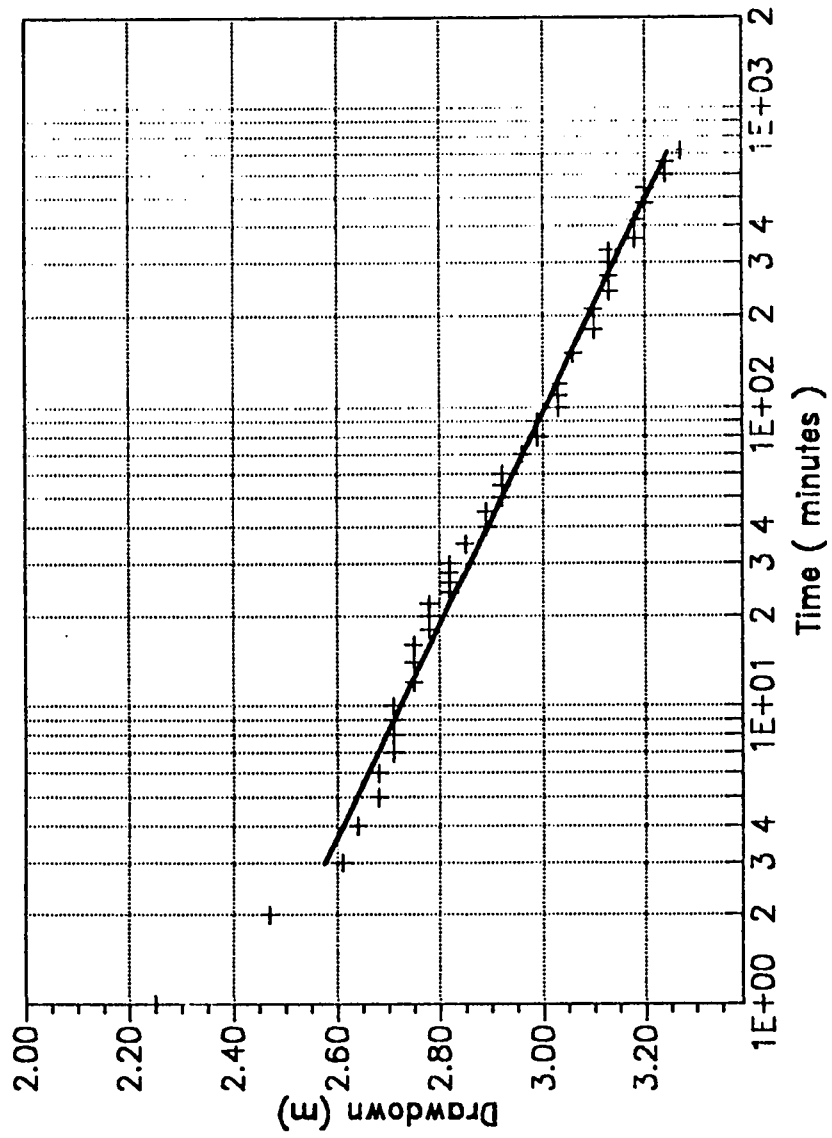
(5)

APPENDIX - A: PUMPING TEST GRAPHS

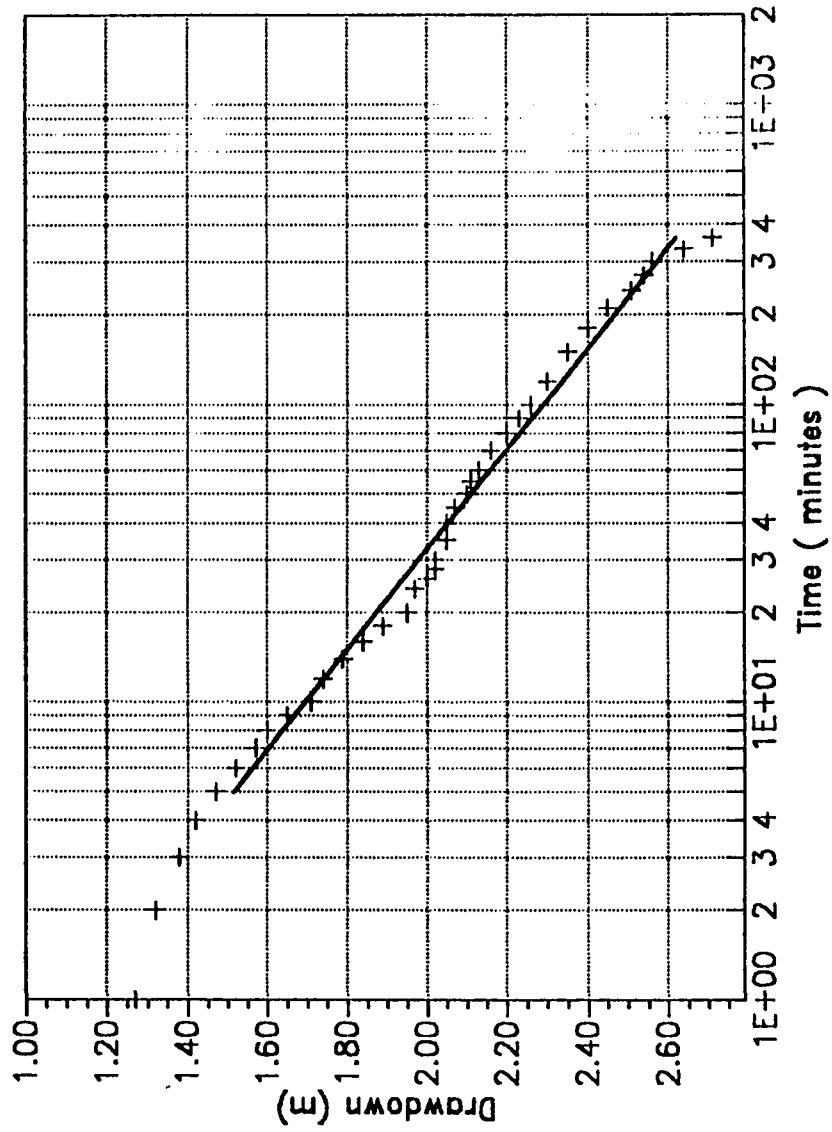
2

APPENDIX - A1: JACOB STRAIGHT LINE METHOD

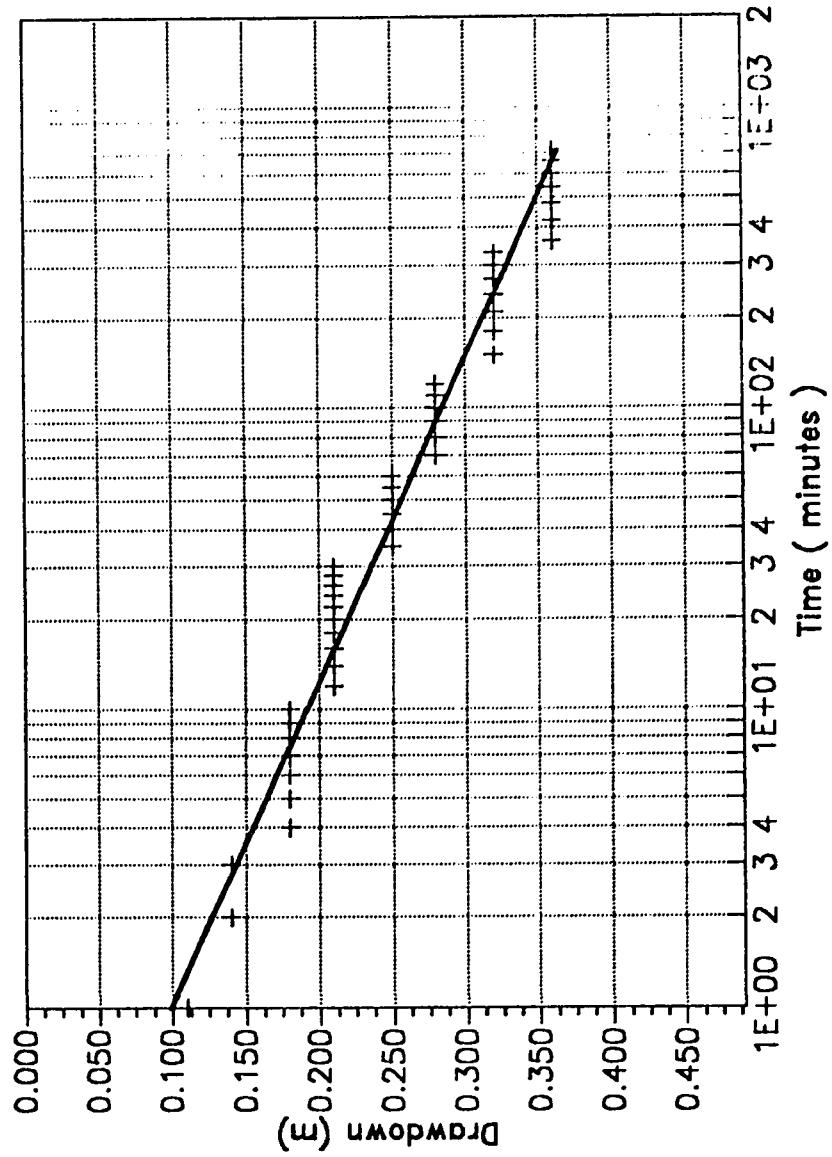
PUMPING TEST (JACOB METHOD) - WELL NO. A6



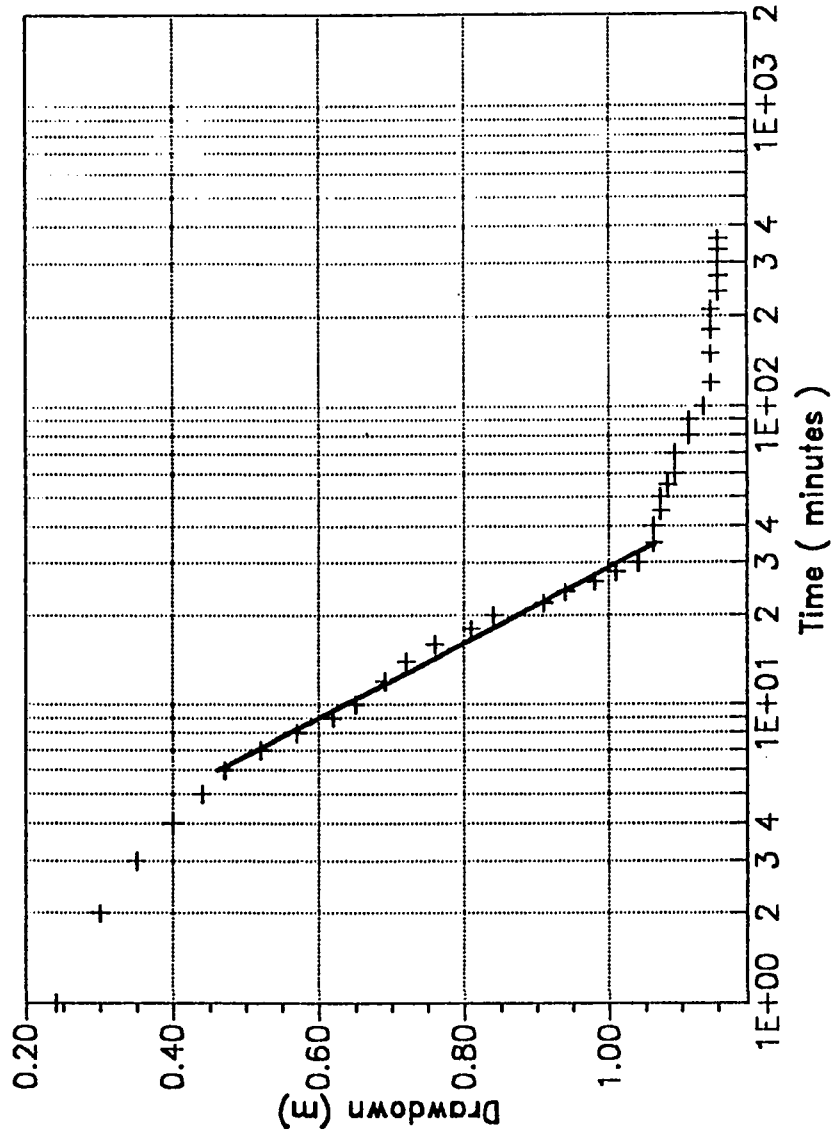
PUMPING TEST (JACOB METHOD) - WELL NO. A8



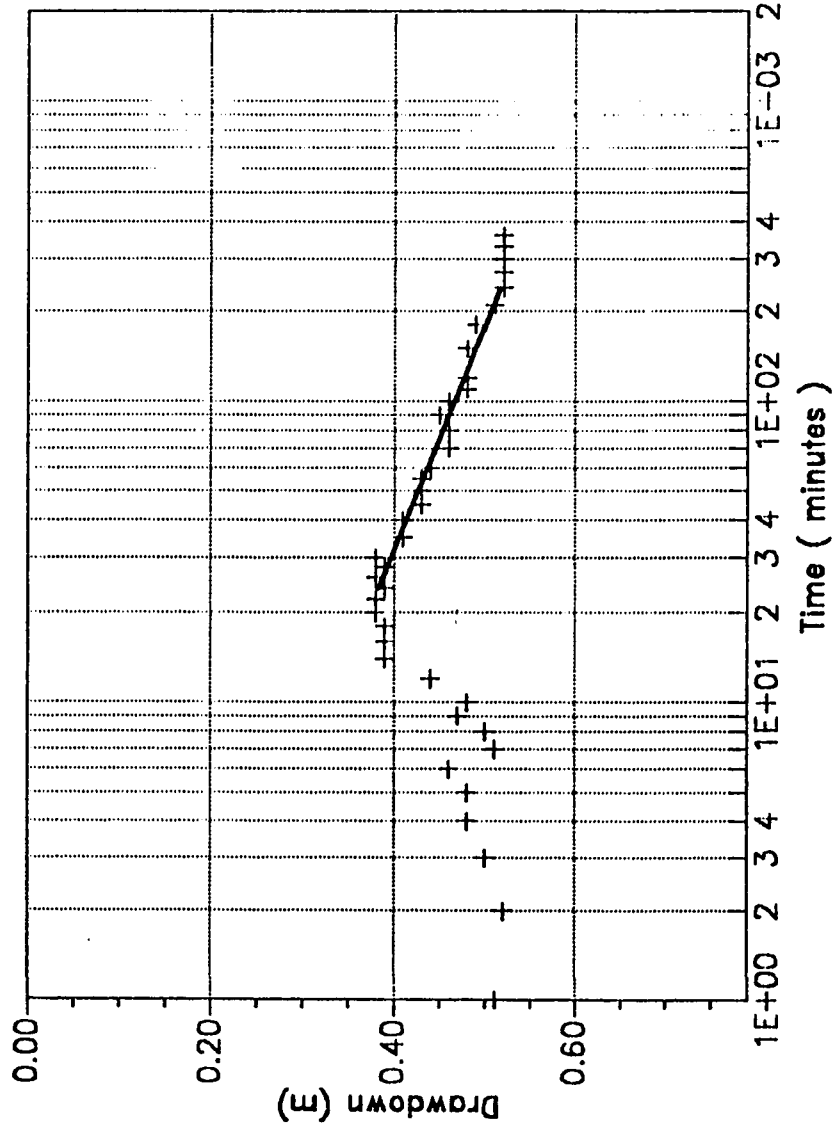
PUMPING TEST (JACOB METHOD) - WELL NO. B2



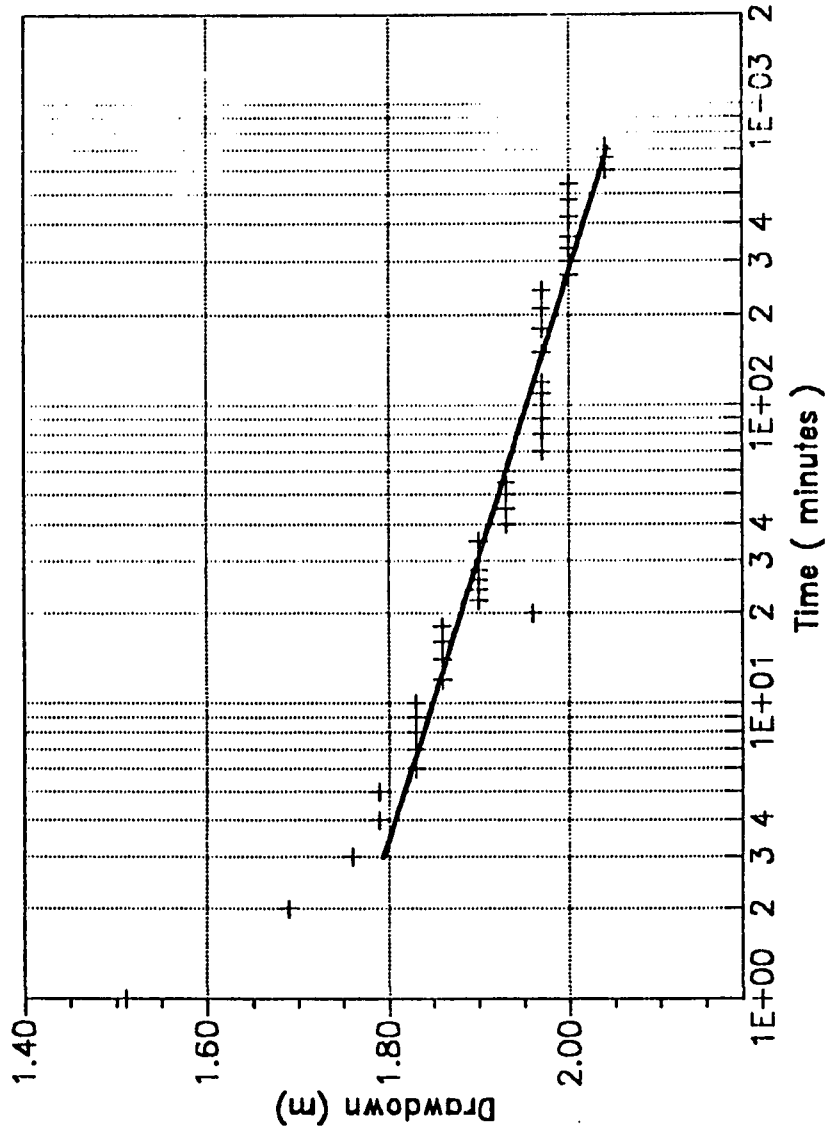
PUMPING TEST (JACOB METHOD) - WELL NO. B3



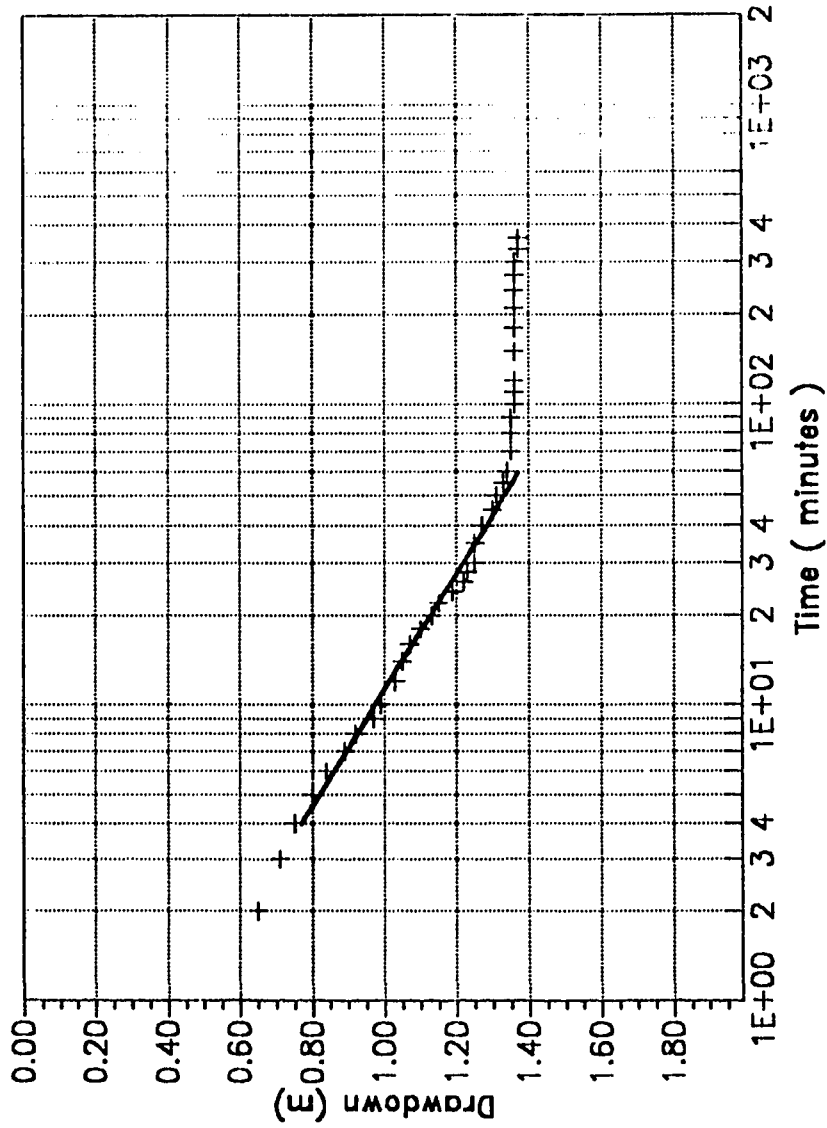
PUMPING TEST (JACOB METHOD) - WELL NO. B5



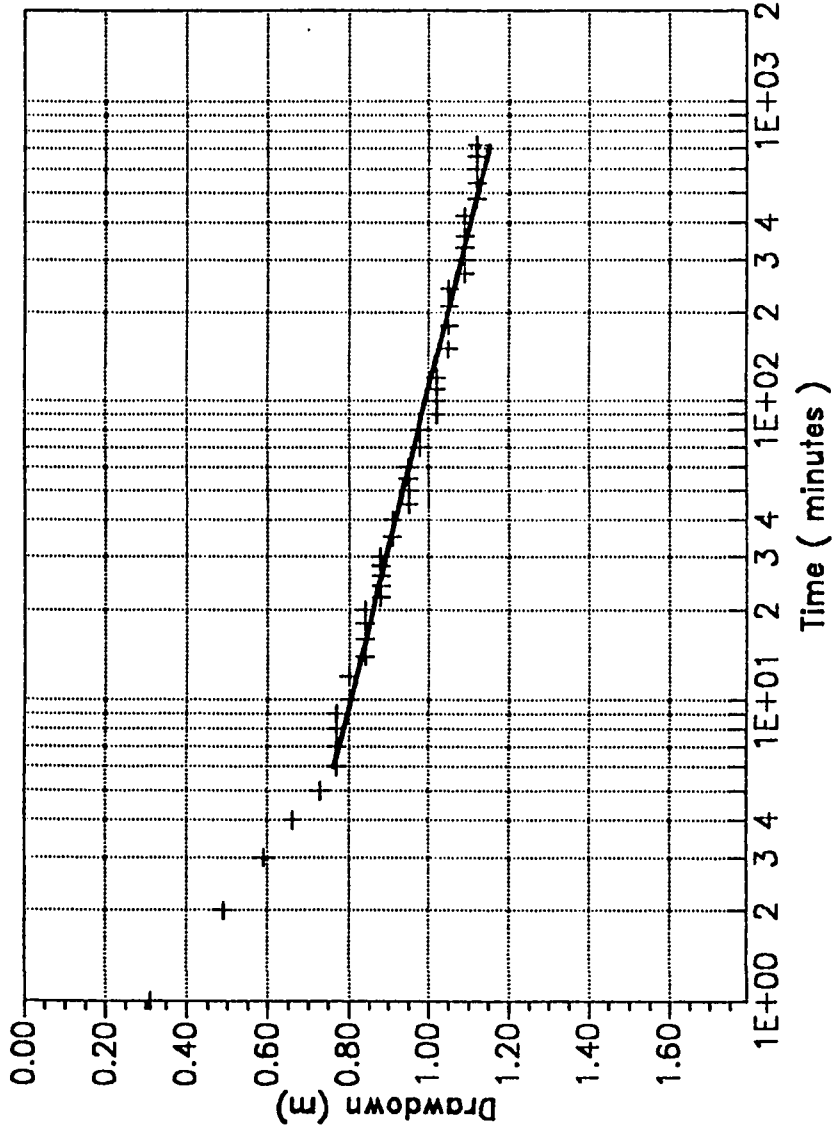
PUMPING TEST (JACOB METHOD) - WELL NO. B6



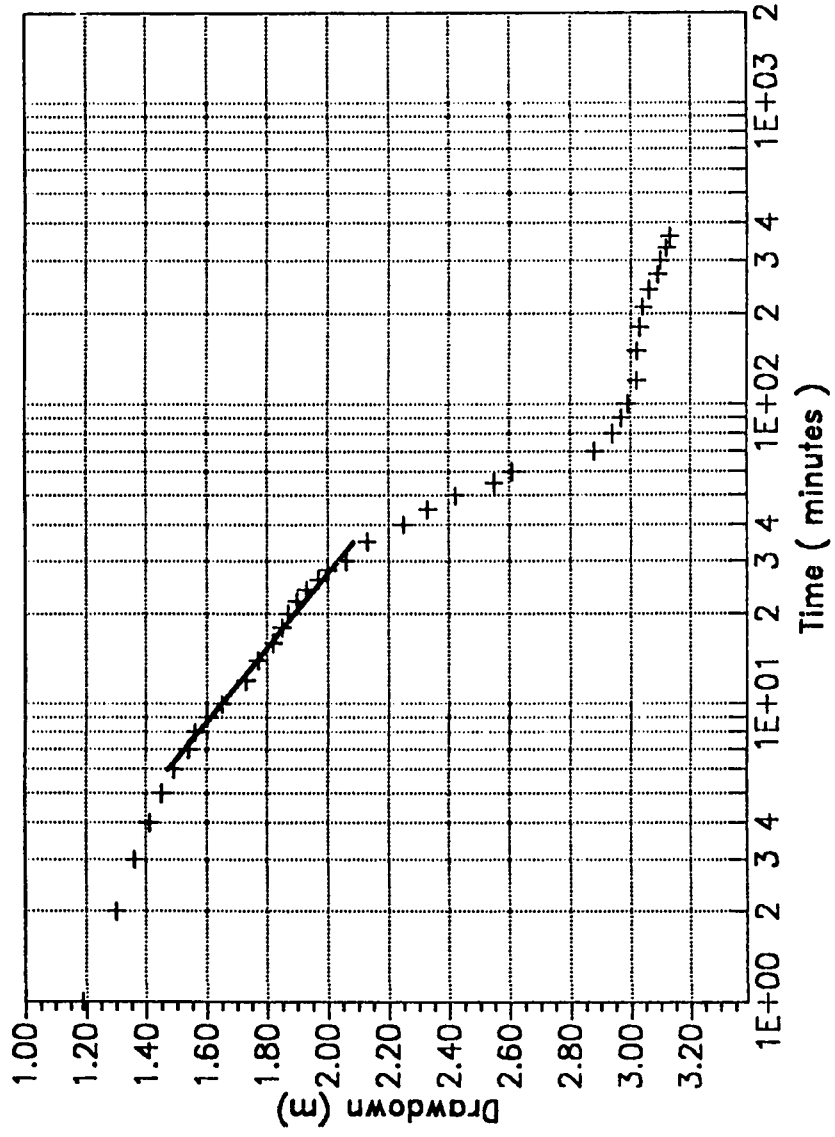
PUMPING TEST (JACOB METHOD) - WELL NO. B8



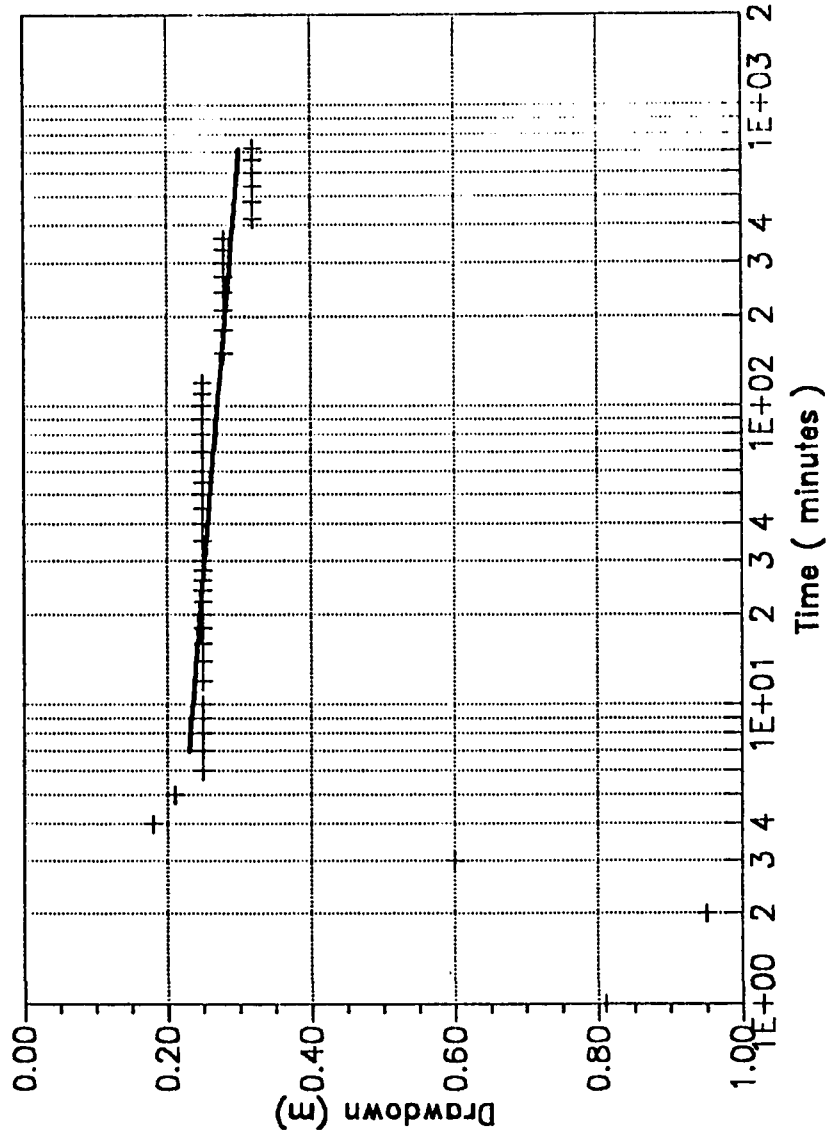
PUMPING TEST (JACOB METHOD) - WELL NO. C2



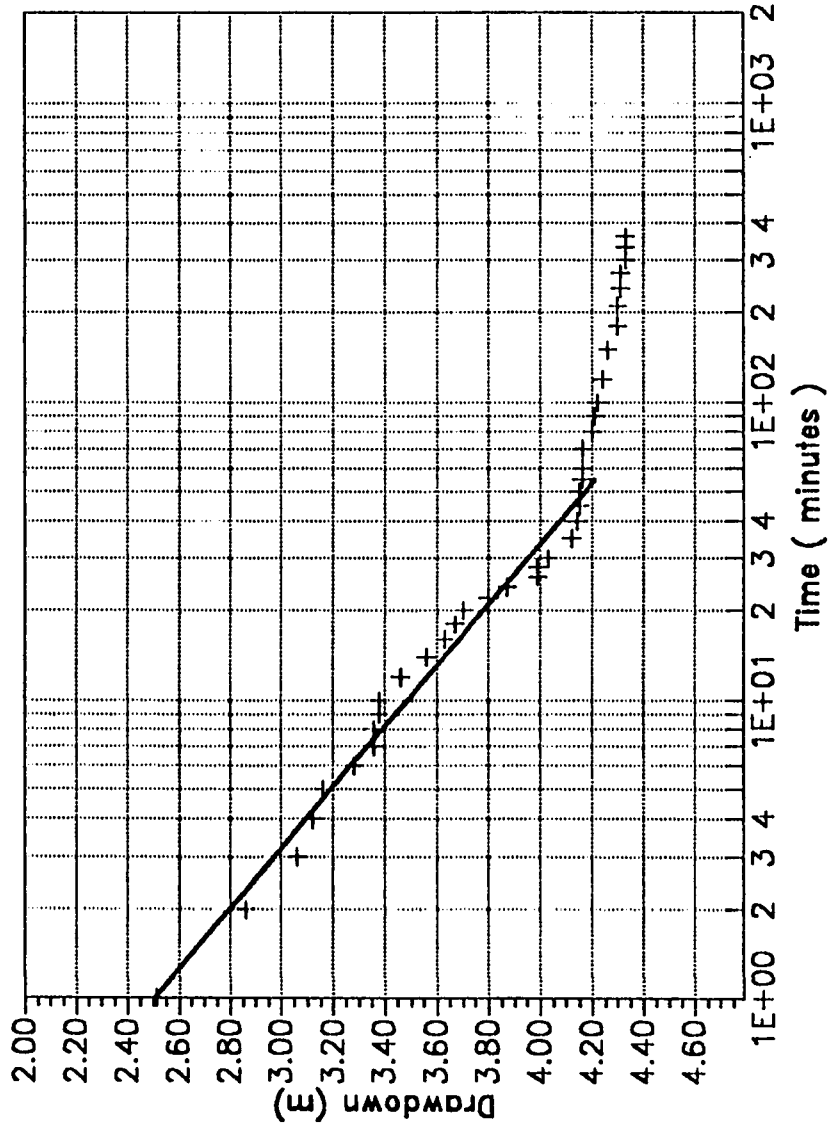
PUMPING TEST (JACOB TEST) - WELL NO. C3



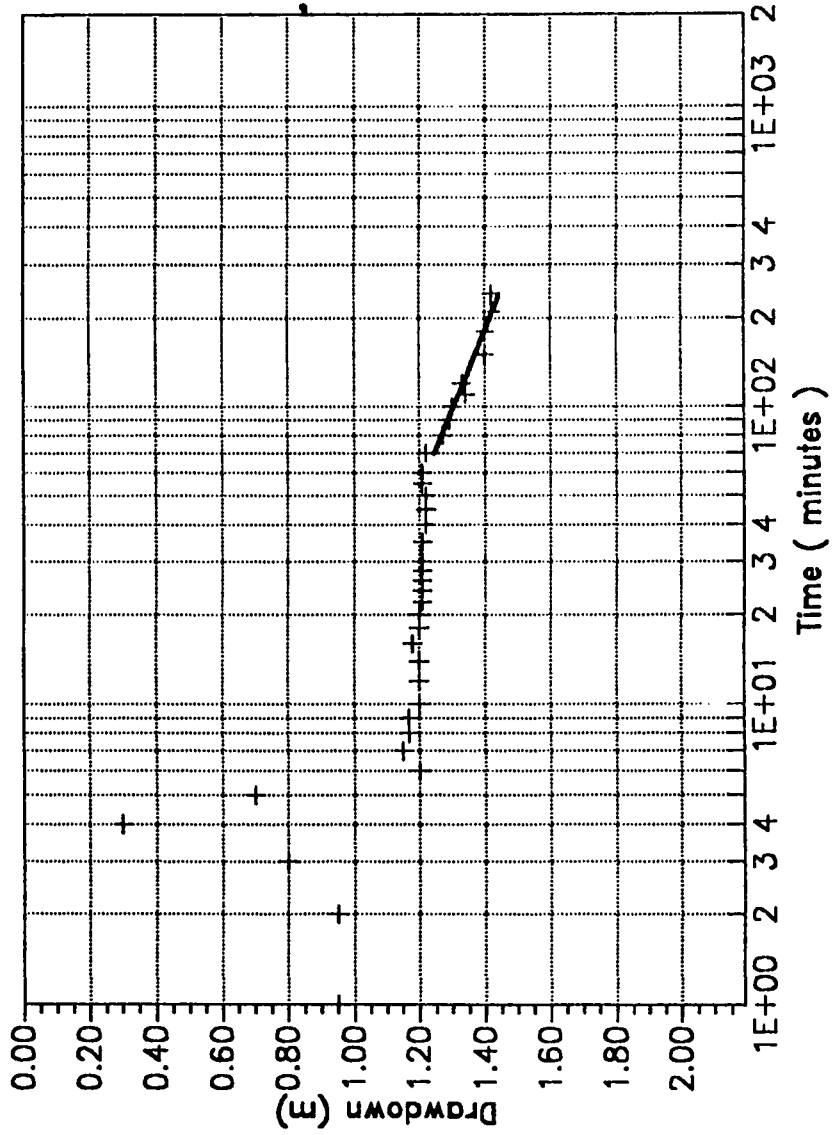
PUMPING TEST (JACOB METHOD) - WELL NO. C6



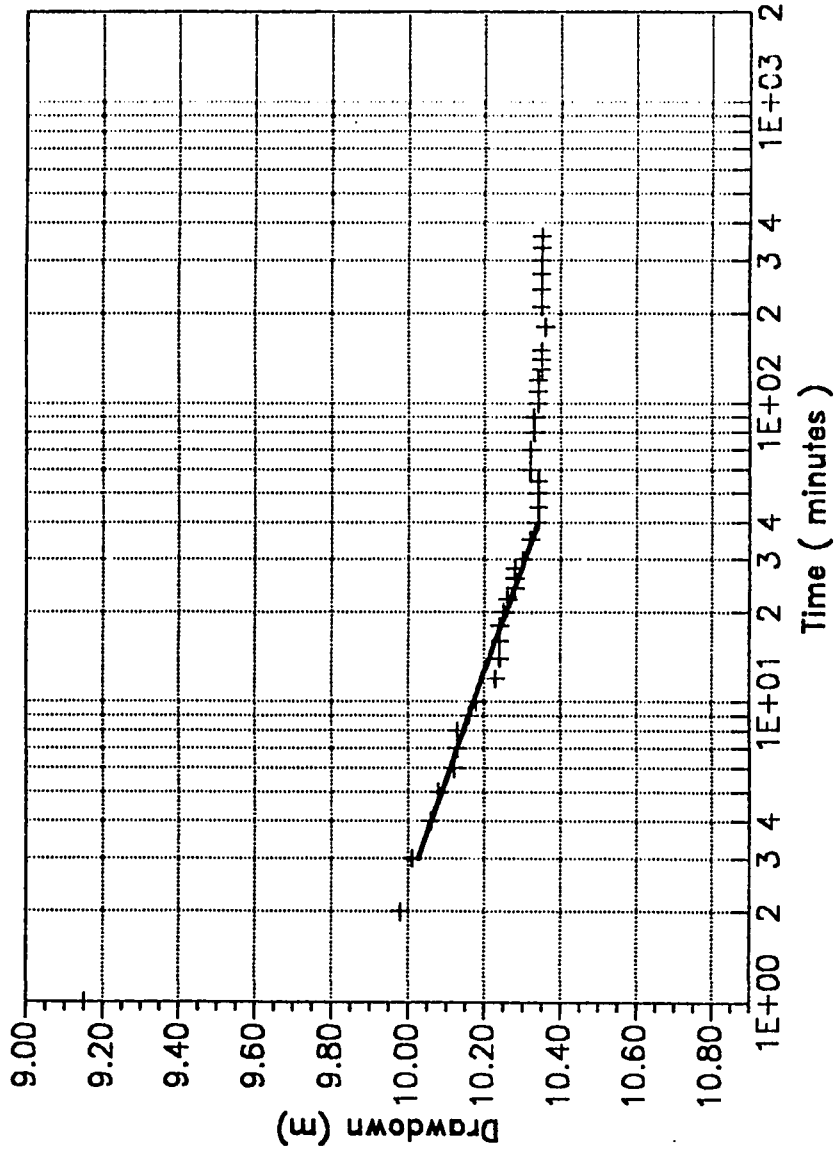
PUMPING TEST (JACOB METHOD) - WELL NO. C7



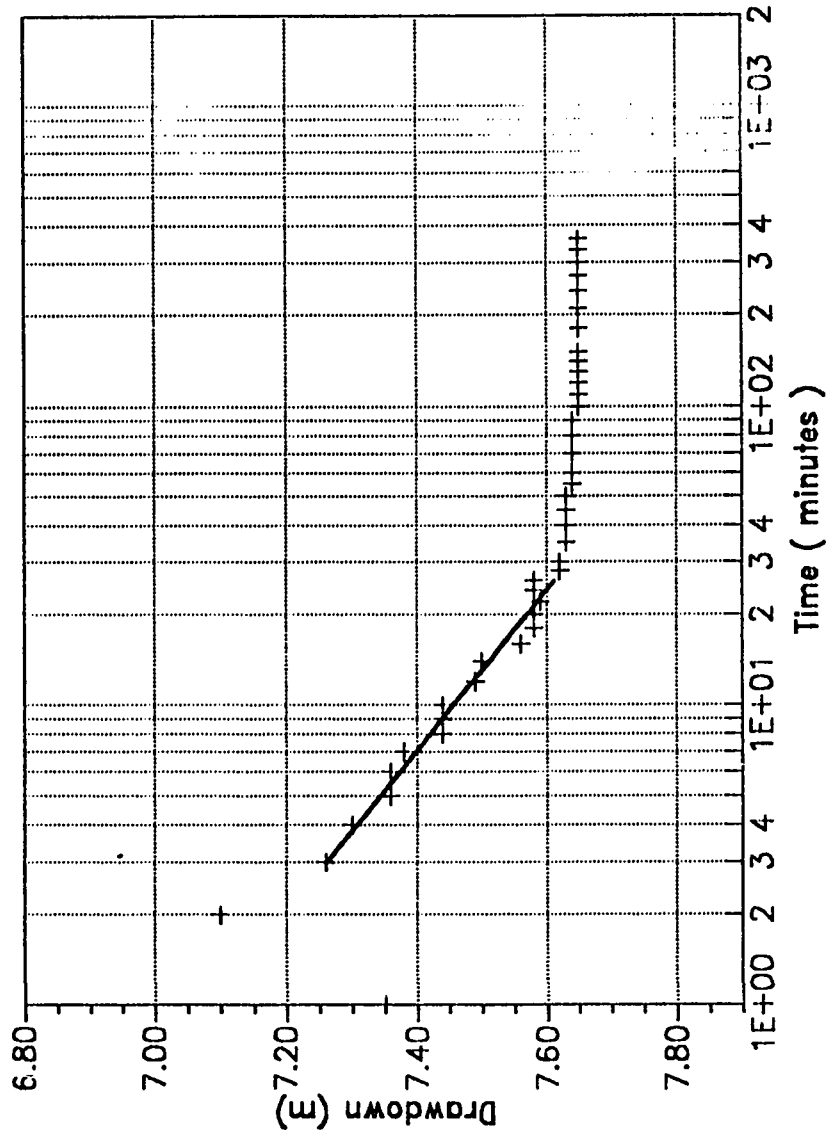
PUMPING TEST (JACOB METHOD) - WELL NO. D9



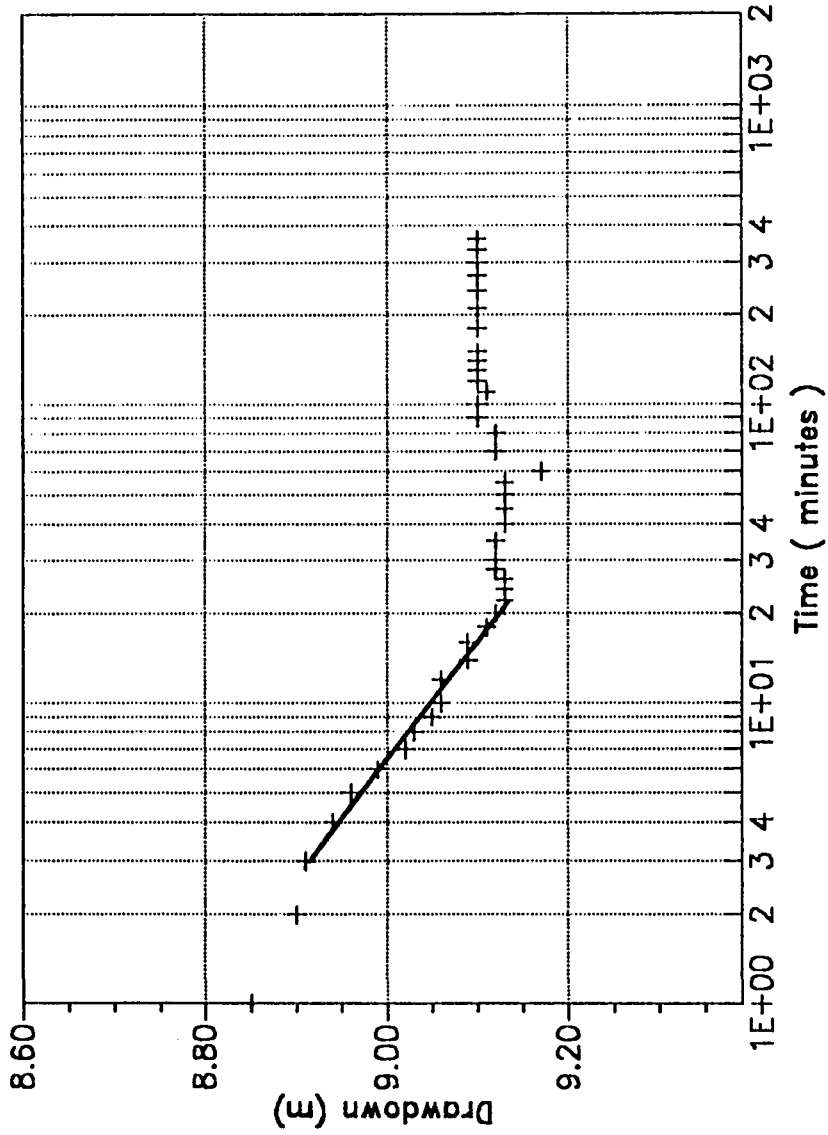
PUMPING TEST (JACOB METHOD) - WELL NO. E7



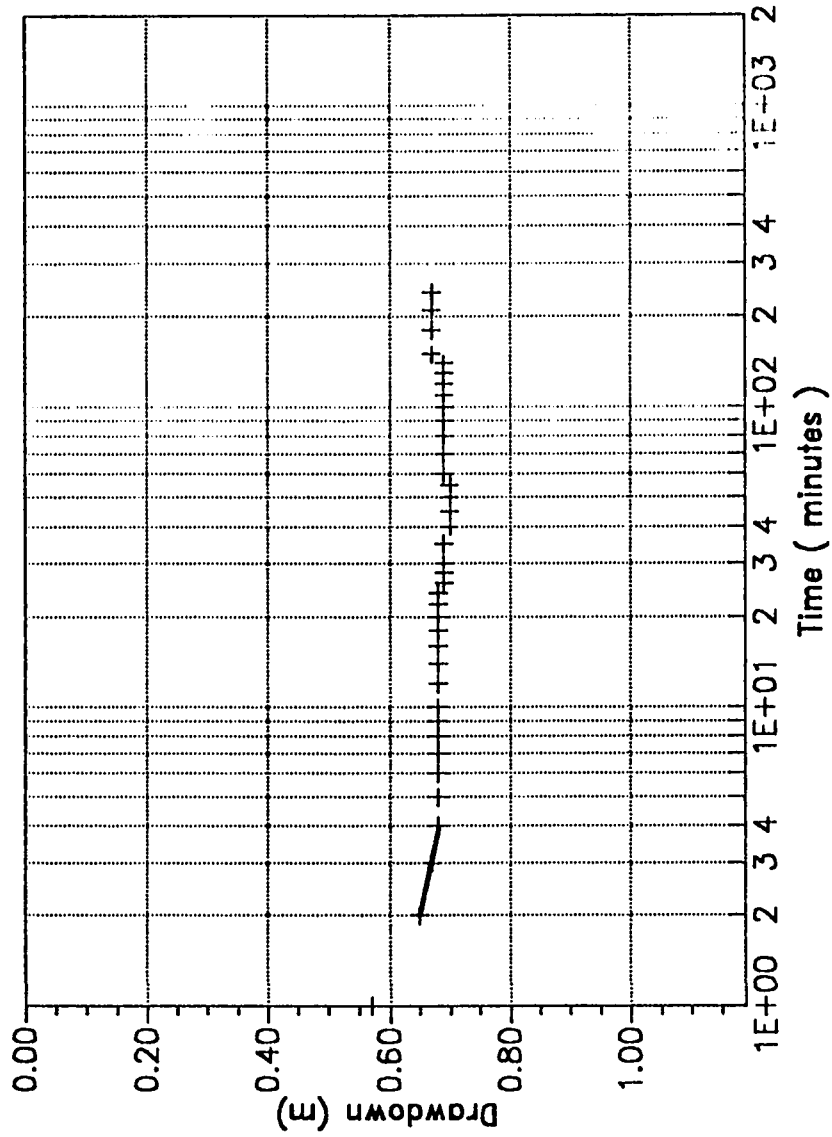
PUMPING TEST (JACOB METHOD) - WELL NO. E8



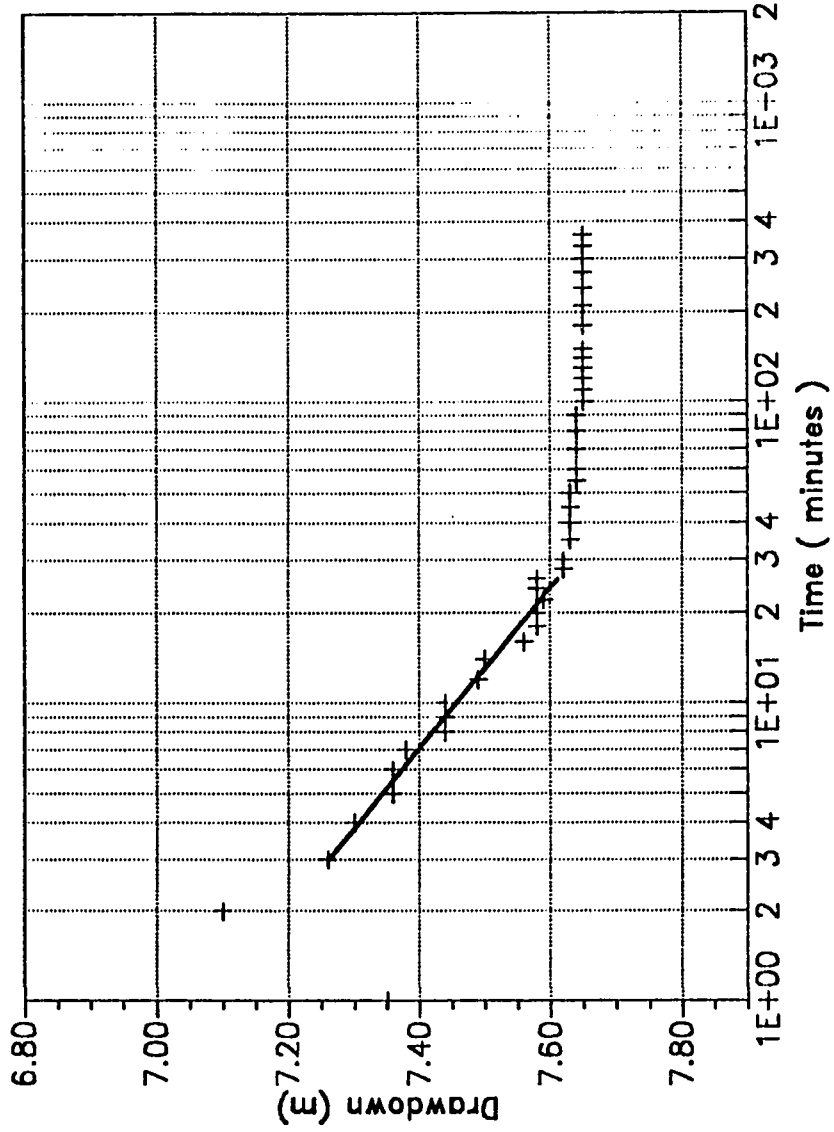
PUMPING TEST (JACOB METHOD) - WELL NO. F6



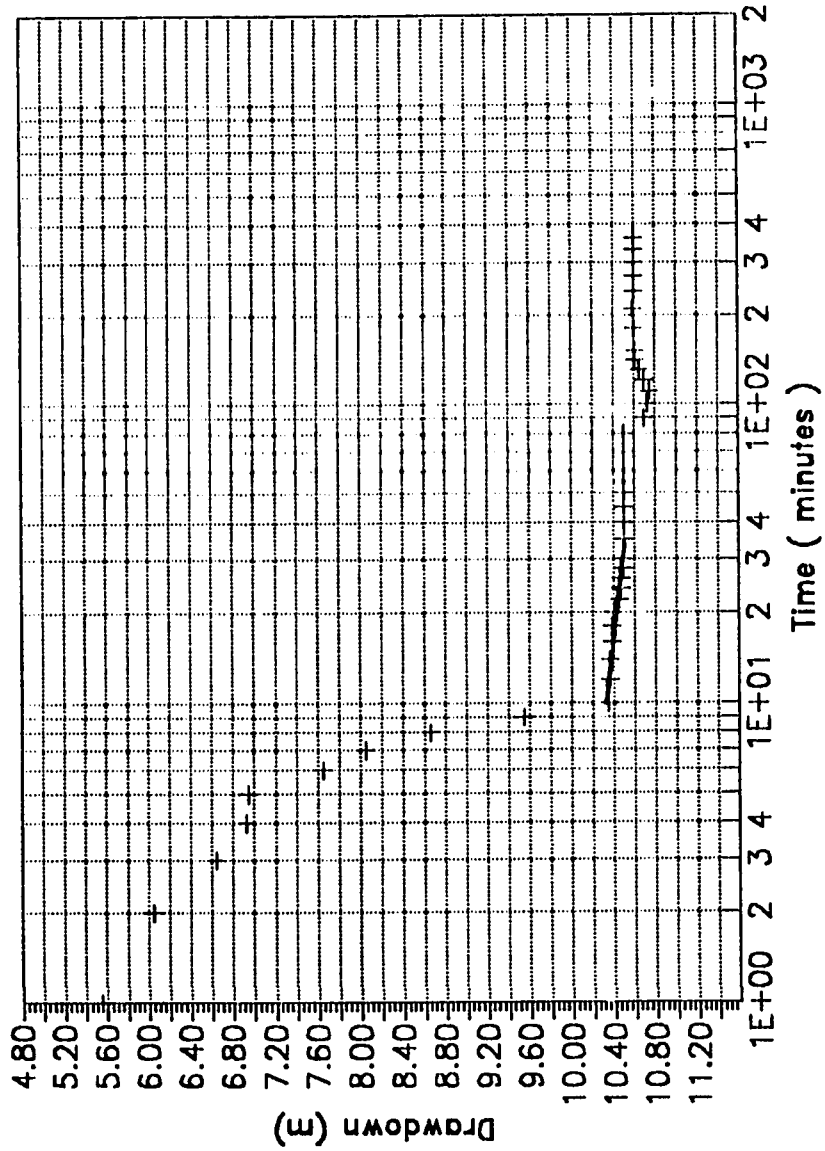
PUMPING TEST (JACOB METHOD) - WELL NO. G6



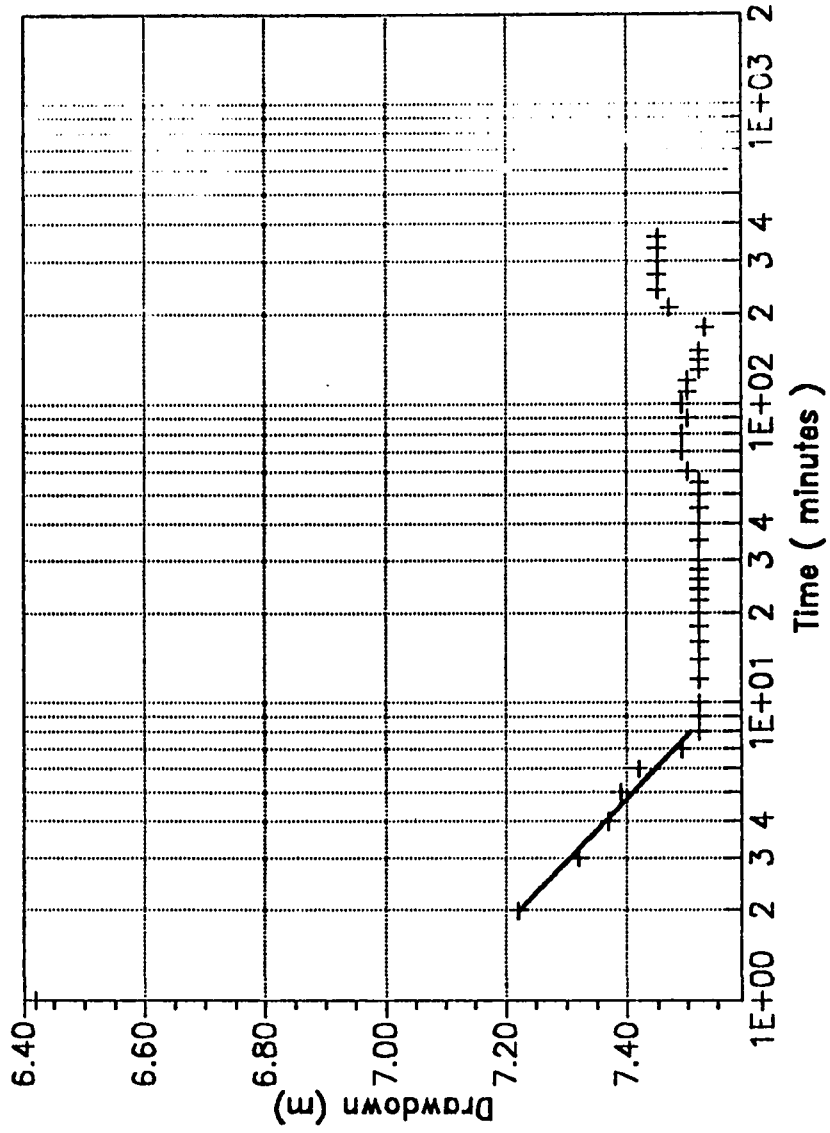
PUMPING TEST (JACOB METHOD) - WELL NO. G7



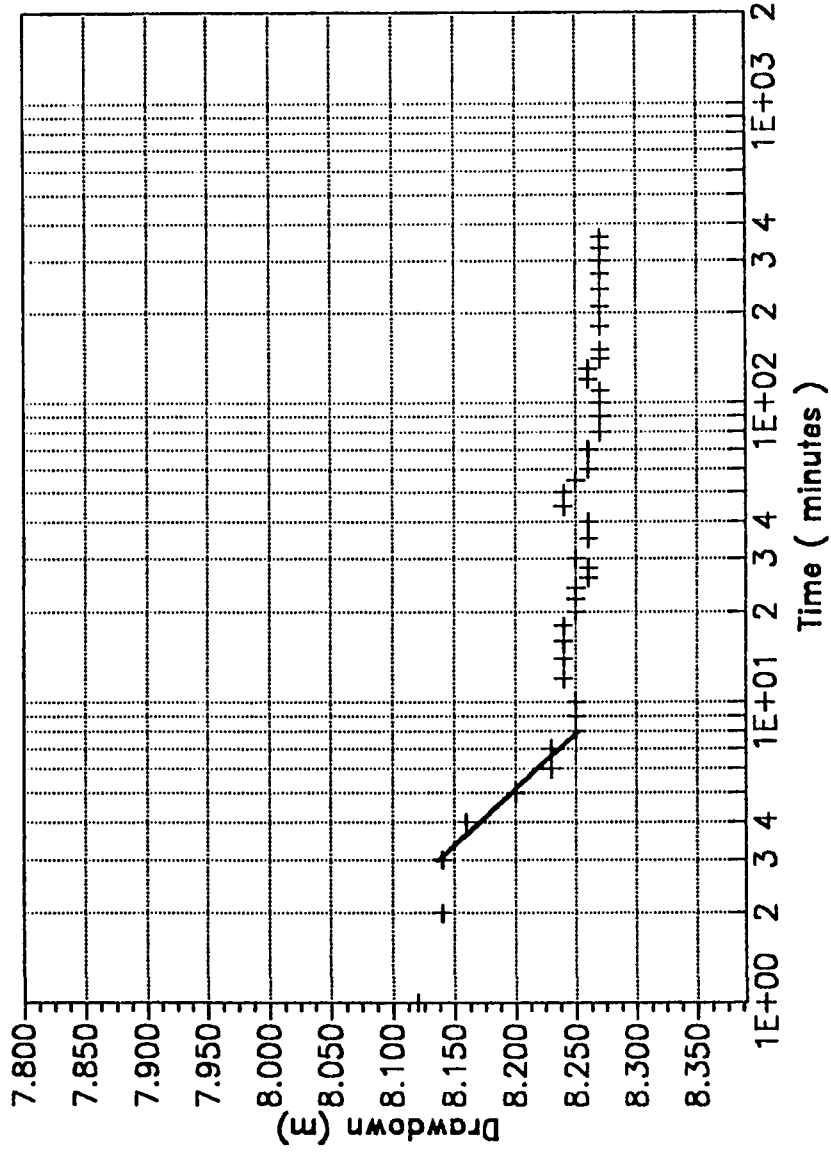
PUMPING TEST (JACOB METHOD) - WELL NO. H5



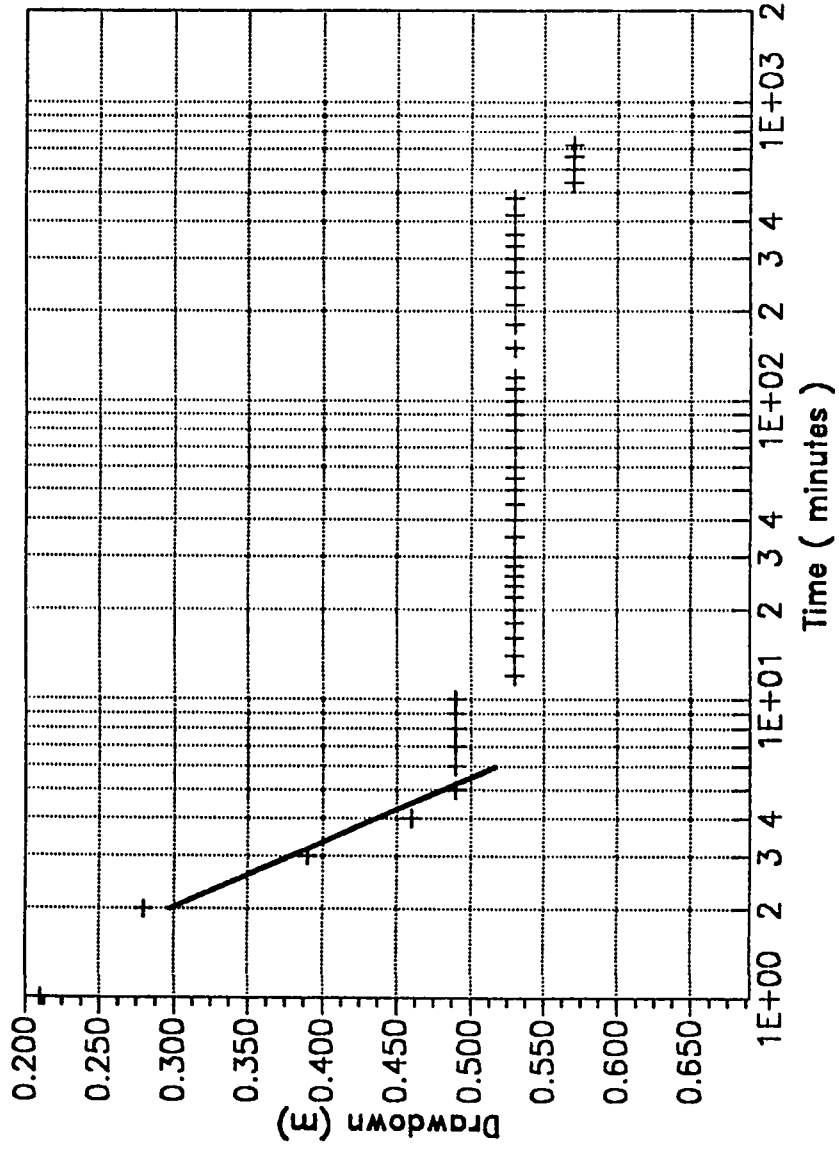
PUMPING TEST (JACOB METHOD) - WELL NO. H6



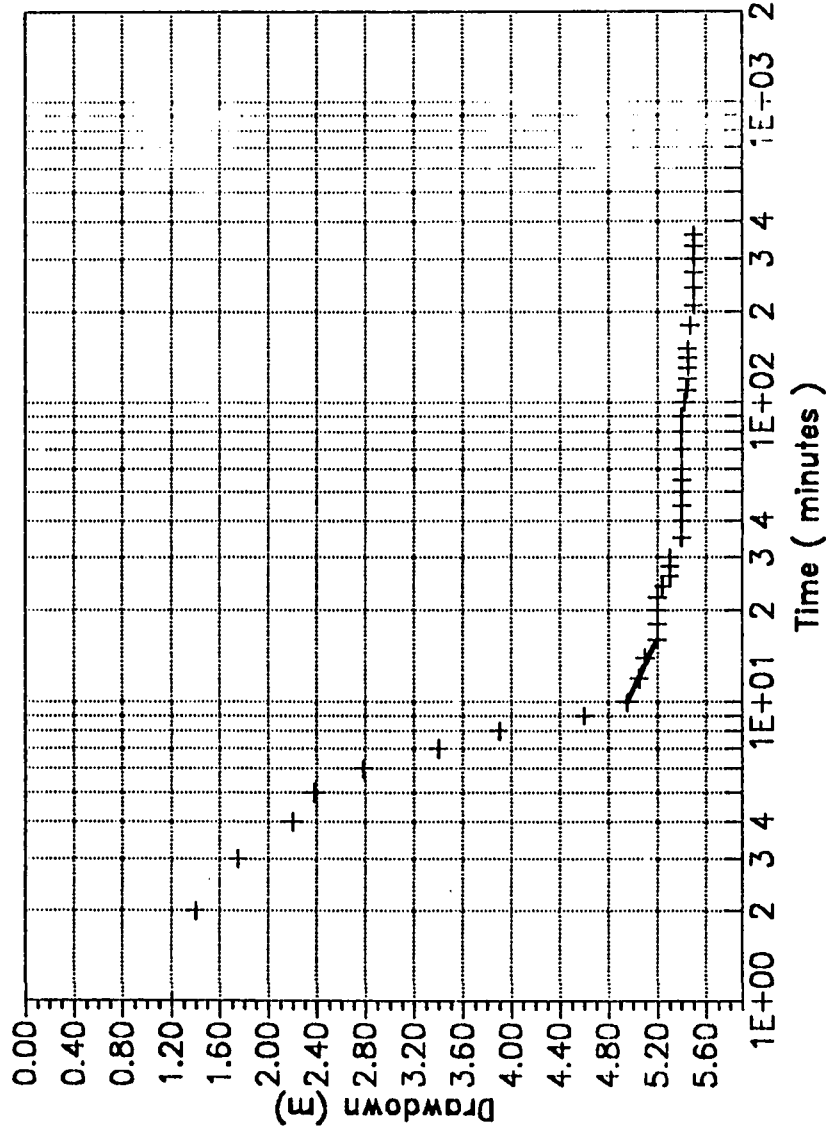
PUMPING TEST (JACOB METHOD) - WELL NO. H7



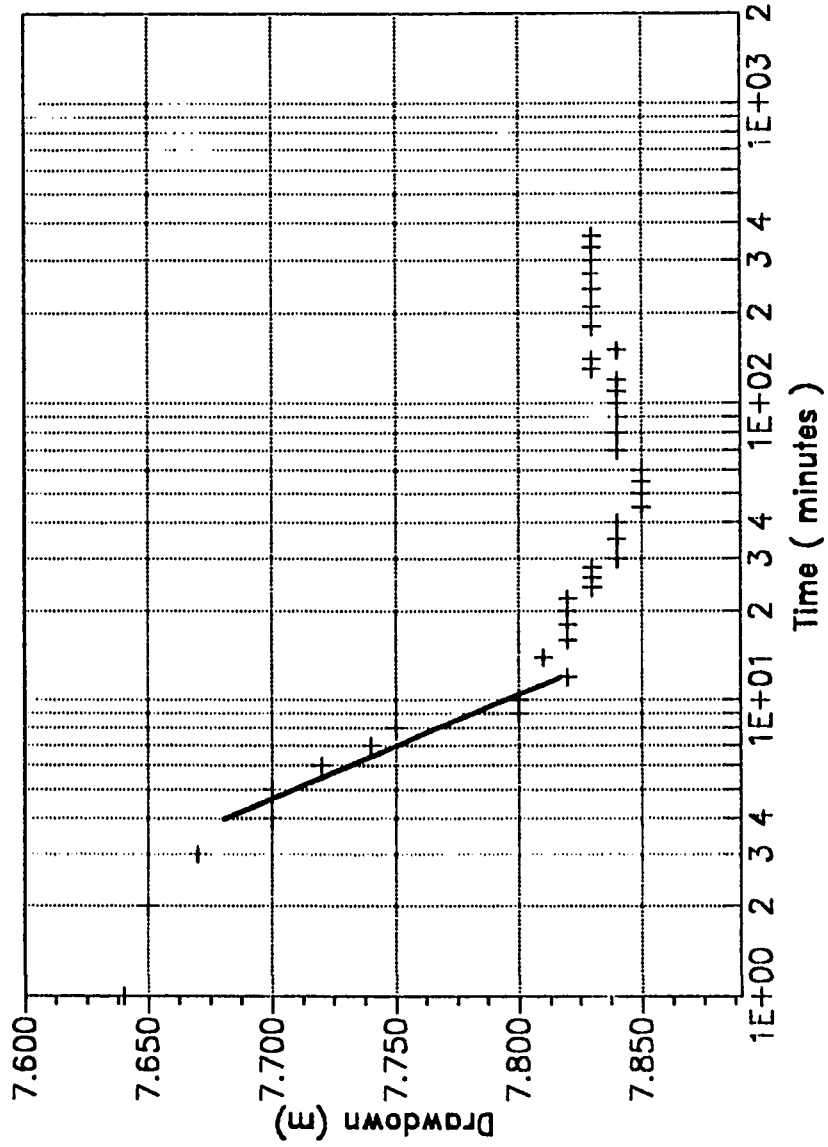
PUMPING TEST (JACOB METHOD) - WELL NO. H9



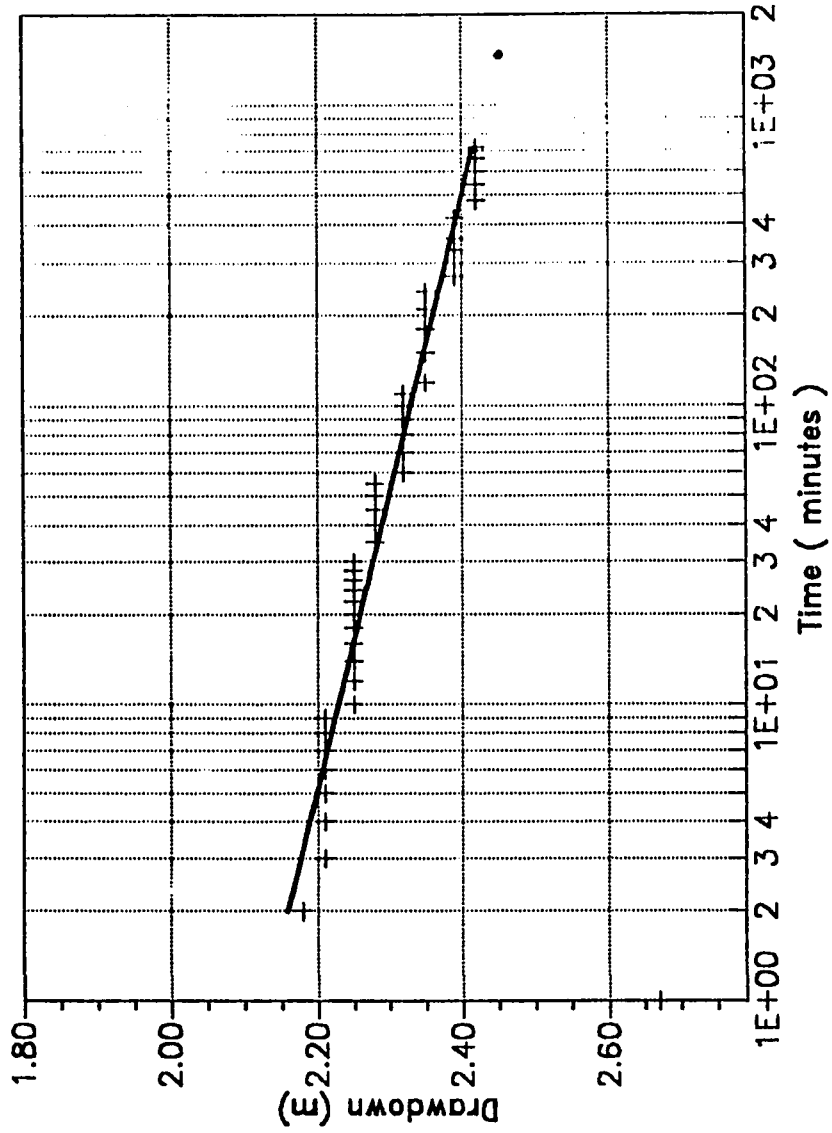
PUMPING TEST (JACOB METHOD) - WELL 15



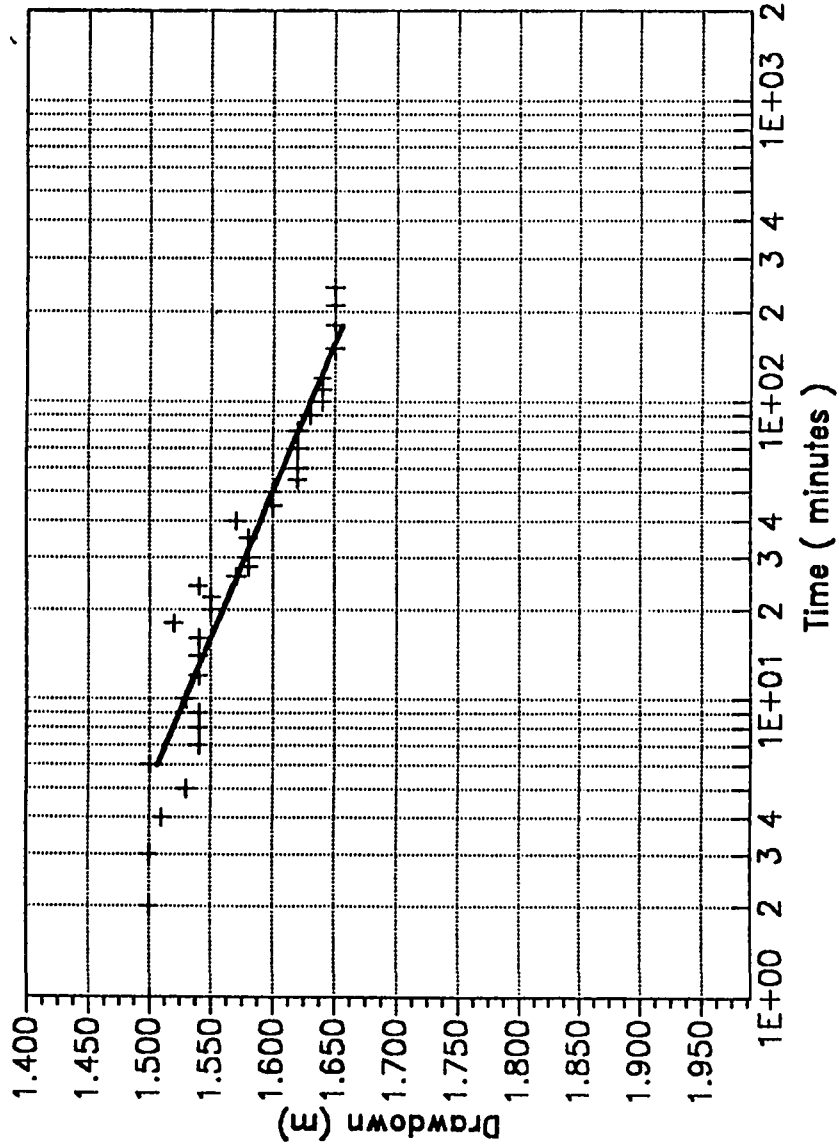
PUMPING TEST (JACOB METHOD) - WELL NO. 17



PUMPING TEST (JACOB METHOD) - WELL NO. 19

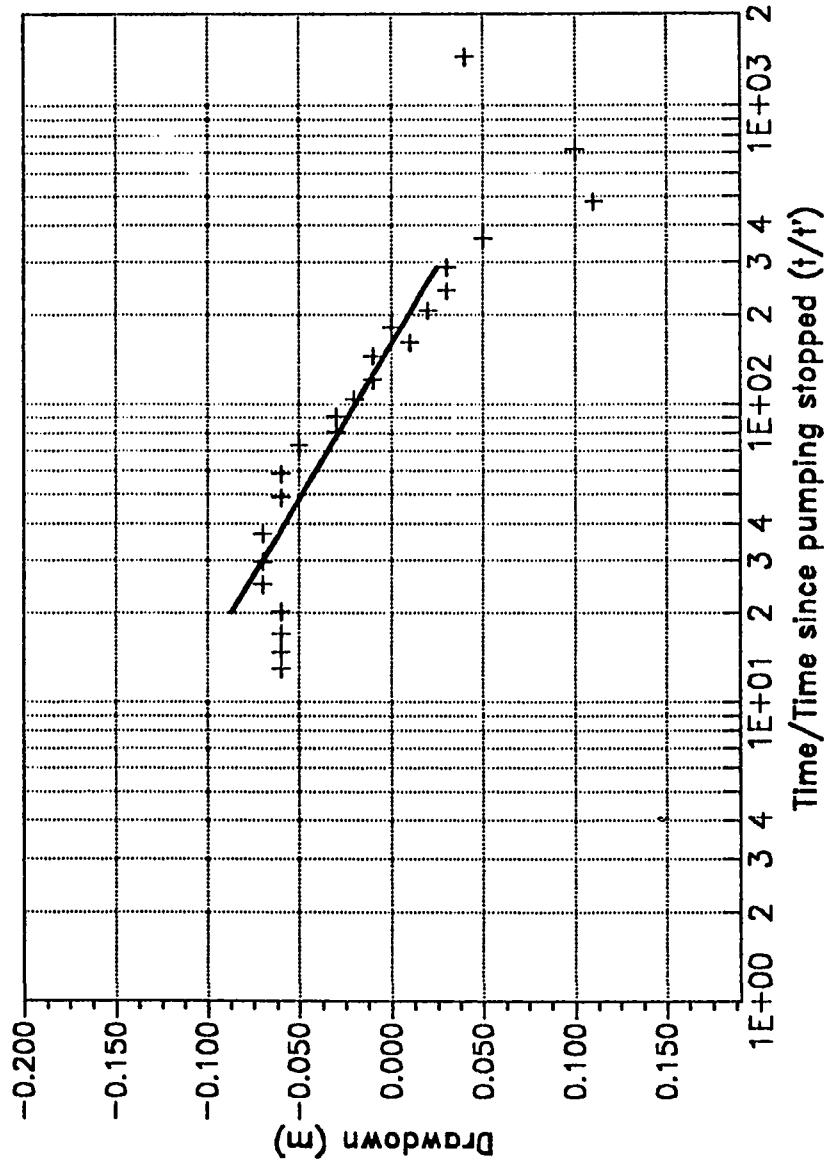


PUMPING TEST (JACOB METHOD) - WELL NO. Z8

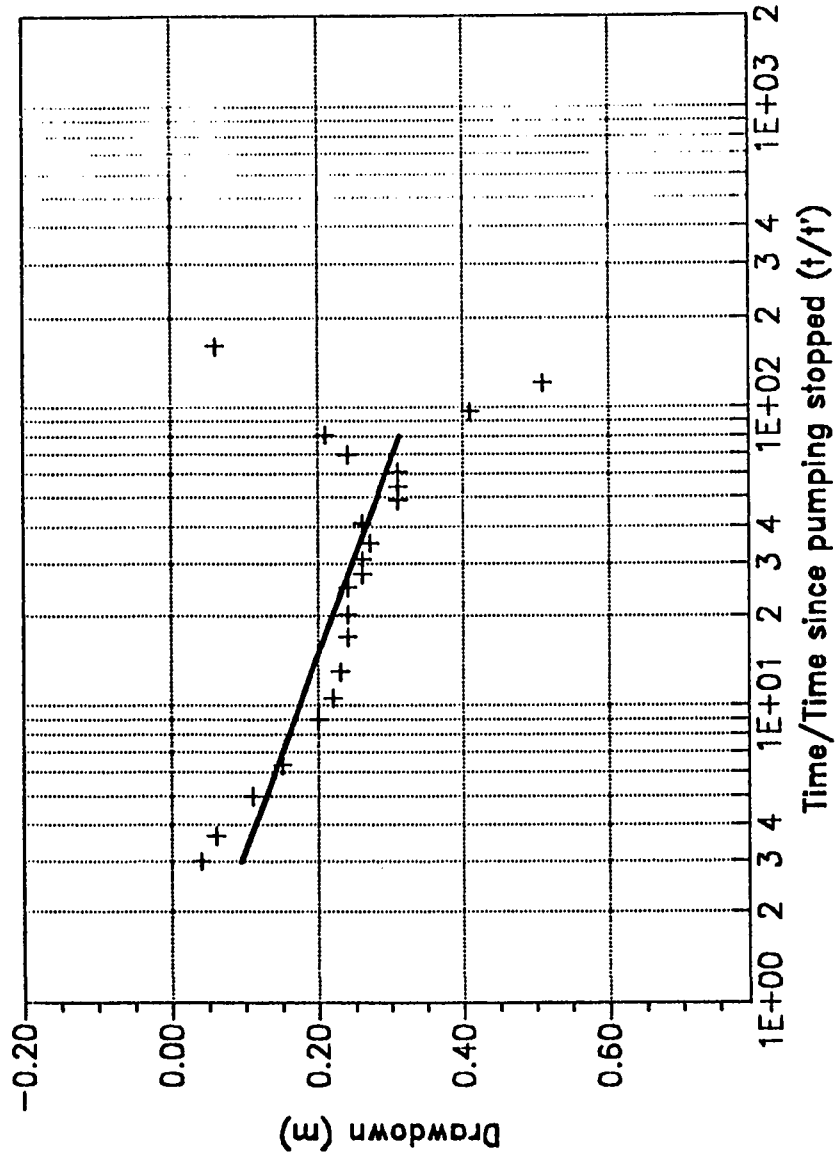


APPENDIX - A2: RECOVERY METHOD

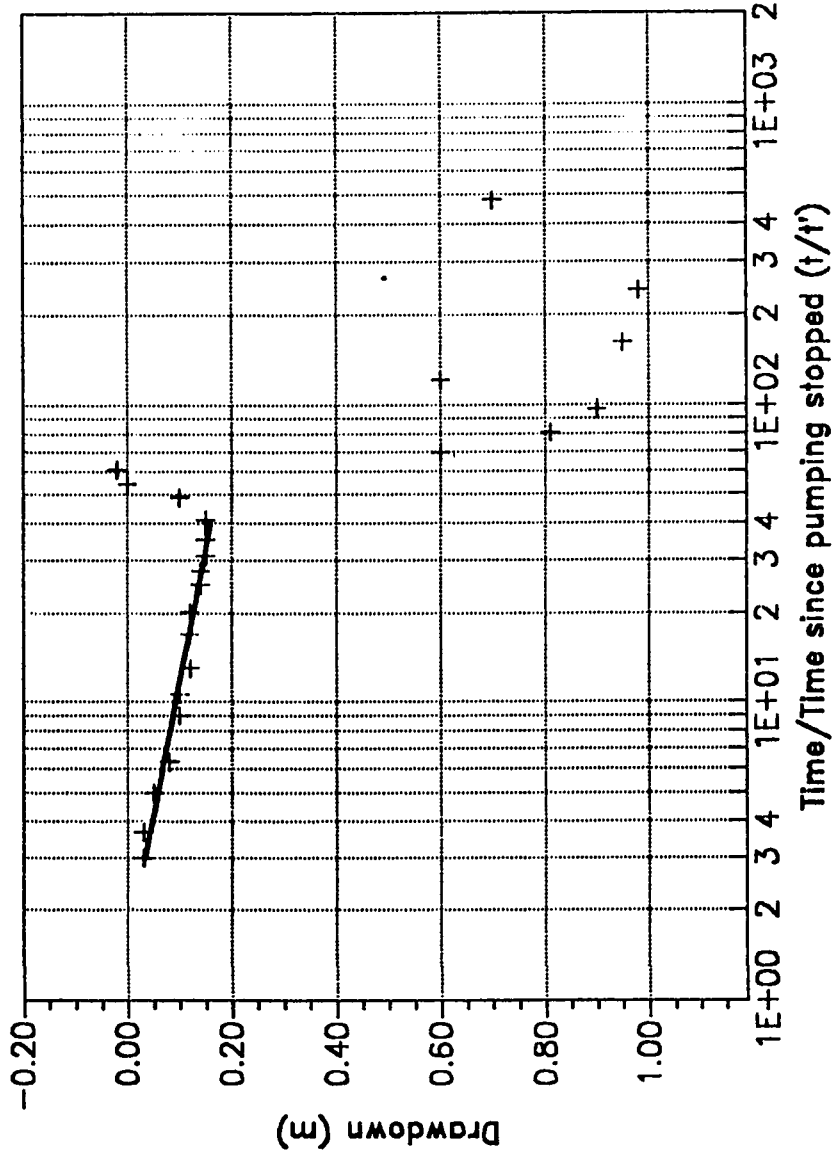
RECOVERY TEST - WELL NO. A2



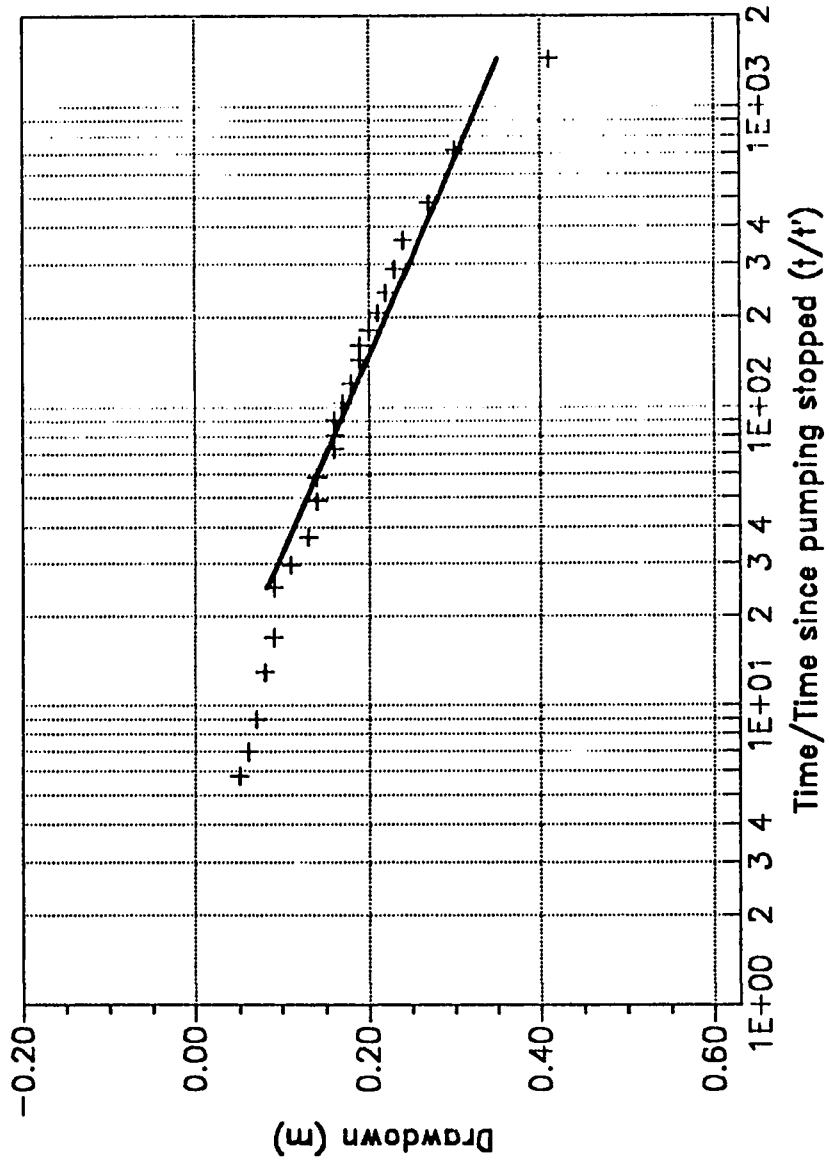
RECOVERY TEST - WELL NO. A3



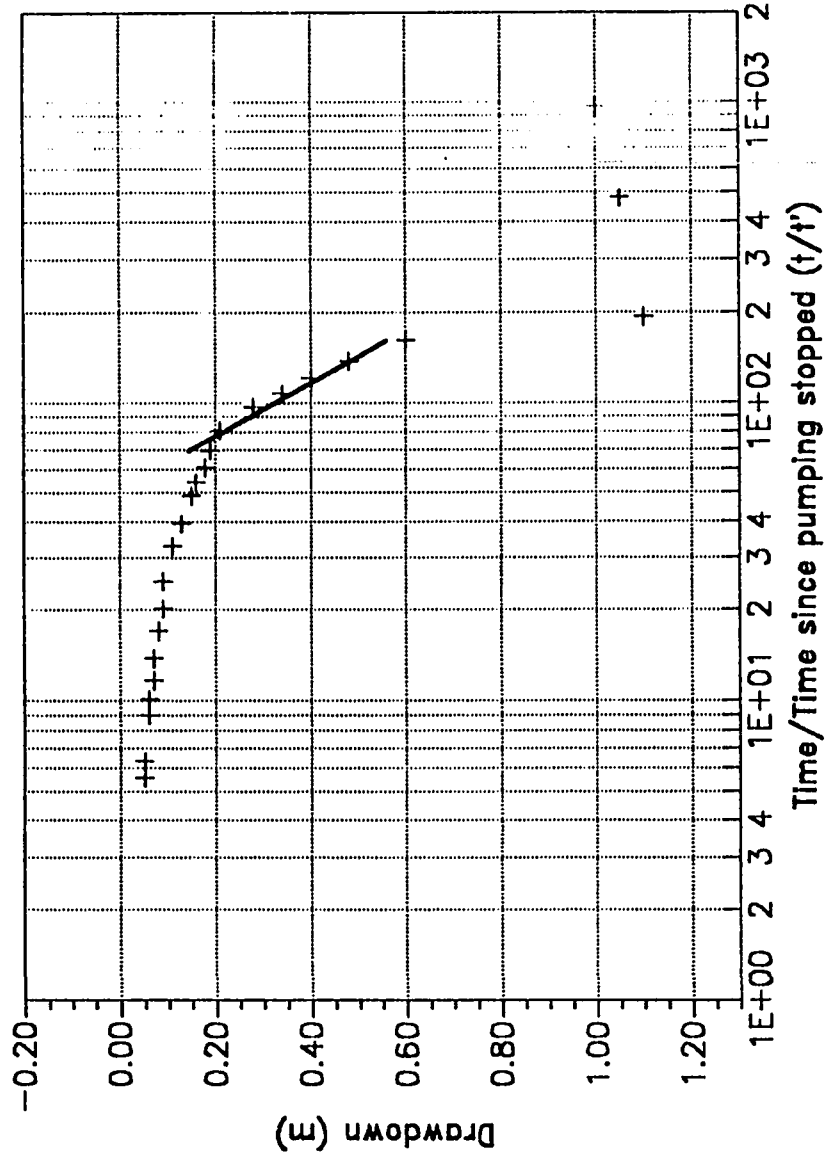
RECOVERY TEST - WELL NO. A4



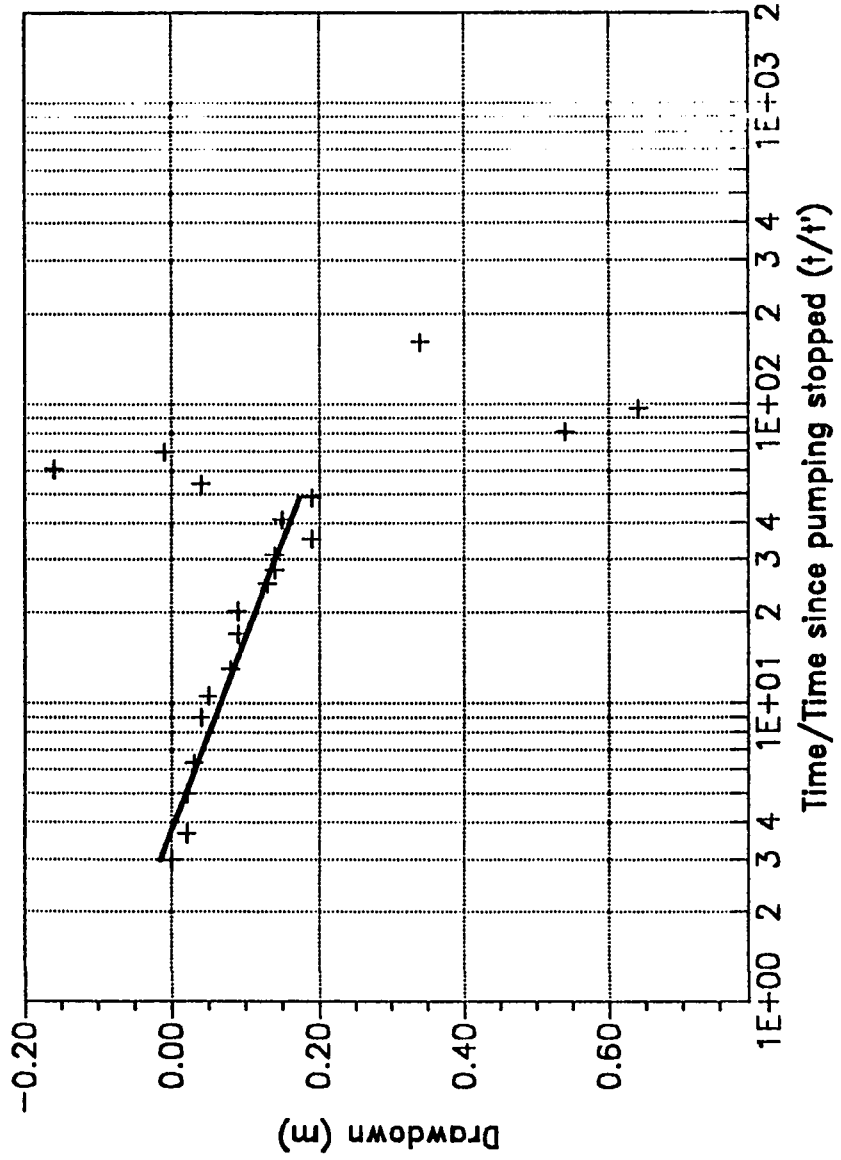
RECOVERY TEST - WELL NO. A7



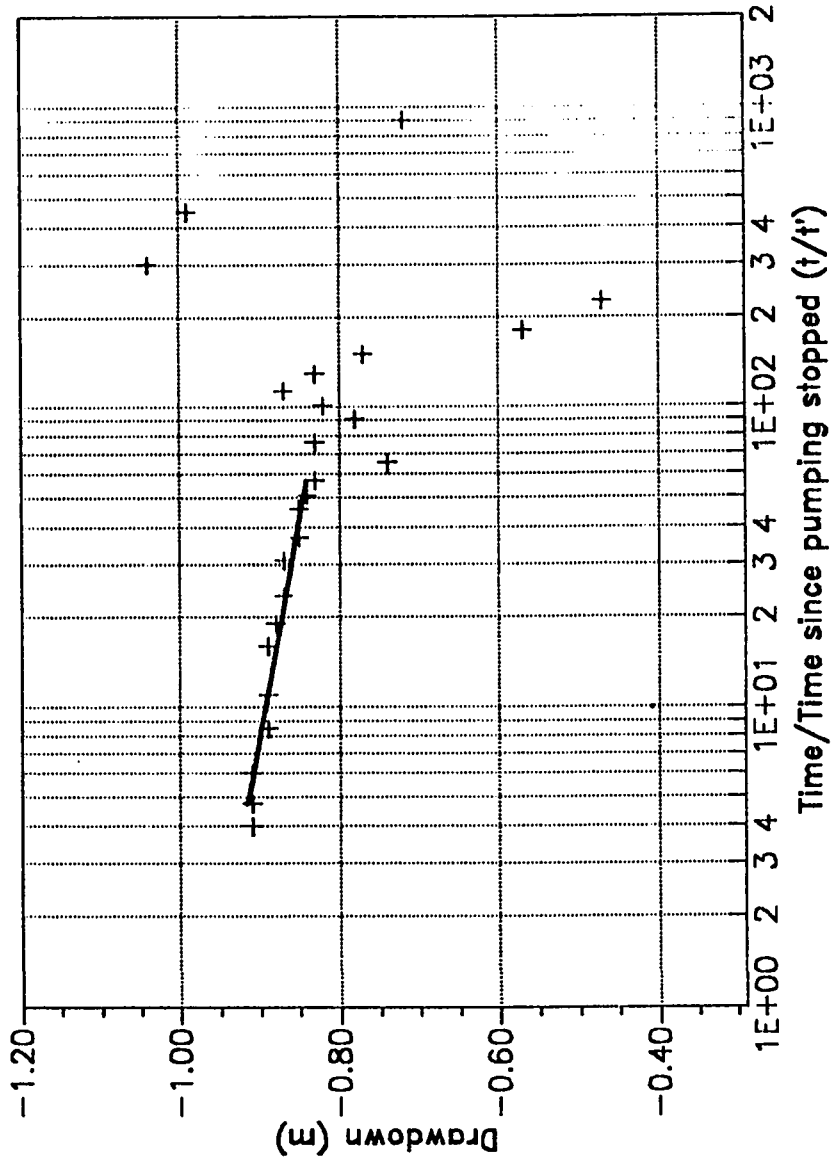
RECOVERY TEST - WELL NO. B1



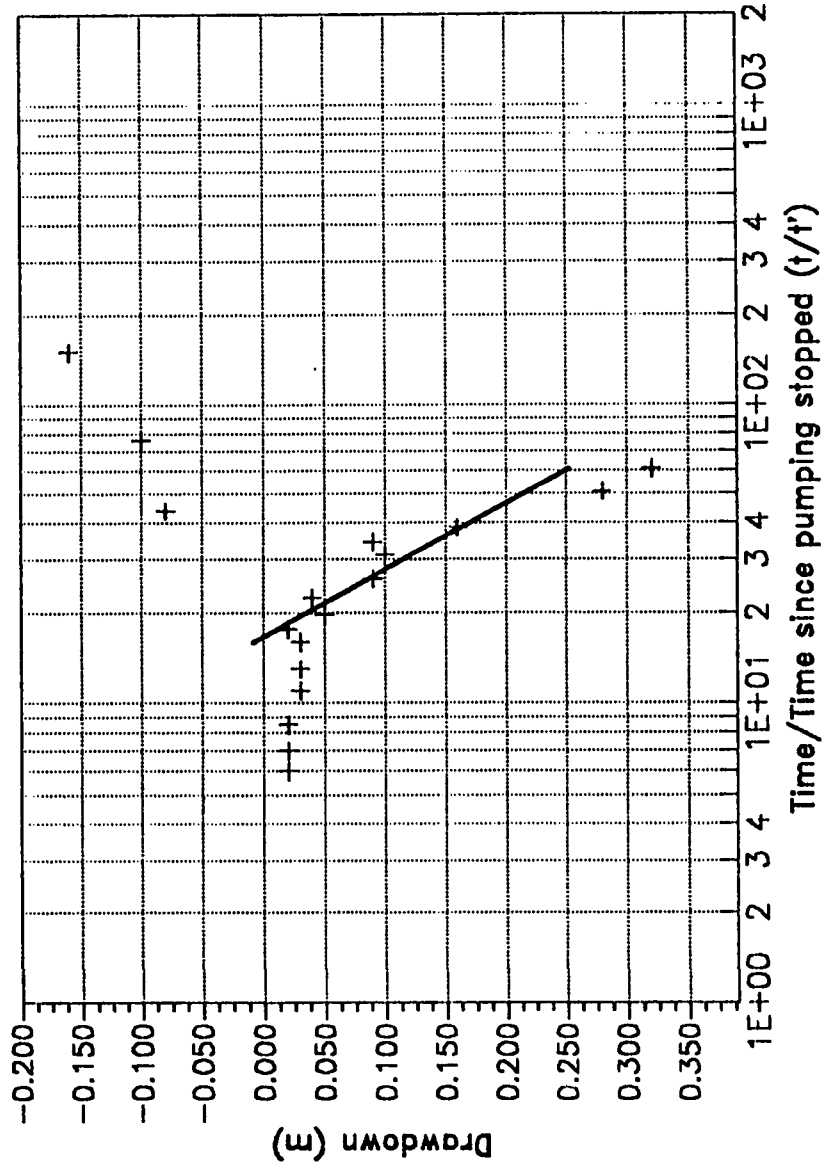
RECOVERY TEST - WELL NO. B4



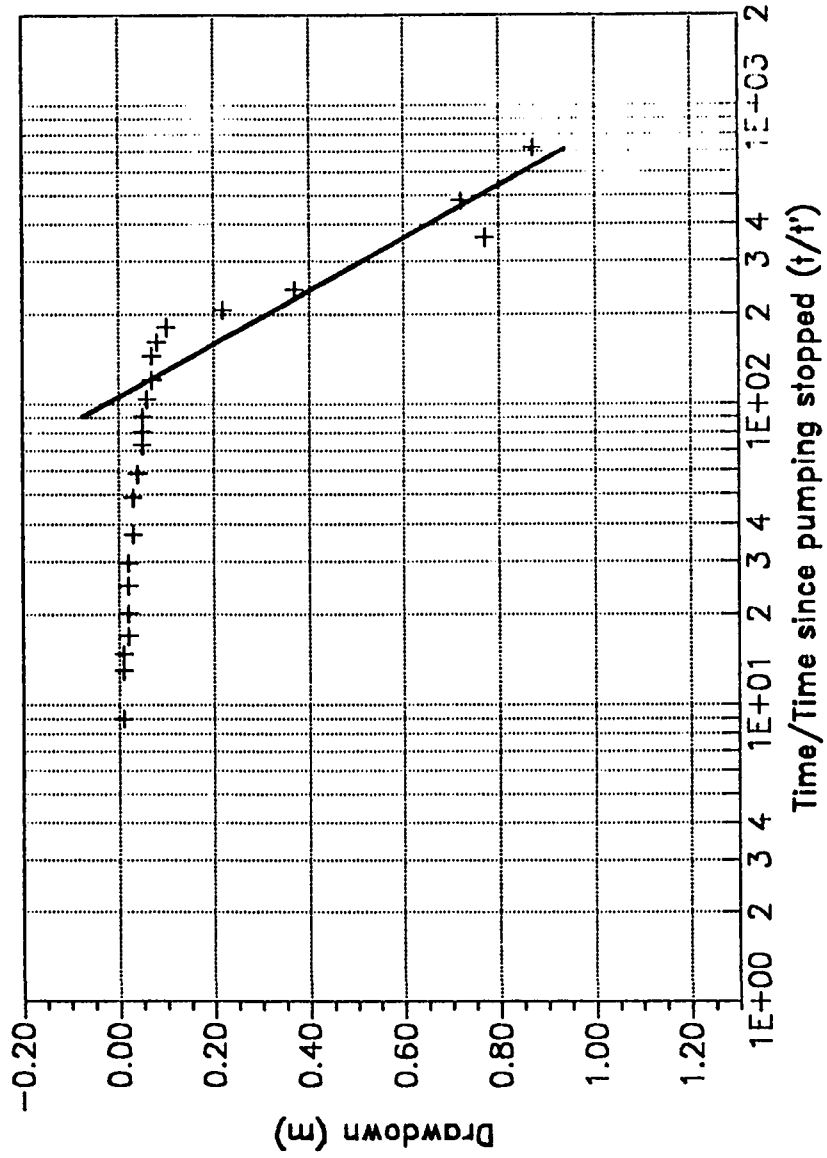
RECOVERY TEST - WELL NO. B7



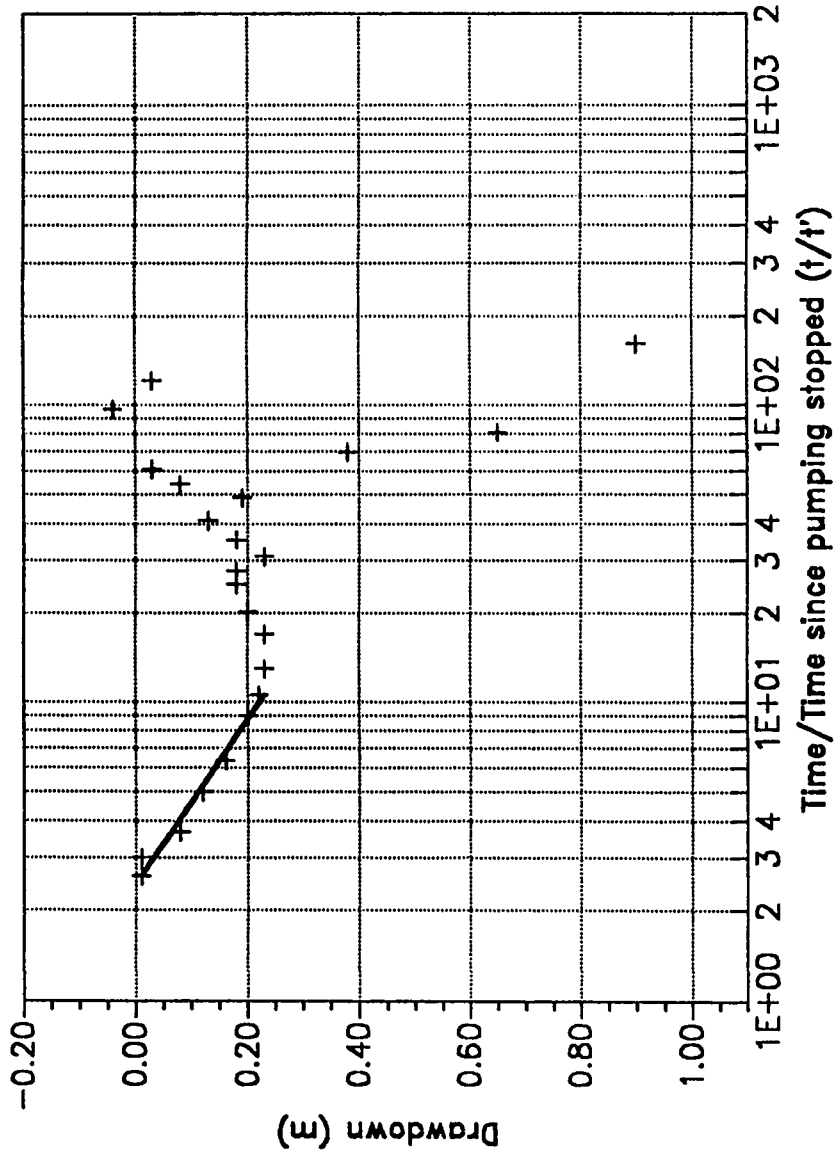
RECOVERY TEST - WELL NO. B9



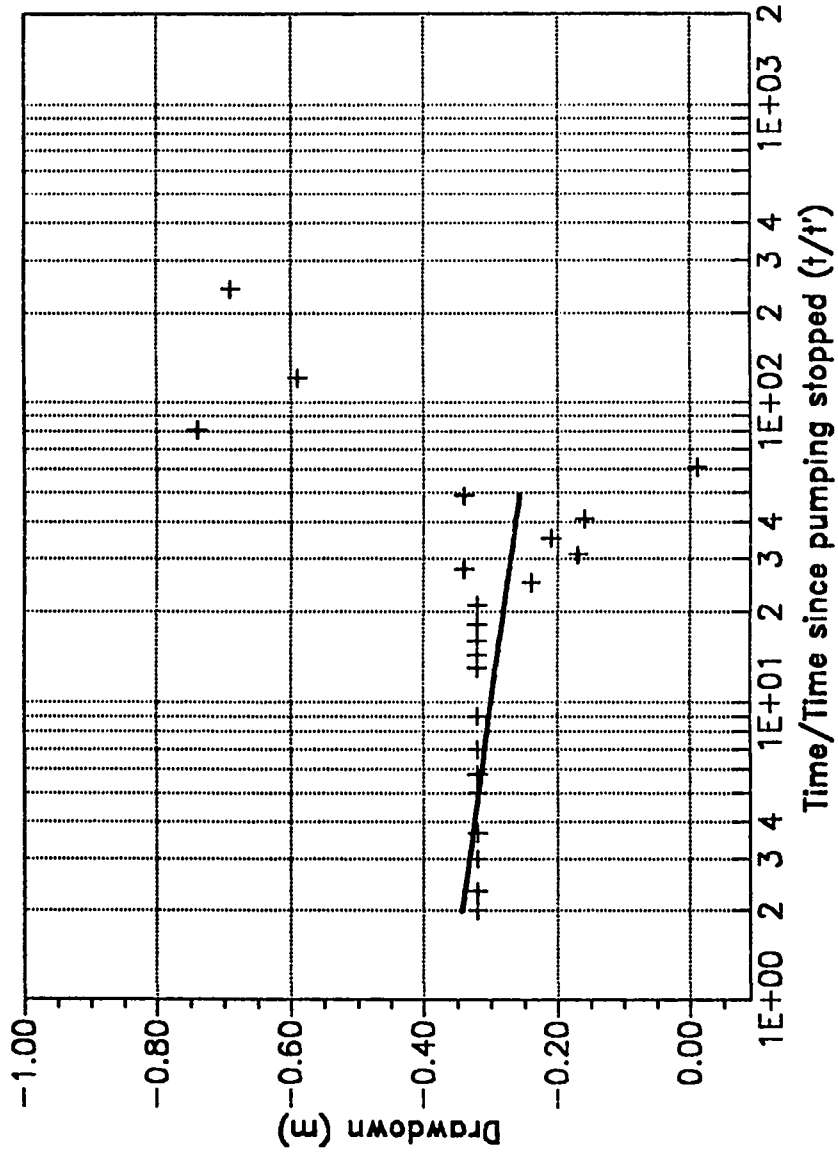
RECOVERY TEST - WELL NO. C1



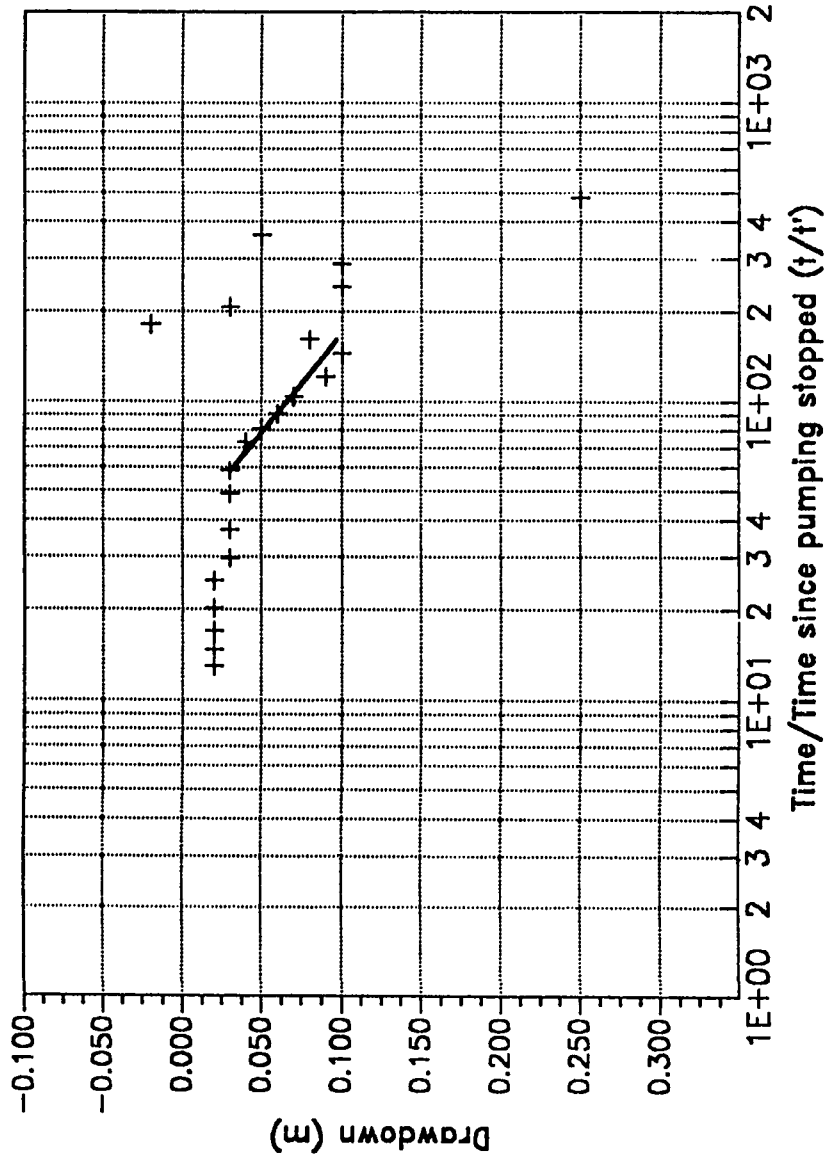
RECOVERY TEST - WELL NO. C4



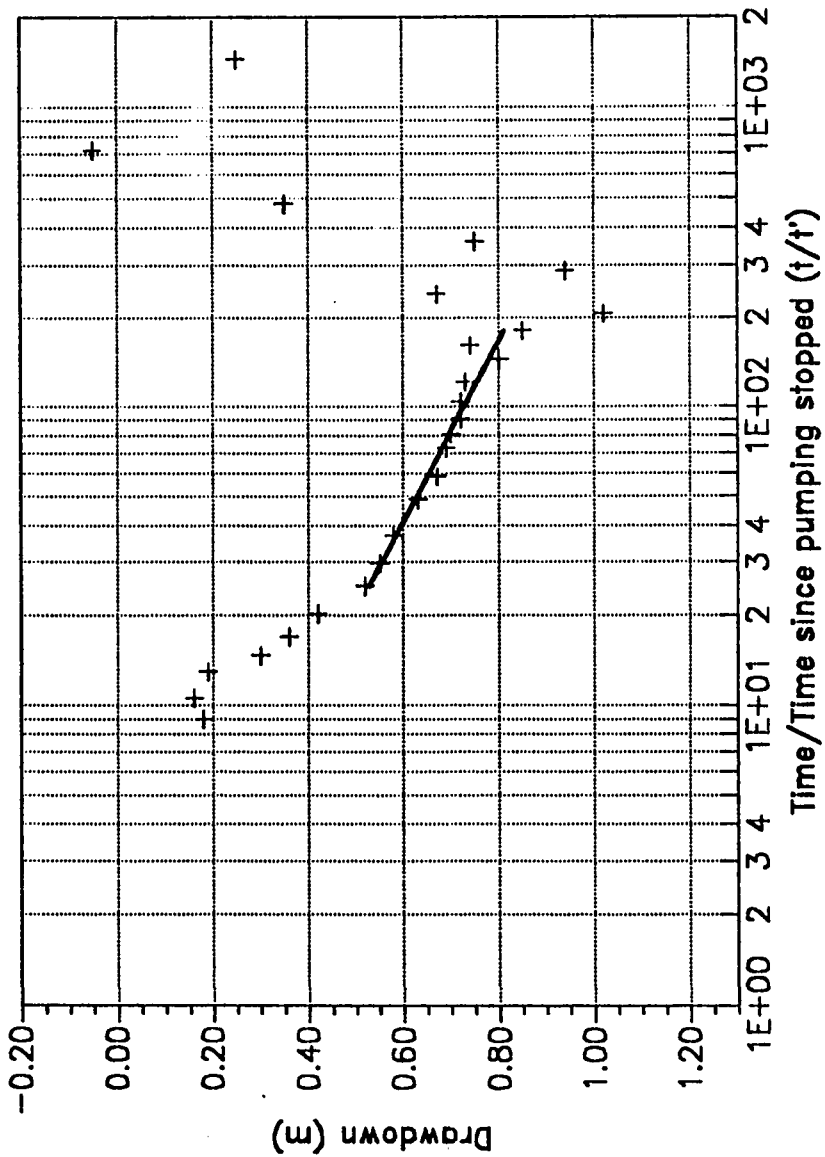
RECOVERY TEST - WELL NO. C9



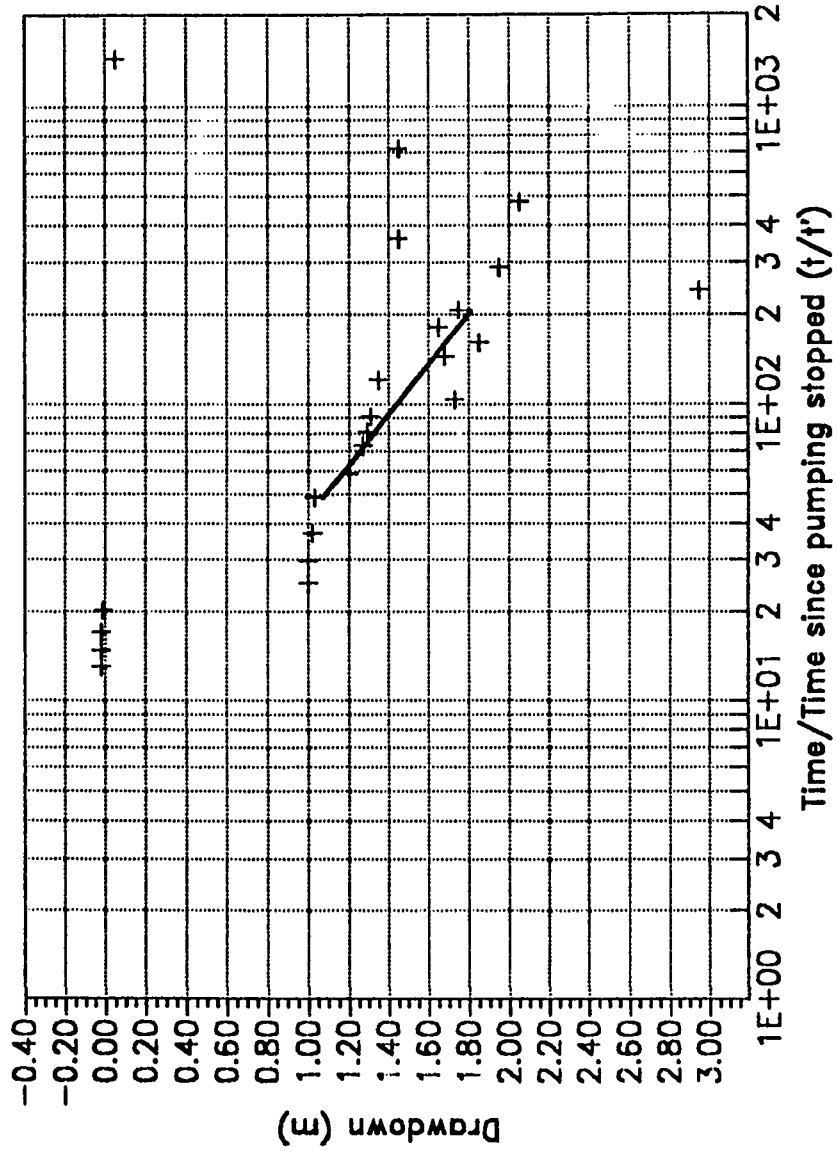
RECOVERY TEST - WELL NO. F2



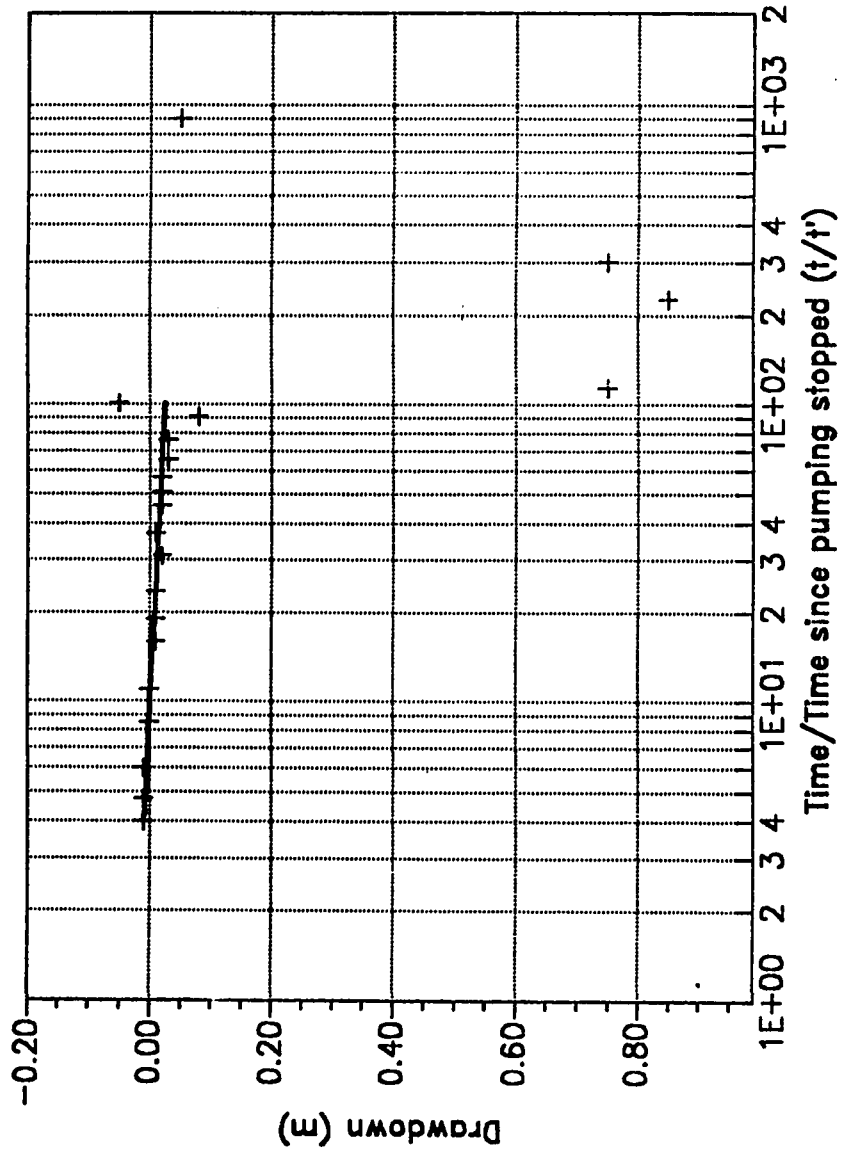
RECOVERY TEST - WELL NO. F3



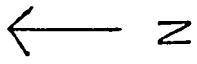
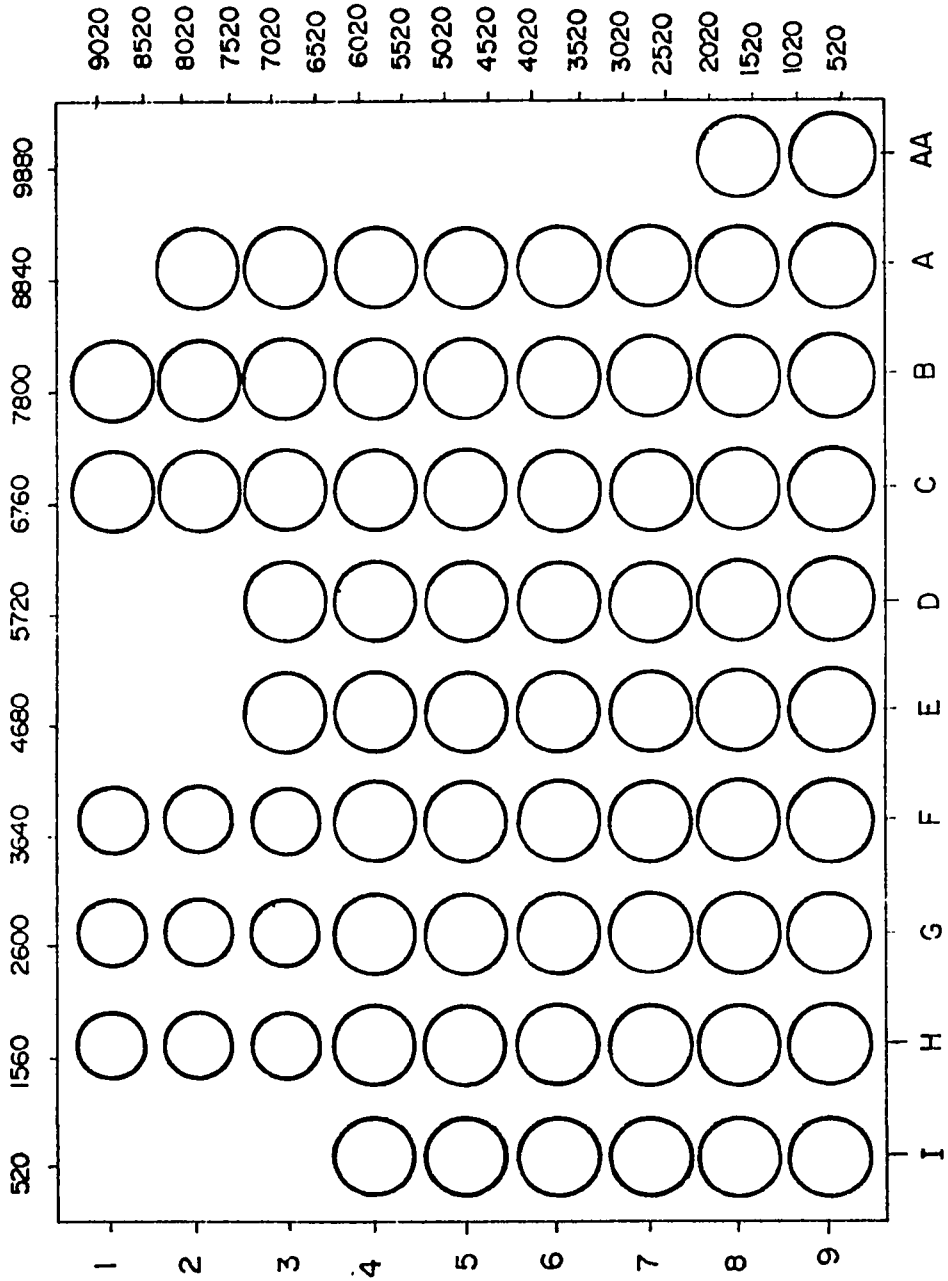
RECOVERY TEST - WELL NO. G3



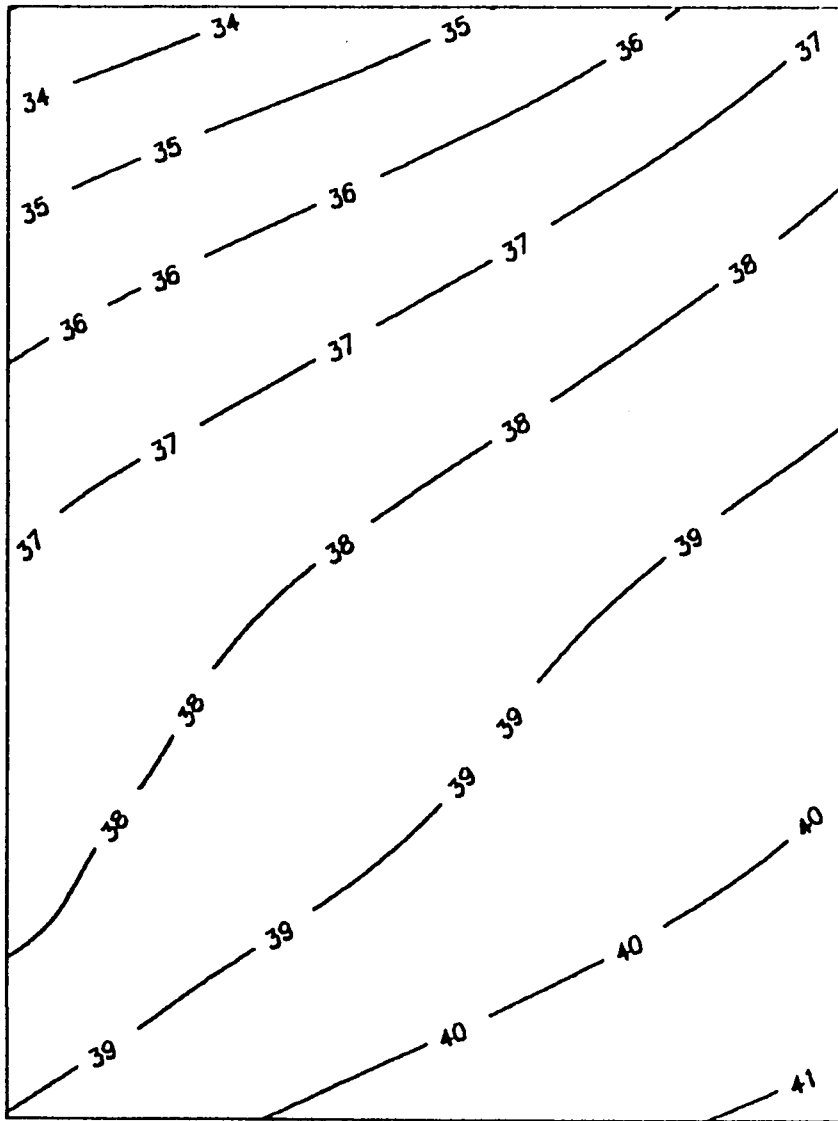
RECOVERY TEST - WELL NO. Z9



**APPENDIX - B: HEADS AT THE END OF
STRESS PERIODS**

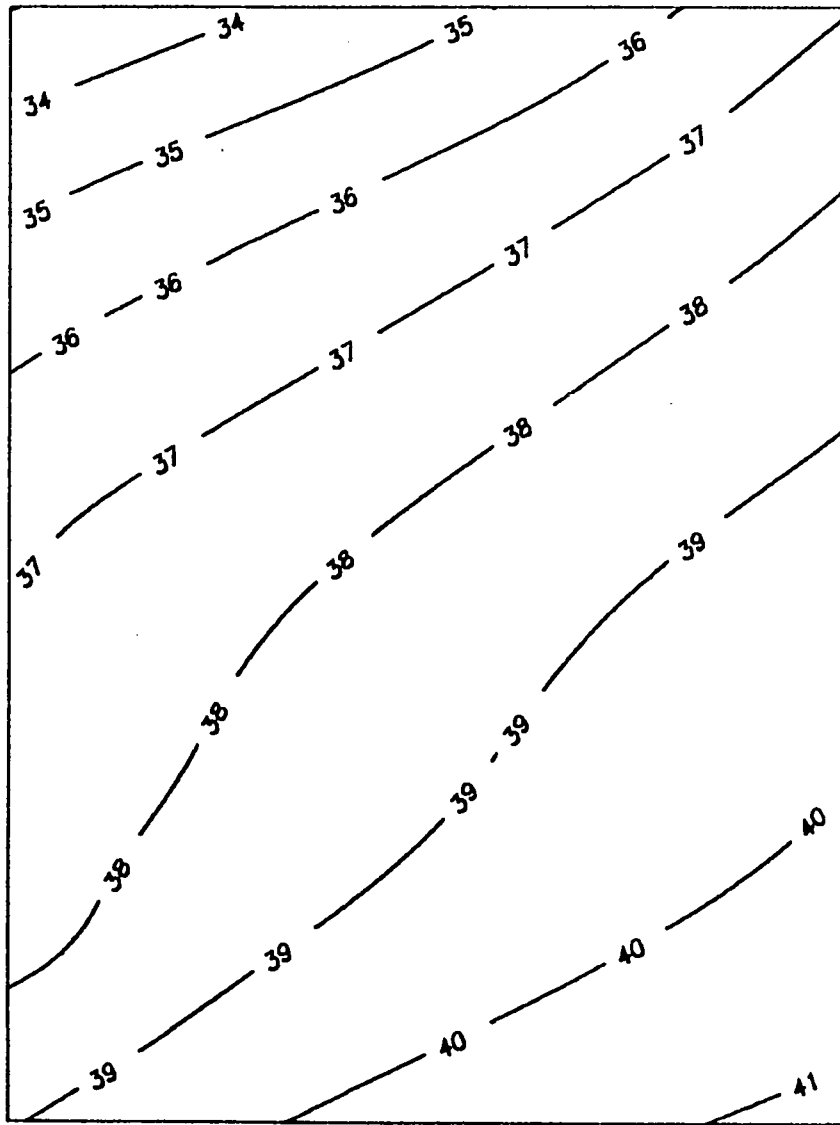


Master Map for the Graphs of Appendix B.

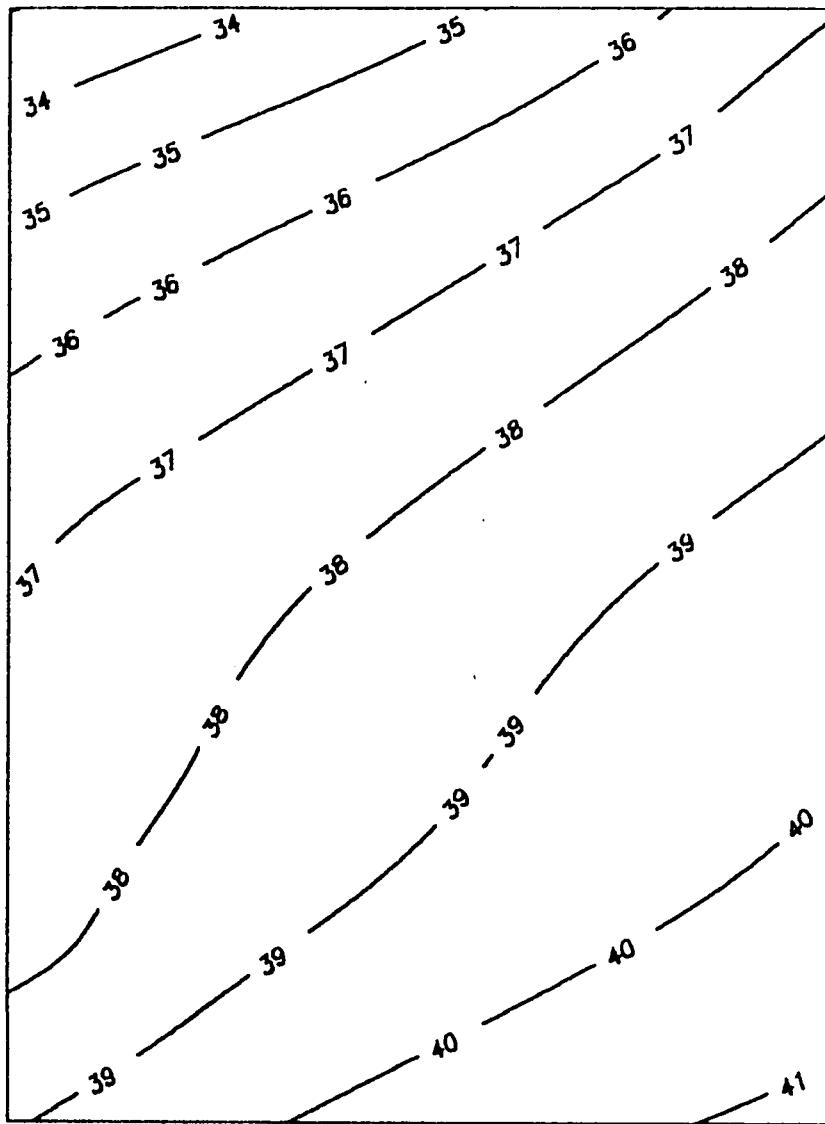


STRESS PERIOD (1)

69

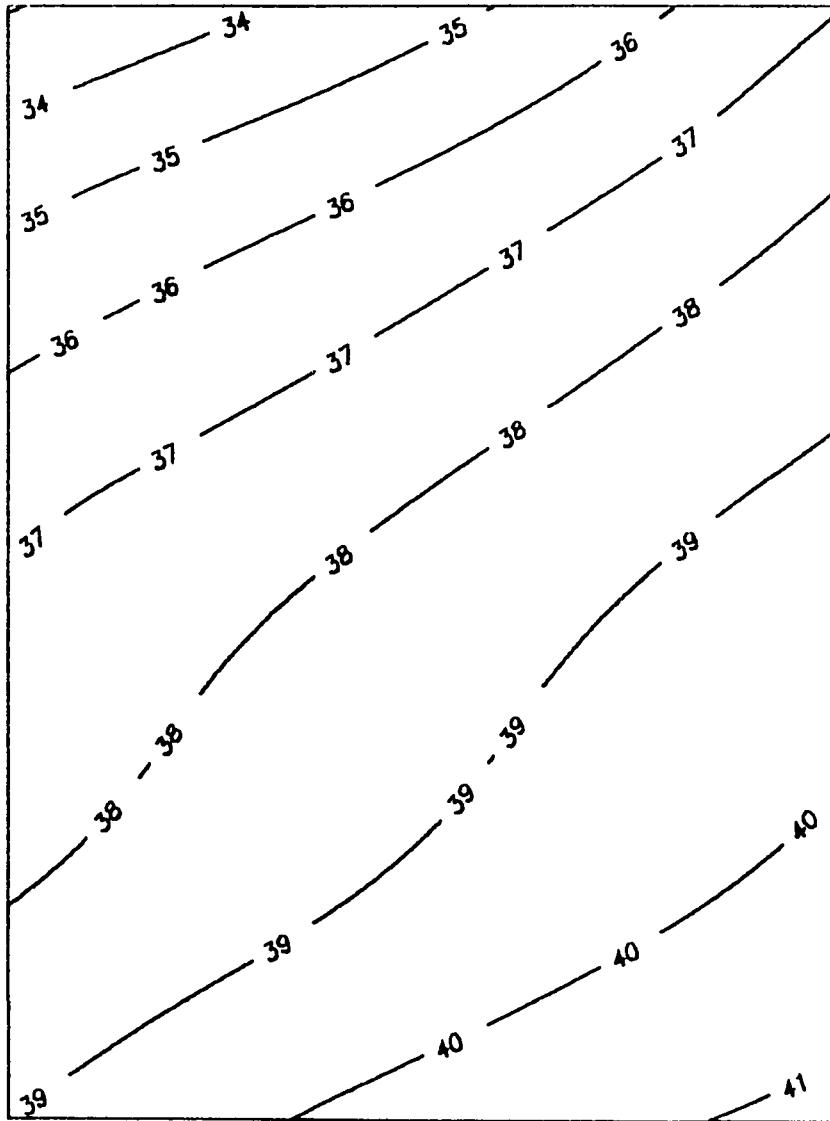


STRESS PERIOD (2)

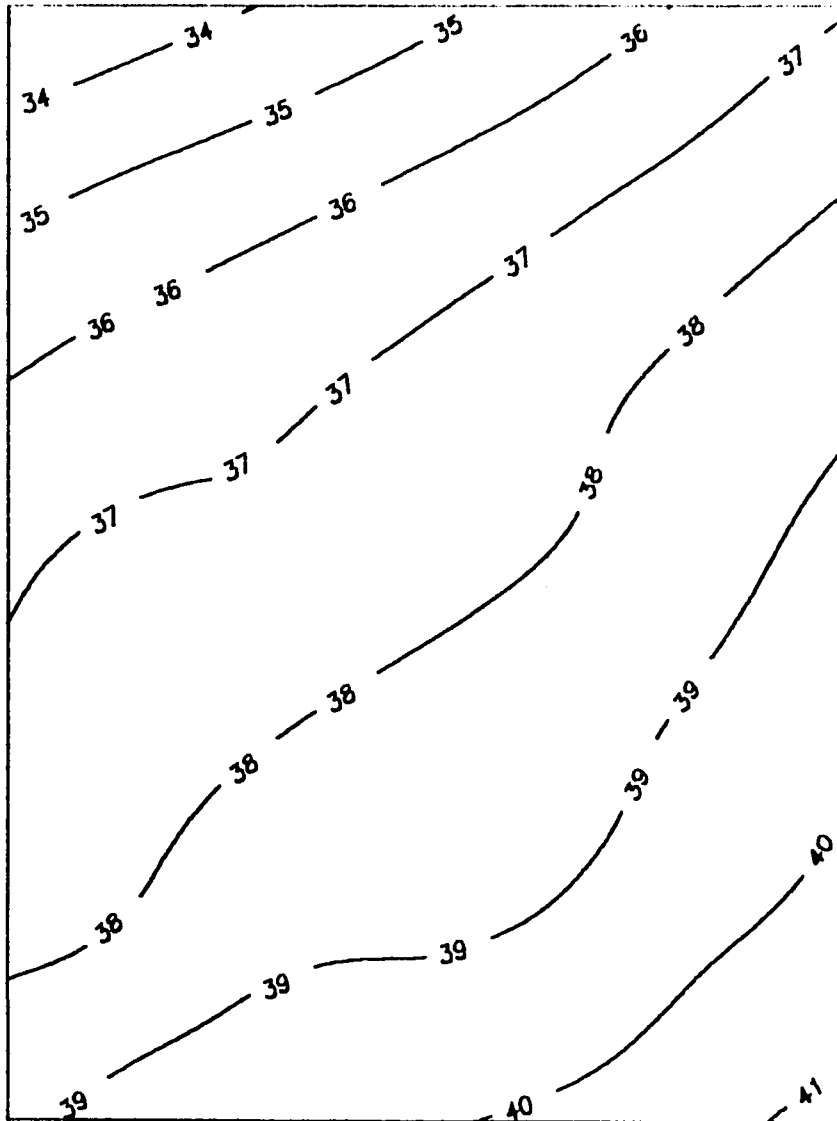


STRESS PERIOD (3)

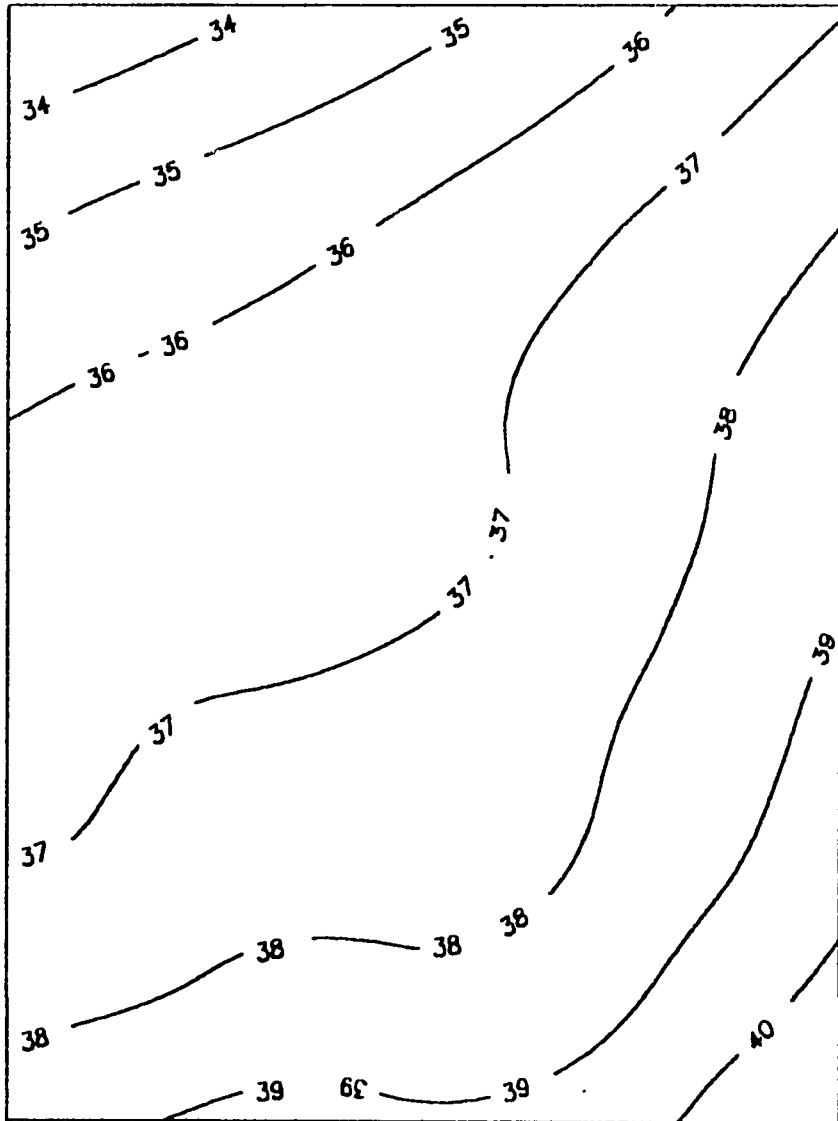
(3)



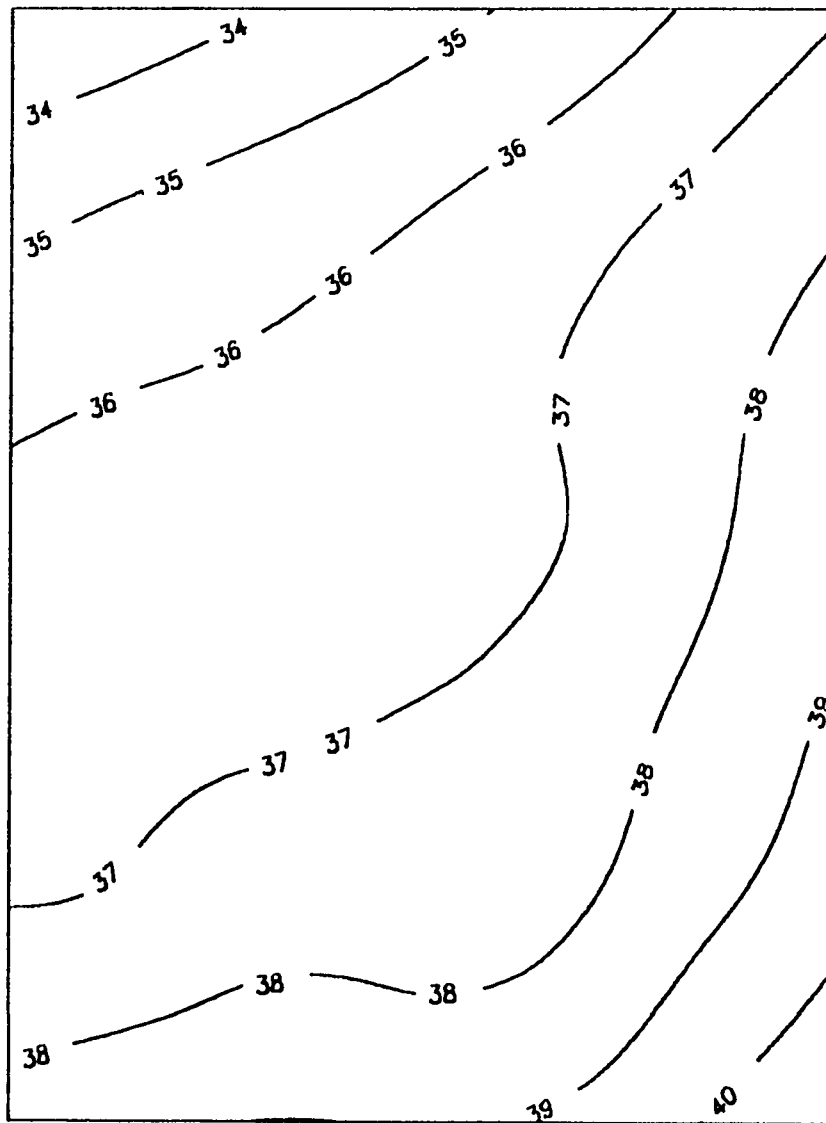
STRESS PERIOD (4)



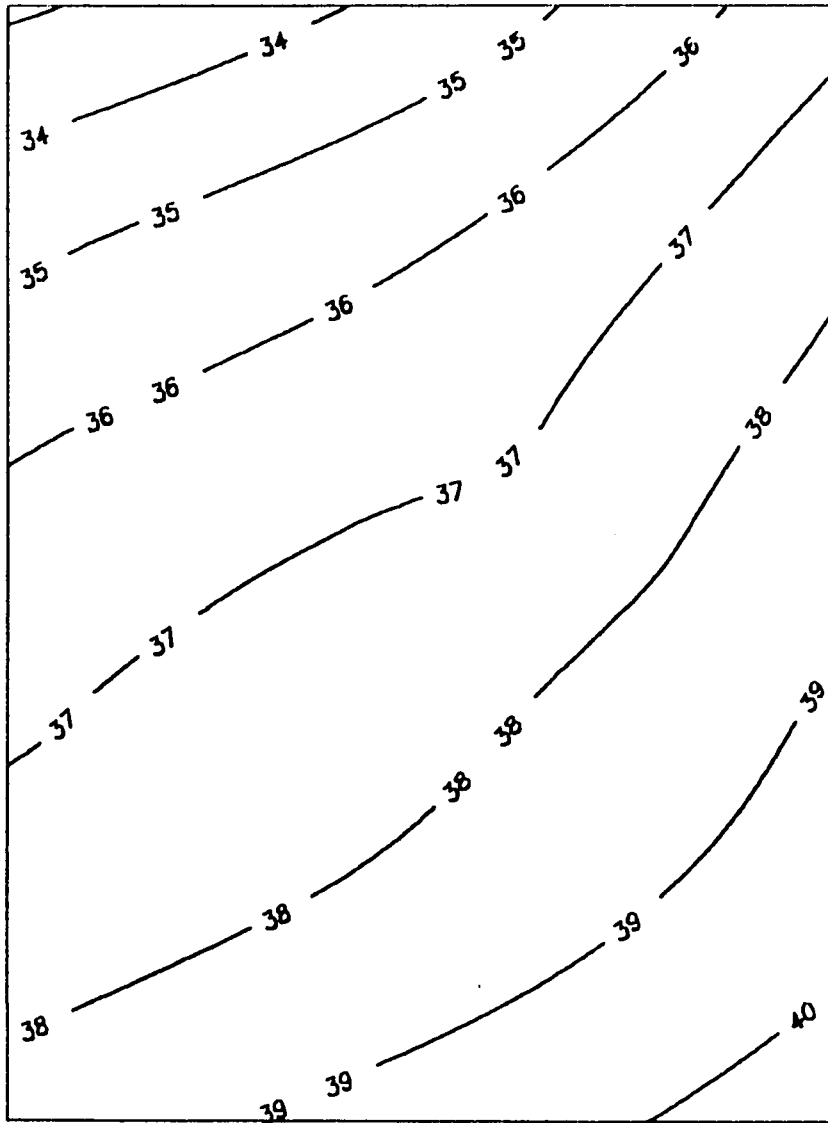
STRESS PERIOD (5)



STRESS PERIOD (6)

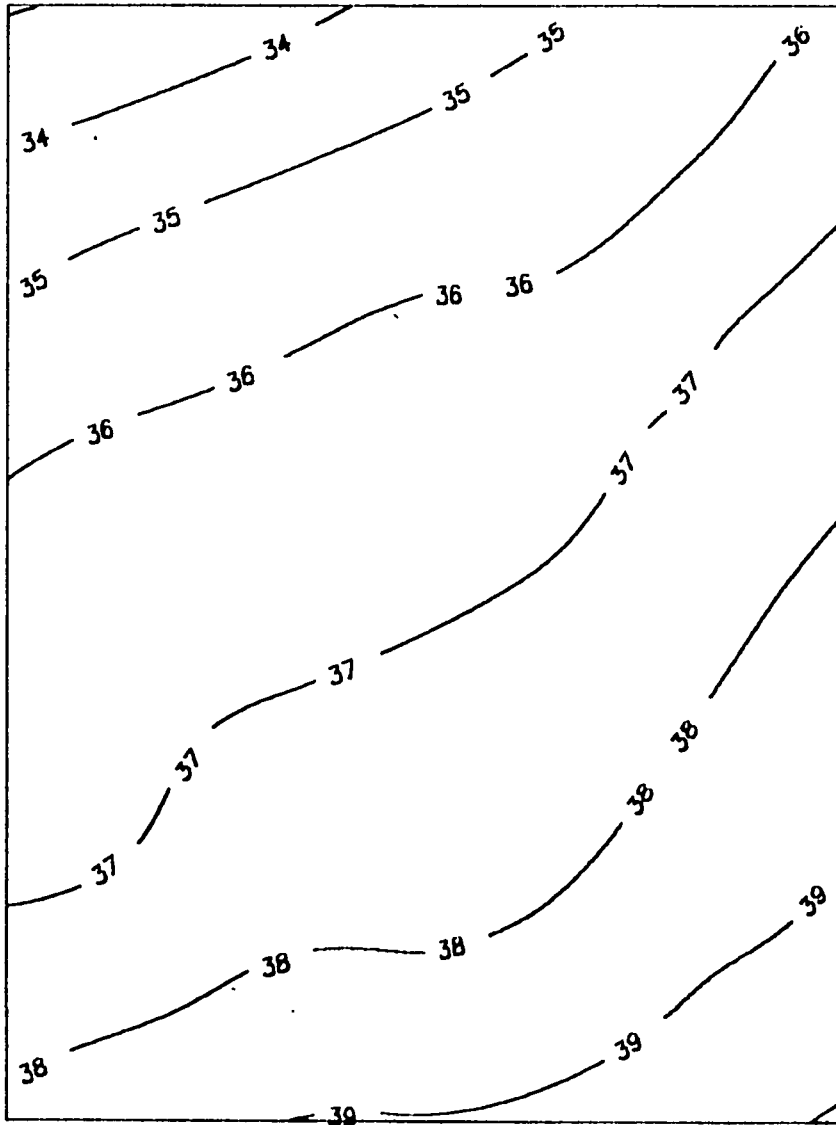


STRESS PERIOD (7)

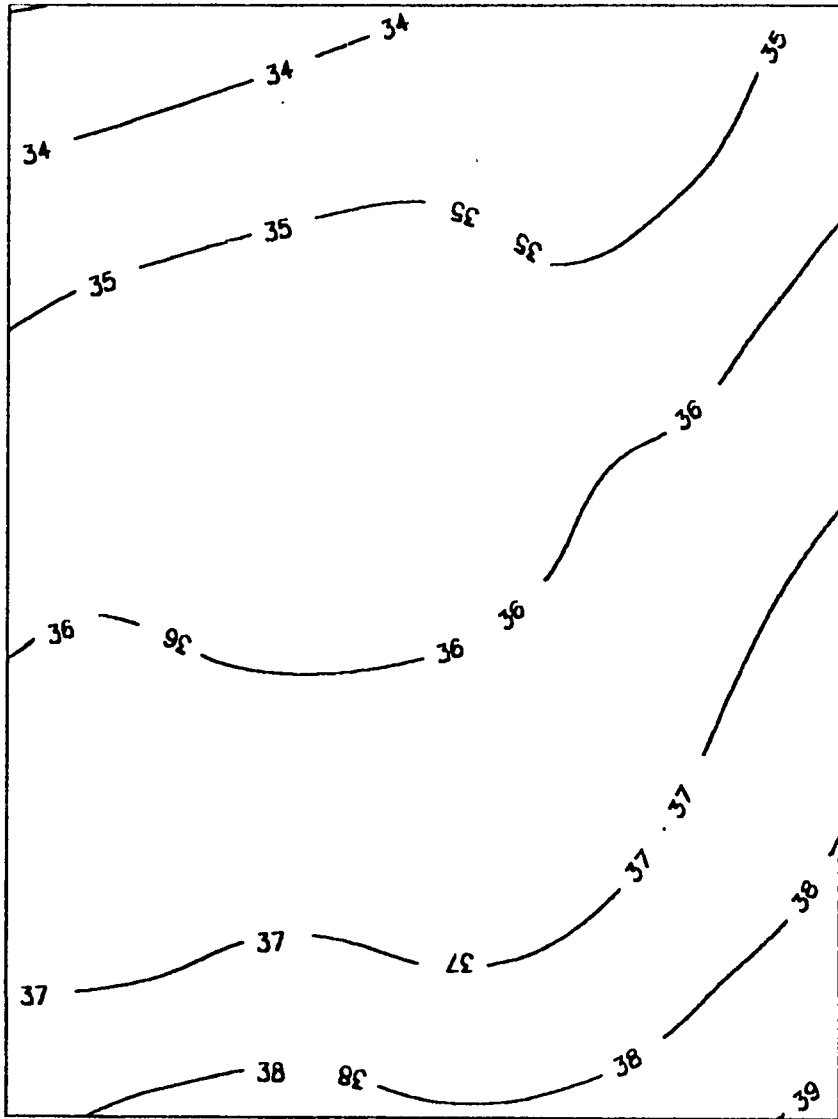


STRESS PERIOD (8)

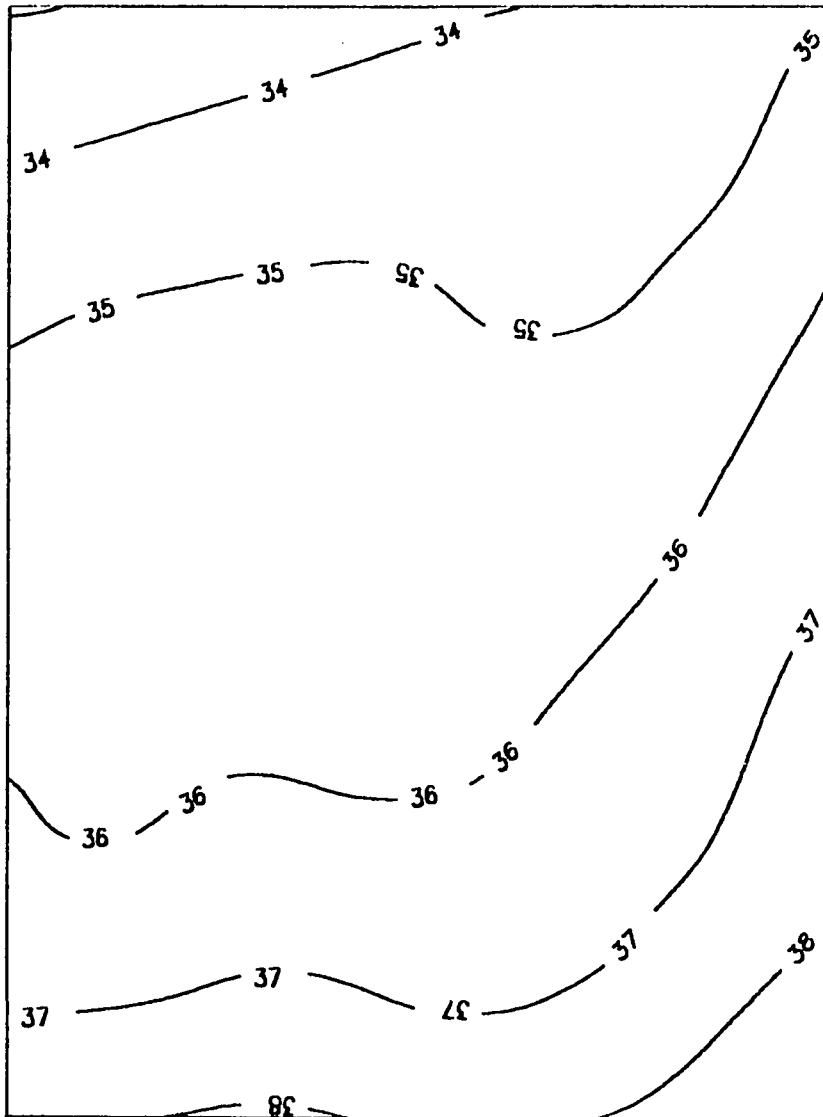
(3)



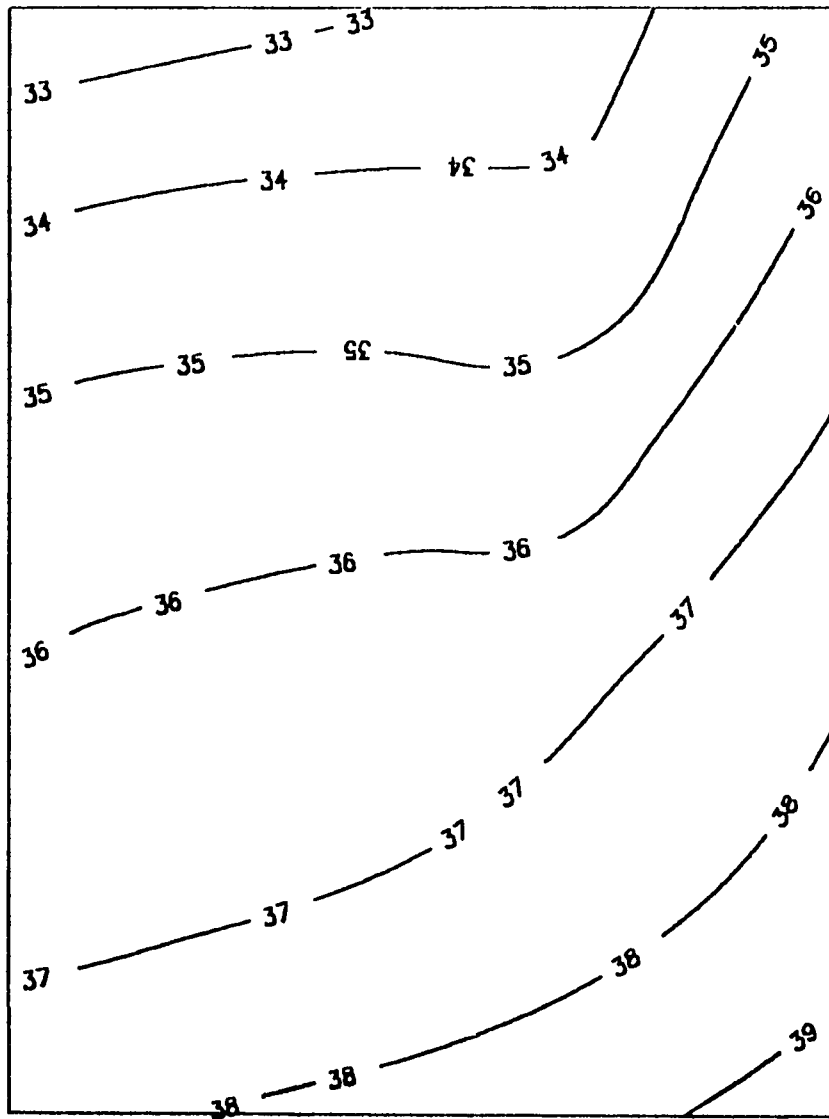
STRESS PERIOD (9)



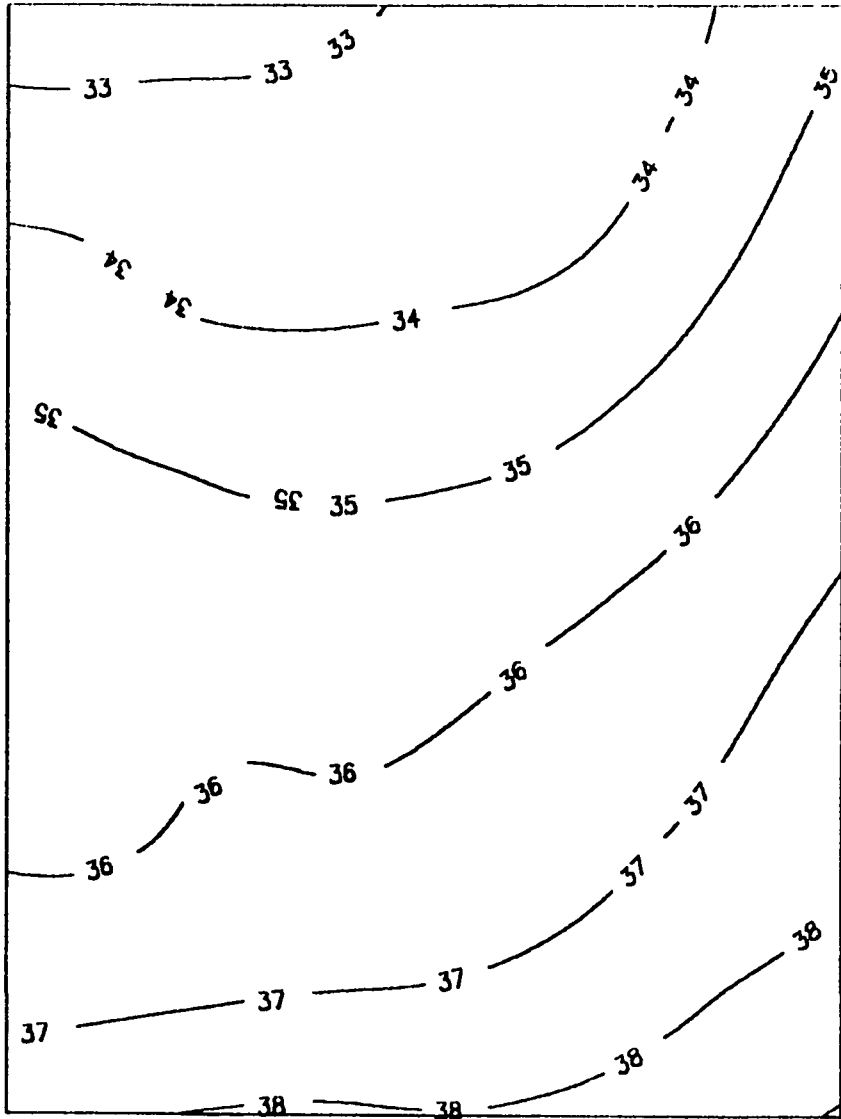
STRESS PERIOD (10)



STRESS PERIOD (11)

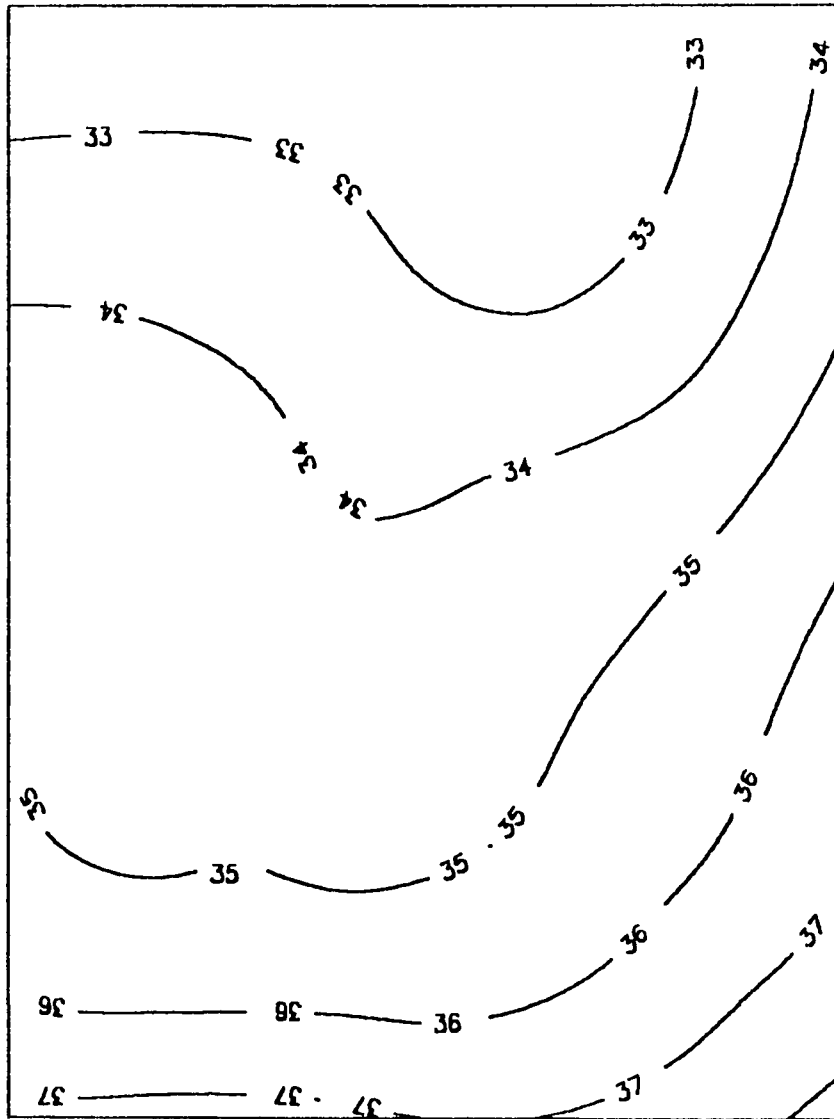


STRESS PERIOD (12)

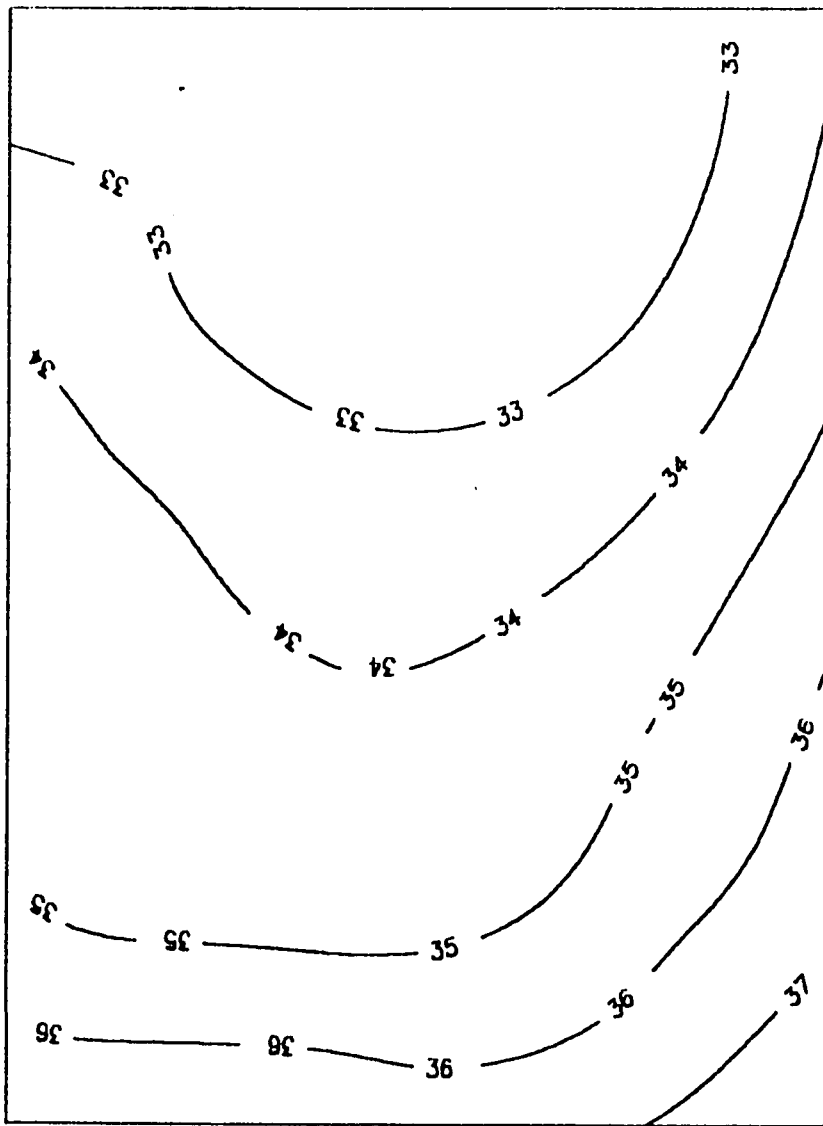


STRESS PERIOD (13)

(7)

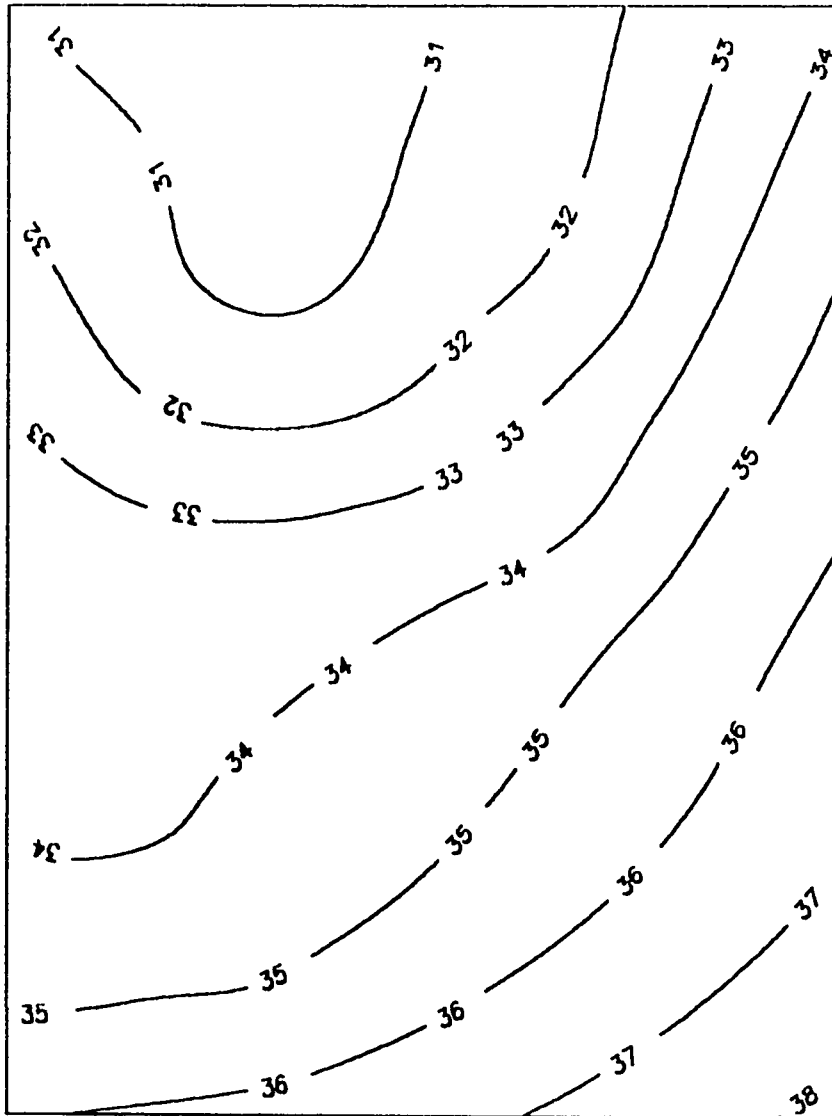


STRESS PERIOD (14)

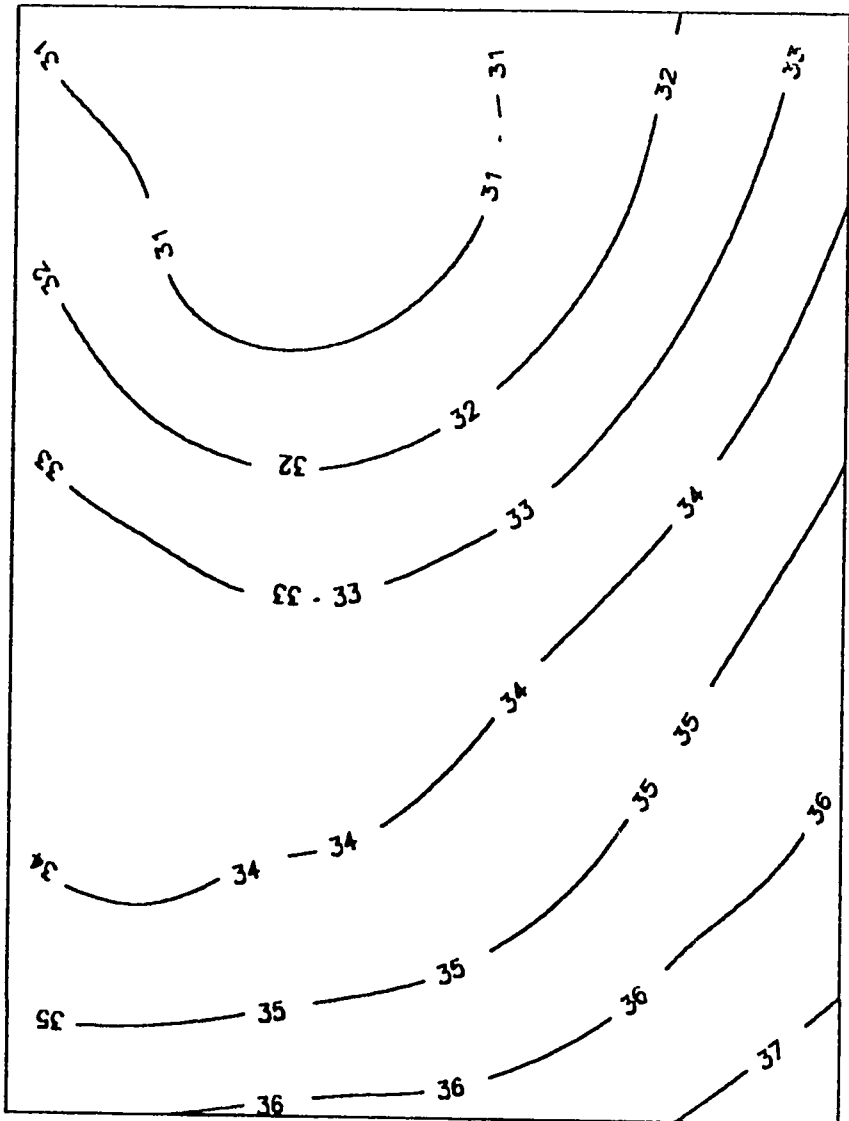


STRESS PERIOD (15)

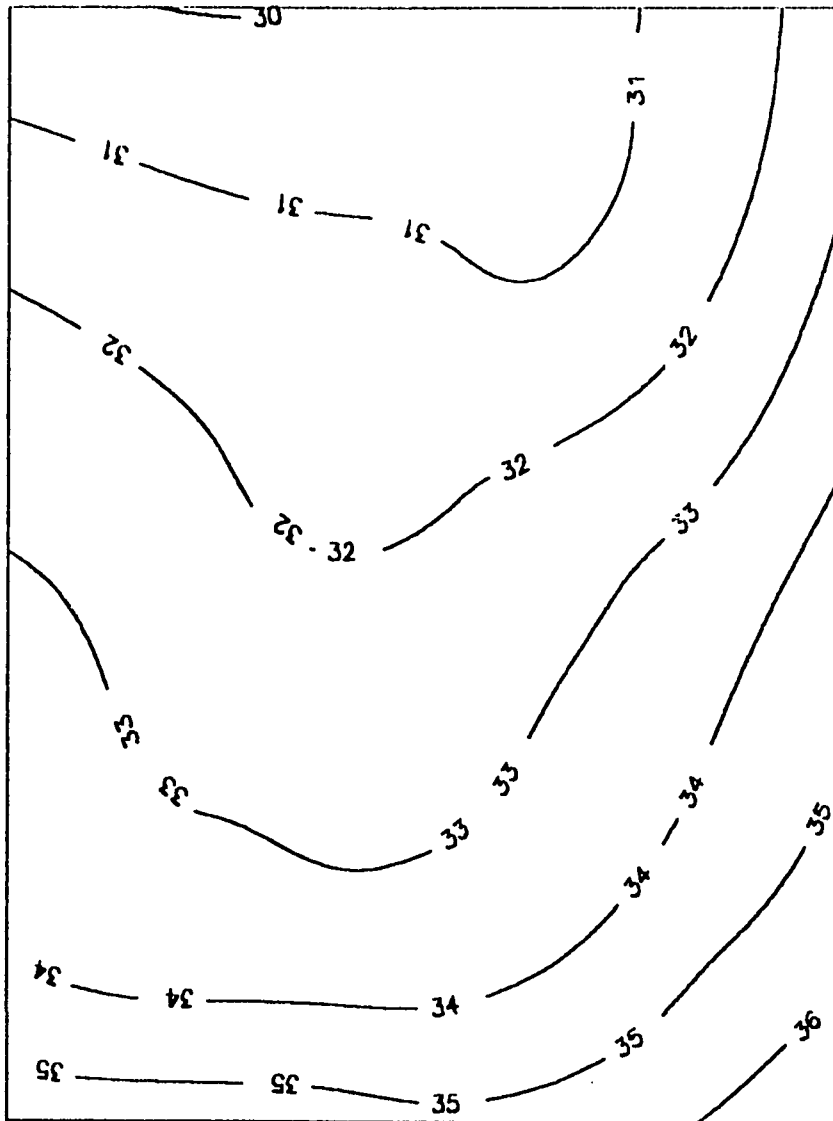
64



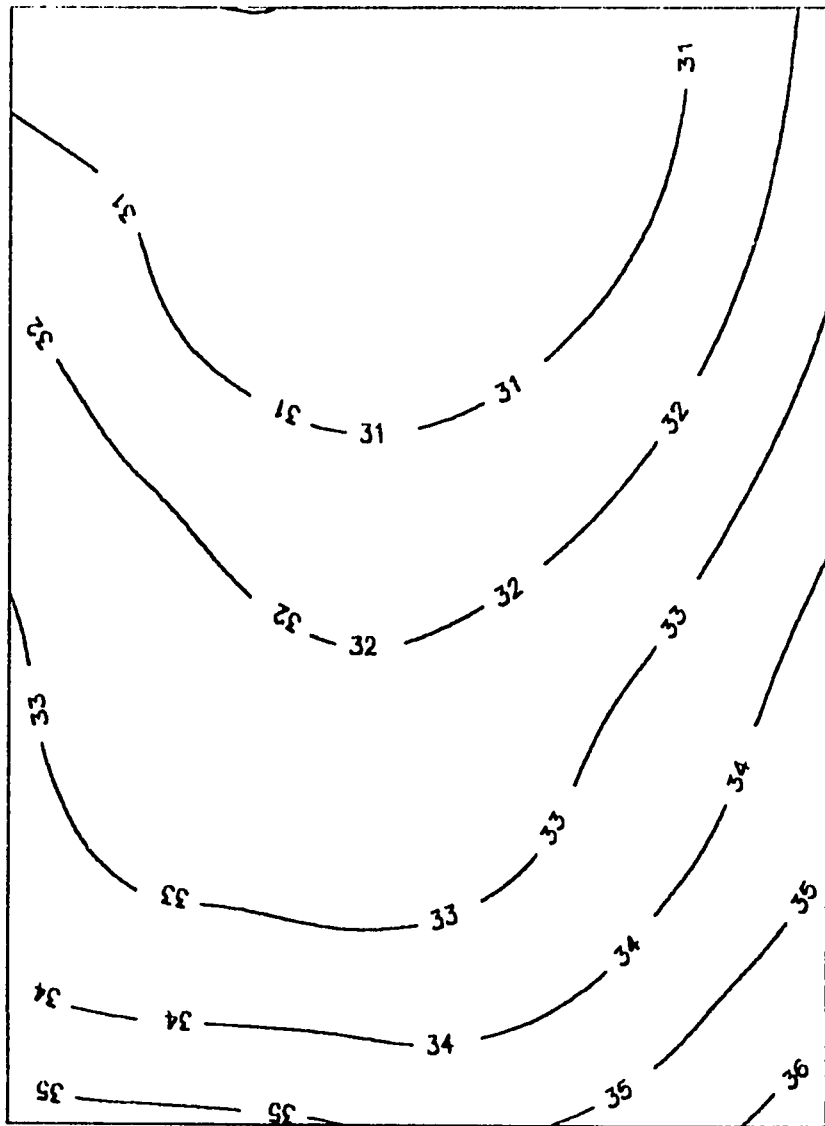
STRESS PERIOD (16)



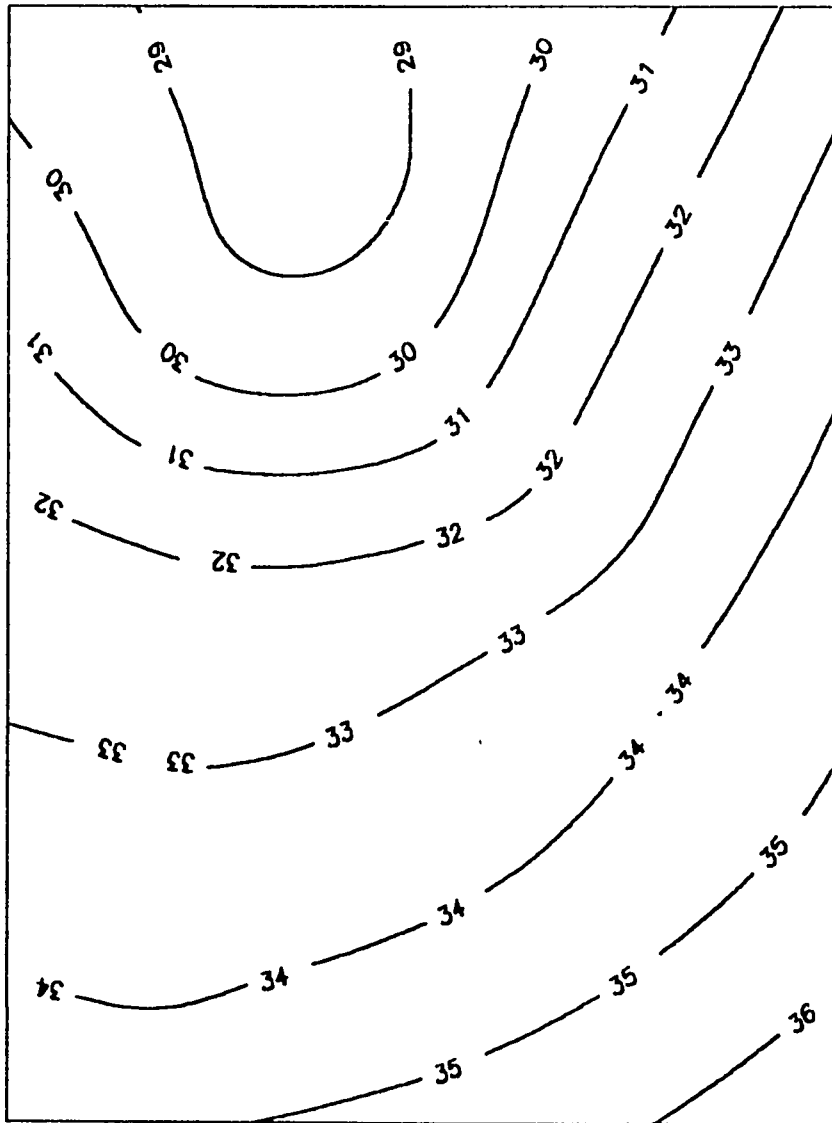
STRESS PERIOD (17)



STRESS PERIOD (18)

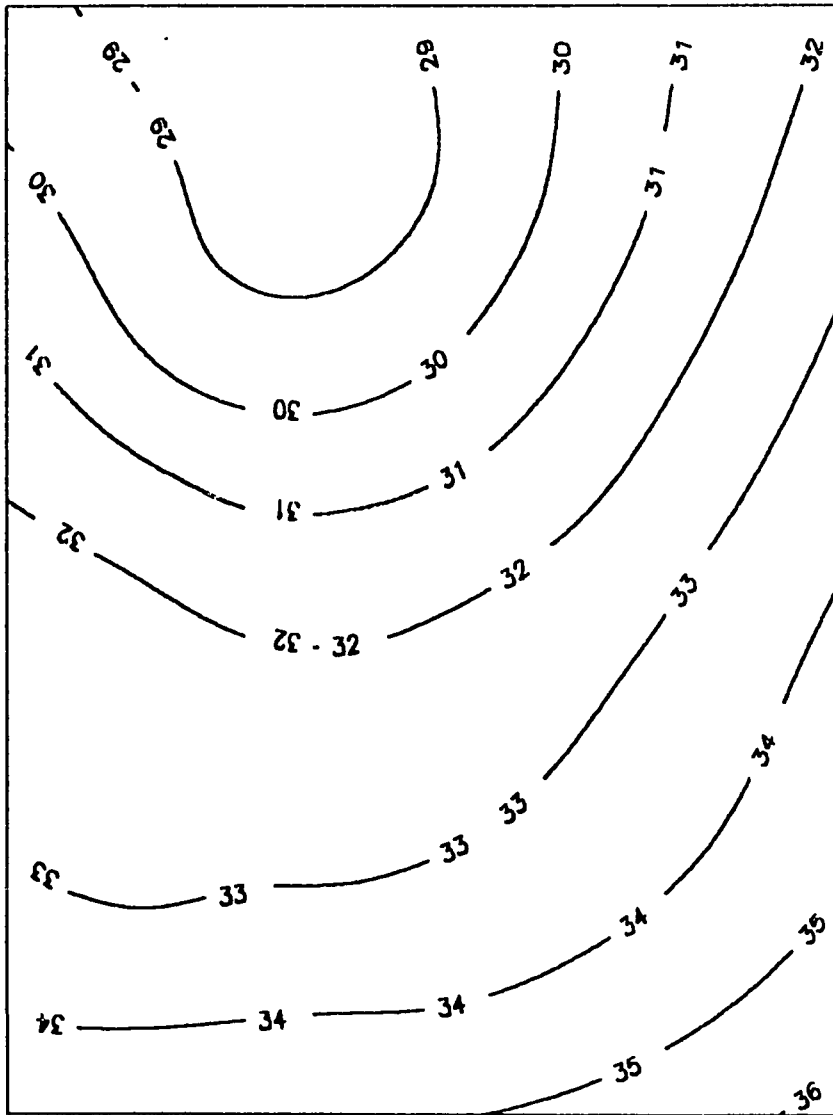


STRESS PERIOD (19)

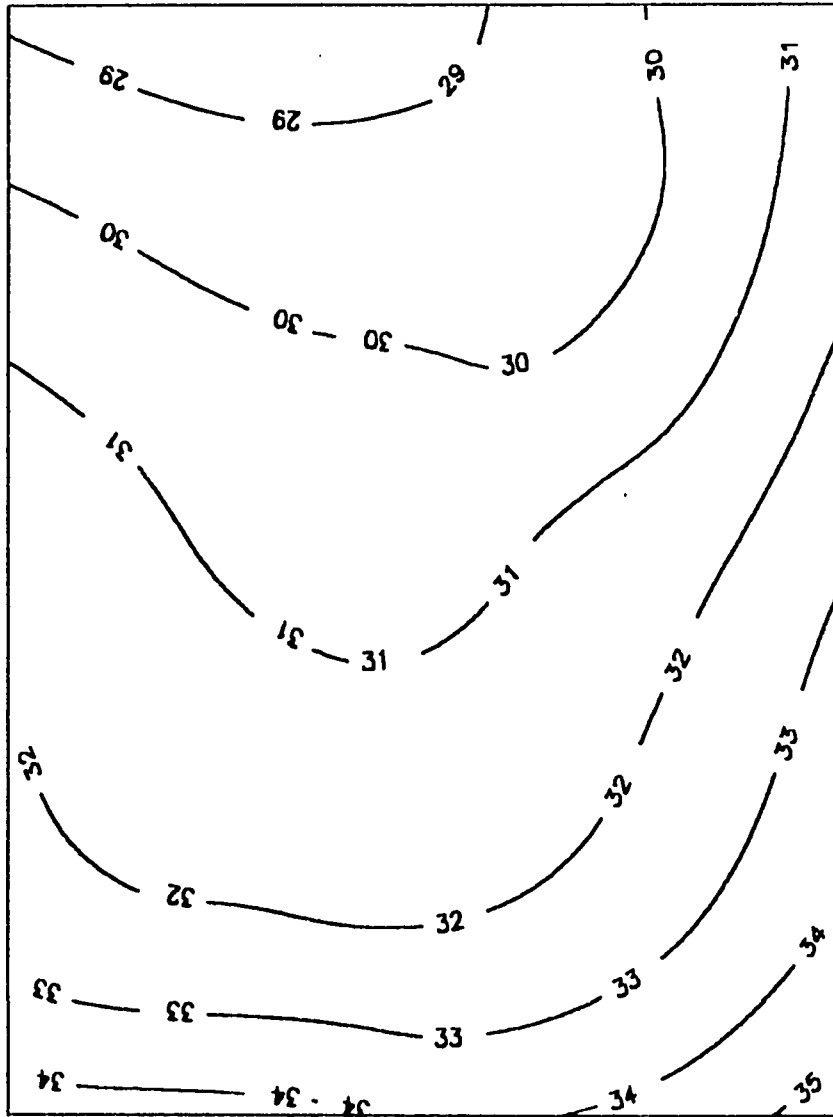


STRESS PERIOD (20)

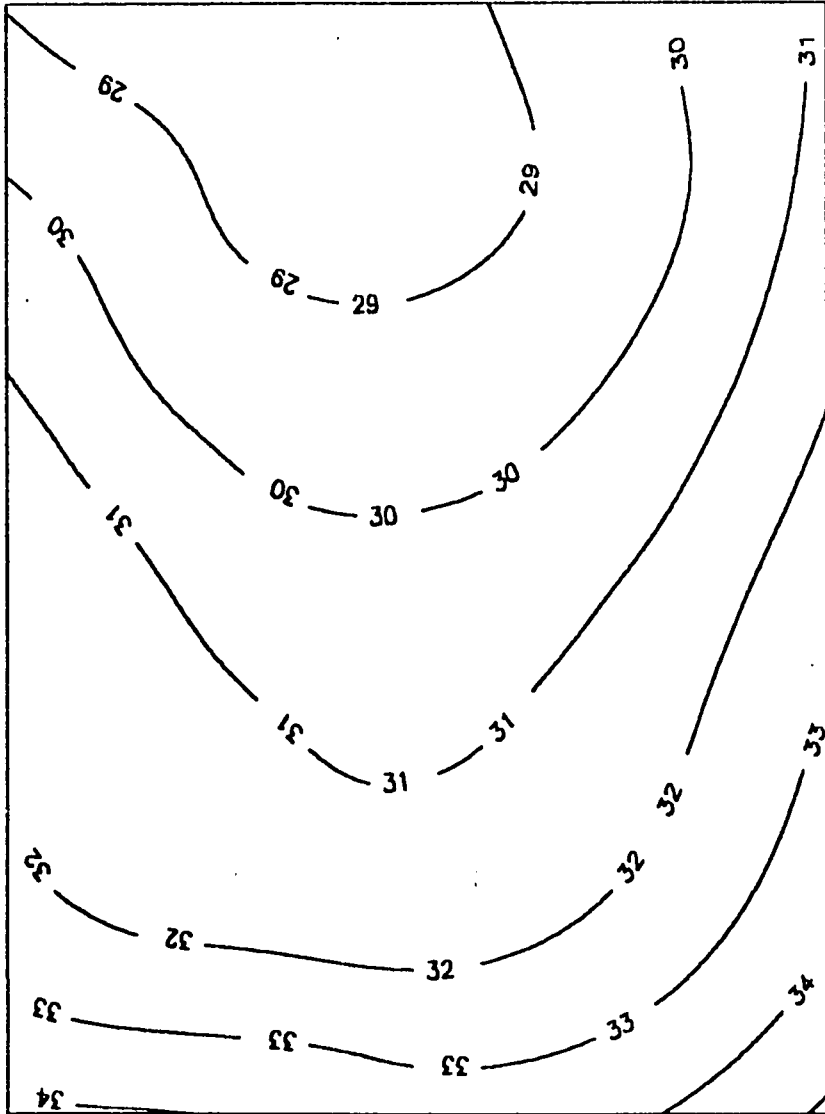
64



STRESS PERIOD (21)

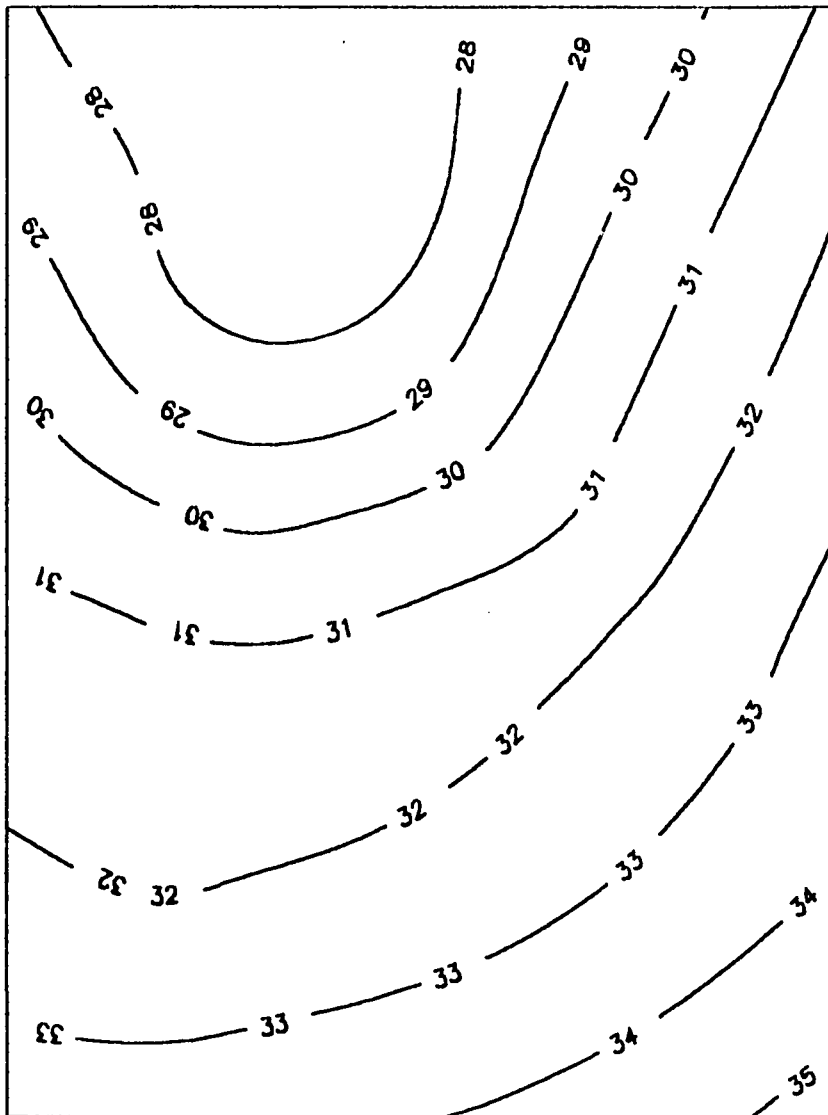


STRESS PERIOD (22)

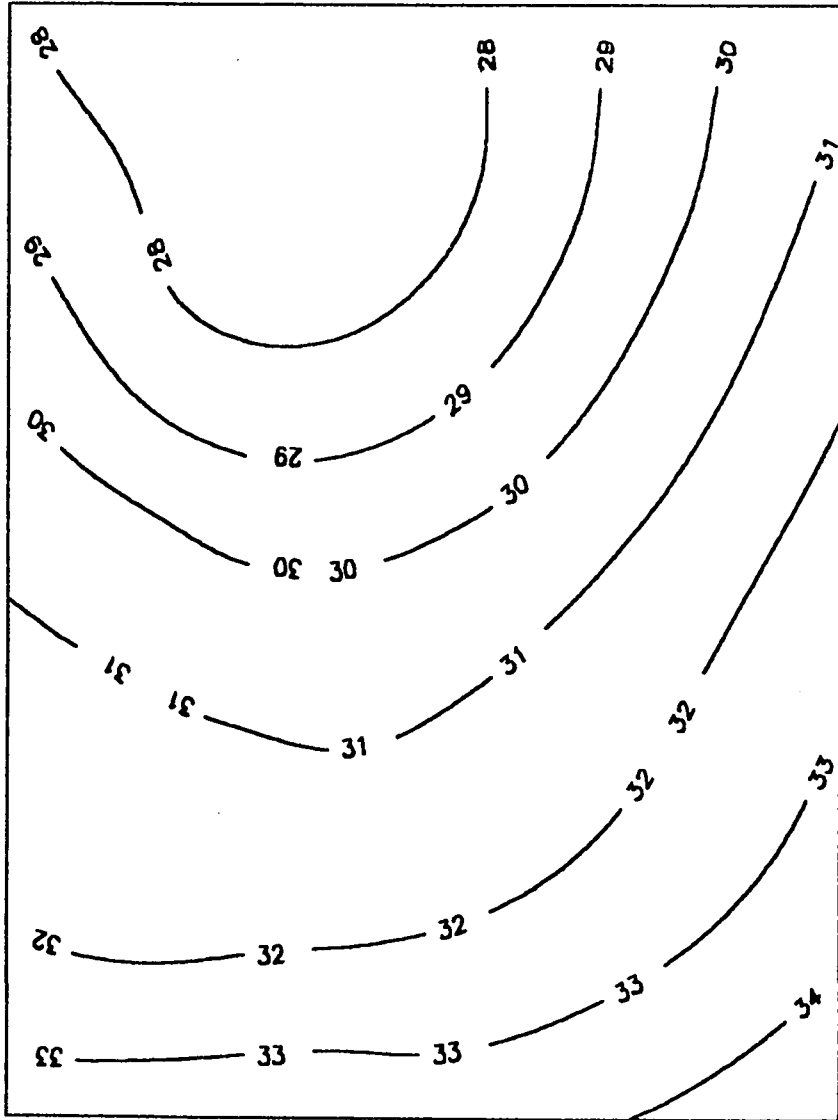


STRESS PERIOD (23)

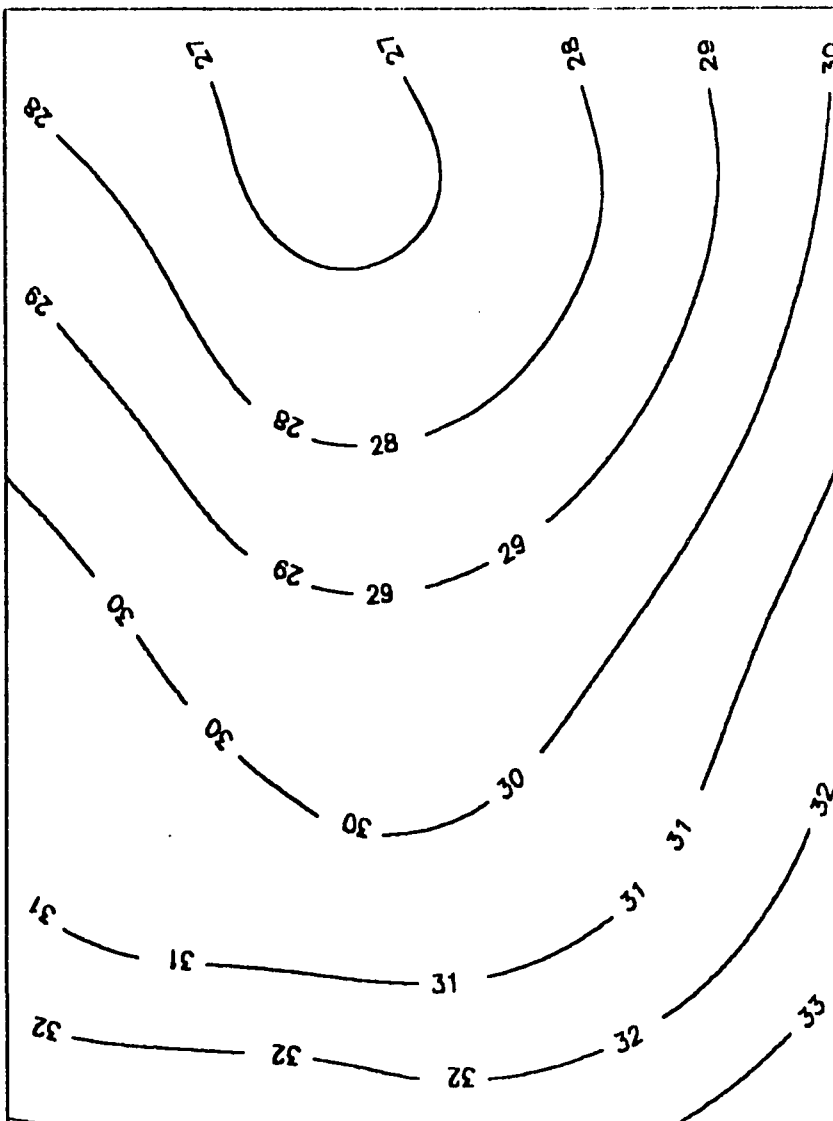
(4)



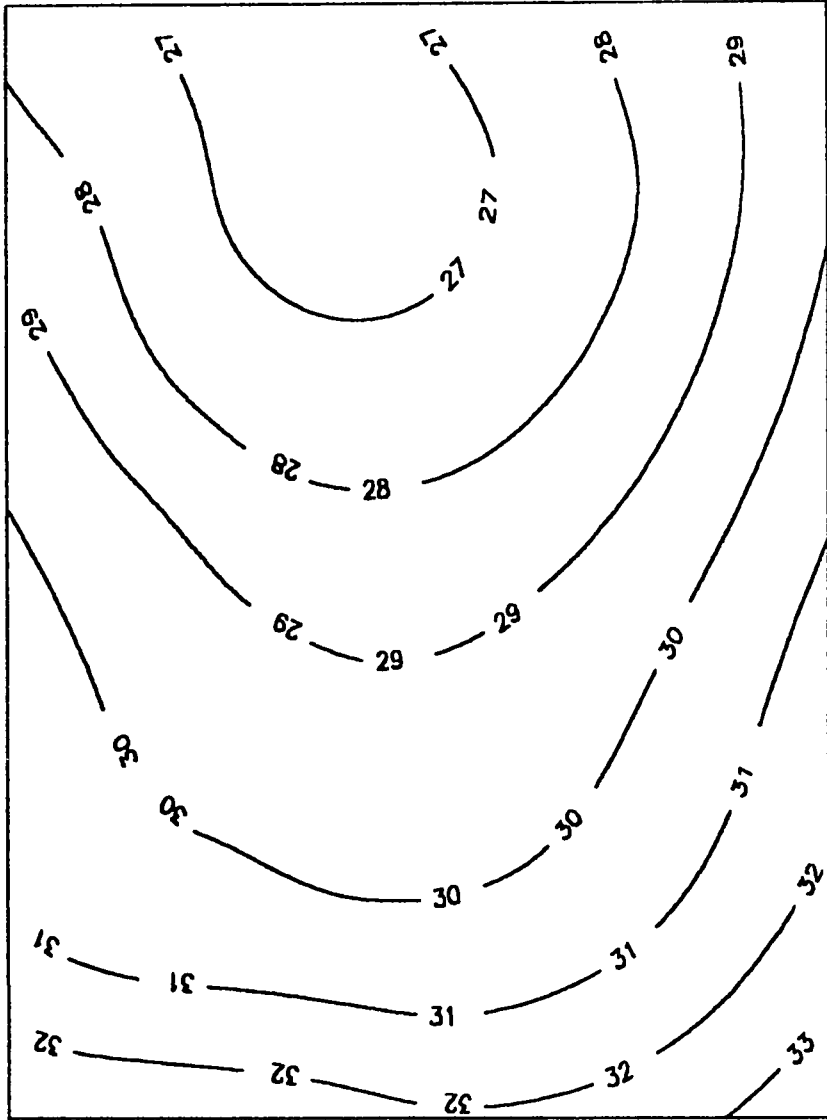
STRESS PERIOD (24)



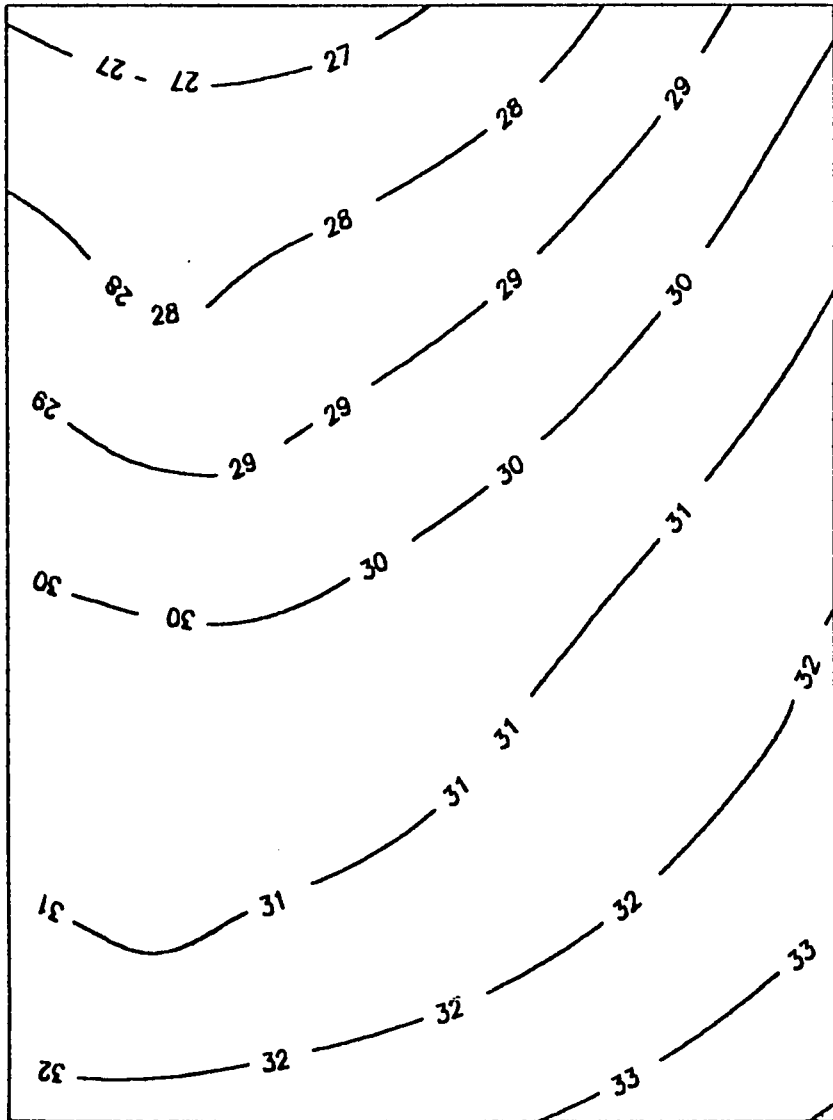
STRESS PERIOD (25)



STRESS PERIOD (26)



STRESS PERIOD (27)



STRESS PERIOD (28)

69